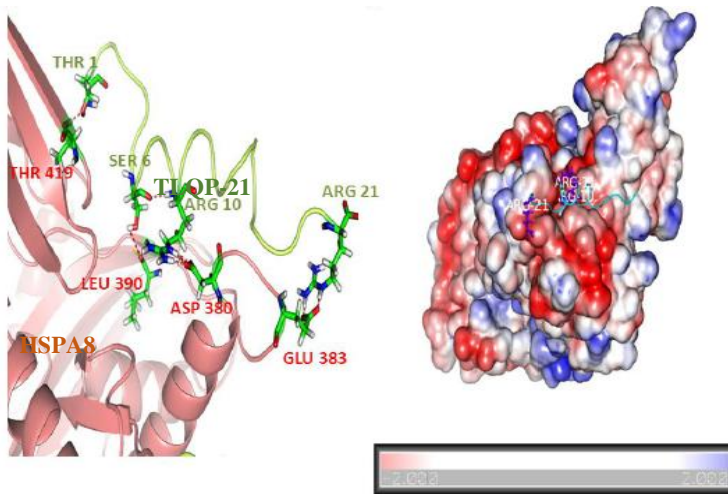


Doctoral Thesis



Isolation of VGF derived neuropeptide receptor

Md Shamim Akhter
Santiago de Compostela, 2015



University of Santiago de Compostela

Faculty of Medicine

Department of Medicine



Isolation of VGF derived neuropeptide receptor

Md Shamim Akhter

Santiago de Compostela, 2015





Jesús Rodríguez Requena, Doctor en Ciencias Químicas, Profesor Contratado Doctor del Departamento de Medicina de la Universidad de Santiago de Compostela,

CERTIFICA:

Que Md. Shamim Akhter ha realizado bajo su supervisión el trabajo titulado: “*Isolation of VGF derived neuropeptide receptor*” (*Isolamento do receptor de neuropeptidos derivados do VGF*), que presenta como Tesis Doctoral para optar al título de Doctor por la Universidad de Santiago de Compostela.

Estimando que el presente trabajo reúne los requisitos exigidos por la normativa vigente, autoriza su presentación a fin de ser evaluado por la Comisión correspondiente.

Dr. Jesús Rodríguez Requena



Acknowledgements

I am heartily thankful to my supervisor, Dr. Jesus Rodriguez Requena, who continuously and convincingly conveyed a spirit of adventure in regard to my research work and the thesis writing. His great efforts to explain things clearly and simply helped to make the research works easier for me. Without his encouragement, sound advice, good teaching, good company, and lots of good ideas from the very beginning to the last level, this thesis would not have been possible.

I am thankful to all of my group members, of past and present, for their continuous support in daily lab works that made my works easier undoubtedly. I am grateful to the group members as well as other friends of Santiago de Compostela for being the surrogate family during the period I stayed here and for their continued moral support thereafter.

I also would like to make a special reference to Mr. Sandipan Chakrobarty for the collaboration works with us and for his permission to include the collaborative works in the thesis.

I take this opportunity to sincerely acknowledge the support and encouragement of my well-wishers and colleagues who supported me in any respect, directly or indirectly, during the completion of the venture.

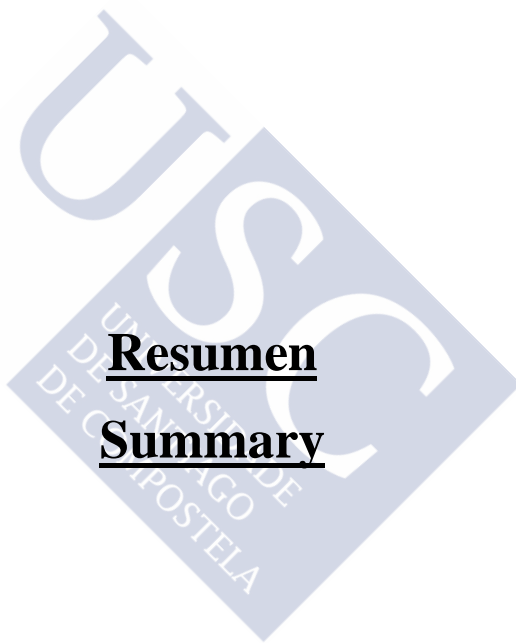
I am indebted to the Erasmus Mundus EXPERTS II scholarship authority who granted me the scholarship to conduct the research work here.

Words fail me to express my appreciation to my family members for their sincere encouragement, inspiration, above all, moral support throughout my research work.

Once again, it is a pleasure for me to express thanks to all of them who contributed in any way to make this study a success.

Also and finally I should like to express my profound gratefulness to the Omnipotent Allah Who has blessed me with sound mind and sound health to complete this piece of work. To Him, I owe all that I have and all that I am.





Resumen
Summary



La VGF es una proteína neurosecretora de ~68 kDa que pertenece a la familia de las graninas. VGF no es un acrónimo, sino que hace referencia a un clon de cADN derivado de un ARN mensajero cuya expresión se indujo en células PC12 mediante tratamiento con la neurotrofina "Nerve Growth Factor (NFG)". Levi y colaboradores designaron este clon como procedente de la placa V de la biblioteca de cADN inducida por el Growth Factor (Levi et al., 1985; Possenti et al., 1989).

La proteína VGF se expresa fundamentalmente en neuronas, como consecuencia de la inducción mediada por NGF y otras neurotrofinas como BDNF. Como se detallará, la VGF es a su vez una neurotrofina, y puesto que el género asignado a BDNF y NGF es el masculino (de "factors"), se utilizará arbitrariamente este mismo género para el VGF, aunque como se ha indicado, VGF no signifique "Growth Factor V".

La secuencia aminoacídica del VGF incluye varios pares de amino ácidos básicos (arginina y lisina) consecutivos, lo que lo convierte en una diana de endoproteasas que lo cortan generando un gran número de péptidos de secreción biológicamente activos. Dichos péptidos se almacenan en vesículas densas hasta el momento de su secreción, que tiene lugar de una forma regulada. Varios de estos péptidos han sido caracterizados y algunas de sus funciones, identificadas. Estas incluyen importantes papeles en la regulación del equilibrio energético, la función reproductiva, la modulación del dolor, el mantenimiento de células neuronales, y la modulación del estado de ánimo.

Uno de los neuropéptidos derivados del VGF mayor caracterizados y estudiados hasta la fecha es el TLQP-21. El nombre de este péptido, siguiendo la pauta utilizada para otros también derivados del VGF, hace referencia al número de aminoácidos que lo componen y a sus cuatro residuos aminoacídicos aminoterminales. Las secuencias de los TLQP-21

humano y murino son relativamente parecidas, aunque con diferencias no desdeñables. Concretamente: TLQPPSALRRRHYHHALPPSR (humana) y TLQPPASSRRRHFHHALPPAR (murina). Como puede apreciarse, la diferencia es de 5 aminoácidos sobre 21, es decir, de aproximadamente un 20%. Esta diferencia se hará particularmente relevante en la discusión sobre las posibles diferencias en la actividad y, sobre todo, los posibles receptores de estos péptidos (ver más adelante).

Se han demostrado efectos del TLQP-21 en los siguientes procesos fisiológicos, entre otros: gasto energético (Possenti et al., 2012; Jethwa et al., 2007; Bartolomucci et al., 2006), metabolismo en general (Bartolomucci et al., 2008), lipólisis (Possenti et al., 2012), secreción de insulina estimulada por la glucosa (Stephens et al., 2012), nociocepción (Fairbanks et al., 2014; Chen et al., 2013; Rizzi et al., 2008; Severini et al., 2008), regulación de la presión sanguínea y control de la hipertensión (Fargali et al., 2014), contractilidad gástrica (Severini et al., 2009; Bartolomucci et al., 2008), regulación de la secreción ácida gástrica (Sibilia et al., 2012; Sibilia et al., 2010a; 2010b), función reproductora (Aguilar et al., 2013; Pinilla et al., 2011) y respuesta al estrés (Razzoli et al., 2012, Bartolomucci et al., 2011).

De entre todos estos efectos, aunque todos importantes, merece la pena destacar la regulación del gasto energético. A grandes rasgos se puede afirmar que el TLQP-21 tiene como efecto un aumento del gasto energético en modelos animales. Este efecto se produce sin que haya una elevación de los niveles séricos de las hormonas tiroideas T3 y T4, y sin un aumento de la actividad locomotora (Bartolomucci et al., 2006; 2009). Sí se acompaña de una elevación de la temperatura rectal. Por otra parte, el tratamiento con TLQP-21 tuvo como consecuencia un aumento de expresión en el tejido adiposo blanco (WAT) de RNA de marcadores catabólicos tales como las isoformas α y β del "peroxisome proliferator-activated receptor" (PPAR), el receptor adrenérgico y la

"uncoupling protein 1" (UCP1, Bartolomucci et al., 2006; 2007). Además, el TLQP-21 produce un aumento de la razón entre ácidos grasos libres y triglicéridos (FFA/TG ratio, según la terminología anglosajona habitual, Bartolomucci et al., 2007). En resumen, el TLQP-21 tiene un efecto catabólico neto, dando lugar a un aumento del gasto metabólico y una disminución de la masa corporal y de grasa (Bartolomucci et al., 2007).

En vista de esta extensa lista de efectos, la identificación del (los) receptor(es) de TLQP-21 se ha convertido, obviamente, en un objetivo de gran interés, por una parte, para poder comprender mejor los mecanismos moleculares de las diversas acciones del péptido, pero por otra, como posible(s) diana(s) terapéutica(s). Recientemente se han publicado dos trabajos en los que se describe la identificación de los receptores de factores del complemento C3AR1 y gC1qR como receptores de el TLQP-21 murino (Hannedouche et al., 2013; Chen et al., 2013). Sin embargo, el TLQP-21 humano muestra una afinidad mucho menor tanto por las versiones murinas como las humanas de estos receptores (Hannedouche et al., 2013; Chen et al., 2013; Cero et al., 2014). Esto sugiere la existencia de otro(s) receptor(es) para el péptido humano.

El C3AR1 es un receptor acoplado a proteína G que se une a dos componentes del sistema de complemento, C3a y C4a (Klos et al., 2013). Hannedouche y cols. partieron del hecho conocido de que en células CHO-K1 la aplicación de TLQP-21 da lugar a un aumento del calcio intracelular (Cassina et al., 2013). Puesto que dicho efecto es inhibido por la toxina pertussis, esos investigadores razonaron que el receptor del TLQP-21 murino (cabe señalar en este punto que las secuencias de la TLQP-21 de diversos roedores como ratón, rata o hámster son idénticas) sería un receptor acoplado a G₀. De acuerdo con esta premisa, realizaron un estudio genómico y concluyeron que el receptor era C3AR1, lo que fue posteriormente confirmado mediante diversos estudios

bioquímicos y moleculares (Hannedouche et al., 2013). Sin embargo, tal y como ya se ha indicado, la unión del TLQP-21 humano a la C3AR1 humana es mucho más débil que la unión del TLQP-21 murino a esa misma proteína. Así, Cero y cols. comprobaron, mediante un ensayo de reclutamiento de arrestina, que si bien la EC_{50} del péptido murino es, en células con sobreexpresión de C3AR1 humana, 3 veces menor que la del agonista por antonomasia de C3AR1, a saber, C3A, la EC_{50} del péptido humano es 22 veces inferior (Cero et al., 2014).

En cuanto al receptor gC1qR, fue identificado por Chen y cols. como un receptor de TLQP-21 murino mediante un estudio de cromatografía de afinidad (Chen et al., 2013). Se trata del receptor de la cabeza globular del componente del complemento C1q ("globular head of the complement component C1q receptor"). Pero ya antes de su identificación como receptor del TLQP-21 murino se sabía que también se une a otros diversos ligandos of origen celular, bacteriano y vírico (Peerschke et al., 2006; Ghebrehiwet et al., 1996; Xu et al., 1999). Es de destacar que el gC1qR tiene una localización en la superficie celular pero también en el citosol, el retículo endoplásmico o las mitocondrias (Peterson et al., 1997), lo que resulta de gran interés en el contexto del presente trabajo (ver más adelante).

En este contexto, la identificación de posibles receptores específicos del TLQP-21 humano es de gran interés. En el presente trabajo se describe la identificación de la proteína "heat shock cognate 71 kDa protein A8 (HSPA8)", como un receptor del TLQP-21 humano. Para ello se utilizó cromatografía de afinidad. Se acopló TLQP-21 humano derivatizado con biotina a una columna de agarosa-avidina. Posteriormente se preparó un homogenado de células de neuroblastoma SH-SY5Y y se pasó por la columna. Las células SH-SY5Y expresan una considerable cantidad de VGF (Ramos et al. 2014), por lo que se supuso que probablemente expresarían también una cantidad

apreciable de receptores de los péptidos derivados de VGF, incluido el TLQP-21, siendo además fáciles de cultivar. Se decidió utilizar inicialmente un homogenado completo, en vez de una fracción de membrana, para evitar pérdidas, maximizando las posibilidades de aislar e identificar proteínas capaces de interactuar con TLQP-21.

La columna se eluyó con biotina, recogiendo varias fracciones que fueron sometidas a electroforesis en gel de poliacrilamida en SDS (SDS-PAGE). Los geles fueron posteriormente teñidos con Sypro Ruby, un colorante de gran sensibilidad. La tinción puso de manifiesto la presencia de una banda correspondiente a una proteína o proteínas con una masa molecular aparente de algo menos de 75 kDa, ausente en fracciones similares eluidas de una columna control no cargada con el péptido TLQP-21 biotinilado. A continuación se cortó la banda, se sometió a reducción, alquilación y digestión con tripsina "en gel" (Shevchenko, 2006), y tras su elución del gel los péptidos trípticos resultantes fueron analizados mediante espectrometría de masas (MS/MS) utilizando un equipo de nanoHPLC (EASY-nLC, Proxeon, Bruker Daltonik GmbH, Alemania) equipado con una nanocolumna de fase reversa (Easy column SC200 C18 3 μ m 120A 360 μ m OD/75 μ m ID, L=10cm, Proxeon-Thermo Scientific, Estados Unidos) cuyo efluente se dirigió a un espectrómetro de masas Bruker Amazon ETD con electrospray y detector de trampa iónica. El análisis automatizado de datos se realizó mediante los programas Data Analysis 4.0 y BioTools 3.2 de Bruker Daltonik GmbH. El análisis mediante el motor de búsqueda Mascot v2.3 (Matrix Science, Reino Unido) utilizando la base de datos SwissProt (release 57.15) reveló la presencia de HSPA8 con una puntuación ("score") de 735.0, una cobertura del 19.8% y 12 péptidos detectados. Dos proteínas adicionales fueron detectadas, Stress-70 protein (HSPA9/mortalin), y 78 kDa glucose-regulated protein (HSPA5), aunque con puntuaciones, coberturas y número de péptidos detectados sensiblemente menores. La identidad de la HSPA8, en la que se han concentrado todos los esfuerzos ulteriores (ver más adelante) fue confirmada

mediante un anticuerpo específico que reaccionó con la banda de ≤ 75 kDa detectada en el gel mediante Sypro Ruby.

La proteína HSPA8 se localiza en diversas fracciones celulares, incluyendo la membrana. No obstante, dado que se habían utilizado homogenados totales de las células SH-SY5Y, y a pesar de que precisamente en estas células se ha descrito la presencia de HSPA8 en la membrana celular, cabía la posibilidad de que la interacción entre la HSPA8 y el TLQP-21 fuese artefactual. Por ello se realizó un experimento para comprobar la unión de TLQP-21 a HSPA8 situado en la superficie celular. Concretamente, se suministró TLQP-21 biotinilado con un residuo extra de cisteína (Biotina-TLQPPSALRRRHYYHHALPPSRC) al medio de células SH-SY5Y vivas en presencia del reactivo de entrecruzamiento bifuncional Sulfo-N-[ϵ -maleimidocaproyloxy]succinimide ester (sulfo-EMCS). El reactivo entrecruzó el péptido y HSPA8 presente en la superficie de las células, como pudo comprobarse tras homogenizar las mismas, someter el homogenado a cromatografía de afinidad en una columna de avidina y finalmente identificar las proteínas adsorbidas mediante inmunodetección con un anticuerpo específico para HSPA8.

Como prueba adicional de que el TLQP-21 se une a un receptor (HSPA8) situado en la membrana de las células SH-SY5Y, se realizó un estudio mediante citometría de flujo (FACS). Se trataron células SH-SY5Y con TLQP-21 humano biotinilado, se utilizó a continuación avidina conjugada con fluoresceína, y se procedió a analizar las células mediante un equipo de citometría de flujo FACScalibur (Becton Dickinson, Estados Unidos). Se observó una fracción creciente de células “decoradas” con fluoresceína, mayor cuanto mayor fue la concentración de TLQP-21 utilizado.

Los resultados anteriores dieron lugar a una colaboración con Sandipan Chakraborty, investigador del departamento de Microbiología la Universidad de Calcuta experto en modelización molecular. Éste realizó un estudio de modelización de la unión y encaje (“docking”) del TLQP-21 humano a HSPA8, utilizando el programa GROMACS 4.5., cuyos resultados sugieren que el péptido encaja muy bien en la cavidad de esta proteína que sirve, precisamente, para unirse a péptidos. La modelización también predice que el péptido, que muestra una estructura desordenada en solución, según otro estudio de modelización previo (Chakraborty et al. 2015) adopta una estructura de hélice α . Igualmente, siempre según la modelización, se produce un elevado número de interacciones iónicas entre el péptido y la cavidad, siendo particularmente reseñables aquellas en las que participan los residuos R₁₀R₁₁ del péptido. La presencia de pares residuos consecutivos de arginina es una conocida característica de otros péptidos que se unen a HSPA8.

La HSPA8 pertenece a la familia de las proteínas de choque térmico (“heat shock proteins, HSPs”), si bien presenta características y particularidades que la hace un miembro muy especial de este grupo. Así, si bien realiza, como otras HSPs, funciones de chaperona, esto es, de asistencia al correcto plegamiento de determinadas proteínas y del mantenimiento del mismo (He et al., 2010), cada vez se van conociendo otras funciones específicas de esta proteína. Además, una característica fundamental de la HSPA8 es que se expresa de manera constitutiva, en contraste con la expresión inducible, particularmente por situaciones de estrés, de sus compañeras de grupo. Además, la HSPA8 es a menudo secretada en vesículas y exosomas (Clayton et al., 2005). Otras funciones importantes de la HSPA8 se relacionan con procesos de inmunidad, antigenicidad, hematopoyesis y autofagia (Stricher et al., 2013; Meimaridou et al., 2009).

Sin embargo, las funciones más interesantes de HSPA8, en el contexto de este trabajo, son aquellas en las que actúa, precisamente, como un receptor. Así, por ejemplo, su actuación como receptor del péptido P140. El P140 es un fosfopéptido artificial (análogo a otro natural) que se une a HSPA8, y que tiene un significativo efecto protector frente al lupus eritematoso (Page et al., 2009; Stricher et al., 2013). De hecho, dicho péptido está siendo sometido a un ensayo clínico de fase III como un posible agente terapéutico para esta enfermedad (Muller et al., 2008; Zimmer et al., 2013; Stricher et al., 2013). Experimentalmente, la unión del P140 a HSPA8 afecta el procesamiento de autoantígenos por parte de células presentadoras de antígenos del sistema inmunitario en el modelo murino de lupus eritematoso MLR/lpr (Page et al., 2011), induciendo una disminución de la señalización asociada a los mecanismos lisosomales. Por otra parte, el HSPA8 también actúa como receptor del virus HTLV-1, con la consiguiente formación de sincitios (Sagara et al., 1998). Por consiguiente, el papel del HSPA8 como receptor de superficie no es una novedad. Más específicamente, su papel como receptor del péptido P140 es de particular relevancia.

El HSPA8 contiene, de hecho, de un dominio de unión a péptidos (Wang, 1993), una característica que comparte con otros miembros de la familia de las HSPs, y más concretamente con la sub-familia HSP70, aunque cada miembro de la familia exhibe propiedades exclusivas y diversificadas de unión (Fourie et al., 1994). En este sentido, se ha visto que la afinidad del dominio de unión a péptidos del HSPA8 aumenta dramáticamente para péptidos que contienen las secuencias KK, KR, o RR (Takenaka et al., 1995). Cabe resaltar que el TLQP-21 humano contiene la secuencia R₉-R₁₀-R₁₁.

En una fase posterior del presente trabajo de investigación se llevaron a cabo dos estudios proteómicos preliminares cuyo objetivo fue comprobar que en nuestro sistema experimental (células SH-SY5Y), el péptido TLQP-21 humano no sólo se une a su

receptor (HSPA8) sino que además esta unión pone en marcha mecanismos moleculares que dan lugar a un efecto biológico; y por otro. Por otro lado, la identificación de alguno de estos efectos (en forma de cambios en la expresión de proteínas o fosfoproteínas) debería abrir la puerta a futuras investigaciones encaminadas a elucidar las rutas de señalización y los mecanismos moleculares mediante los que el TLQP-21 humano realiza sus funciones fisiológicas.

Así, se realizó un estudio proteómico comparativo de extractos de células SH-SY5Y tratadas y sin tratar con TLQP-21. Se separaron las proteínas mediante electroforesis 2D y se cuantificaron las intensidades de las docenas de manchas obtenidas tras teñirse los geles con Sypro Ruby. Mediante el programa Ludesi RedFin, se procedió a comparar las intensidades de 4 geles de muestra tratada con las de 4 geles de muestra control. Se identificaron varias manchas con intensidades diferentes. La identidad de las proteínas correspondientes a estas manchas fue desvelada mediante espectrometría de masas (MS/MS), tal y como se ha descrito para las bandas obtenidas tras SDS-PAGE de las fracciones eluidas de la columna de afinidad con TLQP-21, tras cortarse las áreas de los geles correspondientes a las mismas, y someter dichas muestras a reducción, alquilación y digestión tríplicas “en gel”. El análisis reveló una expresión diferencial de las proteínas: "Mediator of RNA polymerase II transcription, subunit 24"; "Adenylosuccinate synthetase isozyme 2"; "Spindle and kinetochore-associated protein 2"; "1-phosphatidylinositol 3-phosphate 5-kinase (type III PIP kinase)"; "Heat shock protein beta-1" y "Endothelial differentiation-related factor 1" (se indican los nombres en inglés por ser los habituales en la literatura).

En paralelo, y teniendo en cuenta la importancia de los procesos de fosforilación en las rutas de señalización, y aunque HSPA8 no es una quinasa o fosfatasa, se realizó un estudio fosfoproteómico elemental basado en la separación en una dimensión mediante SDS-PAGE de las proteínas correspondientes a muestras de células tratadas y no

tratadas con TLQP-21. Los geles fueron a continuación teñidos con el colorante Diamond Pro-Q, específico de proteínas fosforiladas. Se apreció la disminución de intensidad de 2 bandas correspondientes a proteínas con pesos moleculares aparentes de aproximadamente 55 y 220 kDa. Es intrigante que 220 kDa es precisamente, de forma aproximada, la masa molecular de la "type III PIP kinase", de modo que resulta tentador especular que la mancha de intensidad disminuida correspondiente a dicha quinasa detectada en el análisis proteómico podría quizá corresponder a una isoforma fosforilada, si bien de momento no hay datos experimentales suficientes que permitan llevar esto más allá de la mera especulación. En cualquier caso, será interesante realizar estudios adicionales para investigar esta posibilidad.

En resumen, se ha identificado la proteína de la familia de las chaperonas HSPA8 como un receptor del neuropéptido activo TLQP-21 y se ha comprobado, con células SH-SY5Y, que éste se une a aquella en el contexto de la superficie celular, y que esta unión da lugar a cambios sutiles en la expresión proteica y la fosforilación de determinadas proteínas. Estos estudios abren la posibilidad de buscar agonistas farmacológicos del HSPA8 que pudiesen tener efectos similares a los del TLQP-21, que podrían ser de gran utilidad como agentes para la prevención de la obesidad, entre otros muchos posibles efectos farmacológicos.

(**Nota:** Las referencias citadas pueden encontrarse en forma completa en la sección "**References**" de esta tesis).

VGF (non-acronymic) is a ~68 kDa neurosecretory protein, belongs to the extended granin family of proteins, initially identified as a nerve growth factor (NGF) inducible gene product, is selectively synthesised mostly in neuronal and neuroendocrine cells. Due to the presence of paired basic amino acid residues (R – Arginine, and K – Lysine), the VGF sequence undergoes endoproteolytic cleavage to produce several smaller peptides, released upon stimulation via the regulated secretory pathway both in vitro and in vivo. There are data suggesting that the VGF-derived peptides are the biologically active, stored in dense core vesicles and secreted in order to play a role in inter cellular communication, and responsible for the diverse range of biological functions associated with VGF. Several of these VGF-derived peptides have been characterised and are involved in energy balance, reproductive behaviour, pain modulation and mood order.

Till now, the best characterized VGF derived peptide is designated as TLQP-21. As growing data is accumulating on the several significant biological effects of TLQP-21 like energy balance, pain modulation, gastric, reproduction, stress, diabetes; identification of its receptor(s) is of particular relevance. In light of this extensive array of effects, the very limited knowledge about its molecular mechanisms of TLQP-21 is remarkable. Recently, C3AR1 and gC1qR have been reported as receptors of murine TLQP-21. However, human TLQP-21 whose sequence shows differences with respect to murine TLQP-21, exhibits at best very weak binding to these receptors, suggesting the existence of different receptors for human vs rodent TLQP-21.

Here using affinity chromatography and mass spectrometry-based protein identification, the heat shock cognate 71 kDa protein A8 (HSPA8) has been identified as a receptor of human TLQP-21. Binding of TLQP-21 to membrane associated HSPA8 in live SH-SY5Y cells was confirmed by cross-linking and FACS studies. Furthermore, molecular modeling studies show that TLQP-21 can be docked into the peptide binding pocket of

Summary

HSPA8. The major task moving forward is to elucidate the signaling pathways of the ligand TLQP-21 and its receptor HSPA8. Identification of HSPA8 as a receptor of human TLQP-21 could open new approaches for diagnostics and therapeutics for a wide range of human diseases related with VGF, in particular those in which TLQP-21 has been shown to have an effect.





Index



Index	23
Introduction	31
1. Structure of VGF	31
2. VGF derived peptides	32
3. Tissue distribution of VGF	37
4. Functions of VGF	39
4.1 <i>Regulation of energy homeostasis</i>	39
4.2 <i>Regulation of gastrointestinal function</i>	39
4.3 <i>Regulation of hormone, neurotrophin, and/or neurotransmitter release</i>	40
4.4 <i>Regulation of pain</i>	40
4.5 <i>Regulation of emotion/psychiatric disease</i>	41
4.6 <i>Regulation of sexual function</i>	43
4.7 <i>Regulation of body fluid homeostasis</i>	43
4.8 <i>Role of VGF as neuroprotective agent</i>	44
4.9 <i>VGF derived peptides as diagnostic tools and/or targets in drug discovery</i>	44
4.10 <i>Future perspective</i>	47
5. Significance of TLQP-21 as a bioactive VGF derived peptide	47
5.1 <i>TLQP-21: Feeding, energy balance, obesity and lipolysis</i>	48
5.2 <i>TLQP-21: To modulate pain</i>	50
5.3 <i>TLQP-21: Gastrointestinal function</i>	53
5.4 <i>TLQP-21: Its role in reproduction</i>	54
5.5 <i>TLQP-21 : Glucose metabolism and diabetes</i>	55
6. Receptor(s) for human vs rodent TLQP-21	55

6.1 <i>C3AR1 as a receptor of rodent TLQP-21</i>	56
6.2 <i>gC1qR as a receptor of rodent TLQP-21</i>	60
Objective	65
Materials and methods	69
1. TLQP-21	69
2. SH-SY5Y cell culture	69
3. Detection of a TLQP-21 receptor in SH-SY5Y cells using biotinylated TLQP-21 as a probe	70
3.1 <i>Peptide conjugation</i>	70
3.2 <i>MALDI-TOF mass spectrometry</i>	71
3.3 <i>Crosslinking</i>	71
3.4 <i>SDS-PAGE and Western blot analysis</i>	72
4. Avidin agarose affinity chromatography	72
4.1 <i>SDS-PAGE and SYPRO[®] Ruby protein gel stain</i>	76
4.2 <i>Protein identification</i>	76
4.3 <i>Western blot analysis of the samples obtained from monomeric avidin experiment</i>	78
5. Crosslinking of biotinylated TLQP-21 to SH-SY5Y surface membrane proteins	79
6. Fluorescence-activated cell sorting (FACS) analysis	80

7. Effect of Oxymatrine (OMTR), an inhibitor of HSPA8 expression, on binding of Biotin-TLQP-21 to the surface of intact, live SH-SY5Y cells	81
8. Phosphoprotein gel staining	82
9. Proteomic study	82
9.1 <i>Protein preparation and processing</i>	82
9.2 <i>Protein quantitation</i>	83
9.3 <i>Bi-dimensional (2-D) gel electrophoresis</i>	84
9.3.1 <i>Rehydration of IPG strips</i>	84
9.3.2 <i>Isoelectrofocusing (first dimension)</i>	85
9.3.3 <i>Equilibration</i>	86
9.3.4 <i>SDS-PAGE (second dimension)</i>	87
9.3.5 <i>Staining and scanning</i>	89
9.3.6 <i>Differential image analysis</i>	90
9.3.7 <i>Statistical analysis</i>	92
10. <i>Protein identification using mass spectrometric analysis</i>	93
Results	97
1. Crosslinking and detection of a TLQP-21 binding protein in SH-SY5Y cell homogenate	97
2. Identification of a receptor of human TLQP-21	103
3. Immunochemical validation of HSPA8	107

4. Binding of biotinylated TLQP-21 to HSPA8 on the SH-SY5Y membrane	108
5. Binding of biotin-TLQP-21 to the surface of intact, live SH-SY5Y cells: demonstration by FACS analysis	109
6. Oxymatrine, inhibitor of HSPA8, reduces binding of biotin-TLQP-21 to the surface of intact, live SH-SY5Y cells	113
7. C3AR1 not trapped by TLQP-21 affinity chromatography	125
8. Proteomic study	126
9. Preliminary phosphoproteomic study	129
Discussion	133
1. Identification of HSPA8 as a receptor of human TLQP-21	133
2. Binding of biotinylated TLQP-21 to HSPA8 on the SH-SY5Y membrane	136
3. Binding of biotin-TLQP-21 to the surface of intact, live SH-SY5Y cells: Demonstration by FACS analysis	136
4. OMTR down regulates the expression of HSPA8	137
5. Molecular dynamics study	138
6. HSPA8	139
6.1 <i>Distribution</i>	139
6.2 <i>Functions</i>	140
6.2.1 <i>HSPA8 signaling</i>	140
6.2.2 <i>Protein folding</i>	143
6.2.3 <i>Protein import</i>	144

6.2.4 <i>Immunity</i>	144
6.2.5 <i>Hematopoiesis</i>	144
6.2.6 <i>Autophagy</i>	145
6.3 <i>HSPA8 as receptor/binding partner</i>	145
6.4 <i>HSPs inducers</i>	148
6.5 <i>The HSP family of proteins</i>	153
7. Physiological relevance of the TLQP21- HSPA8 interaction	154
8. Recent identification of murine TLQP-21 receptors	157
9. Receptor(s) for human vs rodent TLQP-21	158
10. Downstream effects of human TLQP-21 binding to its receptor	160
11. Concluding remarks	161
12. Future prospective	162
Conclusions	165
References	169
Annex I. HPLC and MS analysis report of TLQP-21.	205
Annex II. Structural dynamics of TLQP-21 bound to the HSPA8 receptor binding site: Explored by molecular dynamics simulation.	211

Annex III. Probing the conformational dynamics of the bioactive peptide TLQP-21 in solution: A molecular dynamics study.	231
Annex IV. A study on the effect of TLQP-21 on ERK/AKT signaling in SH-SY5Y cells.	253
Annex V. A comparative study on the phosphoproteins and total proteins in TLQP-21 treated vs. control SH-SY5Y cells.	263
Annex VI. A study on the effect of TLQP-21 on the expression of Egr-2 and Grb-2 in SH-SY5Y cells.	271
Annex VII. List of abbreviations.	277





Introduction



VGF (a non-acronymic name) gene was originally identified as a nerve growth factor (NGF) responsive gene and should not be confused with VEGF (vascular endothelial growth factor). NGF33.1, a nervous system-specific mRNA was cloned by treatment of PC12 cells with NGF. After elucidating the nucleic acid as well as amino acid sequences of the NGF33.1 cDNA clone, Levi et al. (1985) designated this clone corresponding to the NGF-inducible mRNA as VGF. The term 'VGF' derived from the selection of this clone from plate **V** of the nerve **G**rowth **F**actor induced PC12 cell cDNA library (Levi et al., 1985; Possenti et al., 1989). Indeed, in response to NGF treatment, VGF was independently identified by several groups using differential hybridization techniques (Cho et al., 1989; Levi et al., 1985; Salton et al., 1991).

Structure of VGF:

The human and mouse VGF genes are located on chromosome 7q22.1 and 5 (Hahm et al., 1999; Canu et al., 1997a; Canu et al., 1997b) and encode a 615 amino acid (human) and 617 amino acid (rat), respectively (Levi et al, 1985). VGF is a single copy gene (Canu et al., 1997a) and is simply organized as depicted in Figure 1 and 2. It is composed of 3 exons but the complete VGF protein is encoded by exon 3 only while two introns interrupt the region encoding the 5' untranslated sequence of VGF (Hahm et al., 1999). C-terminal peptide regions encode a number of bioactive peptides. As depicted in Table 1, VGF is a proline, and glycine rich and acidic polypeptide. Although there are evolutionary conservation of other invertebrate granins (a family of proteins comprising chromogranins, secretogranins and some other related proteins (Bartolomucci et al., 2011) found in the secretory granules of endocrine, neuroendocrine cells and neurons (Deftos et al., 1986; Fischer-Colbrie et al., 1987), that function to control the supply of neurotransmitters, hormones, growth factors and peptides (Bartolomucci et al., 2011); no invertebrate VGF proteins have been identified so far. And several regions of high

sequence conservation were found in both lower and higher vertebrate VGF proteins (Figure 3).

Table 1: Introductory informations on VGF, at a glance. (Number of amino acids (AA) and calculated molecular mass (MM) of the preprotein, number of amino acids and calculated molecular mass of the mature protein, observed molecular mass of the mature protein, number of dibasic sites, number/content of proline, number/content of glutamate, calculated (calc) and observed (obs) pI, and secondary structure (percent - helix) are shown for human (h), ND, not determined. From Bartolomucci et al., 2011).

	Preprotein		Mature protein			Dibasic sites ^h	AA/% proline ^h	AA/% glutamate ^h	pI calc ^h /obs	% α -Helix ^h
	AA ^h	Calculated MM ^h (kDa)	AA ^h	Calculated MM ^h (kDa)	Observed MM (kDa)					
VGF	615	67	593	65	90 ^h	10	77/12.5	97/15.8	4.5/ND	39

VGF derived peptides:

In human, rat, mouse and chimpanzee (Hahm et al., 1999; Canu et al., 1997a; Possenti et al., 1989), VGF protein possesses ten (Levi et al., 2004) paired basic amino acid residues (as illustrated in the Figure 3) having potential cleavage sites for the best characterized mammalian prohormone processing enzymes, prohormone convertases (PCs), members of the family of subtilisin/kexin-like serine proteinases (Seidah and Chretien, 1999; Steiner, 1998). For example, TLQP-62 is produced by PC1/3, while NAPP-129 has been produced by the action of either PC1/3 or PC2 (Trani et al., 2002). N-terminal VGF peptides (human) are not compatible with known motifs required for PCs. So some VGF peptides must be generated by other yet unidentified endoproteases. As mentioned earlier, in rat, mouse and human VGF protein comprises at least 10 basic amino acid residues susceptible to potential PC cleavage. Hence the number of known VGF derived peptides is likely to increase further. To understand the contributions of 'such a variety of VGF peptides' individually as well as their mode of action has now become a big challenge.

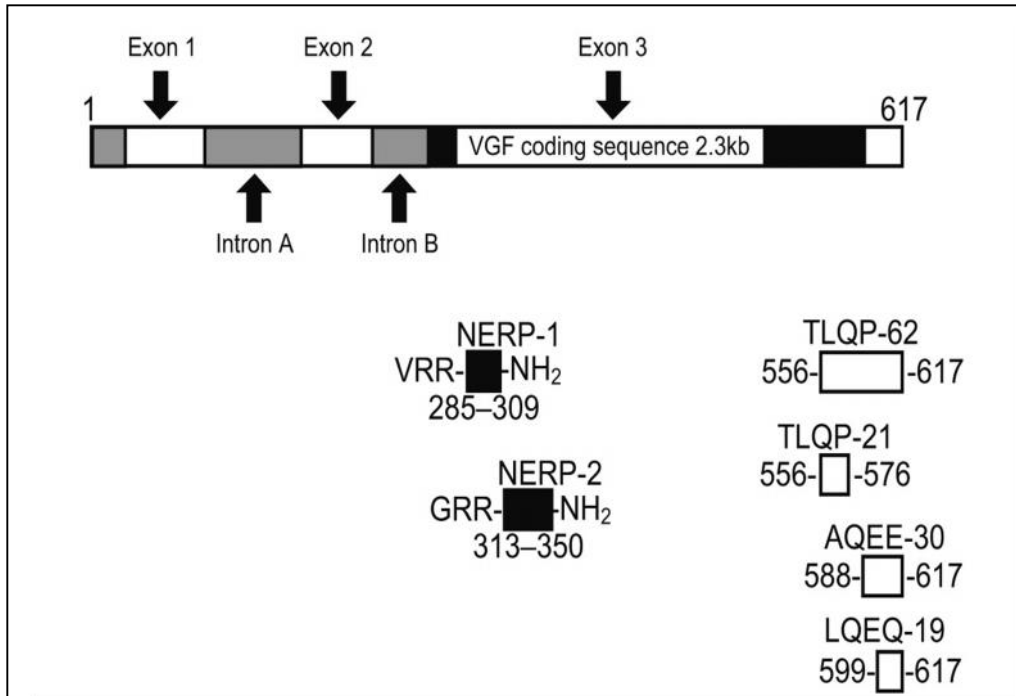


Figure 1: Schematic diagram of the VGF gene and its derived peptides (mouse). The numbers correspond to the positions of amino acid residues in mouse VGF protein. The closed black boxes represent neuroendocrine regulatory peptides (NERPs): NERP-1 and NERP-2 and the rest of the boxes represent other peptides: TLQP-62, TLQP-21, AQEE-30 and LQEQ-19. (From Toshinai and Nakazato, 2009).

VGF in PC12 cells appears as a doublet of 80–90 kDa when analysed by Western Blot though its calculated molecular weight is 68 kDa. The lower band was confirmed to be generated from the upper, probably due to limited proteolysis, providing that no post-translational modification occurred (Levi et al., 1985). Finally it was concluded that the

very high proline content accounts for the lower than expected electrophoretic mobility of the protein. In addition to a doublet of 80–90 kDa, several smaller peptides were identified in rat brain homogenates, neuronal, endocrine and pancreatic beta cell lines, in extracts of primary cultures of cerebellar granule cells in response to the antibodies raised against the C-terminal nonapeptide of rat VGF protein (Possenti et al., 1999; Trani et al., 1995). Several VGF peptides were revealed out in rat brain homogenates by mass spectroscopy followed by affinity purification with C-terminal antiserum, in addition to more lower molecular-weight peptides detected by Western Blot Analysis (Trani et al., 2002).



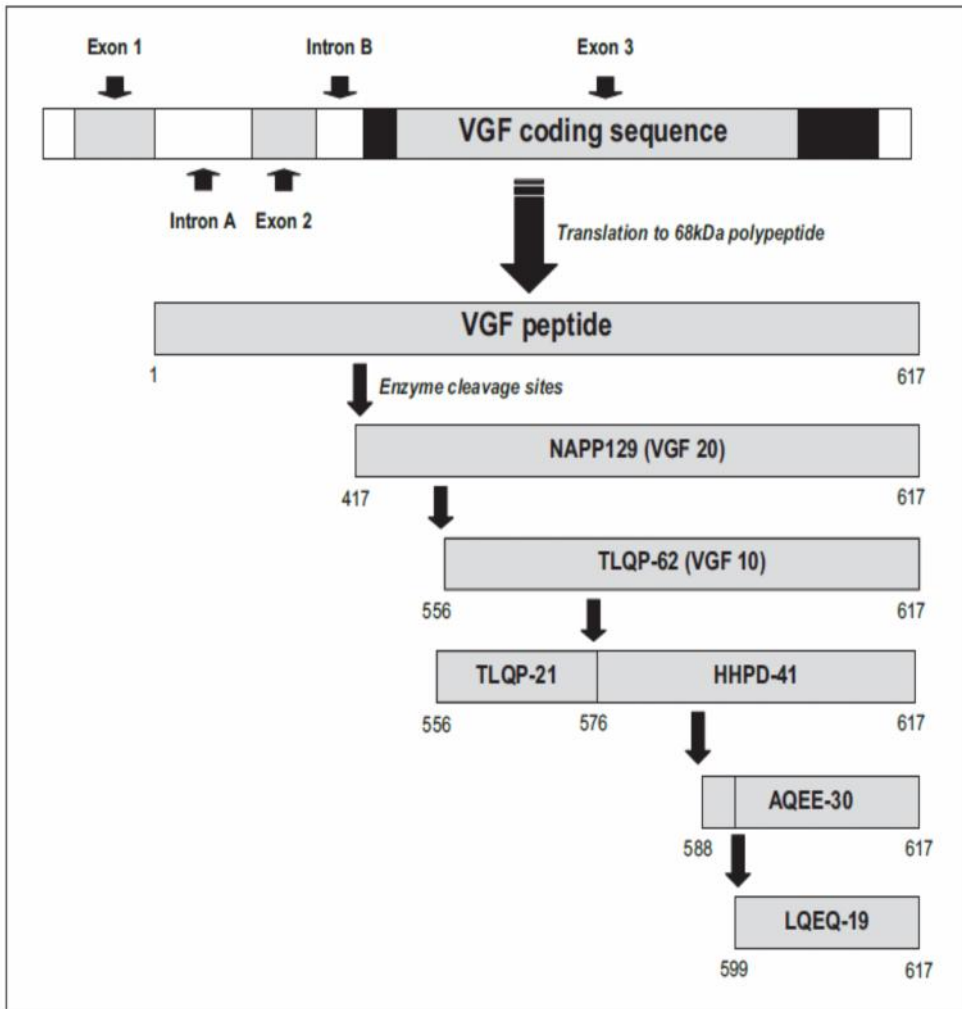


Figure 2: Schematic diagram of the VGF gene and its derived peptides (mouse). VGF gene with its simple structure encodes a 617-amino acid protein in rats, and a 615-amino acid protein in humans, subjected to cleavage into several peptides. Two introns interrupt the region encoding the 5' untranslated sequence of VGF, and the entire VGF protein is encoded by exon 3. Most of the fragments are capable to show biological activity, indicated in Table 2 (From Jethwa and Ebling, 2008).

Table 2: A listing of VGF derived peptides. Nomenclature of the peptides was simplified by the first four amino acids and by its length, such as: TLQP-21 and TLQP-62 are two peptides with TLQP (Thr-Leu-Gln-Pro, respectively) sequences at N-terminus with total length 21 and 62 amino acids, respectively except the neuroendocrine regulatory peptides, NERPs (an acronym for neuroendocrine regulatory peptides) and VGF 20 (20 kDa, based on the apparent molecular weights observed by Western blot analysis). (Adapted from Jethwa and Ebling, 2008).

Peptide names	Amino acid position on VGF precursor	Length	Biological activity known?
APPG-40	23-62	40	No
APPG-37	23-59	37	No
GRPE-37	26-62	37	No
NERP-1	302-309	8	Yes
NERP-2	341-350	10	Yes
NAPP-129 (VGF 20)	417-617	201	No
VGF 18	Unknown	---	No
TLQP-62 (VGF 10)	556-617	62	Yes
HFHH-51 (VGF 6)	567-617	51	No
HHPD-41	576-617	41	No
AQEE-30 (Peptide V)	588-617	30	Yes
LQEQ-19	599-617	19	Yes
<u>TLQP-21</u>	556-576	21	Yes

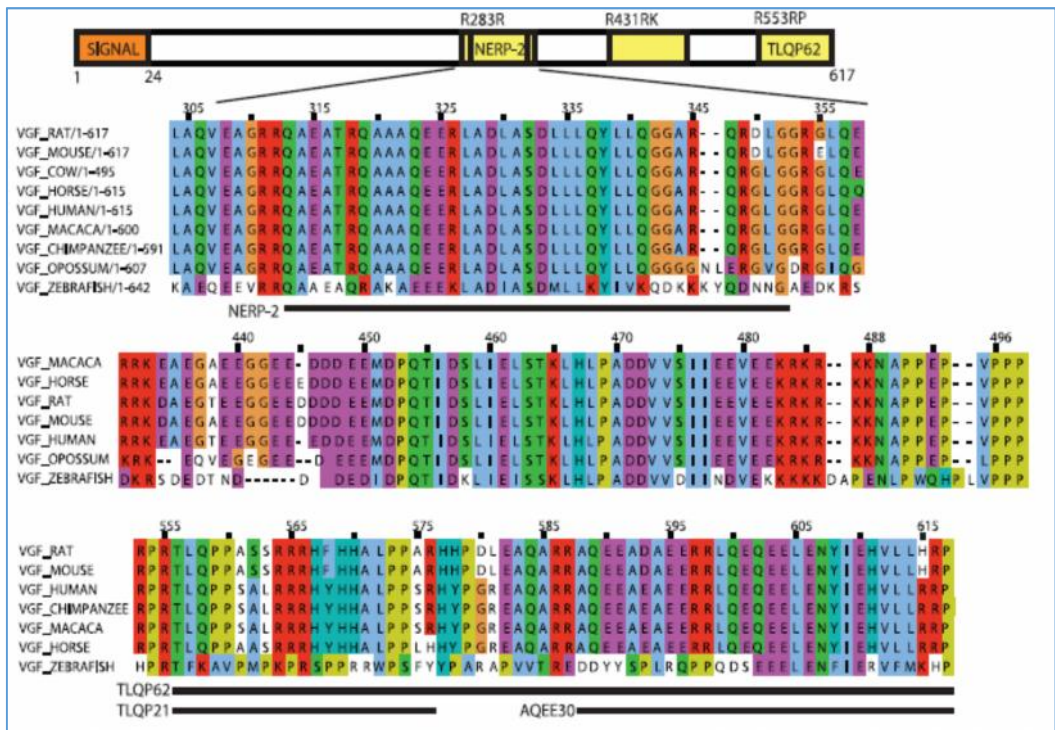


Figure 3: Evolutionary conservation of VGF. Each of the three highly conserved regions of VGF: NERP-2, TLQP and AQEE peptides, are conserved in both higher and lower vertebrates (From Bartolomucci et al., 2011).

Tissue distribution of VGF:

VGF mRNA is expressed in the main and accessory olfactory bulbs, hippocampus, cortex, basal ganglia, thalamus, amygdala, midbrain and the brainstem, with the highest expression in neurons in the hypothalamus and in the granular layer of the cerebellum (van den Pol et al., 1989; 1994; Snyder et al., 1997; 1998). After birth, rats express VGF throughout brain (in neurons exclusively), and in peripheral endocrine and neuroendocrine tissues (Snyder et al., 1998). Later on in the adult rat brain, VGF mRNA

becomes widely distributed in the spinal cord, olfactory system, cerebral cortex, hypothalamus, and hippocampus, and also in thalamic, septal, amygdaloid, and brain stem nuclei (Snyder et al., 1998; van den Pol et al., 1989; 1994). Before birth, rats express VGF at first on embryonic day 11.5 in the dorsal root and sympathetic ganglia, neural crest cells migrating to enteric ganglia and in primordia of the vagal (X) complex (Snyder et al., 1998). VGF mRNA continues to be expressed in the ventral spinal cord, cranial nuclei, basal forebrain, adrenal and pituitary in between of embryonic day 13.5 to 15.5. Later in embryogenesis, VGF expression starts to additional CNS sites as well as becomes prevalent in the esophagus, stomach (both in endocrine cells and myenteric plexus), and pancreas in between of embryonic day 17.5 to 19.5). High expression of VGF mRNA was evident in oligodendrocyte precursors though it was found to disappear following differentiation (Dugas et al., 2006; Cheishvili et al., 2007). VGF derived peptides were also found to be expressed in peripheral leukocytes (Cattaneo et al., 2010) and glial fibrillary acidic (GFA) protein-expressing astrocytes of the spinal cord in transgenic mutant SOD1G93A mice. In the spinal cords of sporadic amyotrophic lateral sclerosis (ALS) patients, VGF expression was found low in comparison to control patients. A small molecule, SUN N8075 was capable to slow down disease progression in SOD1 mouse and rat models of ALS, resisting the lowering of VGF level in the spinal cords of ALS mice (Shimazawa et al., 2010). However, further investigation regarding the unexpected localization of VGF may point out towards unexpected functional roles. To summarize, VGF is synthesized by neurons in the CNS and PNS, as well as in the adult pituitary, adrenal medulla, endocrine cells of the stomach and pancreatic beta cells, moreover, VGF mRNA is obvious at embryonic day 11.5 in the rat dorsal root and sympathetic ganglia (Snyder et al., 2003).

All these informations regarding tissue specific expression and distribution of VGF suggest that VGF has different roles in the concerned tissues.

Functions of VGF:*Regulation of energy homeostasis:*

Studies on VGF knockout mice demonstrated that they were hyperactive, hypermetabolic, lean, and small with less abdominal fat (Hahm et al., 1999). VGF derived peptide, TLQP-21 was found to decrease food intake and to rise energy expenditure in Siberian hamsters (Jethwa et al., 2007). Also in mice fed high-fat diet (HFD) for 14 days, TLQP-21 decreased body weight and white adipose tissue (WAT) blocking hormonal changes associated with HFD and provoking the autonomic activation of the adrenal medulla and adipose tissue. Furthermore, intracerebroventricular (icv) administration of TLQP-21 reduced early phase diet induced obesity (Bartolomucci, et al., 2006). Thus, VGF derived peptide TLQP-21 shows catabolic activity (Jethwa et al., 2007; Bartolomucci et al., 2006) whereas VGF knockout mice demonstrated the opposite trend (Hahm et al., 1999). The hypothesis to explain this inconsistency could be: one or more VGF derived peptides possess opposite biological roles with respect to TLQP-21. There are evidences that upkeep the hypothesis: administration of TLQP-62, HHPD-41 increased food intake in fasting mice (Bartolomucci et al., 2007). While, NERP-2 icv administration to rats and mice increased food intake, body temperature, O₂ consumption, locomotor activity promptly (Yamaguchi et al., 2007; Toshinai and Nakazato, 2009; Toshinai et al., 2010).

Regulation of gastrointestinal function:

There are evidences suggestive of the central role of TLQP-21 in intermediating gastroenteric functions by the initiation of prostaglandin (PG) synthesis. Icv, but not intraperitoneal (ip), or intravenous (iv) injection of TLQP-21 inhibited gastric emptying almost ~40% in a time (Severini et al., 2009) as well as dose dependent manner and

reduced ethanol induced gastric lesions in rats through nitric oxide synthase and PG E₂. It also reduced gastric acid secretion through somatostatin and PG (Sibilia et al., 2010a; 2010b). The peptide also induced contraction of gastric fundic strips ex vivo by PG mucosal release (Severini, et al., 2009).

Regulation of hormone, neurotrophin, and/or neurotransmitter release:

TLQP-62, in hippocampal slices, provoked electrical potentiation that was found to be blocked by the brain-derived neurotrophic factor (BDNF) scavenger TrkB-Fc, Trk tyrosine kinase inhibitor K252a, and tissue plasminogen activator STOP (Bozdagi et al., 2008), pointing out the probable role of TLQP-62 in inducing release of BDNF in the hippocampus and other regions of CNS. The BDNF-receptor, TrkB, is progressively activated in vitro by TLQP-62 to initiate the TLQP-62 induced proliferation of neural progenitor cells (NPCs) (Thakker-Varia et al., 2014) in consistent with the upregulation of VGF protein by BDNF treatment (Alder et al., 2003). Accordingly, AQEE-30 and LQEQ-19 upregulate phosphorylation of MAPK p³⁸ in microglia (Riedl et al., 2009) in nociceptive signaling with the probable induction of BDNF (Coull et al., 2005). Another VGF derived peptide, neuroendocrine regulatory peptide (NERP) increased food intake in mice through the activation of an orexin dependent mechanism indicating that NERP induces the release of neuropeptide orexin in hypothalamus (Toshinai K et al., 2010).

Regulation of pain:

In the first study highlighting the role of TLQP-21 in pain modulation , the forepaw-injected formalin test confirmed the induction of analgesic effect by TLQP-21, additionally it was established that the inflammatory modulatory effects of TLQP-21 depend on the route of administration : being pronociceptive at the periphery and

antinociceptive at the central level (Rizzi et al., 2008). TLQP-21 has been found to provoke a hyperalgesic response when it was subcutaneously injected into the hind paw of mice. Mechanical hypersensitivity was apparent in rat following inoculation of TLQP-21-stimulated macrophages into rat hind paw and intracellular Ca^{2+} levels in macrophages was lessened via siRNA suggesting that TLQP-21 plays an important role in inducing hepergesia/hepersensitivity/chronic pain through activation of macrophages (Chen et al., 2013). Moreover, in vivo, long-lasting mechanical and cold behavioural allodynia (pain produced by stimuli which usually do not provoke pain (Merskey and Bogduk, 1994) like temperature, cold or physical stimuli (Hooshmand and Hooshang, 1993) was persuaded by TLQP-62 (Moss et al., 2008). AQEE-30 and LQEQ-19 caused hyperalgesia via microglial p38 MAPK activation (Riedl et al., 2009). To sum up, both the short and long VGF derived peptides like LQEQ-19 (Riedl et al., 2009), TLQP-21 (Fairbanks et al., 2014; Chen et al, 2013; Rizzi et al., 2008), AQEE-30 (Riedl et al., 2009), TLQP-62 (Moss et al., 2008) were found to be responsible for the consistent induction of analgesia/hyperalgesia/hepersensitivity/chronic pain in diverse models of pain.

Regulation of emotion/psychiatric disease:

Probably out of the granin family members, VGF has been the most explored for its role as well as mechanism in emotional behavior and psychiatric disease (Bartolomucci et al., 2011), while there are very few data suggesting the role of other granin family members like secretogranin II (SgII)-derived peptides GE19, GAIPIRR and SN (secretoneurin) in emotional behavior (Wakonigg et al., 2002). Since the time period when VGF mRNA was found in the hippocampal areas, VGF was thought to play a crucial role in this area (Snyder and Salton, 1998) which was later confirmed.

VGF has antidepressant-like actions in rodents (Hunsberger et al., 2007, Thakker-Varia et al., 2007; 2010). For the last two decades, this VGF peptide is getting more importance due to the unveiling of its role as an anti-depressant. VGF^{+/-} mice exhibit deficits in experimental paradigms of depression (Hunsberger et al., 2007). VGF mRNA extensively co-localizes throughout the central nervous system (CNS) with mRNA encoding brain derived neurotrophic factor (BDNF) and the BDNF receptor, TrkB (Snyder et al., 1997), suggesting that VGF could potentially mediate some of the behavioral and electrophysiological actions ascribed to BDNF signalling. BDNF is a central player in the “adult neurogenesis theory of depression” (Gilhooley et al., 2010). Recently, using a proteomic approach, VGF was found to be one of the proteins whose expression more conspicuously decreased as a result of ShRNA-based DISC1 (Disrupted-in-schizophrenia 1, one of the very few genes directly correlated with psychiatric illness and was co-segregated with schizophrenia, bipolar disorder and major depression in a large Scottish pedigree (Chubb et al., 2008) silencing in human SH-SY5Y neuroblastoma cells. Subsequently, this result was confirmed by means of Western blot analysis in the same cells and in ShRNA-silenced murine primary neurons (Ramos et al., 2014). In this context, the finding that silencing of DISC1 causes a marked decrease of expression of VGF, a protein that is so critically involved in depression, bipolar disorder, and schizophrenia, is of particular relevance. Further, a recent study found that NPAS3, a transcription factor that is a replicated genetic risk factor for psychiatric disorders, regulates VGF (Sha et al., 2012). Therefore, three independent proteins with strong associations with mental disease, DISC1, NPAS3 and BDNF, seem to have VGF as a downstream effector, making VGF, and more specifically, the putative receptor of VGF-derived peptides, a very attractive target of pharmacological intervention to develop new drugs effective in the treatment of mental diseases. Though till to date, VGF derived peptide TLQP-62 (Lin et al., 2014; Bozdagi et al., 2008) has been found to be linked up with mental depression, etc., not TLQP-21.

Regulation of sexual function:

In consistent with both male and female infertility observed in VGF knockout mice (Hahm et al., 1999; 2002), following repeated administration of TLQP-21 on adolescent males with chronic food deprivation the gonadotrophin response of hypothalamic-pituitary-gonadal axis was reduced. However, in case of properly nourished fed mice, only puberty onset was late (Pinilla et al., 2011). Other VGF derived peptides namely AQEE-11, LQEQ-19, AQEE-30 and HHPD-41 were found to facilitate penile erection capability in rats via the mechanism of nitric oxide production in the paraventricular nucleus (PVN) followed by the activation of PVN oxytocinergic neurons (Succu et al., 2004; 2005).

Regulation of body fluid homeostasis:

With the aid of immunogold electron microscopy, neuroendocrine regulatory peptides (NERPs) colocalization was confirmed with vasopressin in storage granules (Toshinai and Nakazato, 2009). VGF mRNA in rats was found to be upregulated as a consequence of water deprivation, in consistent with the upregulation of the vasopressin mRNA. VGF mRNA was also increased with vasopressin mRNA level following salt inoculation into the brain of rats (Mahata, et al., 1993). Icv inoculation of hypertonic NaCl stimulated vasopressin release while inoculation with NERP-1 and 2 inhibited the NaCl induced vasopressin release. Moreover, NERP antibodies were found to reduce plasma vasopressin following water loading (Yamaguchi et al., 2007). All these data including in vivo and immunocytochemical observations suggest the possible roles of VGF derived peptides, NERPs in modulation of the central body fluid balance.

Role of VGF as neuroprotective agent:

TLQP-21 was found to protect the cerebellar granule cells (CGCs) dose-dependently in rats which (CGCs) were supposed to go through cell death due the serum and potassium deprivation via the modulation of extracellular signal-regulated kinase1/2, ERK1/2 and by the enhancement of intracellular Ca^{2+} release (Severini, C. et al, 2008). SUN N8075, an inducer of VGF mRNA, protected cells from ER stress induced cell death. But its protective mechanism was entirely diminished by VGF knockdown with siRNA validating that the protective effect of SUN N8075 is mediated by VGF. VGF level was found to be lower in the spinal cords of sporadic ALS patients. This inducer was also found to slow the disease progress in the mutant SOD1 animal models of familial ALS and thus elongating the survival of the animals (Shimazawa et al., 2010). From all these findings, the involvement of SUN N8075/ VGF, either unconnectedly or concurrently, in progression of ALS can be speculated, and either or both of them may become a potential therapeutic candidate for treatment of ALS.

VGF derived peptides as diagnostic tools and/or targets in drug discovery:

It has already become evident that VGF derived peptides are produced at altered levels in different disease conditions. VGF expression is down regulated in the brains of rodents subjected to animal depression paradigms (Thakker-Varia et al., 2007). VGF is also reduced in postmortem brain of patients with bipolar disorder and contributes to some of the behavioral and molecular effects of lithium, the canonical drug used to treat this disorder (Thakker-Varia et al., 2010).

Data referring to expression of VGF in schizophrenia are conflicting: one study reported increased VGF expression in prefrontal cortex of four brains from schizophrenic

patients, and an increased concentration of in CSF of a 40-amino acid VGF-derived peptide, VGF 23–62, in CSF of first-onset, drug-naïve schizophrenia patients and, to a lesser degree, in patients with depression. Interestingly, a VGF 26–62 peptide with an identical sequence to the VGF 23–62 peptide, except for the first three amino-terminal amino acids, did not appear to be differentially expressed in CSF from schizophrenia or depression patients compared to healthy volunteers, in the same study (Huang et al. 2006). On the other hand, results from the Stanley Medical Research Institute Genomics Database showed decreased VGF in prefrontal cortices of schizophrenia and bipolar disorder patients (Thakker-Varia et al., 2010). More recently, a reduced density of hypothalamic VGF-immunoreactive neurons was detected in post-mortem brains from patients with schizophrenia as compared to control subjects (Busse et al., 2012). All these strongly suggest that VGF does play an important role in the development of schizophrenia.

Like schizophrenia, VGF derived peptides are also related to some other diseases as summarized in Table 3.

Table 3: VGF derived peptides linked to diseases in humans and animals, at a glance. (Bartolomucci et al., 2010).

Disease	Peptide/fragment aa residue (species)	Effect	Stage	Reference
Neurological disease				
Alzheimer's disease	378–397 (human) Fragment not specified (human)	Decreased in patient's CSF Decreased in patient's CSF	Identified as potential biomarker Identified as potential biomarker	Carrette et al., 2003 Simonsen et al., 2007
Amyotrophic lateral sclerosis	308–411 (human) Entire pro-peptide (human) Entire pro-peptide (mouse)	Decreased in patient's CSF Decreased in patient's CSF Decreased in CSF, serum and motor neurons	Identified as potential biomarker Identified as potential biomarker Pre-clinical	Pasinetti et al., 2006 Zhao et al., 2008
Frontotemporal dementia	26–62 (human)	Decreased in patient's CSF	Identified as potential biomarker	Ruetschi et al., 2005
Pain	TLQP-21 556–576 (mouse) TLQP-62 556–617 (mouse, rat) AQEE-30 588–617 (mouse, rat) LQEQ-19 598–617 (mouse, rat)	Hyperalgesia (peripheral) analgesia (icv) Allodynia Hyperalgesia Hyperalgesia	Pre-clinical Pre-clinical Pre-clinical Pre-clinical	Rizzi et al., 2008 Moss et al., 2008 Riedi et al., 2009 Riedi et al., 2009
Psychiatric disease				
Schizophrenia/depression	23–62 (human)	Increased in patient's CSF	Identified as potential biomarker	Huang et al., 2006, 2007
Depression	TLQP-62 556–617 (mouse, rat)	Antidepressant-like effect	Pre-clinical	Thakker-Varia et al., 2007
Depression/anxiety	AQEE-30 588–617 (mouse, rat)	Antidepressant- and anxiolytic-like effects	Pre-clinical	Hunsberger et al., 2007
Other disease				
Obesity/eating disorders	TLQP-21 556–576 (mouse, hamster) NERP2 313–350 (rat) TLQP-62 and HHPD-41 556–617 and 577–617 (mouse)	Limits diet induced obesity (mice, hamster) anorexia (hamster) Enhance food intake in an orexin-dependent manner Enhanced food intake	Pre-clinical Pre-clinical Pre-clinical	Bartolomucci et al., 2006; Jethwa et al., 2007 Toshina et al., in press Unpublished, referred to by Bartolomucci et al., 2007

The number of diseases for which VGF-derived peptides have already been proved or are being investigated to act as disease biomarkers are increasing day by day. Some of them are namely breast cancer, gastroenteric tumors, insulinoma, lung tumors, medullary thyroid carcinoma, neuroblastoma, ganglioneuroma, parathyroid adenoma, pheochromocytoma, pituitary carcinoma, fronto-temporal dementia (FTD), schizophrenia (SCZ), major depressive disorder (MDD), alzheimer's disease (AD), Amyotrophic lateral sclerosis (ALS) (Bartolomucci et al., 2011). Though the number of experimental proofs are increasing day by day to recommend VGF derived peptides for widespread clinical use, not yet enough data confirmed the clinical utility of the VGF derived peptides as 'surrogate endpoints' for diseases, especially for life threatening, extensively prevalent neurological, psychiatric disorders (Bartolomucci et al., 2010). It

should be noted that it took forty five years for the first granin protein, chromogranin A (CgA) to be used as a biomarker for neuroendocrine tumors (Harsha et al., 2009).

Future perspective:

Biological activities of a number of VGF derived peptides as well as their diverse tissue specific distribution and their corresponding multi-functional roles have already been elucidated with experimental evidences, as described earlier. What is now left and of utmost important in the field of VGF is complete elucidation of physiologically important receptors/binding proteins/partners with further characterization of receptor-dependent and/or receptor-independent signaling pathways.

Significance of TLQP-21 as a bioactive VGF derived peptide:

Out of several bioactive peptides derived from VGF, TLQP-21 is of great importance because of its many physiological roles, some of which have already been mentioned in the previous sections in which a general overview of VGF was provided. In the following sections, the specific significance of TLQP-21 will be discussed. Thus, TLQP-21 plays a key role in energy expenditure (Possenti et al., 2012; Jethwa et al., 2007; Bartolomucci et al., 2006), metabolic functions (Bartolomucci et al., 2008), lipolysis (Possenti et al., 2012), glucose-stimulated insulin secretion (GSIS) (Stephens et al., 2012), nociception (Fairbanks et al., 2014; Chen et al., 2013; Rizzi et al., 2008), blood pressure/hypertension regulation (Fargali et al., 2014), gastric contractility (Severini et al., 2009; Bartolomucci et al., 2008), regulation of gastric acid secretion (Sibilia et al., 2012; Sibilia et al., 2010a; 2010b) reproduction (Aguilar et al., 2013; Pinilla et al., 2011), stress (Razzoli et al., 2012, Bartolomucci et al., 2011), neuroprotective agent (Severini et al., 2008), anorexia (Bartolomucci et al., 2006; Jethwa et al., 2007).

TLQP-21 was the first identified VGF-derived peptide involved in energy homeostasis (though the first identified VGF-derived peptide was AQEE-30 (Liu et al., 1994) which added a new aspect to the study of energy homeostasis and nutrigenomics (Kaput et al., 2006; Bartolomucci et al., 2007) as previously several findings identified some other different genes contributing in energy homeostasis (Cederberg et al., 2001; Obici et al., 2003; Riu et al., 2003; Zhang et al., 2005; Netea et al., 2006).

Growing biological significant effects of TLQP-21 has reached momentum:

TLQP-21: Feeding, energy balance, obesity and lypolysis:

TLQP-21 increased energy expenditure (as mentioned earlier) along with elevation of rectal temperature, serum epinephrine but with decrease of norepinephrine levels accompanied by no fluctuation in the level of free T₃ and free T₄ serum levels, in addition, no change was evident in locomotor activity (Bartolomucci et al., 2006; 2009). Moreover, catabolic markers like peroxisome proliferator-activated receptor α , β -adrenergic receptor and uncoupling protein 1 (UCP1) mRNA in white adipose tissue (WAT) were upregulated by TLQP-21 while hypothalamic mRNA encoded metabolically active hypothalamic peptides and hematological biomarkers were unchanged (Bartolomucci et al., 2006; 2007). TLQP-21 was found to increase FFA/TG (free fatty acids/ triglycerides) ratio as TLQP-21 down regulated the level of TG keeping FFA consistent. Glucose level after TLQP-21 treatment was found unaffected while there was non-significant reduction of leptin level and WAT (Bartolomucci et al., 2007). Jethwa et al., 2007 also validated the similar findings like Bartolomucci et al., 2006; 2007; 2009 confirming that TLQP-21 confers catabolic effects decreasing bodyweight and adipose fat mass. To sum up, the effects of TLQP-21 on energy balance has been characterized but receptor mediated TLQP-21 effects have not yet been well characterized, and findings on the mechanism of action of TLQP-21 in this regard is yet

to be clarified (Cassina et al., 2013). However, it has been validated that TLQP-21 induced energy expenditure follows the same mechanism of action of CNS constitutive COX-2 (cyclooxygenase-2) stimulation and gastric PG (prostaglandin) production (Sibilia et al., 2010b) : the effect of TLQP-21 induced gastric fundus strips contraction was prevented by COX inhibitors, indomethacine and naproxen and by PG receptor antagonists, PGF₂ dimethyl-amide and SC-19220. Presence of PGs (PGF₂, PGD₂ and PG E₂) were additionally confirmed in the medium after incubation of rat fundus dissections and TLQP-21. PGs, specially, PG E₂ has been found to induce energy expenditure (Amir and Schiavetto, 1990; Heleniak and Aston, 1989; Konsman et al., 2002). α -adrenergic (AR) stimulation also controls energy expenditure (Jimenez et al., 2002; Larsen et al., 2002; Bachman et al., 2002). In consistent with the α -adrenergic (AR) controlled energy expenditure, α -2 AR expression in brown adipose tissue (BAT) and α -3 AR in white adipose tissue (WAT) were increased by TLQP-21 (Bartolomucci et al., 2007). TLQP-21 induced upregulation of PPAR- α expression (Bartolomucci et al., 2007) also contributes in energy expenditure by fatty acid oxidation and energy uncoupling in WAT (Wang et al., 2003; Evans et al., 2004; Cannon and Nedegaard., 2004). Overall, TLQP-21 increses energy expenditure through the induction of central PG, peripheral adrenomedullary activities and catabolic activities of adipose tissue. Accordingly, by virtue of these effects of the peptide (as mentioned above), it also controls weight gain, obesity and lipolysis (see below), given that all the effects relating to energy balance and obesity were found in rodents using TLQP-21 of rodent version.

Due to the increasing spread of obesity problem, especially in industrialized countries (Cassina et al., 2013), the role of TLQP-21 in preventing obesity (Jethwa et al., 2007; Bartolomucci et al., 2006) and decreasing adipocyte diameter (Possenti et al., 2012) is getting utmost importance. In highly fed TLQP-21 mice, serum leptin increased while ghrelin was found to decrease along with keeping endocrine biomarkers steady

(Bartolomucci et al., 2007). TLQP-21-induced increase of energy expenditure, temperature and adipose tissue catabolic mediators is compatible with the preventing of obesity and adiposity (Lowell and Spiegelman, 2000; Lowell and Flier, 1997; Schwartz et al., 2000). TLQP-21 induced upregulation of AR stimulation and PPAR-expression (Bartolomucci et al., 2007) contributes in preventing obesity and fatty acid oxidation (Wang et al., 2003; Evans et al., 2004; Cannon and Nedegaard, 2004). It has been validated that TLQP-21 plays role in lipolysis (Hannedouche et al., 2013) , later on, confirming it in 2014 by Cero et al. though the mechanism is yet to be more clarified. To sum up, TLQP-21 confers its role in energy expenditure, obesity and adiposity through the stimulation of autonomic nervous system by central PG induction, peripheral adrenomedullary actions and catabolism of adipose tissue (Bartolomucci et al., 2007).

Due to the identification of TLQP-21 as the first metabolically active VGF peptide (Bartolomucci, et al., 2006), this peptide is now being considered as a key regulator of energy balance, obesity and lipolysis. Key challenge is now ahead to clarify its mechanisms of action in details targeting to develop metabolically active drugs.

TLQP-21: To modulate pain:

TLQP-21 is a modulatory peptide for pain (Fairbanks et al., 2014; Chen et al., 2013, Rizzi et al., 2008). The role of this peptide in pain modulation was confirmed by formalin tests in two phases: in the first phase, there is local response because of direct chemical stimulation of nociceptors that lasts for 5-10 minutes following the formalin injection. This early phase results in nociceptor activation suggesting that formalin prompts actions in C-fibers, not in A afferents (Porro and Cavazzuti 1993; Tjolsen et al., 1992; Heapy et al., 1987). Later on, it has been shown that formalin provokes

primary afferent sensory neurons through TRPA1 channels (McNamara et al., 2007). The last phase continues for 30-60 minutes which starts after 15-20 minutes following the injection of formalin. This phase is characterized by the inflammatory reaction in the peripheral tissue and functional changes in the dorsal horn of the spinal cord. The functional changes seem to be initiated by the C-fiber activity of the early phase, provoking the activity-dependent sensitization of the CNS neurons in the dorsal horn (Tjolsen et al., 1992). As an effect of peripheral injection of TLQP-21, a remarkable increase of pain-related licking response was observed while there was an analgesic effect without pain following the icv injection of the peptide (Rizzi et al., 2008). All these studies suggest that this peptide is involved in inflammatory pain in vivo and acts differently at the peripheral and central levels of the nociceptive pathways : being pronociceptive at the periphery and antinociceptive at the central level.

Other VGF derived peptides like LQEQ-19 induces hyperalgesia dose dependently mediating by p38 MAPK phosphorylation in microglia cells in the spinal cord while SB 202190, the p38 MAPK phosphorylation inhibitor, was found to inhibit the induction of hyperalgesia (Riedl et al., 2009). In addition, another VGF derived long peptide, TLQP-62 also showed its role in pain modulation (Moss et al., 2008). Interestingly, TLQP-62 is composed of both TLQP-21 and LQEQ-19 suggesting that VGF derived these peptides have direct effects as well as may interact each other to induce more (synergistic) or less (antagonistic) effect simultaneously or when undergo differential proteolytic cleavage (Trani et al., 2002; Seidah and Chretien, 1999).

Macrophages have been shown to be involved in neuropathic pain maintenance after stimulation by TLQP-21, additionally downstream signaling following the TLQP-21 treatment may control chronic pain (Chen et al., 2013). Chen et al., 2013 also confirmed TLQP-21 stimulated upregulation of intracellular Ca^{2+} in macrophages inducing nitric

oxide and TNF- synthesis (Brown et al., 2004; Korhonen et al., 2001). Xiao et al., 2001 showed IL-8 (interleukin-8) expression through MAP kinase pathways. Following nerve injury, plenty of macrophages (Mueller et al., 2001) and monocytes flow at the injured site (Abbadie et al., 2003) that was already evident while reduction of macrophages was shown to result in the reduction of mechanical hypersensitivity following nerve injury (Liu et al., 2000) and delayed onset of pain in diabetic condition (Mert et al., 2009). Pap/Reg2, the macrophage chemoattractants were found to increase in the rat models of neuropathic pain (Maratou et al., 2009). All these data suggest that TLQP-21 induced macrophage stimulation may influence the process of synthesis and secretion of some cytokines possibly following MAP kinase pathway, in order to modulate pain.

Recently, Fairbanks et al., 2014 illustrated the effects of the peptide TLQP-21 in spinal mechanisms of continuous pain: TLQP-21 induced dose-dependent thermal hyperalgesia was inhibited by a p38 mitogen-activated protein kinase inhibitor, as well as inhibitors of cyclooxygenase (COX) and lipoxygenase. Moreover, intradermal injection with complete Freund adjuvant, intrathecal treatment with anti-TLQP-21 immediately prior to or 5 hours after induction of inflammation inhibited tactile hypersensitivity and thermal hyperalgesia in a dose dependent manner. These results provide credence that TLQP-21 peptide contributes to the mode of action of spinal neuroplasticity after inflammation and nerve injury (Fairbanks et al., 2014).

Overall, *in vivo* data suggest that TLQP-21 is a modulator in pain that acts at the peripheral and central levels of the nociceptive pathways (Rizzi et al., 2008), possibly via the interaction of TLQP-21 with microglia: either by direct actions of TLQP-21-activated microglia on neurons or microglia mediate activity of other cells like glia, including astrocytes, as well as other immune cells. However, there is a possibility that the mechanisms of action of TLQP-21 for pain modulation is yet to be unveiled (Ayub,

2012). But till now, there is growing data confirming the involvement of TLQP-21 in pain modulation, now urge to further elucidate the molecular mechanisms of action of the peptide on different cells, specially dorsal root ganglion (DRG) neurons and microglia, in the PNS and CNS that are involved in the pathway of pain modulation in order to confirm the target of TLQP-21 as a drug/novel analgesics/hyperalgesics for the treatment of pain.

TLQP-21: Gastrointestinal function:

TLQP-21 confers potential roles in gastroenteric function of rat (Bartolomucci et al., 2008). In vivo and ex vivo experiments confirmed that TLQP-21 treatment provoked the contraction of gastric fundus strips, though it failed to induce contraction of stomach antrum or more distal gut portions like jejunum and ileum. PG E2 and PG F2 were synthesized and secreted from the mucosal layer while due to the pretreatment with PG antagonists and the COX (cyclooxygenase) inhibitors : indomethacin and naproxen, the fundus strip contraction was diminished (Severini et al., 2009; Sibilia et al., 2010b). In support of the involvement of TLQP-21 in the outflow pathway from CNS to gastrointestinal tract, acute icv, not ip or iv, administration of the peptide reduced ethanol-induced gastric lesions (Sibilia et al., 2010a) and repressed gastric emptying in a time and dose dependent manner (Severini et al., 2009). A significant upregulation in the expression of gastric PG E2 and COX1 was found as the resultant effect of the TLQP-21 induced gastroprotective effect. Treatment with NG-nitro-L-arginine methyl ester (nitric oxide synthase inhibitor) and indomethacin (COX inhibitor) diminished the activity of TLQP-21 induced gastroprotection, gastric emptying (Severini et al., 2009), gastric acid secretion (Sibilia 2010b). To sum up, both in vivo and in vitro, the peptide exerts its gastrointestinal effect via PG-dependent mechanism: in vivo, the peptide showed a central inhibitory role on gastric emptying, involving PG release while in

vitro, TLQP-21 stimulated contraction of the rat longitudinal forestomach (RLF) strip through the discharge of PGs within the mucosal layer of the cells. Further studies are now required to validate the downstream effectors contributing to the biological activity of TLQP-21 regarding gastrointestinal functions in vivo.

TLQP-21: Its role in reproduction:

Upon injection of several VGF derived peptides including TLQP-21 into the hypothalamic Paraventricular Nucleus (PVN), the male erectile behavior was modulated (Pinilla et al., 2011) via nitric oxide mediated excitation of an oxytocinergic pathway (Succu et al., 2004; 2005). The nitric oxide synthase inhibitor, L-NG-nitro-L-arginine methyl ester, the oxytocin receptor antagonist d-[CH (2)](5) Tyr(Me)-Orn(8)-vasotocin, morphine and muscimol inhibited TLQP-21 induced penile erection partially (Succu et al., 2004; 2005). TLQP-21 administration showed : acute gonadotrophin response through stimulation of Gonadotrophin releasing hormone (GnRH), Leutinizing hormone (LH) secretion from pubertal, not adult, male rat pituitary, human chorionic gonadotrophin (hCG) induced testosterone secretion by adult testicular tissue. TLQP-21 administration on pubertal chronic undernourished males ameliorated the hypogonadotrophic condition whereas in properly fed males it delayed the onset of puberty. Thus Pinilla et al., 2011 for the first time by both in vivo and in vitro analyses documented complex and multifaceted mechanisms of accomplishment of TLQP-21 at different levels of the male hypothalamic-pituitary-gonadal (HPG) axis with predominant stimulatory consequences, establishing a reasonable concrete base for the direct reproductive function of TLQP-21.

All these findings are consistent with the reproductive phenotypes of VGF knockout mice, characterized by delayed puberty, reduced fertility, decreased ovarian and uterus

weights, and low mRNA levels and protein contents of LH and FSH (follicle-stimulating hormone) α -subunits at the pituitary, strongly suggesting that the products of VGF, including TLQP-21 are directly or indirectly involved in the control of the reproductive events (Hahm et al., 2002; 1999). Hence, VGF derived peptides like TLQP-21 could be a target to be used in the stimulation/modulation of reproductive phenomena.

TLQP-21: Glucose metabolism and diabetes:

Stephens et al., 2012 showed that TLQP-21 is capable to potentiate glucose-stimulated insulin secretion (GSIS) in isolated rat and human pancreatic islets. Consistently, administration of TLQP-21 to Wistar rats upregulated the circulating insulin in response to a glucose challenge, confirming the increase glucose tolerance. TLQP-21 induced insulin secretion occurs in concert with an upregulation of cAMP, indicating that the effect of TLQP-21 is mediated by downstream targets of activated PKA, as with other cAMP-raising agents such as glucagon-like peptide-1 (GLP-1), glucose-dependent insulinotropic polypeptide (GIP), and vasoactive intestinal peptide (VIP). A role for PKA (protein kinase A) in the TLQP-21 signaling pathway is supported by the finding that inhibition of PKA blocks the ability of TLQP-21 to suppress thapsigargin-induced islet cell death. Unlike GLP-1, TLQP-21 does not hamper gastric emptying or boost up heart rate. Taken together all these findings, TLQP-21 is a targeted agent for uplifting of islet β -cell survival period of time and functionality, ultimately for the treatment/improvement of diabetes (Stephens et al., 2012).

Receptor(s) for human vs rodent TLQP-21:

For the last two decades the effects of TLQP-21 have been demonstrated and characterized but till now, not enough has been elucidated about its molecular mechanism in physiological system. Being one of the bioactive peptides of VGF, the

elucidation of the biological activity of the peptide is under investigation but there is lacking of the informations on the receptor-dependent or receptor independent signaling pathways.

TLQP-21 was found to bind to adipocyte membranes, expressing stimulatory pro-lipolytic effect (Possenti et al., 2012) and unique binding sites of TLQP-21 were revealed on living Chinese hamster ovary (CHO) cell lines with the aid of atomic force microscopy (AFM) (Cassina et al., 2013) but there was little information about the mechanisms of action of the peptide as well as about putative receptor that mediate the TLQP-21 effects, as mentioned earlier. Very recently, complement component-3a receptor 1 (C3AR1) (Cero et al., 2014; Hannedouche et al., 2013), and globular head of the complement component C1q receptor (gC1qR) (Chen et al., 2013) have been identified as receptors of murine TLQP-21.

C3AR1 as a receptor of rodent TLQP-21:

C3AR1 is a G protein-coupled receptor protein that binds both C3a (complement component-3a) and C4a (complement component-4a) though its official name implies that it only binds C3a (Klos et al., 2013). Before discovery of its role as a receptor of rodent TLQP-21, its activity was thought to be involved in innate immune system showing roles in the complement system. But its roles are not limited only to complement system, its roles also found in neurogenesis (Klos et al., 2013), cancer (Opstal-van Winden et al., 2012) and hormone release from pituitary gland (Francis et al., 2003). Moreover, C3AR1 knockout mice were found to be resistant to diet-induced obesity and high fat diet induced insulin suggesting its role in metabolism (Mamane et al., 2009).

Hannedouche et al. 2013 conducted studies on signaling activity in rodent cell lines, CHO-K1 and O-342, that led to the discovery of its cognate receptor C3AR1. CHO-K1

cells responded to TLQP-21 showing increase in intracellular calcium (Cassina et al., 2013) though ATP priming was necessary to get a vigorous signal suggesting that the expected TLQP-21 receptor is not Gq- coupled GPCR (G-protein coupled receptor). cAMP or Inositol phosphates accumulation was not found in TLQP-21-induced signaling events in CHO-K1 cell line. Moreover, increase in intracellular calcium influx induced by TLQP-21 treatment was blocked by pertussis toxin (PTX). The authors therefore concluded that it was highly likely that the G-protein mediated effects were to be G₀ due to all the findings regarding PTX sensitivity and lack of cAMP modulation. Subsequently, RNA sequencing was carried on both TLQP-21 responsive, CHO-K1 and TLQP-21 non-responsive, CCL39 cell line in order to have more informations on the molecular mechanisms of TLQP-21 induced actions. A total of 21 GPCRs were identified after unbiased genome-wide sequencing of the transcriptome that were speculated to bring about TLQP-21 mediated biological activity, considering that GPCRs expression would be more in CHO-K1 than CCL39 cell line.

To confirm the identity of GPCR of TLQP-21, a panel of antagonists were used to inhibit the peptide response in CHO-K1 cell line. Out of the well characterized antagonists, SB290157 was proved as the most potential antagonist which was a C3AR1 antagonist (Ames et al., 2001). In another TLQP-21 responsive cell line O-342, the antagonist SB290157 was tested to confirm that this cell line would express the homologous receptor like CHO-K1 that was further confirmed by qRT-PCR showing that O-342 cells express the C3AR1.

To further validate C3AR1 as a receptor of TLQP-21, siRNA screening was performed. A total 63 siRNAs were tested against all the 21 genes that were confirmed by the transcriptomic analysis earlier. The only gene knockdown was found to reduce the TLQP-21 mediated response consistently was siRNAs against C3AR1. Thus, C3AR1

was confirmed as a potential receptor for TLQP-21 in rodents using defined receptor antagonist and siRNA techniques.

However, this finding was not translatable to the human receptor. For example, the authors tried to show the TLQP-21 signaling in HEK293 cells expressing the human C3AR1 but failed whereas in hamster and rat C3AR1, it was successful. This might be due to the fact that human TLQP-21 is remarkably different than rodent version (Hannedouche et al. 2013) (see below, in details, about the difference between human and rodent version of the peptide). All these studies led the authors to conclude that there might be a receptor other than C3AR1 for human TLQP-21.

Later on, Cero et al., 2014 confirmed C3AR1 as a receptor of TLQP-21. By photoactivated crosslinking, the peptide was found to bind to a ~56 kDa (equivalent to molecular weight of C3AR1) protein in 3T3L1 and CHO cell lines. The same binding experiment was performed using SB290157, a C3AR1 antagonist (Ames et al., 2001) and the binding was found reduced in presence of the antagonist suggesting that SB290157 competes with C3AR1 for binding with TLQP-21. Furthermore, β -arrestin recruitment assay in HTLA cells transfected with human C3AR1 (Lin et al., 2013) added more credence to the interaction of TLQP-21 and C3AR1 as it demonstrated that TLQP-21 acts as an agonist for the human C3AR1: half maximal effective concentration (EC_{50}) for mouse TLQP-21 was about 3 times lower than that of C3A while the EC_{50} for human TLQP-21 was about 22 times lower than that of C3A, suggesting that human and mouse version of the peptide show activity toward human C3AR1 with different potency.

Further experiments were targeted to find out the hot spots for biological function in the sequence of the peptide based on the bioassay for the peptide function of the contraction of the stomach fundus strips (Severini et al., 2009). The peptide showed ~69% contraction promoted by acetylcholine at a dose of 3 μ M of the peptide. Two truncated TLQP-21 peptide fragments were used, TLQP-11 (the C-terminus sequences with the

first 11 amino acids) and HFHH-10 (the N-terminus sequences with the latter 11 amino acids) showing that TLQP-11 is completely inactive whereas HFHH-10 is modestly active demonstrating 2.6 %, 62%, 75% response at a dose of the peptide 3, 6, 10 μM , respectively while TLQP-11 showed zero response even at the dose of 10 μM). This suggests that hot spots in the peptide responsible for biological activity lies in the C termini, not in the N-termini. Accordingly, Ala scanning mutagenesis in the C-terminal of the peptide was performed to observe the biological effect of the mutated peptide. It was found that this mutation had no significant effects excepts P18A mutant, P19A and R21A that showed biological activity 65%, 19%, nil, respectively. Amidation of the capping of the C-terminal resulted in the complete loss of biological activity. Notably, in this experiment human TLQP-21 showed 20% response while rodent version of the peptide showed 100% activity as expected suggesting that human peptide shows five times less biological activity to the rodent receptor compared to the rodent version of the peptide (Cero et al., 2014). Moreover, C3AR1 has been confirmed as a receptor of TLQP-21 pointing out the folding-upon-binding Mechanism : TLQP-21 is intrinsically disordered but upon binding with its receptor C3AR1, it goes from disordered to ordered shift adopting α -helical conformations (Cero et al., 2014) in consistent with a molecular dynamics study exploring that the peptide is not absolutely random coil but it also possesses stretches of distinct structural region that adopts a very much compact globular structure stabilized by π -cationic interactions and several hydrogen bonding interactions, finally validating that the peptide exhibits very flexibility in solution and that three C-terminal residues, P₁₉-R₂₁, and the region A₇-R₉ shows strong helical tendency (Chakraborty et al., 2015).

In fact, the study by Cero et al., 2014 supplemented the finding of Hannedouche et al. 2013 that there is possibly a receptor other than C3AR1 in humans, as human TLQP-21 is different from its rodent version sequence by four amino acids (Bartolomucci et al., 2011), highlighting the dissimilar biological function of human and rodent TLQP-

21(Cero et al., 2014), as described earlier. Cero et al. 2014 suggested that this finding might be connected with the human susceptibility to obesity due to less potency of human TLQP-21 toward receptor C3AR1 resulting in less lipolysis of adipocytes (Possenti et al., 2012). This could be one of the reasons of being more susceptible to obesity by human than other species (Cero et al., 2014).

All in all, considering all potential functions of TLQP-21 (as illustrated earlier), there should be another receptor in humans to which human version of the peptide will bind and potentiate 100% biological activity.

gC1qR as a receptor of rodent TLQP-21:

The globular head of the complement component C1q receptor, gC1qR, also known as C1QBP, TAP, HABP1, p³³ and p³², is a multiligand binding and ubiquitously expressed protein. It is found in mitochondria (Dedio et al., 1998), nucleus, endoplasmic reticulum(ER)(Petersen-Mahrt et al., 1999), cytosol(Peterson et al., 1997) and cell surface(Peerschke and Ghebrehiwet, 2007): interacting with a variety of ligands of cellular, bacterial and viral origin (Peerschke et al., 2006; Ghebrehiwet et al., 1996; Xu et al., 1999). It has been observed to play important role in carcinogenesis (Ghebrehiwet et al., 2001), bacterial and viral infections (Ghebrehiwet and Peerschke, 2004), immune cell modulation and complement activation (Peerschke et al., 2006), adipogenesis (Kim et al., 2009) and pain modulation (Chen et al., 2013). Recently, it has been validated as a receptor of murine TLQP-21 highlighting its role in pain modulation (Chen et al., 2013).

In order to search for the receptor, Chen et al., 2013 used chemical cross-linking, affinity chromatography followed by mass spectrometry analysis: a heterobifunctional crosslinker, Sulfo-EMCS was conjugated with biotinylated TLQP-21 followed by cross-linking reaction between this peptide and membrane proteins obtained from whole brain

and spinal cord of 6 weeks old female Wistar rat. A ~30 kDa protein was detected by Western blot, probing with HRP-conjugated Streptavidin, from the sample obtained after cross-linking reaction. Further experiment was performed by attaching the peptide to avidin monomeric column followed by incubation with three types of membrane protein fractions of post-natal day 4 rat forebrain: whole cell lysate, cytosolic and membrane & associated protein fractions. The elutants were analysed by silver-staining showing ~30 kDa protein which was identified as gC1qR after nanoLC-MS/MS analysis.

Further experiments showed that electroporation of siRNAs against gC1qR remarkably lowered the gC1qR level in macrophages. The siRNAs also reduced the quantity of macrophages responding to the peptide observed in live cell Ca^{2+} imaging. A considerable reduction of the response to the peptide was evident after incubation of macrophages with neutralizing gC1qR monoclonal antibodies. Furthermore, to elucidate the role of gC1qR in pain modulation, the following experiment was performed using gC1qR antibody : the gC1qR antibody was applied to the site of the nerve ligation of partial sciatic nerve ligation (PSNL) model rats that resulted in the drop of punctuate mechanical threshold. Again, the gC1qR antibody application caused delay of the inception of the hypersensitivity linked with PSNL (Chen et al., 2013). All these results validate the gC1qR as a receptor that activates macrophages in response to TLQP-21, playing a crucial role in pain modulation.

It was proposed by Chen et al., 2013 that both receptors, gC1qR and C3AR1 functions in response to TLQP-21, either simultaneously or sequentially as it has not yet been disclosed that whether the receptors interact each other or not, in response to the peptide. However, the functional and structural similarity between gC1qR and the peptide TLQP-21 is apparently absent (Gaboriaud et al., 2003). Moreover, the possibility of the existence of the second receptor, in addition to C3AR1, in CHO or 3T3L1 cells is not

supported by the recent and previous works (Cero et al., 2014; Hannedouche et al., 2013; Cassina et al., 2013; Possenti et al., 2012).

All these studies confirm the existence of cell surface membrane receptor of TLQP-21 in rodents. It is noteworthy that almost all of these works with TLQP-21 were performed with rat/mouse TLQP-21, except, so far it has been known, very few works that were performed by Hannedouche et al., 2013 and Cero, et al., 2014 with human TLQP-21; provided that due to the difference in biological activities between human and rodent TLQP-21 (as discussed earlier) (Cero et al., 2014) as well as due to the difference in respect of the sequences between human (TLQPPSALRRRHYHHALPPSR) and rodent version (TLQPPASSRRRHFHHALPPAR) of the peptide, it is highly expected that there is different receptor(s) for human as mentioned by Hannedouche et al., 2013. No doubt left, identification of the receptor of VGF-derived human peptide TLQP-21 will offer a very interesting pharmacological target to develop drugs for the treatment not only of obesity related disorders but also for improving the treatment for hypertension, stress, reproduction and diabetes. In addition, it should help understand the molecular mechanisms in human underlying these ailments.

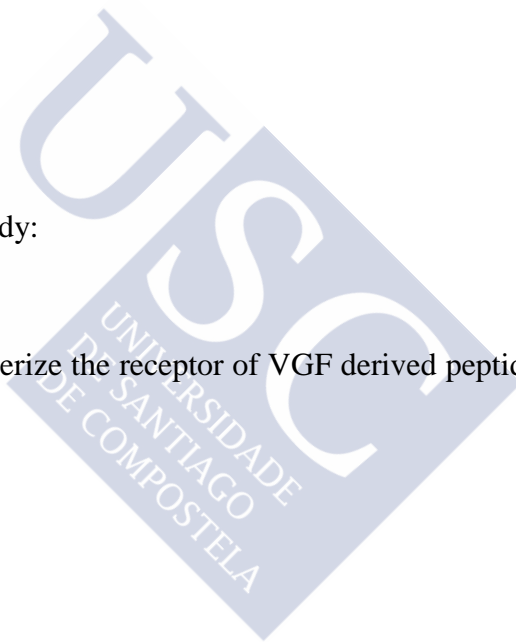


Objective



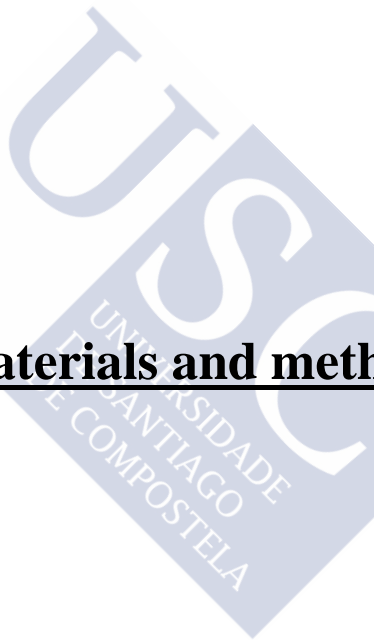
The objective of this study:

-To identify and characterize the receptor of VGF derived peptide human TLQP-21.





Materials and methods





TLQP-21:

TLQP-21(human, molecular weight 2490.88 Da) and biotinlyted TLQP-21(human) containing an extra cysteine residue at the C-terminus with total molecular weight 2820.32 Da, were purchased from ChinaPeptides Co. Ltd., Shanghai; peptide purity >95%, confirmed by HPLC and MS analysis (Figure 24 and 25, respectively, Appendix I). It was in the form of white lyophilized powder and stored at -21°C immediately upon arrival for short time storage and at -80 °C for long term storage, as per instruction of the supplier. The peptide sequence is –

Biotin-TLQPPSALRRRHYYHALPPSR-C

Biotin-Thr - Leu - Gln - Pro - Pro - Ser - Ala - Leu - Arg - Arg - Arg - His - Tyr - His - His - Ala - Leu - Pro - Pro - Ser – Arg- Cys

To prepare solutions of TLQP-21 and Biotin-TLQP-21-C, the lyophilized powder was dissolved in filtered (0.22 µm, Millex, Merck Millipore Ltd.) PBS, used instantly or was kept at -80 °C for long term storage. It should be noted here that in all the experiments Biotin-TLQP-21-Cys was used except phosphoprotein gel staining and proteomic study, where TLQP-21 was used.

SH-SY5Y cell culture:

SH-SY5Y (European Collection of Cell Cultures, ECACC; catalog number-94030304) is a thrice cloned (SK-N-SH SH-SY SH-SY5 SH-SY5Y) subline of the neuroblastoma cell line SK-N-SH which was established in 1970 from a metastatic bone tumor of a four year-old female with neuroblastoma (Biedler et al, 1973; 1978). The cells were grown at 37 °C in a 5% CO₂-humidified incubator on a culture medium composed of 1:1 Earle's Balanced Salt Solution (EBSS) (Sigma Aldrich) and F12

HAM (Sigma Aldrich) supplemented with 15% fetal bovine serum (FBS) (Gibco), 1% Glutamine (Gln) (Sigma Aldrich), 1% Non-Essential Amino Acids (NEAA) (Sigma Aldrich), and 1% Penicilin-Streptomycin (P/S) (Invitrogen) in 100×20 mm Falcon Petri dishes (Life Sciences). The cells were always used at less than 20 passages.

Petri dishes with confluent SH-SY5Y cells were washed twice with cold PBS, followed by solubilization in lysis buffer, composed of 20 mM HEPES, 2mM EGTA, 1mM DTT, 1mM sodium orthovanadate, 1% Triton X-100, 10% Glycerol, 2µM leupeptin, 400 µM PMSF, 50 µM -glycerophosphate, 100 µg/ml trasylol. The cells were scrapped on ice for 10 minutes and were incubated on ice for 30 minutes with periodic vortexing at each 5 minutes interval, followed by centrifugation for 20 minutes at 14000g at 4 °C. The supernatant was saved for further use. Protein concentration was quantified using the BCA protein assay kit (Pierce Chemical).

Detection of a TLQP-21 receptor in SH-SY5Y cells using biotinylated TLQP-21 as a probe:

Peptide conjugation:

Sulfo-N-[-maleimidocaproyloxy]succinimide ester (sulfo-EMCS) cross-linkers are moisture-sensitive. So, to avoid moisture condensation inside the container the vial was equilibrated to room temperature. Dissolving in Conjugation buffer (PBS, 0.1M sodium phosphate, 0.15M NaCl, pH 7.2, Thermo Scientific), 1 mM Sulfo-EMCS (Thermo Scientific) solution was freshly prepared, to which 0.1 mM Biotin-TLQP-21 peptide was added, making final volume 1 ml and incubation continued on ice for 2 hours. The resultant conjugated peptide was then checked by Matrix Assisted Laser Desorption

Ionization Time-of-Flight (MALDI-TOF) mass spectrometry (MS) and subsequently was used for the crosslinking step.

MALDI-TOF mass spectrometry:

Sulfo-ECMS-conjugated peptides were identified using a 4800 MALDI-TOF/TOF analyzer (Applied Biosystems). Peptides were dissolved in 4 μL of 0.5% formic acid. The same volumes (0.5 μL) of peptide and matrix solution, composed of 3 mg alpha-cyano-4-hydroxycinnamic acid (-CHCA) were dissolved in 1ml of 50% acetonitrile in 0.1% trifluoroacetic acid (TFA), then deposited using the thin layer method, onto a 384 Opti-TOF MALDI plate (Applied Biosystems). Mass spectrometric data were obtained in an automated analysis loop. MS spectra were attained in reflectron positive-ion mode with aNd:YAG, 355 nm wavelength laser, averaging 1000 laser shots and using at least three trypsin autolysis peaks as internal calibration.

Crosslinking:

Followed by confirmation of the peptide conjugation, the cross linking reactions were accomplished. For the crosslinking reaction, the resulting activated peptide solution (5 μl) was mixed with 5 μl of SH-SY5Y cell homogenate, equivalent to 10 μg of protein (final activated peptide concentration, 10 μM) and allowed the reaction for 2 hours on ice. To optimize the conditions, the cross linking reaction was also performed with higher amount (50 and 100 μg) of cell homogenate protein as well as with higher amount (20 and 100 μM) of conjugated peptide. Finally, the reaction was terminated adding 50 mM Tris buffer (pH 8.0), containing primary amines reacting with

unconjugated crosslinker, if any. As a control, cell homogenate, unconjugated Sulfo-EMCS and conjugation buffer, without conjugated peptide were incubated. Then the samples were subjected to SDS-PAGE and Western blot analysis.

SDS-PAGE and Western blot analysis:

All the samples obtained from crosslinking were boiled in 2XLaemmli sample buffer (Bio-Rad) for 10 minutes at 100 °C, spun, loaded and subjected to SDS-PAGE in a 12% gel. After electrophoresis (200V, 01h), proteins were transferred onto PVDF (Polyvinylidene fluoride) membranes (Millipore, Bedford) in the condition of 0.8 mA/cm² for 90 minutes using semi-dry method (Trans-blot SD semi-dry transfer cell, Biorad). The PVDF membranes were then blocked with 5% BSA in TBS-T solution (Tris-buffered saline with 0.1% Tween - 20) for 1 hour at room temperature, followed by three washes with TBS-T solution each for 10 minutes. The membrane was then probed by Pierce high sensitivity streptavidin- HRP (Thermo Scientific) at 1:20000 dilution in TBS-T. Then the PVDF membranes were washed 3 times with TBS-T for 10 minutes each wash, followed by incubation for 5 minutes with the chemiluminescence solution Luminata Forte Western HRP substrate (Merck Millipore) wrapping the PVDF membrane containing container to shield it from light, and finally developed using, Hypercassette and Amershamhyperfilm (GE Healthcare).

Avidin agarose affinity chromatography:

The Pierce Monomeric Avidin Kit (Thermo) was used. It contains a monomeric avidin column (2 ml prepacked column containing monomeric avidin immobilized to 4% beaded agarose, supplied as a 50% slurry (i.e., 4 ml of slurry equals 2 ml of settled

resin); binding capacity is 1.2 mg biotinylated BSA/ml settled resin), Wash buffer-BupHTM phosphate buffered saline (PBS) pack (equivalent to 0.1 M sodium phosphate, 0.15M NaCl, pH 7.2 when reconstituted with 500 ml of ultrapure water; to store buffer for >1 week, preservative 0.02% sodium azide was added.), biotin blocking & elution buffer (having 2 mM D -biotin in PBS), regeneration buffer (contains 0.1M glycine, pH 2.8).

The column has 2 porous discs: to produce a stop-flow action preventing resin from drying when left unattended for short period and to stop automatically the solution flow applied to column when the liquid level reaches the top disc. The monomeric avidin resin can be regenerated at least 10 times with negligible loss in binding capability. Upon receipt, all of the kit components were stored at 4°C.

After equilibration of the necessary kit components to room temperature, the storage solution of the column was drained out. The column was washed with 8 ml PBS followed by addition of 6 ml biotin blocking & elution buffer (2 mM D-biotin in PBS) to block any non-reversible biotin binding sites. Regeneration buffer (0.1M glycine, pH 2.8, 12 ml) was added to remove biotin from the reversible binding sites followed by addition of 8 ml of PBS to wash the column again. The column was then ready to add protein or peptide samples. Air bubbles introduced into column resin beds may impede the flow of solutions column, so extra care was taken to prevent air bubbles to enter into the resin by removal top column cap before bottom cap all the time.

To attach biotin-TLQP-21 to the column, 2 ml of solution consisting of 1 ml of 0.1 mM biotin-TLQP-21, 900 µl of wash buffer and 100 µl of 1mM TCEP (to prevent biotin-TLQP-21 peptides to form disulphide bonds due to the extra cysteine residues at their C-termini) were applied to the column, which was incubated for an hour at room temperature. The column was subsequently washed by 12 ml wash buffer, then the column was ready to add SH-SY5Y cell homogenate.

A 700 μ l SH-SY5Y cell homogenates with a protein concentration of 10 μ g/ μ l were diluted into 1.3 ml wash buffer to make the total volume 2 ml, then applied to the column already supposed to be attached with the biotin-TLQP21. The column was then washed with 12 ml washing buffer followed by addition of 10 ml of elution buffer. Fractions of 500 μ l were collected and stored on ice until further use for analysis by SYPRO[®] Ruby Protein Gel Stain (Lonza), and Western blot. As control, cell lysate solution was added under the same conditions to a column without biotin-TLQP-21 attached, and processed under the described conditions.



Box 1: Avidin affinity chromatography, at a glance.

The immobilized monomeric avidin protein bound biotin with high specificity and moderate affinity, allowed non-biotin molecules to be washed away and then the bound biotin-labeled molecules were competitively eluted using 2mM biotin in phosphate buffered saline (PBS) (biotin blocking and elution buffer) and thus provided the gentlest elution conditions for biotinylated protein purification, in more details : avidin with strong binding features was immobilized in monomeric avidin immobilization. These high affinity biotin-binding sites were first blocked with biotin-containing buffer (biotin blocking and elution buffer). Biotin molecules were eluted from monomers with the glycine solution (regeneration buffer, pH 2.8) revealing the reversible binding sites. The biotinylated specimens of interests were then applied for purification, followed by elution through ligand competition using the biotin-containing solution (biotin blocking and elution buffer) (Strachan, et al, 2004). Thus, the monomeric avidin agarose resin resulted in the high-binding capability with least nonspecific binding and last of all, excellent recovery of biotinylated molecules was performed.

To regenerate column after use, it was washed two times with 4 ml of regeneration buffer to strip the column of residual bound biotin without losing the ability to bind another biotinylated sample. For storage, column was washed with 5 ml of PBS containing the preservative 0.01% sodium azide. A supplied white tip was placed on the column and additional preservative-containing PBS was added above the top disc before replacing the top cap. Finally, it was stored at 4°C for use next time.

SDS-PAGE and SYPRO[®] Ruby Protein Gel Stain:

Samples (25 μ l) from the different fractions eluted from Pierce monomeric avidin agarose affinity chromatography were boiled in 2X Laemmli buffer (Bio-Rad) for 10 minutes at 100 °C, spun, and loaded to SDS-PAGE gel. After electrophoresis (200V, 01h), the gel was washed in dH₂O for 10 minutes. Then the gel was incubated with fixing solution (10% methanol, 7% acetic acid) for 1 hour at room temperature in an orbital shaker step at 50 rpm, followed by overnight incubation with SYPRO[®] Ruby Protein Gel Stain at room temperature with shaking.

The gel was then placed into a staining container covering with a lid to protect it from the light, in addition, the container was wrapped in aluminium foil to further shield the stain from light during the staining process, as per instruction of the supplier. After overnight staining, the gel was transferred to a clean staining dish, washed with the fixing solution in the same condition of staining followed by 5 minutes washing in dH₂O. Finally, the gel was taken from the container to take the image in a Molecular Imager[®] Gel Doc[™] system (Bio Rad, Hercules) using the highest sensitivity of the CCD camera at a resolution of 1392 x 1040 pixels with 12 bit gray scale levels per pixel.

Protein identification:

Following Pierce monomeric avidin agarose affinity chromatography, SDS-PAGE gel run and SYPRO[®] Ruby Protein Gel Staining, the protein bands found (but not in the control lane) were carefully excised from the gel using a clean, sterile razor blade in a laminar flow hood to avoid dust and keratin contamination and, subjected to in-gel

reduction, alkylation and trypsin digestion, according to the method of Shevchenko et al., (2006). Extracted peptides were analysed by LC-MS/MS.

Digested peptide mixtures were dried in a centrifugal evaporator (Speedvac, Savant) and dissolved in 0.1% formic acid followed by separation in an EASY-nLC (Proxeon, Bruker Daltonik GmbH) with a reverse phase nanocolumn (Easy column SC200 C18 3 μ m 120A 360 μ m OD/75 μ m ID, L=10cm) from Proxeon. Peptides were ionized and examined in a Bruker Amazon ETD ion trap. Automated analysis of mass data was performed by Data Analysis 4.0 and BioTools 3.2 from Bruker Daltonik GmbH. Database search was done with the Mascotv2.3 search tool (Matrix Science, London, UK) screening SwissProt (release 57.15). Searches were limited to human taxonomy permitting carbamidomethyl cysteine as a fixed modification and oxidized methionine as potential variable modification. Both the precursor mass tolerance and the MS/MS tolerance were fixed at 0.3 and 0.4 Da, respectively, with 1 missed tryptic cleavage site. All spectra and database results were scrutinized manually in details using the above software, especially in the case of identifications based on one peptide hit. Positive identification by MS was only accepted when more than 50% y-ions were obtained for a peptide comprising at least eight amino acids long and no missed tryptic cleavage site. Positive hits corresponded to Mascot scores > 40 plus the fulfillment of the above criteria.

Western blot analysis of the samples obtained from monomeric avidin experiment:

As per standard protocol for Western blot analysis, samples (25 μ l) obtained from monomeric avidin experiment were boiled in 2X Laemmli sample buffer (Bio-Rad) for 10 minutes at 100 °C, loaded to SDS-PAGE gel. After electrophoresis (200V, 01h), proteins were transferred onto Polyvinylidene fluoride (PVDF) membrane (Millipore, Bedford, MA) in the condition of 0.8 mA/cm² for 90 minutes using semi-dry method (Trans-blot SD semi-dry transfer cell, Biorad). The PVDF membrane was then blocked by 5% BSA (Bovine Serum Albumin) in TBS-T solution (Tris-buffered saline with 0.1% tween 20) for 01 hour at room temperature, followed by three washes by TBS-T each for 10 minutes and then, the membranes were probed by Anti-Hsc 70/HSPA8 (Abcam) antibody at 1:500 dilution in TBS-T. Then the PVDF membrane was washed 3 times with TBS-T for 10 minutes each wash, followed by incubation with the secondary Anti-rabbit antibody (Dako) at 1 : 2000 dilution in TBS-T. The membrane was washed 3 times with TBS-T for 10 minutes each wash. Subsequently, the membrane was incubated with chemiluminescence solution Luminata Forte Western HRP substrate (Merck Millipore) for 5 minutes covering the membrane containing container to protect it from light and was developed using Hypercassette and Amershamhyperfilm (GE Healthcare).

Additionally, the same PVDF membrane was stripped by incubation in Restore Plus Western Blot Stripping Buffer (Thermo Scientific) as per instruction of the supplier and finally was probed with Anti-C3AR1 antibody(Sigma-Aldrich) at a 1:200 dilution, followed by incubation with anti-mouse secondary antibody (GE Healthcare, UK) at a 1:5000 dilution. But it could not recognize any protein in the membrane, concluding that it is not C3AR1 protein.

Crosslinking of biotinylated TLQP-21 to SH-SY5Y surface membrane proteins:

SH-SY5Y cells were grown as described above. Culture medium from the Petri dishes with confluent SH-SY5Y cells were removed followed by washing three times with PBS. Subsequently, the dishes were incubated with 10 ml of PBS containing 1 mM Sulfo-EMCS and 0.1 mM biotin-TLQP-21 for 30 minutes at room temperature. The cross-linking reaction was stopped adding Tris-HCl, pH 7.8 to a final concentration 50mM. Cells were then harvested as described above. Briefly, Petri dishes were washed twice with cold PBS, then solubilization in lysis buffer(20 mM HEPES, 2mM EGTA, 1mM DTT, 1mM sodium orthovanadate, 1% Triton X-100, 10% Glycerol, 2 μ M leupeptine, 400 μ M PMSF, 50 μ M β -glycerophosphate, 100 μ g/ml trasylol). The cells were scrapped on ice for 10 minutes and were incubated on ice for 30 minutes with vortexing at each 5 minutes interval, finally centrifuged for 20 minutes at 14000 g at 4 °C. The supernatant was collected for the next step use and the pellet was discarded.

The Pierce monomeric avidin agarose affinity chromatography kit components were equilibrated to room temperature. The column was extensively washed with 8 ml PBS, then added 6 ml biotin blocking & elution buffer to block any non-reversible biotin binding sites. Regeneration buffer (12 ml) was added to remove biotin from the reversible binding sites followed by washing again with 8 ml of PBS. Thus the column was prepared to add solubilized biotinylated SH-SY5Y membrane protein samples.

Two ml of solubilized biotinylated SH-SY5Y membrane proteins were applied to the Pierce avidin-agarose affinity column. The column was then washed with 12 ml washing buffer and eluted with 10 ml of elution buffer. Fractions of 500 μ l were collected and stored on ice and subsequently subjected to SDS-PAGE and Western blotting as described above.

Fluorescence-activated cell sorting (FACS) analysis:

To further confirm binding of TLQP-21 to the surface of viable SH-SY5Y cells, FACS analysis was performed. Adherently growing SH-SY5Y cells were washed with room temperature PBS. Then for detachment from the bottom of the Petri dish, cells were incubated with 1.5 ml of 0.05% Trypsin/EDTA solution (1×Gibco, Life Technologies) at 37 °C with 5% CO₂ for 2-5 minutes and finally cell detachment was empirically assessed by visual inspection. Subsequently, 1.5 ml of SH-SY5Y culture medium was added and mixed gently by pipetting. Cells were taken in a Falcon tube and spun down at 1500 rpm for 10 minutes. Cells were resuspended in PBS containing 1% BSA at a concentration of $0.5-2 \times 10^6$ cells/ml, as determined by counting using a FACSCalibur™ (Becton Dickinson; San Jose).

Biotin-TLQP-21 (28, 10 or 5 µl of a 0.1 mM solution in filtered PBS, corresponding to 2.8, 1.0 and 0.5 mmoles of biotin-TLQP-21) was added to resuspended cells, and the mixture incubated at 4 °C for 30 minutes. The cells were then washed twice with PBS supplemented with 1% BSA (wash buffer), followed by centrifugation at 1500 rpm for 7 minutes. After the second wash, the supernatant was discarded gently, followed by vortexing to resuspend the pellet. Fluorescein-conjugated avidin (Thermo Scientific) was added at 10 or 20 µg/ml as per instructions of the supplier, and the mixture incubated at 4 °C for 30 minutes in the dark. Then after washing two times as before, the cells were measured with a FACSCalibur™ (Becton Dickinson; San Jose). When necessary, propidium iodine was added before analysis to exclude nonviable cells, using 10000 cells per treatment. Gates were set by forward and side scatter. For analysis, cells were calculated using Cell Quest Software (Becton Dickinson). As control, cells were treated with fluorescein-conjugated avidin (Thermo Scientific) only.

Effect of Oxymatrine (OMTR), an inhibitor of HSPA8 expression, on binding of Biotin-TLQP-21 to the surface of intact, live SH-SY5Y cells:

OMTR, an inhibitor of HSPA8 protein expression, with purity >97% was purchased from the Selleck Chemicals, USA.

SH-SY5Y cells treated with OMTR (0.4 mg/ml; 1.51 mM) and untreated control cells were collected. The cell suspension was further processed for flow cytometry analysis, as described before.

Box 2: Oxymatrine (OMTR), at a glance.

Over 70 candidate compounds were screened by Wang et al., 2010 to find out HSPA8 inhibitor. Among the compounds examined, Oxymatrine (OMTR), molecular weight (MW) 264.31 (Figure 15) an alkaloid extract from *Sophera flavescens* (Ling et al., 2007) (popularly known as ku shen plant, Figure 16), showed significant activity to down regulate the expression of HSPA8 in HepG2 liver cells without showing any toxicity to the cells. Additionally, Western blotting confirmed the reducing effect at the protein level showing reduction of HSPA8 protein in the OMTR treated cells (Wang et al., 2010).

Phosphoprotein gel staining:

Petri dishes with confluent SH-SY5Y cells were incubated for 6 hours with the peptide TLQP-21 at a concentration of 1µg/ml. Then the cell homogenates were prepared as discussed above. As control, cells without peptide incubation were grown, then homogenized under the same conditions as treated cells.

Cell homogenate samples (20 µl) were boiled in 2X Laemmli buffer (Bio-Rad) for 10 minutes at 100 °C, spun, and loaded to SDS-PAGE gel. After electrophoresis (200V, 01h), the gels were washed in dH₂O for 10 minutes. Then the gels were incubated with fixing solution (50% methanol and 10% acetic acid) for 30 minutes at room temperature in an orbital shaker step at 50 rpm. The fixation step was repeated once. Followed by washing the gel with water three times each for ten minutes, the gels were incubated for one and half hour with Pro-Q^R Diamond (Invitrogen) gel stain in the dark with agitation at 50 rpm. The gels were then destained with Pro-Q^R Diamond phosphoprotein gel destaining solution (20 % acetonitrile, 50 mM sodium acetate, pH 4) for 30 minutes with shaking. The destaining procedure was repeated two times more, followed by washing the gels two times with water, each for 5 minutes. Finally, the gel was imaged using a Typhoon FLA9500 scanner at a 100µm resolution at 532nm green laser.

Proteomic study:

Protein preparation and processing:

SH-SY5Y cells were grown as described earlier in the SH-SY5Y cell culture section. Petri dishes with confluent SH-SY5Y cells were incubated for 6 hours with the TLQP-21 peptide at a concentration of 1µg/ml. Then the cell homogenates were prepared as discussed above. As control, cells without peptide incubation were grown, then

homogenized under the same conditions as treated cells. Both the cell homogenates treated with peptide and control (without peptide treatment) were precipitated with 60% trichloroacetic acid in acetone as follows:

Frozen extracts were resuspended in half of their volume with a 60% TCA/acetone solution and kept during 45 minutes on ice. The samples were then centrifuged at 10000 g during 1 minute at 4°C and the supernatant was discarded. The pellet was resuspended in 500 µl of cold acetone and sonicated with 3-4 pulses in the ultrasonic cell disruptor Sonifier 150 (Branson) until it was broken up. The sample had to be maintained cold, so for this purpose it was kept on ice. The samples were then centrifuged at 10000 g during 1 minute at 4°C. Precipitation and resuspension steps were repeated twice. The last supernatant was discarded and the last pellet was left to air dry.

The dry pellet was finally resuspended in a minimum volume of 2D sample buffer (5 M urea, 2 M thiourea, 2 mM tributyl-phosphine, 65 mM DTT, 65 mM CHAPS, 0.15 M NDSB-256, 1 mM sodium vanadate, 0.1 mM sodium fluoride, and 1 mM benzamidine). Thus the sample was ready to quantify.

Protein quantitation:

Protein quantitation was performed with the Coomassie Plus protein reagent (Thermo Scientific) that is a compatible method with the 2D buffer used to solubilize the samples. Samples in 2-DE buffer, 50 µL of Coomassie Plus and BSA (2 mg/mL) solution (BSA was resuspended in PBS) were allowed to reach room temperature. A standard curve was constructed as follows: six different points were obtained with consecutive dilutions 1:2 of a BSA solution (1 mg/mL), using as solvent the buffer in which the sample was diluted, i.e. 2-DE buffer. For the first data point 20 µL of 2-DE buffer and 20 µL of BSA

solution (2mg/ml) were mixed. The six points of the standard curve had the following concentrations of BSA: 1000; 500; 250; 125; 62,5; 31,25 $\mu\text{g/mL}$. Two μl of each sample were analyzed. The Coomassie reagent was allowed to stand at room temperature, and then 600 μl were added to each sample. They were mixed and let stand at RT during 5 minutes. Absorbance at 595 nm was then measured in a Genesis 20 spectrophotometer (Thermo Scientific). A blank was prepared with the solvent (20 μL) and Coomassie (600 μL) for the samples of the standard curve and 2 μl of the solvent and 600 μl of Coomassie for the samples of unknown concentration. Each sample was measured twice; in case both measurements diverged more than 10%, the sample was prepared and measured again. With all the measurements, a standard curve was constructed with the Excel program (Microsoft).

Bi-dimensional (2-D) gel electrophoresis:

Cell homogenates treated with peptide and control (without peptide treatment) were subjected to two dimensional gel electrophoresis-based proteome analysis.

Rehydration of IPG strips:

Rehydration of the IPG strips is a passive rehydration that takes place during 14-16 hours. The strips used had a pH gradient of pH 4-7 and 24 cm (GE Healthcare) and the final volume of rehydration buffer was 500 μl . 600 μg of the sample was mixed with 1,6% (v/v) of ampholytes (pH 4-7) (SERVA Electrophoresis GmbH). 2-DE buffer (see previous section) was added to a final volume of 500 μl . The mixture was vortexed and centrifuged during 5 min at 10000g to avoid any type of impurities. The sample was pipetted in a lane of the rehydration tray (Immobiline Dry Strip Reswelling Tray, GE Healthcare). The gel of the strip was in contact with the sample. The strip was covered with mineral oil Dry Strip Cover Fluid (GE Healthcare) to avoid evaporations and it was

left in rehydration overnight. The following day the strip was blotted on a filter paper to remove oil. Finally, the strips were placed in a Multiphor II electrophoresis unit (GE Healthcare) to perform the first dimension separation.

Isoelectrofocusing (first dimension):

The IPG strips were placed in the Multiphor II electrophoresis unit with the gel up. Small pieces of electrode paper were humidified with milliQ water and placed in the ends of the strips to absorb the remaining salts. The IPG strips were covered with mineral oil. The electrodes were set in place and the programme was set as described in Table 4. The first dimension was carried out at 17°C.

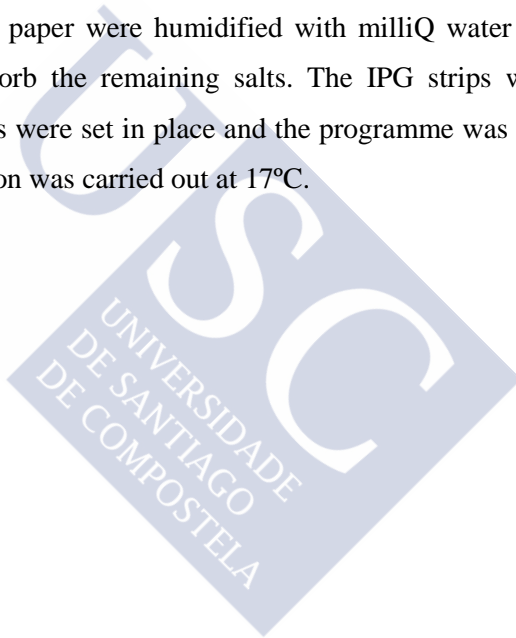


Table 4: Conditions of the isoelectrofocusing performed in the first dimension.

PHASE	VOLTAGE	AMPERAGE	WATTAGE	TIME
1	300V	3mA	5W	1 minute
2	300V	10mA	5W	2 hours
3	3500V	10mA	5W	3 hours
4	3500V	10mA	5W	21 hours

Equilibration:

After the first dimension the strips were equilibrated, reduced and alkylated: First the strips were treated 15 minutes at room temperature and in agitation with the reducing buffer (50 mMTris, pH 8,8; 4M urea; 2% (v/v) SDS; 30%(v/v) glycerol; 2% (w/v) DTT and traces of bromophenol blue).After this, the strips were gently washed with milliQ water and incubated this time in an alkylating buffer (same composition as the reducing buffer but without DTT and with 2.5% (w/v) iodoacetamide Alkylation with

iodoacetamide after cysteine reduction results in the covalent addition of a carbamidomethyl group (57.07 Da) and prevents the regeneration of disulfide bonds. The strips were incubated in this buffer during 15 minutes at RT and in agitation. Finally the strips were washed gently with milliQ water.

SDS-PAGE (second dimension):

The second dimension was performed on 10% large polyacrylamide gels. The DALT six Gel Caster system (GE Healthcare) was used to polymerize the gels. With this system it is possible to prepare 6 gels at the same time, therefore, the reproducibility of the system is higher. Bis-acrylamide (37.5:1, 30% w/v) was used in the presence of N,N,N',N'-tetrametil-etilendiamine (TEMED) and ammonium persulfate, (APS) (Table 5). The gels were prepared the day before their use and they were allowed to polymerize during 5 hours at room temperature. After this, the gels were kept at 4°C overnight protected with a storage solution (0.1% SDS, 375mM Tris pH 8.8) to avoid dehydration. The equilibrated strips were placed onto the gel with a 0.5% (w/v) agarose solution avoiding bubbles between the strip and the gel.

Table 5: Reagents used for the preparation of the gels.

REAGENTS	6 gels 10%
Bis-Acrylamide	150 mL
Tris pH 8,8 1,5M	113 mL
SDS 10% (filtered)	4,50 mL
Water milliQ	147,23 mL
APS (10%)	4,50 mL
TEMED (10%)	0,77 mL
Rhinohide	30 mL

The second dimension was carried out in the EttanDALT six system (GE Healthcare), with electrophoresis buffer (0.25 M Tris BASE, 1.92 M Glycine, 1% (w/v SDS) for 5 hours at 10°C with the program detailed in Table 6.

Table 6: Program for the second dimension (25x20 cm gels).

PHASE	VOLTAGE (v)	AMPERAGE (mA)	WATAGE (W)	TIME
1	80	20/gel	2/gel	1 hour
2	500	40/gel	17/gel (100W as maximum)	6 hour

Staining and scanning:

The gels were stained with Sypro Ruby fluorescent dye (Lonza). When the second dimension was finished, the gels were extracted carefully from the glasses and they were washed with water during 10 min. Gels were washed for 1 hour in 10% methanol/7% acetic acid, followed by stained overnight with Sypro Ruby solution. Gels had to be protected from the light. For this purpose the boxes that contained the gels were covered with a black plastic bag. After staining, gels were washed with 10% methanol/7% acetic acid during 1 hour, and subsequently in milliQ water for 10 minutes. All these steps were carried out with enough volume of solutions (300 ml) and in constant agitation. Finally the gels were scanned in a Typhoon 9410 scanner (GE Healthcare). The programme used to scan the images was Typhoon Scanner Control, version 5.0 and the following parameters were chosen: resolution 200 μm , blue laser with an excitation wavelength of 488nm, filter 610 nm, medium sensitivity, and photomultiplier 600V.

After scanning the images were converted to a high resolution TIF format to be imported to the image analysis software: Ludesi REDFIN 3 (Ludesi, Malmö, Sweden) The gels were kept in plastic bags in vacuum and they were stored at 4°C until spot excision.

Differential image analysis:

Images were processed using Ludesi REDFIN 3 Software. Four gels from each sample were analyzed. Images were analyzed using the LudesiRedfin Solo protocol. In this approach, spot detection and image segmentation takes place in a composite image (see below) and the same spot positions and borders are then applied to all images, after compensation for geometric distortions. The advantages of this protocol are its simplicity and that every detected protein spot will be assigned a volume in each image. A disadvantage is that some spots may be assigned misshaped/misaligned borders, leading to an incorrectly measured spot volume. The results may later be quality controlled by inspection of the individual images and errors can be manually corrected. The steps performed in this process were:

- 1) Image registration and alignment: The first step is to register matching points in the gel images, based on features or patterns that can be seen in the image. Using this information the images can be aligned and geometrically transformed (warped) so that matching protein spots appear at the same position in the warped images. The spots should overlap when the warped images are stacked on top of each other. LudesiRedfin Solo uses a semi-automatic approach, where a human indicates matching points in the images, which are subsequently improved by computer algorithms. One gel is selected as the reference gel, and all other gels are aligned/warped to it.

2) Composite image: A composite image (consensus image or fusion image) is created by merging all the gel images into a single representative image. This image will then contain all the spots from the individual gels. In order to avoid artifacts, such as cracks or large stains, from being included in the composite image, it is possible to choose to exclude some images, or image regions, when creating the fusion image.

3) Spot detection: Spot detection involves using algorithms to detect all real protein spots in the images, while avoiding falsely detecting anything in the images that does not represent a true spot. The sensitivity of the spot detection algorithm is adjusted to work well with the specific images. The detected spot positions should be checked for both falsely detected spots and undetected spots.

4) Segmentation: The image segmentation step determines which region in the images contains each protein spot. The region outline (spot border) should encompass all of the stained area belonging to the spot and nothing from nearby spots. In the Redfin Solo protocol, spot borders are determined in the composite image and are then applied, after warping, to all the individual images. After this, verification and adjustment of spot positions and borders can be done in each individual image.

5) Quantitation: Quantitation is the process of measuring the cumulative staining intensity contained within a spot which in turn corresponds to the relative protein volume. This involves calculating the local background level around a spot, and subtracting this background level from the staining level contained within the spot as defined by the spot border. The result is a calculation of the total, background corrected, and staining level of the spot.

6) Normalization: Normalization is the process of making these spot volumes comparable between gel images in the face of technical differences in staining, scanning, sample volume, and so on. Ludesi uses a method of normalization that works with gel

pairs. The algorithm computes a normalization factor for each gel and uses it to normalize the spot volumes in that gel:

- For each gel pair that has been matched, all matches between the two gels are extracted. The top 50% matches, based on the spot volumes, are kept.
- A spot volume ratio is calculated between each kept spot pair match. A pair-wise normalization factor between the gels is computed by taking the median of these ratios. This ensures robustness and accuracy even if the project contains up to 50% regulated spot volumes.
- Each gel normalization factor is computed by optimizing an over-determined equation system, resulting from the pairwise normalization factors.
- Finally, the spot volumes in each gel are multiplied with the corresponding gel normalization factor.

Statistical analysis:

To help determine statistically significant differences between groups of samples One-way ANOVA ("Analysis Of Variance") method for statistical hypothesis testing was employed. For each spot ID, ANOVA p-value was calculated using the quantified and normalized volumes for the matched spot in each of the images. ANOVA is a parametric method that assumes independency and normal distribution of all values and is capable of comparing multiple groups. For comparisons between two groups only, the ANOVA becomes equivalent to the two-sided Student's t-test. In this study differential expression

of proteins was defined on the basis of >1.5-fold change between group averages and $p < 0.05$.

Protein identification using mass spectrometric analysis:

Spots chosen for mass spectrometric analysis were excised from the gels with a pipette tip and manually in-gel digested with trypsin following the protocol described by Shevchenko et al., 2006. The excised spots were washed three times with 100 μ l of ammonium bicarbonate 50 mM in 50% methanol (grade HPLC Scharlau) and reduced with 10 mM DTT (SERVA Electrophoresis GmbH). After this, the gel pieces were washed three times with ammonium bicarbonate, dried in a SpeedVac (Thermo Scientific) and alkylated with 55 mM Iodoacetamide (IAA) (Sigma- Aldrich). The gel pieces were washed again with ammonium bicarbonate, dehydrated with acetonitrile and dried again in a SpeedVac (Thermo Scientific). Porcine modified trypsin (Promega) was added to a final concentration of 20 ng/mL in 20 mM ammonium bicarbonate and digestion let proceed overnight at 37°C.

Peptide extraction from the gel pieces was carried out three times with 40 μ L of 60% acetonitrile in 0.5% of formic acid. Extracts were pooled, dried in the SpeedVac (Thermo Scientific) and stored at -20°C. After digestion the spots were identified using a model 4800 MALDITOF/TOF mass spectrometer (ABSciex, Framingham, MA, EEUU) at the Proteomics Lab of the Foundation IDICHUS (Hospital Clínic, University of Santiago de Compostela), as per protocol described above. All MS/MS spectra were performed by selecting the precursor ions with a relative resolution of 300 (FWHM) and metastable suppression. Automated analysis of mass data was achieved by using the 4000 Series.

Explorer Software V3.5. MS and MS/MS spectra data were combined through the GPS Explorer Software v3.6. Database search was performed with the Mascot v2.1 search tool (Matrix Science, London, UK) screening SwissProt (release 56.0). Searches were restricted to human taxonomy, setting carbamidomethyl cysteine as a fixed modification and oxidized methionine as potential variable modification. Both the precursor mass tolerance and the MS/MS tolerance were set at 30 ppm and 0.35 Da, respectively, allowing 1 missed tryptic cleavage site. All spectra and database results were manually inspected in detail using the above software.





Results



Crosslinking and detection of a TLQP-21 binding protein in SH-SY5Y cell homogenate:

In order to confirm the presence of a TLQP-21 receptor or receptors in SH-SY5Y cell homogenates, a modified version of the approach described by Ayub (2012) was used. Such approach relies on probing a cell homogenate with biotinylated TLQP-21; after chemical cross-linking with the hetero-bifunctional reagent Sulfo-EMCS (Figure 4) to stabilize any putative receptor: peptide complex, the reaction mixture is subjected to SDS-PAGE, transferred to a PVDF membrane and probed with HRP-avidin, so as to detect any protein bound to the biotinylated peptide.

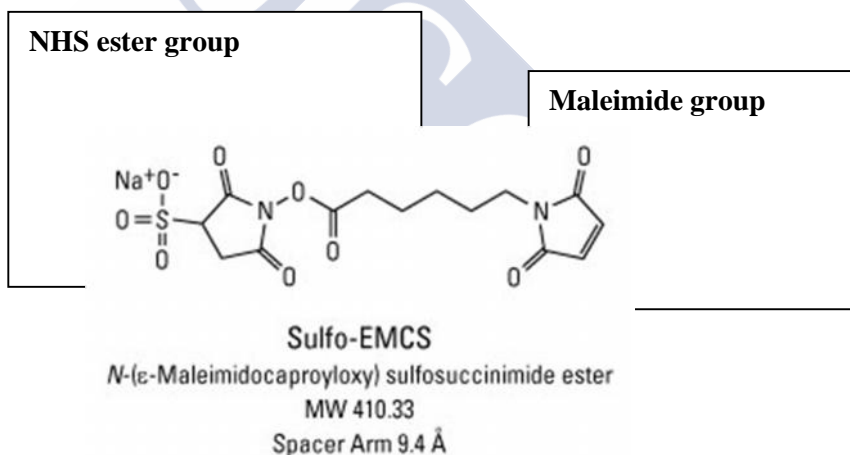


Figure 4: Chemical structure of Sulfo-EMCS crosslinking reagent highlighting NHS ester and maleimide group.

The cross-linking reaction is carried out in two steps: first, the maleimide moiety in sulfo-EMCS reacts with the extra C residue in the specially designed biotinyl-TLQP-21; then, this “activated” biotinyl-TLQP-21 is mixed with the cell homogenate and the

sulfo-NHS-ester “traps” any free amino group that is within reach, i.e., that is part of a protein bound to the activated, biotinylated TLQP-21 (Figure 5).

While the two steps of the reaction are carried out one immediately after the other, following the steps of Ayub (2012), the correct activation of the biotinylated peptide was checked by MALDI-TOF mass spectrometry (MS) to be sure that the peptide TLQP-21 was conjugated correctly to Sulfo-EMCS under the conditions used.

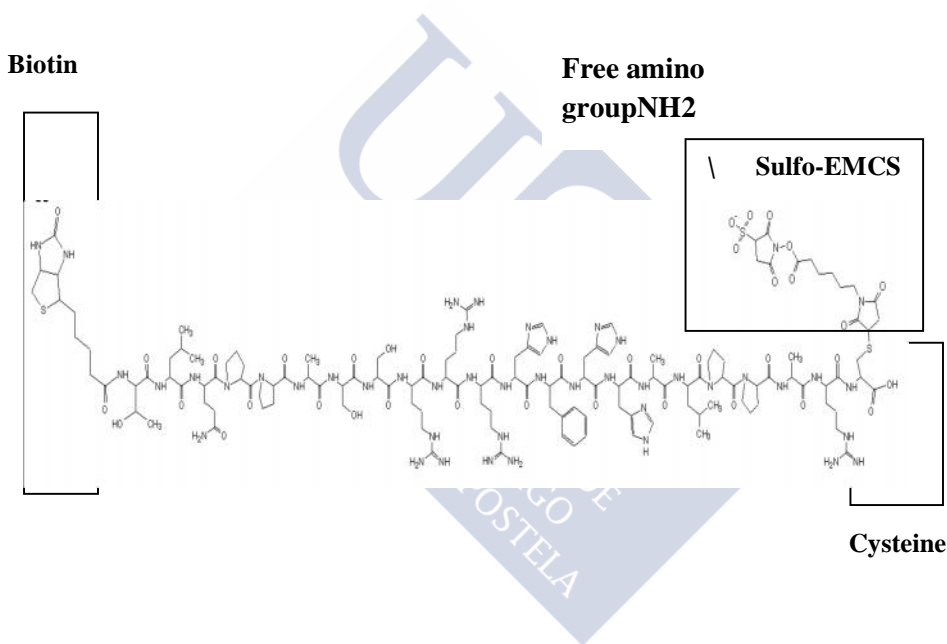
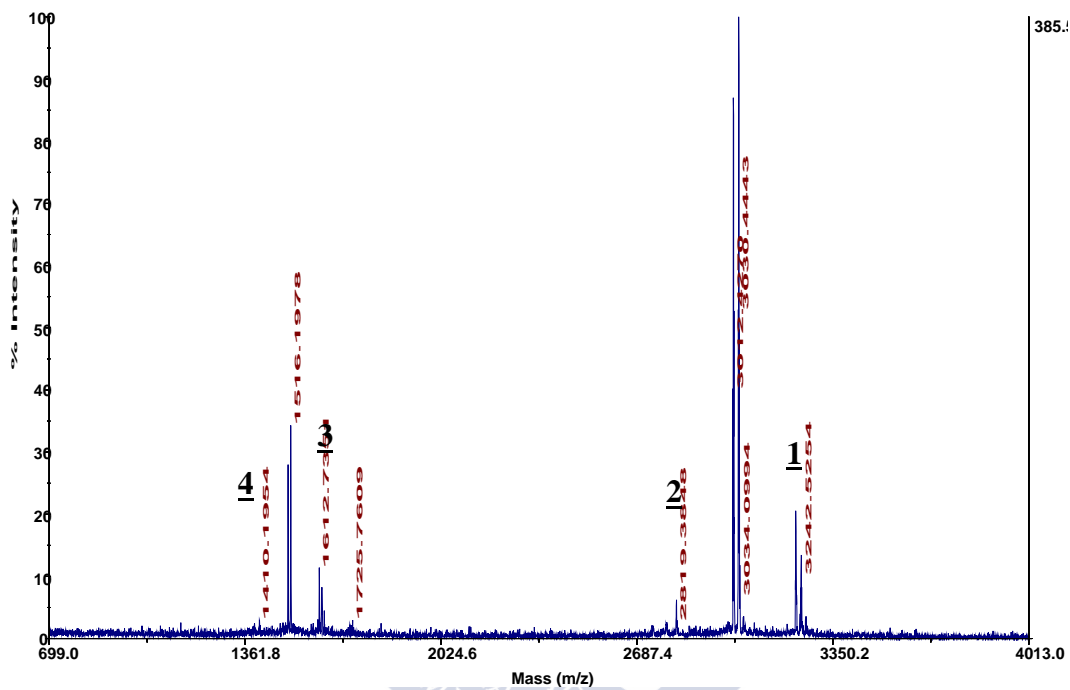


Figure 5: The structure of the conjugated TLQP-21 with Sulfo-EMCS that traps free amino group.

A.

4700 Reflector Spec #1 MC[BP = 3031.4, 385]

UNIVERSITY OF
MILANO
DIPARTIMENTO DI
FARMACIA
E BIOTECNOLOGIA
FARMACIA
E BIOTECNOLOGIA

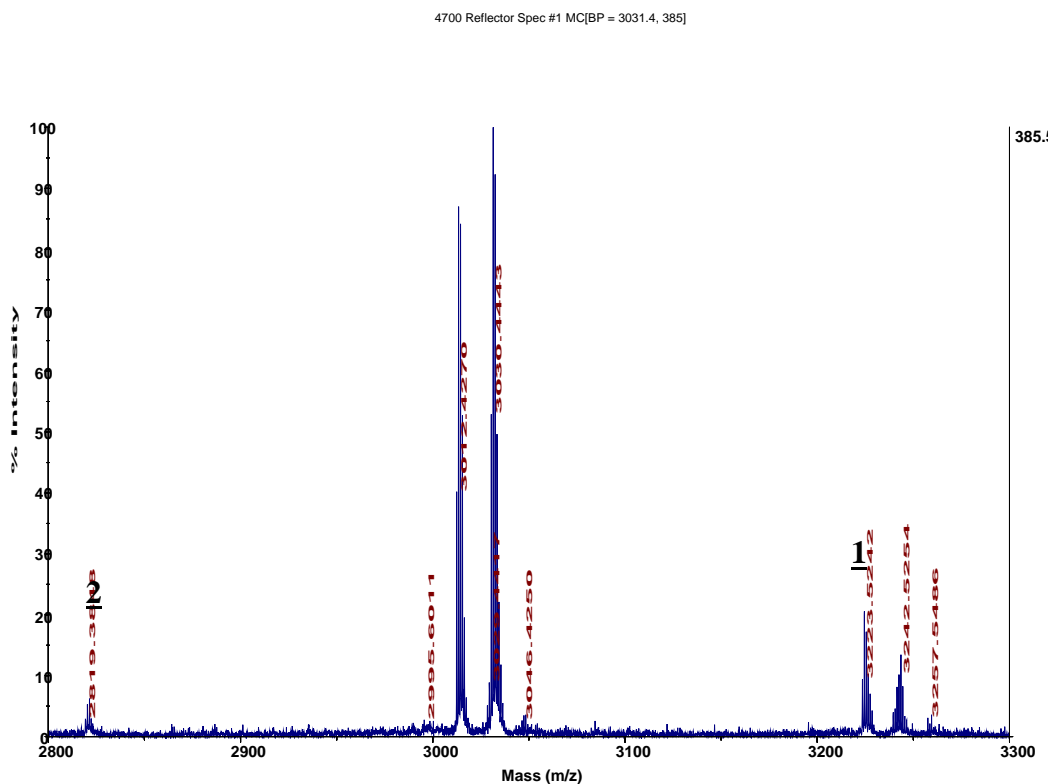
B.

Figure 6: MALDI-TOF MS confirmation of formation of a stable thioether linkage between Sulfo-EMCS and Biotin-TLQP-21. Biotin-TLQP-21 was conjugated to Sulfo-EMCS, followed by sample clean up using C₁₈ resin Zip Tips (Millipore) and MALDI-TOF MS analysis. **A:** full spectrum; **(1)**The peak at m/z 3223.52 corresponds to TLQP-21 conjugated to Sulfo-EMCS. **(2)** The peak at m/z 2819.38 corresponds to unconjugated TLQP-21. **(3)** The peak at m/z 1612.73 corresponds to doubly charged Sulfo-EMCS conjugated to the peptide. **(4)** The peak at m/z 1410.19 corresponds to doubly charged, unconjugated TLQP-21. **B:** zoom on the m/z range where the peaks of interest appear; **(1)**The peak at m/z 3223.52 corresponds to TLQP-21 conjugated to Sulfo-EMCS. **(2)**The peak at m/z 2819.38 corresponds to unconjugated TLQP-21. See text for additional details.

MALDI-TOF spectra of reaction products showed generation of the expected thioether adduct (Figure 6): the theoretical MW of the peptide + Sulfo-EMCS thioether adduct is 3208 Da (with Na^+ being replaced by H^+ as a consequence of protonation of the sulfo group under the strongly acidic conditions of sample preparation for MALDI). A peak with an m/z of 3223.52 was detected; the ~ 17 kDa difference agrees with the characteristic -OH addition and rearrangement of the maleimide moiety during MALDI (Borges & Watson, 2003, Figure 7). Additional peaks in the spectrum correspond to doubly charged products.

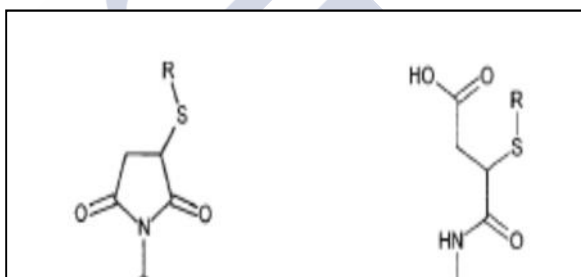


Figure 7: Rearrangement of cysteine maleimide adducts during MALDI (From Borges & Watson, 2003).

Once it was ascertained that the reaction conditions were adequate for generation of a stable activated peptide, the crosslinking reaction was carried out by conjugation of Sulfo-EMCS to TLQP-21 and then immediate reaction of the activated peptide with an SH-SY5Y cell homogenate on ice for 2 hours, terminated by 50 mM Tris buffer (pH 8.0), which contains primary amines reacting with unconjugated crosslinker, if any; followed by separation by SDS-PAGE and Western blotting using high sensitivity streptavidin-HRP, as the peptide had biotin tagged at N-terminal end.

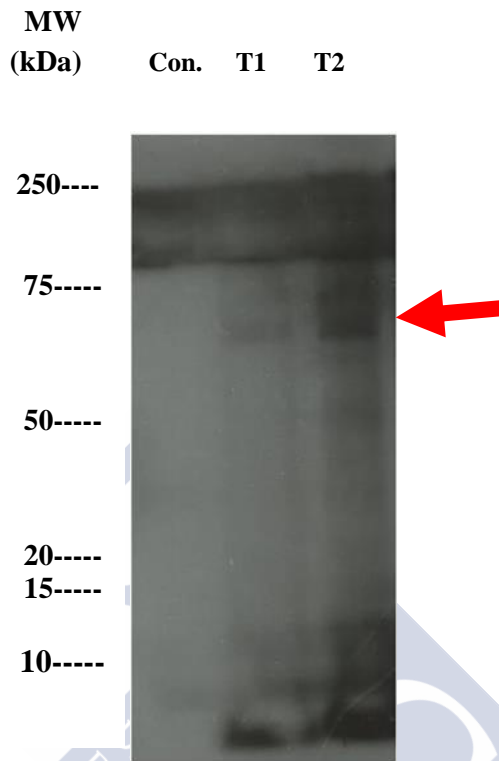


Figure 8: The crosslinking reaction of Sulfo-EMCS conjugated VGF-derived peptide TLQP -21 to SH-SY5Y cell homogenate traps a 75 kDa TLQP-21-binding protein. The Sulfo-EMCS conjugated peptide biotin-TLQP-21 was incubated with SH-SY5Y cell homogenates followed by resolving by SDS-PAGE, and probed with HRP-avidin. A 75 kDa protein band is visible in the reaction mixture containing TLQP-21 (T1 and T2), whereas in the control sample (C, homogenate incubated with unconjugated Sulfo-EMCS crosslinker and conjugation buffer, without any conjugated peptide) no band was detected. T2 lane corresponds to the double amount of sample loaded as compared to T1.

As shown in Figure 8, a 75 kDa protein band is visible in T1 and T2 lanes. In T1 lane, the band was less prominent as the amount of loaded protein sample was doubled in T2

lane whereas in control lane no protein band was found there. All these indicate that the intensity of the 75 kDa band in the sample is enormous greater than the control lane.

To optimize the conditions, the crosslinking reaction was also performed with higher amount (50 and 100 μg) of cell lysate protein as well as with higher amount (20 and 100 μM) of conjugated peptide. But the best result was obtained using 10 μg of protein added to 10 μM conjugated peptide (data not shown).

Identification of a receptor of human TLQP-21:

Once the presence of a TLQP-21-binding protein in SH-SY5Y cell homogenates was confirmed, cell homogenates were subjected to affinity chromatography on a biotinyl-TLQP-21-loaded avidin column to adsorb and isolate the 75 kDa binding protein that was cross-linked to TLQP-21. Following affinity chromatography, SDS-PAGE of eluted fractions and SYPRO[®] Ruby protein staining, a protein band of 75 kDa was detected that was not present in the elution fractions of the control sample applied to an avidin agarose column lacking the biotinyl-TLQP-21 peptide (Figure 9). This band was excised and analyzed by nanoHPLC-electrospray MS/MS. MASCOT analysis of the spectra (Table 7) identified total 3 proteins, considering exclusion parameters (Nesvizhskii et al., 2007): Heat shock cognate 71 kDa protein (HSPA8/HSC70), Stress-70 protein (HSPA9/mortalin), and 78 kDa glucose-regulated protein (HSPA5). Sequence coverages and scores varied from highest for HSPA8 (19.8, 735), middle for HSPA9 (12.5, 431), to lowest for HSPA5 (5.4, 216) (Table 7, Figure 10). For this latter protein, only 3 peptides were identified, at the borderline of exclusion parameters; therefore, we concentrated our attention on HSPA8 and HSPA9. Given the predominantly mitochondrial localization of HSPA9/mortalin (Deocarlis et al., 2008; Kaul, 2002; 2006; Bhattacharyya et al., 1995) compared to the known presence of HSPA8 in the cell membrane (Shin, et al., 2002; Liao and Tang, 2014; Mambula et al., 2006; Kettner et al., 2007; Powers et al., 2008),

we further narrowed our interest on HSPA8 as the most promising candidate to be a receptor of VGF-derived peptide TLQP-21, which was further validated afterwards (see below).

MW CF2 CF3 CF4 CF5 CF6 TF2 TF3 TF4 TF5 TF6
(kDa)

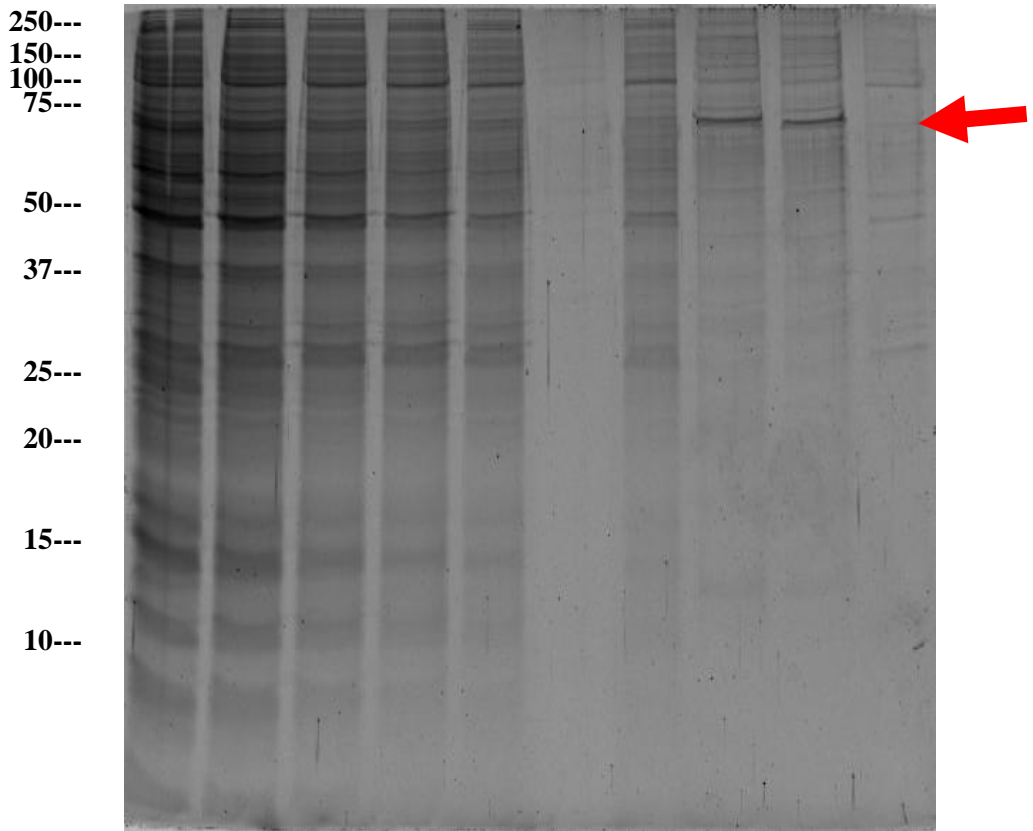


Figure 9: Biotin-TLQP-21 interacts with a 75 kDa protein in SH-SY5Y cell homogenate. SH-SY5Y cell homogenates were applied to the monomeric avidin column loaded with biotin-TLQP-21. The eluted fractions were resolved by SDS-PAGE and analysed by Sypro ruby staining. A 75 kDa protein band was apparent in (fractions eluted from the TLQP-21 column, TF 4-5) but not in the corresponding elution fractions obtained from column without TLQP-21 attached (control fraction, CF4-5).

Table 7: MASCOT analysis of tryptic peptides extracted from the 75 kDa band.

Protein	Score	MW(kDa)	Sequence coverage	Number of unique peptides
Heat shock cognate 71 kDa protein(HSPA8)	735.0	70.9	19.8	12
Stress-70 protein (HSPA9/mortalin)	430.0	73.6	12.5	07
78 kDa glucose-regulated protein (HSPA5)	216.0	72.3	5.4	03

A.

10	20	30	40	50	60	70	80
MSKGPVAGID	LGTTYSCVGV	FQHGKVEIIA	NDQGNRTTPS	YVAFDTERL	IGDAAKQVA	MNPTNTVFDA	KRLIGRRFDD
90	100	110	120	130	140	150	160
AVVQSDMKHW	PFMVNDAGR	PKVQVEYKGE	TKSFYPEEVS	SMVLTKMKEI	AEAYLGKTVT	NAVVTVPAYF	NDSQRQATKD
170	180	190	200	210	220	230	240
AGTIAGLNVL	RIINEPTAAA	IAYGLDKKVG	AERNVLIFDL	GGTFDVSIL	TIEDGIFEVK	STAGDTHLGG	EDFDRMNVNH
250	260	270	280	290	300	310	320
FIAEFKRKHK	KDISENKRAV	RLRTACERA	KRTLSSSTQA	SIEIDSLYEG	IDFYTSITRA	RFEELNADLF	RGTLDPVEKA
330	340	350	360	370	380	390	400
LRDAKLDKSQ	IHDIVLVGGS	TRIPKIQLL	QDFPNGKELN	KSINPDEAVA	YGAAVQAAIL	SGDKSENVQD	LLLLDVTPLS
410	420	430	440	450	460	470	480
LGIETAGGVM	TVLIKRNTTI	PTKQTQTFTT	YSDNQPGVLI	QVYGERAMT	KDNNLGKFE	LTGIPPAPRG	VPQIEVTFDI
490	500	510	520	530	540	550	560
DANGILNLSA	VDKSTGKENE	ITITNDKGRLL	SKEDIERMVQ	EAEKYKAED	KQRDKVSSKN	SLESYAFNMK	ATVEDEKLQG
570	580	590	600	610	620	630	640
KINDEKQKI	LDKNEIINW	LDKNTAEKE	EFEHQQKELE	KVCNPIITKL	YQSAGGMPGG	MPGGFPGGGA	PPSGGASSGP
650							
TIEEVD							

B.

10	20	30	40	50	60	70	80
MISASRAAAA	RLVGAAASRG	PTAARHQDSW	NGLSHEAFRL	VSRRDYASEA	IKGAVVGIDL	GTTNSCVAVM	EGKQAKVLEN
90	100	110	120	130	140	150	160
REGARTTPSV	VAFPTADGERL	VMMPAKRQAV	TNPNTFYAT	KRLIGRRYDD	PEVQKDIKNV	PFKIVRASNG	DAWVEAHGKL
170	180	190	200	210	220	230	240
YSPSQIGAFV	LMKMKETAEN	YLGHTAKNAV	ITVPAYFNDS	QRQATKDAQG	ISGLNVLRVI	NEPTAAALAY	GLDKSEDKVI
250	260	270	280	290	300	310	320
AVYDLGGGTF	DISILEIQKG	VFEVKSTNGD	TFLGGEDFDQ	ALLRHIVKEF	KRETGVDLTK	DNMALQVRRE	AAEKAKCELS
330	340	350	360	370	380	390	400
SSVQTDINLP	YLTMDSSGPK	HLNMKLTRAQ	FEGIVTDLIR	RTIAPCQKAM	QDAEVSKSDI	GEVILVGGMT	RMPKVOQTVQ
410	420	430	440	450	460	470	480
DLFGRAPSKA	VNPDEAVAIG	AAIQGGVLAG	DVTDVLLLDV	TPLSLGIETL	GGVFTKLINR	NTTIPTKKSQ	VFSTAADGQT
490	500	510	520	530	540	550	560
QVEIKVQGE	REMAGDKGTG	GQFTLIGIPP	APRGPVQIEV	TFDIDANGIV	HVSAKDKGTG	REQQIVIQSS	GGLSKDIEIN
570	580	590	600	610	620	630	640
MVKNKAEYAE	EDRRKKEVE	AVNMAEGLH	DTETKMEEFK	DQLPADECNK	LKEEISKMRE	LLARKSETG	ENIRQAASSL
650	660	670	680				
QQASLKLIFEM	AYKMASERE	SGSGSGTGEQ	KEDQKEEKQ				

C.

10	20	30	40	50	60	70	80
MKLSLVAAML	LLLSAARAE	EDKKEDVGTV	VGIDLGTTYS	CVGVFKNGRV	EIIANDQGNR	ITPSYVAFPT	EGERLIGDAA
90	100	110	120	130	140	150	160
KNQLTSPEN	TVFDAQRLIG	RTWNPDSVQQ	DIKFLPFKVV	EKKTKPIYQV	DIGGGQTKTF	APEEISAMVL	TKMKETAEAY
170	180	190	200	210	220	230	240
LGKKVTHAVV	TVPAYNDAQV	RQATKAGTI	AGLNVMRIIN	EPTAAAIAYG	LDKREGEKNI	LVFDLGGGTF	DVSLLTIDNG
250	260	270	280	290	300	310	320
VFEVVAINGD	THLGGEDFDQ	RVMEHFILKY	KKKTGKDVVK	DNRAVQKLR	EVEKAKRALS	SQHARIEIE	SFYEGEDFSE
330	340	350	360	370	380	390	400
TLTRAKFEEL	NMDLFRSTMK	FVQKVLESD	LKKSDEIV	LVGGSTRIPK	IQQLVKEFFN	GKEPSRGINF	DEAVAYGAAV
410	420	430	440	450	460	470	480
QAGVLSGDQD	TGDLVLLDVC	PLTLGIETVG	GVMTKLIPRN	TVVPTKKSQI	FSTASDNQPT	VTIKVYEGER	PLTKDNHLLG
490	500	510	520	530	540	550	560
TFDLTGIPPA	PRGVPQIEVT	FEIDVNGILR	VTAEDKGTGN	KNKITITNDQ	NELTPEEIER	MVNDAEKFAE	EDKCLKERID
570	580	590	600	610	620	630	640
TRNELESYAY	SLKNQIGDKE	KLGGKLSSED	KETMEKAVEE	KIEWLESHQD	ADIEDFKAKK	KELEEIVQPI	ISKLYGSAGP
650	660						
PPTGEEDTAE	KDEL						

Figure 10: Comparative peptide coverage of tryptic peptides extracted from the 75 kDaband. **A.** ForHSPA8, there were 12 unique peptides identified, in red, with score: 735.0, MW [kDa]: 70.9, sequence coverage [%]: 19.8 **B.** For HSPA9/mortalin, there were 7 unique peptides identified, in red, with score: 430.9, MW [kDa]: 73.6, sequence Coverage [%]: 12.5 **C.** For HSPA5, there were 3 unique peptides identified, in red, with score: 216.0, MW [kDa]: 72.3, sequence coverage [%]: 5.4

Immunochemical validation of HSPA8:

The samples corresponding to fractions 4 and 5 (Figure 9) in which the 75 kDa band was detected by Sypro[®] ruby staining, were pooled together subjected to Western blot analysis with an anti-Hsc70 (HSPA8) antibody. As seen in Figure 11, the antibody reacted positively with the protein but not in the corresponding control fractions.

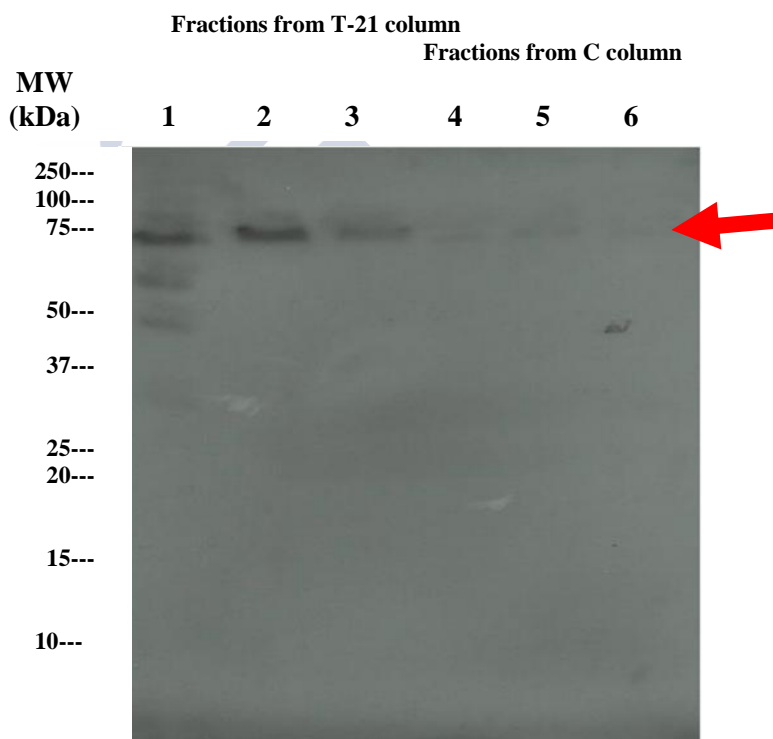


Figure 11: Immunochemical validation of HSPA8 as a TLQP-21 binding protein. The HSPA8 was confirmed at ~71 kDa by Western blot analysis of the fractions eluted from the column loaded with biotin-TLQP-21 (“TF”, T-21 column), but not in the equivalent fractions eluted from a control column not loaded with biotin-TLQP-21(C column).

Binding of biotinylated TLQP-21 to HSPA8 on the SH-SY5Y membrane:

Since we used, for practical reasons, whole cell homogenates in the experiments that led to identification of HSPA8 as a putative human TLQP-21 receptor, and considering that a considerable fraction of HSPA8 is localized in the cytoplasm, there was the possibility that its interaction with TLQP-21 might be artifactual, and it was imperative to demonstrate that TLQP-21 actually binds HSPA8 on the cell membrane. For this, biotinylated TLQP-21 was added to intact, live SH-SY5Y cells and cross-linked to putative membrane receptors with the bi-functional crosslinking reagent Sulfo-EMCS. Subsequently, the cells were homogenized and the homogenate subjected to affinity chromatography using a monomeric avidin column. Eluted fractions were resolved by SDS-PAGE, blotted, and membranes probed with anti-HSPA8 antibody. A positive ~71 kDa band corresponding to HSPA8 was detected in fractions 3, 4 and 5 (Figure 12), though in the previous monomeric avidin column purification fractions used for Sypro ruby staining, it was visible in 4 and 5 fractions, not in fraction 3 (Figure 9). The small mass increment added by biotin-TLQP-C (2820 Da) to HSPA8 is not sufficient to be detected in our SDS-PAGE system.

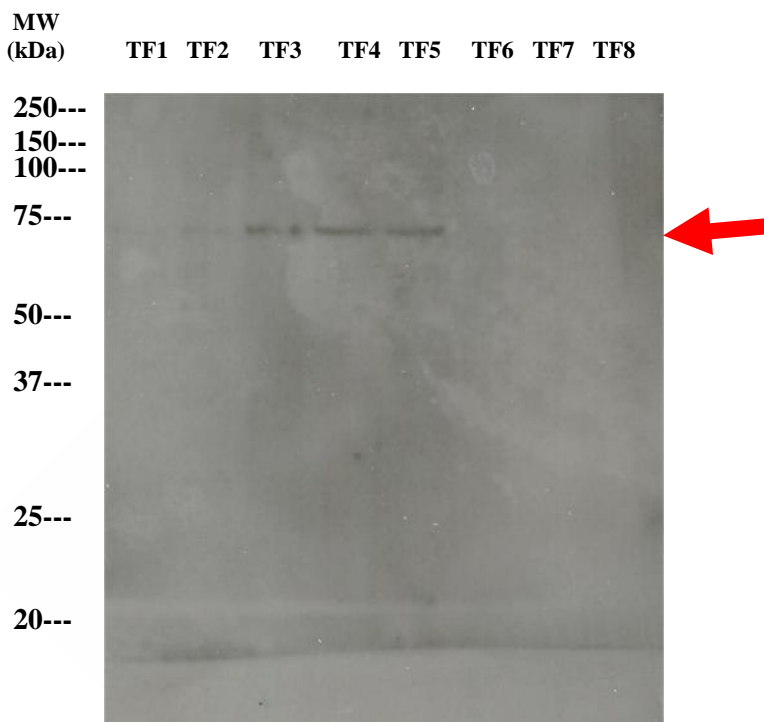


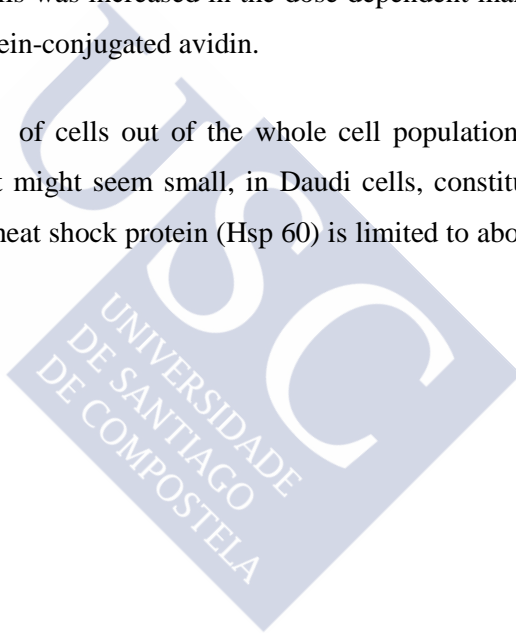
Figure 12: Binding of biotinylated TLQP-21 to HSPA8 on the SH-SY5Y membrane. Following biotinylation of membrane proteins, they were applied onto the monomeric avidin column. Finally, eluted proteins were recognized by Anti-HSPA8 antibody in fractions TF3, TF4 and TF5 lanes.

Binding of Biotin-TLQP-21 to the surface of intact, live SH-SY5Y cells: Demonstration by FACS analysis:

Live SH-SY5Y cells were incubated with 3 different volumes of 0.1 mM biotin-TLQP-21: 5, 10 and 28 μ l, respectively. Subsequently, cells were treated with fluorescein-conjugated avidin and subjected to FACS analysis. Phenotypic expression of surface binding of biotinyl-TLQP-21 by the cells was increased in the dose-dependent manner of

biotin-TLQP-21. Surface binding of biotin-TLQP-21 by the cells were 5.16%, 8.77% and 10.30% when the SH-SY5Y cells were incubated with 0.1 mM biotin-TLQP-21 with 5, 10 and 28 μ l, respectively that showed the tendency of an increasing dose-dependent manner. However, out of the whole cell population maximum 10.30% cells were proved to display positive staining expression of surface binding of biotinyl-TLQP-21 by the cells (Figure 13). Figure 14 shows the almost same result as Figure 13 though in that case, fluorescein-conjugated avidin was used 50% less showing that surface binding of biotin-TLQP-21 by the cells was increased in the dose-dependent manner due to biotin-TLQP-21, not for fluorescein-conjugated avidin.

However, only a 10.37% of cells out of the whole cell population display positive staining, a proportion that might seem small, in Daudi cells, constitutive cell surface expression of the 60 kDa heat shock protein (Hsp 60) is limited to about 10% (Cicconi, et al., 2004).



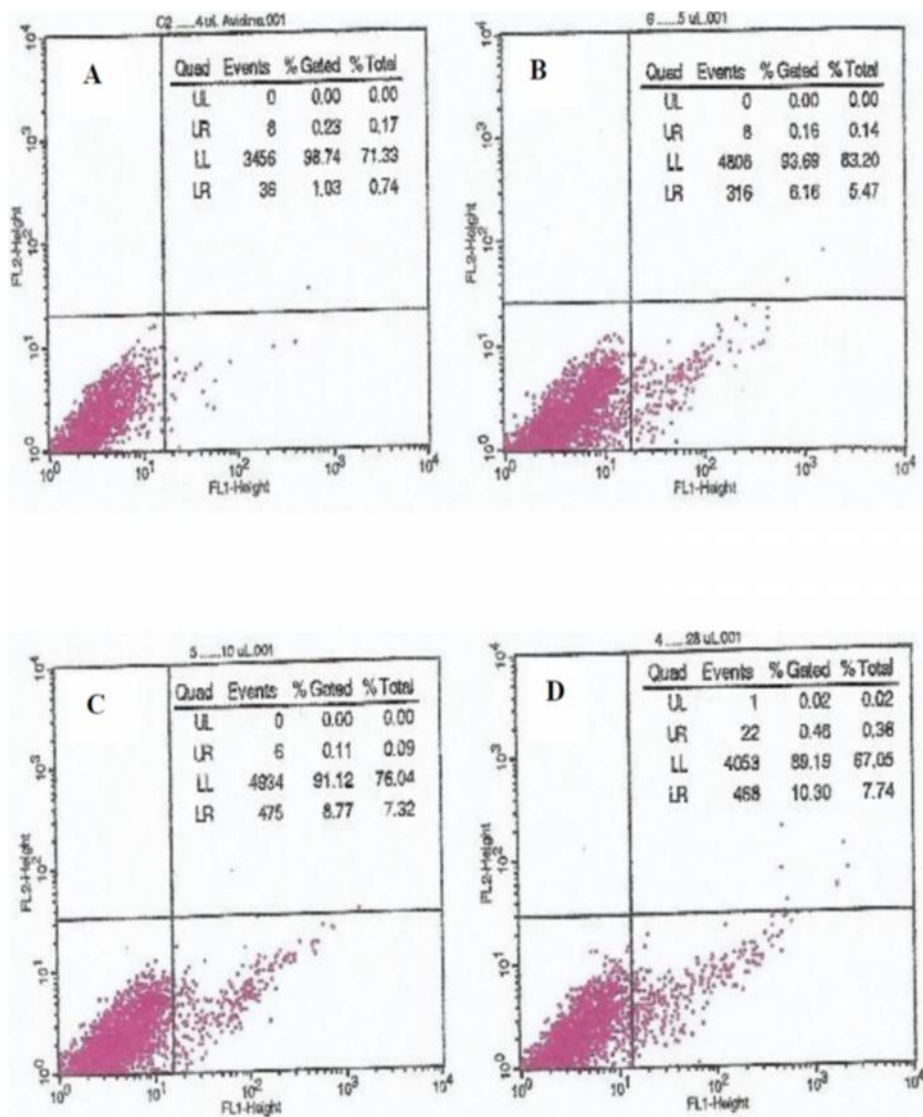


Figure 13: Binding of Biotin-TLQP-21 to SH-SY5Y cells analyzed by FACS. Incubation of SH-SY5Y cells with 0.1 mM Biotin-TLQP-21 with 5 μ l (B), 10 μ l (C) and 28 μ l (D), respectively followed by staining with avidin, fluorescein conjugated (20 μ g/ml) showed surface binding of biotin-TLQP-21 as 5.16%, 8.77% and 10.30%, respectively representing the tendency of an increasing dose-dependent manner.

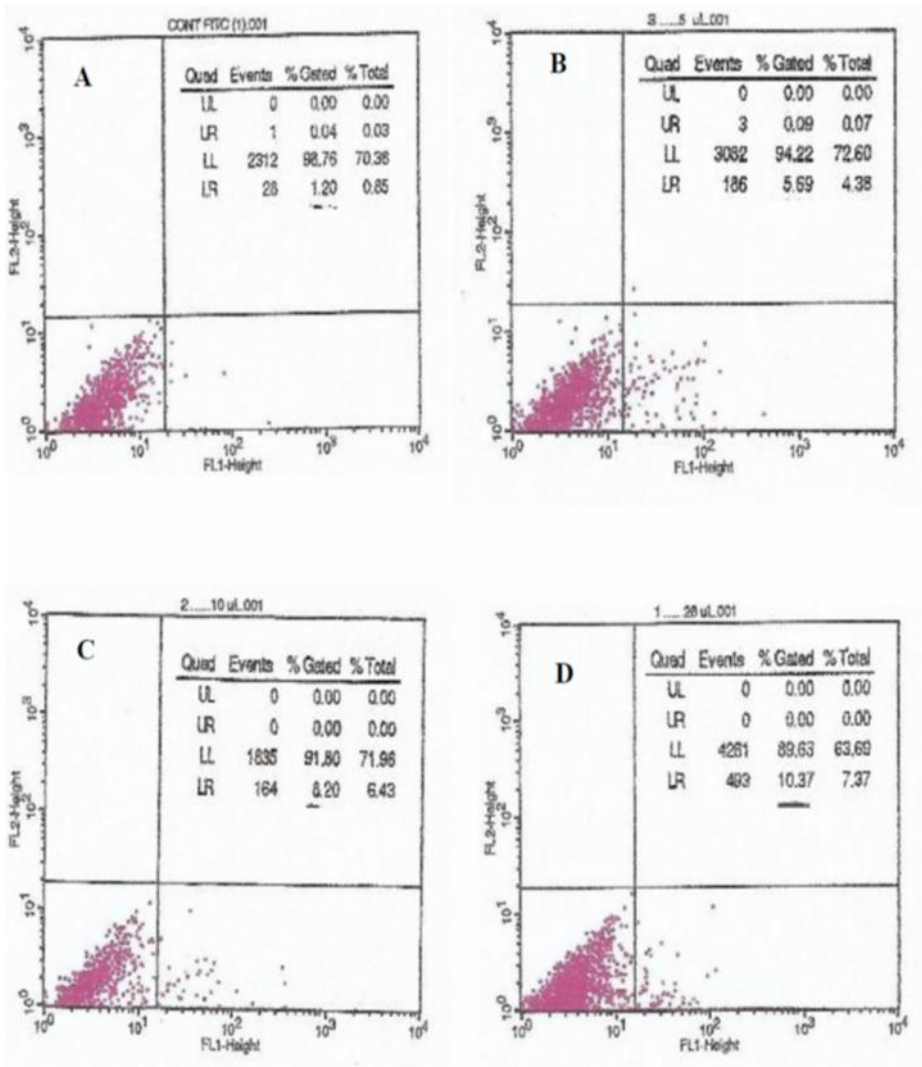


Figure 14: Binding of Biotin-TLQP-21 to SH-SY5Y cells analyzed by FACS. Incubation of SH-SY5Y cells with 0.1 mM Biotin-TLQP-21 with 5 μ l (B), 10 μ l (C) and 28 μ l (D), respectively followed by staining with avidin, fluorescein conjugated (10 μ g/ml) showed surface binding of biotin-TLQP-21 as 5.69%, 8.20% and 10.37%, respectively representing the tendency of an increasing dose-dependent manner.

Oxymatrine, inhibitor of HSPA8, reduces binding of biotin-TLQP-21 to the surface of intact, live SH-SY5Y cells:

OMTR reduces the binding of Biotin-TLQP-21 to the surface of intact, live SH-SY5Y cells: Live SH-SY5Y cells, treated and not treated with OMTR, at a concentration known to inhibit expression of HSPA8 (Wang et al. 2010), were incubated with 3 different volumes of 0.1 mM biotin-TLQP-21: 5, 10 and 28 μ l, equivalent to 0.5, 1.0 and 2.8 mmoles of biotin-TLQP-21 respectively. Subsequently, cells were treated with fluorescein conjugated avidin and subjected to FACS analysis.

SH-SY5Y cells treated with OMTR showed a significant reduction of binding of the peptide, particularly at the optimum conditions (16.66%, Figure 19): this is, when the cells were incubated with 5 μ l of the peptide (corresponding to 0.5 mmole) followed by the addition of fluorescein-conjugated avidin was added at a concentration of 20 μ g/ml.

Under other conditions, the inhibitory effect was also found: Surface binding of biotinyl-TLQP-21 by the cells treated with OMTR were 2.81% (control, Figure-17A), 57.37% (Figure-17C), 53.61% (Figure-17E) and 53.16% (Figure-17G); while surface binding of biotinyl-TLQP-21 by the cells not treated with OMTR were 2.28% (control, Figure-17B), 57.36% (Figure-17D), 59.33% (Figure-17F) and 58.73% (Figure-17H) when the SH-SY5Y cells were incubated with 0.1 mM biotin-TLQP-21 with 5, 10 and 28 μ l, respectively. In this case, fluorescein-conjugated avidin was added at a concentration of 10 μ g/ml.

In addition, using fluorescein-conjugated avidin at double concentration, 20 μ g/ml ; surface binding of biotinyl-TLQP-21 by the cells treated with OMTR were 1.98% (control, Figure-18I), 30.78% (Figure-18K), 32.64% (Figure-18M) and 50.36% (Figure-18O); whereas surface binding of biotinyl-TLQP-21 by the cells not treated with OMTR were 3.51% (control, Figure-18J), 32.13% (Figure-18L), 40.75% (Figure-18N) and 61.16% (Figure-18P) when the SH-SY5Y cells were incubated with 0.1 mM biotin-TLQP-21 with 5, 10 and 28 μ l, respectively.

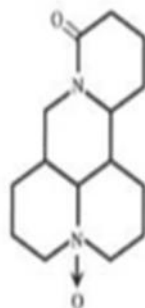


Figure 15: Chemical structure of OMTR.



Figure 16: *Sophora flavescens* : A Chinese herb, popularly known as Ku shen: a typical traditional Chinese medicine plant (Cai et al., 1997).

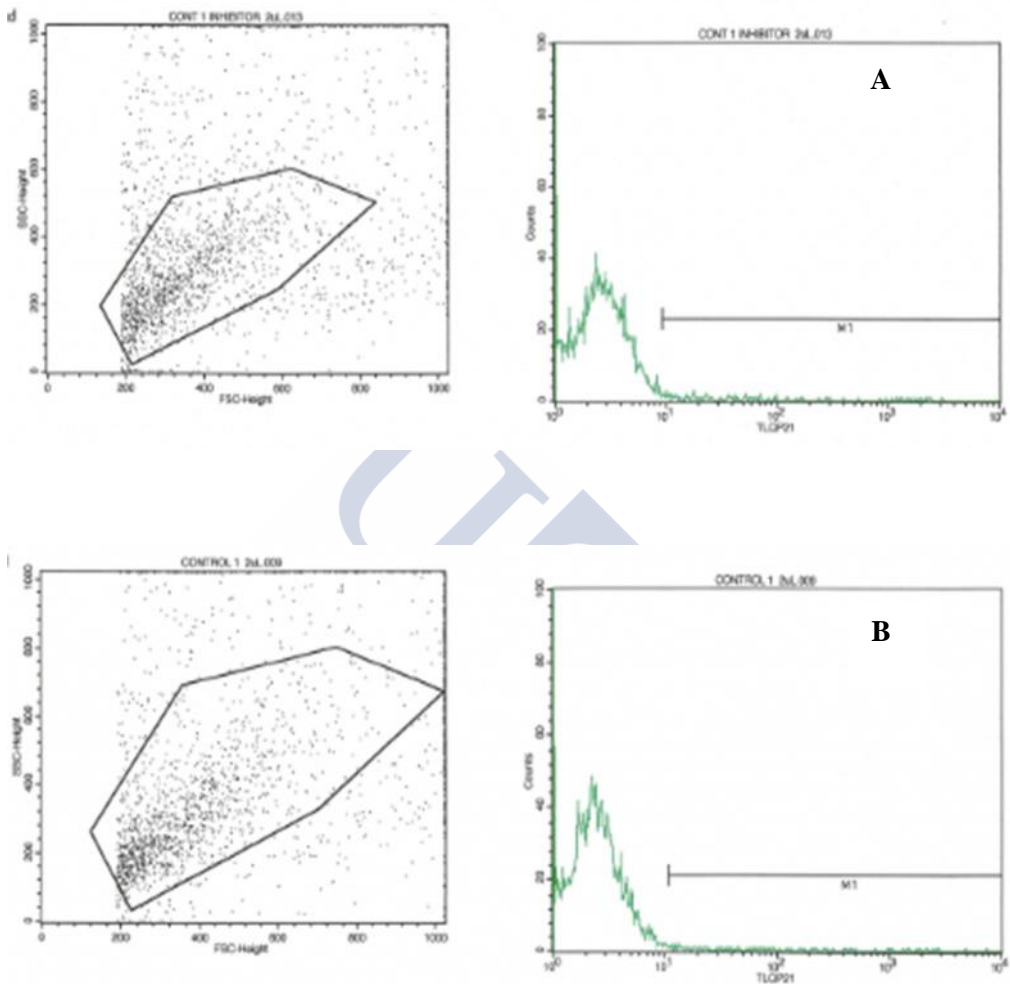


Figure 17(A-B): Expression of HSPA8 protein in SH-SY5Y cells reduced in flow cytometry assays (24 hours treatment). Incubation of SH-SY5Y cells without biotin-TLQP-21, staining with avidin, fluorescein conjugated at a concentration of 10 $\mu\text{g/ml}$ showed as 2.81% (control, with inhibitor, A) and 2.28 % (control, without inhibitor, B).

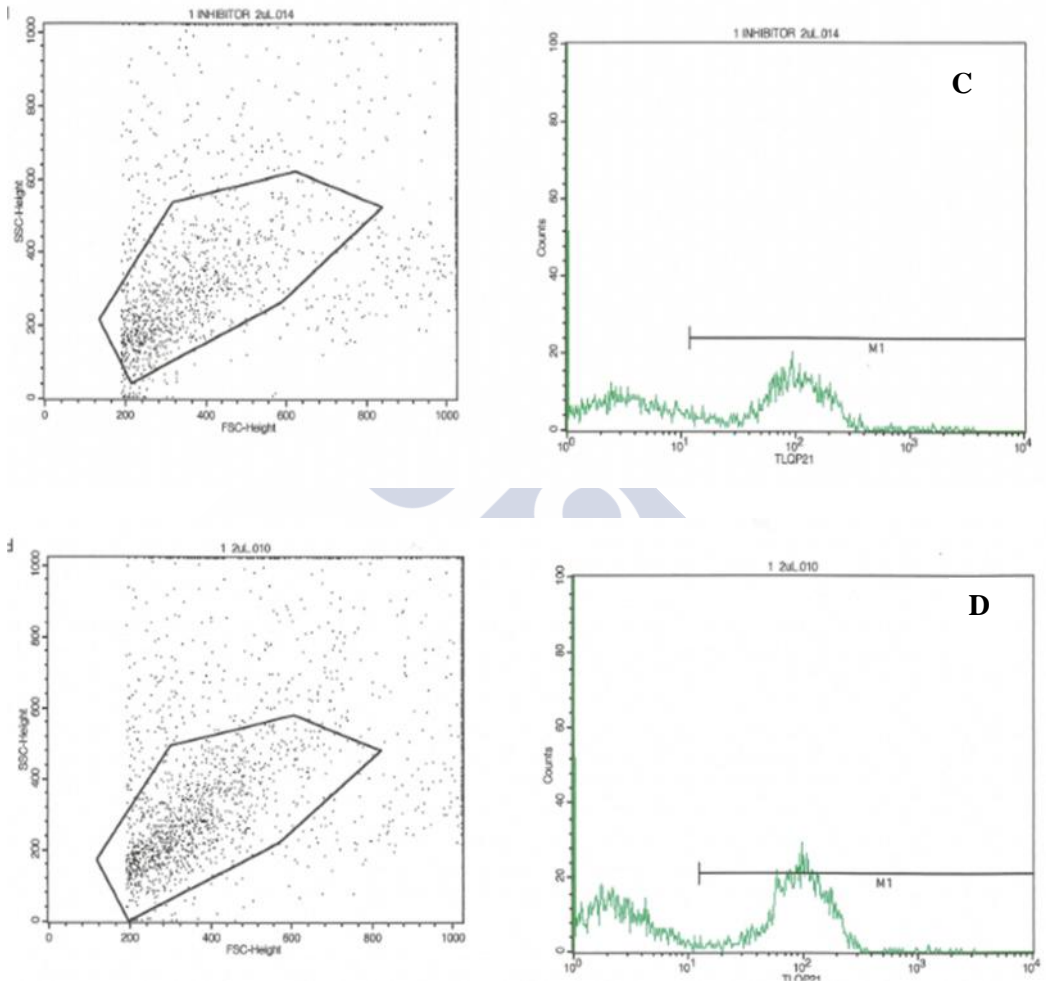


Figure 17(C-D): Expression of HSPA8 protein in SH-SY5Y cells reduced in flow cytometry assays (24 hours treatment). Incubation of SH-SY5Y cells with 28 μ l of 0.1 mM Biotin-TLQP-21 followed by staining with avidin, fluorescein conjugated (10 μ g/ml) showed surface binding of biotin-TLQP-21 as 57.37% (with inhibitor, C), and 57.36% (without inhibitor, D).

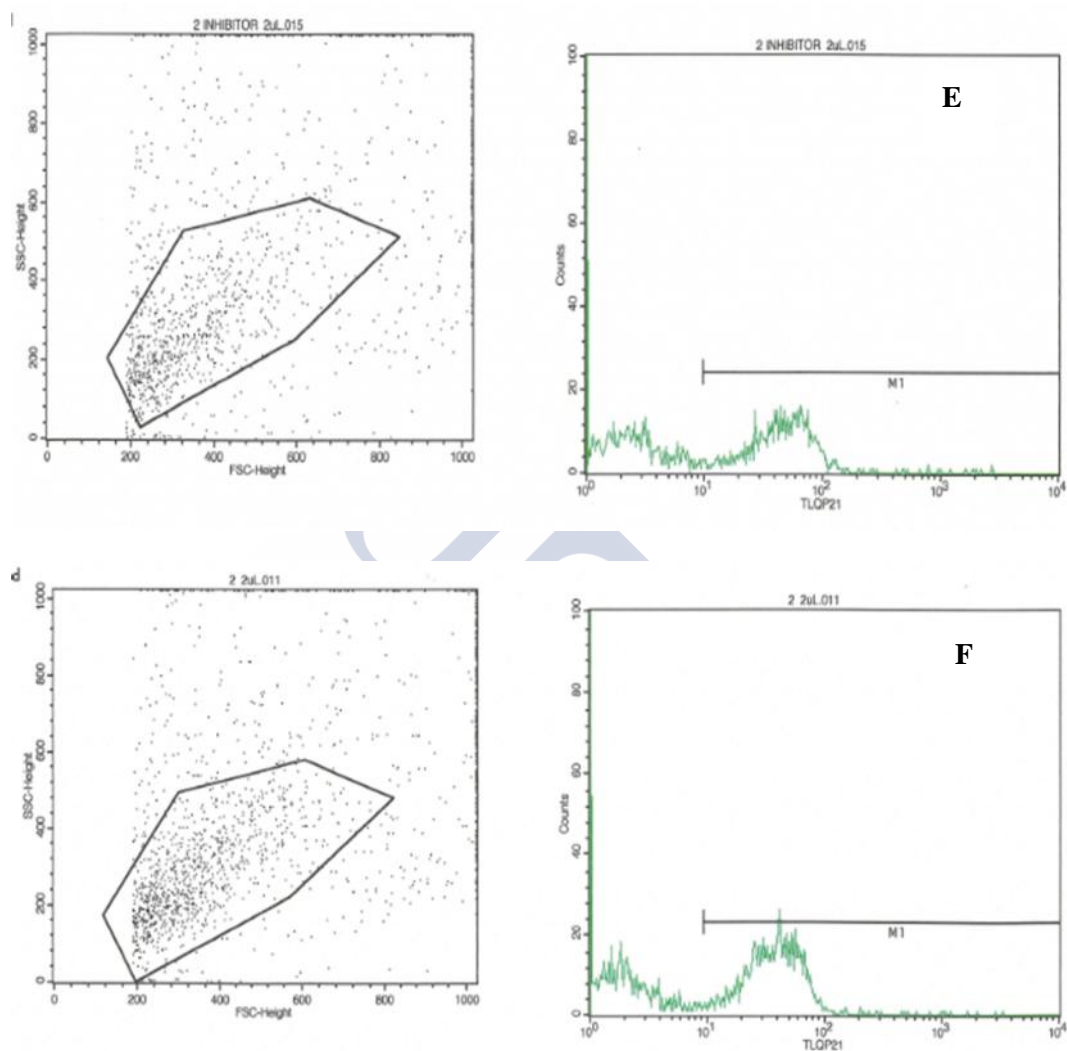


Figure 17(E-F): Expression of HSPA8 protein in SH-SY5Y cells reduced in flow cytometry assays (24 hours treatment). Incubation of SH-SY5Y cells with 10 μ l of 0.1 mM Biotin-TLQP-21 followed by staining with avidin, fluorescein conjugated (10 μ g/ml) showed surface binding of biotin-TLQP-21 as 53.61% (with inhibitor, E), and 59.33% (without inhibitor, F).

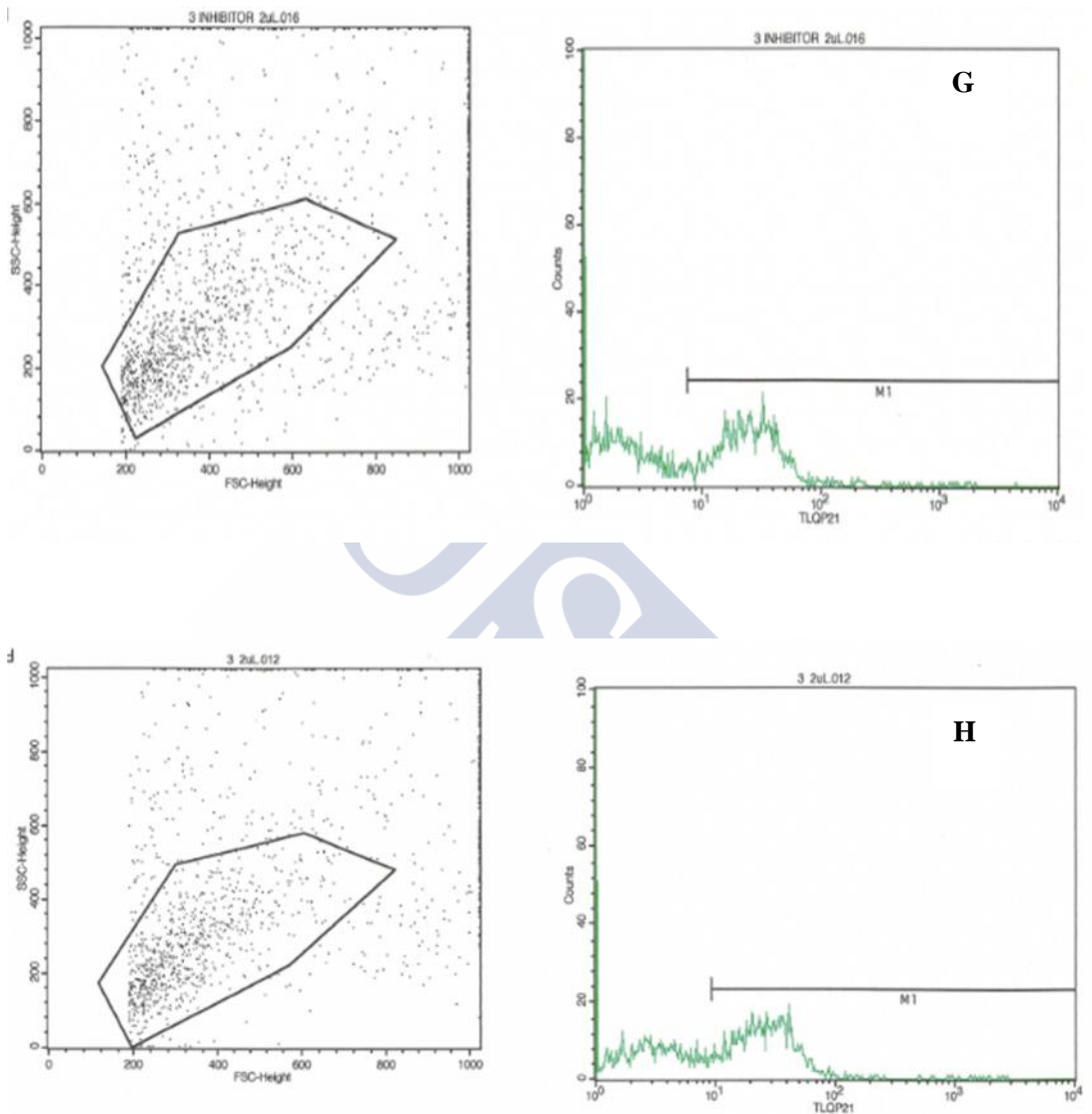


Figure 17(G-H): Expression of HSPA8 protein in SH-SY5Y cells reduced in flow cytometry assays (24 hours treatment). Incubation of SH-SY5Y cells with 5 μ l of 0.1 mM Biotin-TLQP-21 followed by staining with avidin, fluorescein conjugated (10 μ g/ml) showed surface binding of biotin-TLQP-21 as 53.16% (with inhibitor, G), and 58.73% (without inhibitor, H).

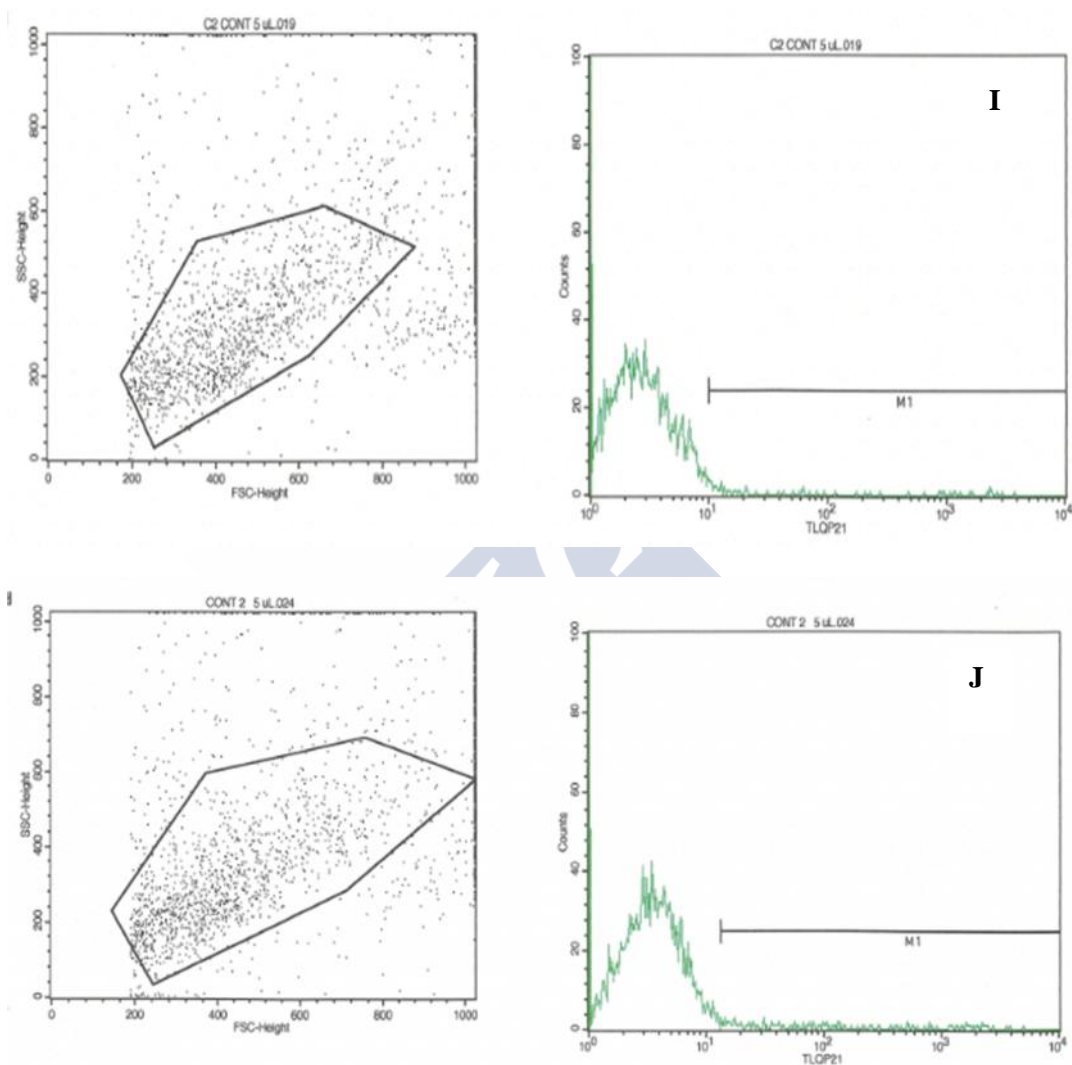


Figure 18(I-J): Expression of HSPA8 protein in SH-SY5Y cells reduced in flow cytometry assays (24 hours treatment). Incubation of SH-SY5Y cells without Biotin-TLOP-21, staining with Avidin, fluorescein conjugated at a concentration of 20 $\mu\text{g/ml}$ showed as 1.98% (control, with inhibitor, I) and 3.51% (control, without inhibitor, J).

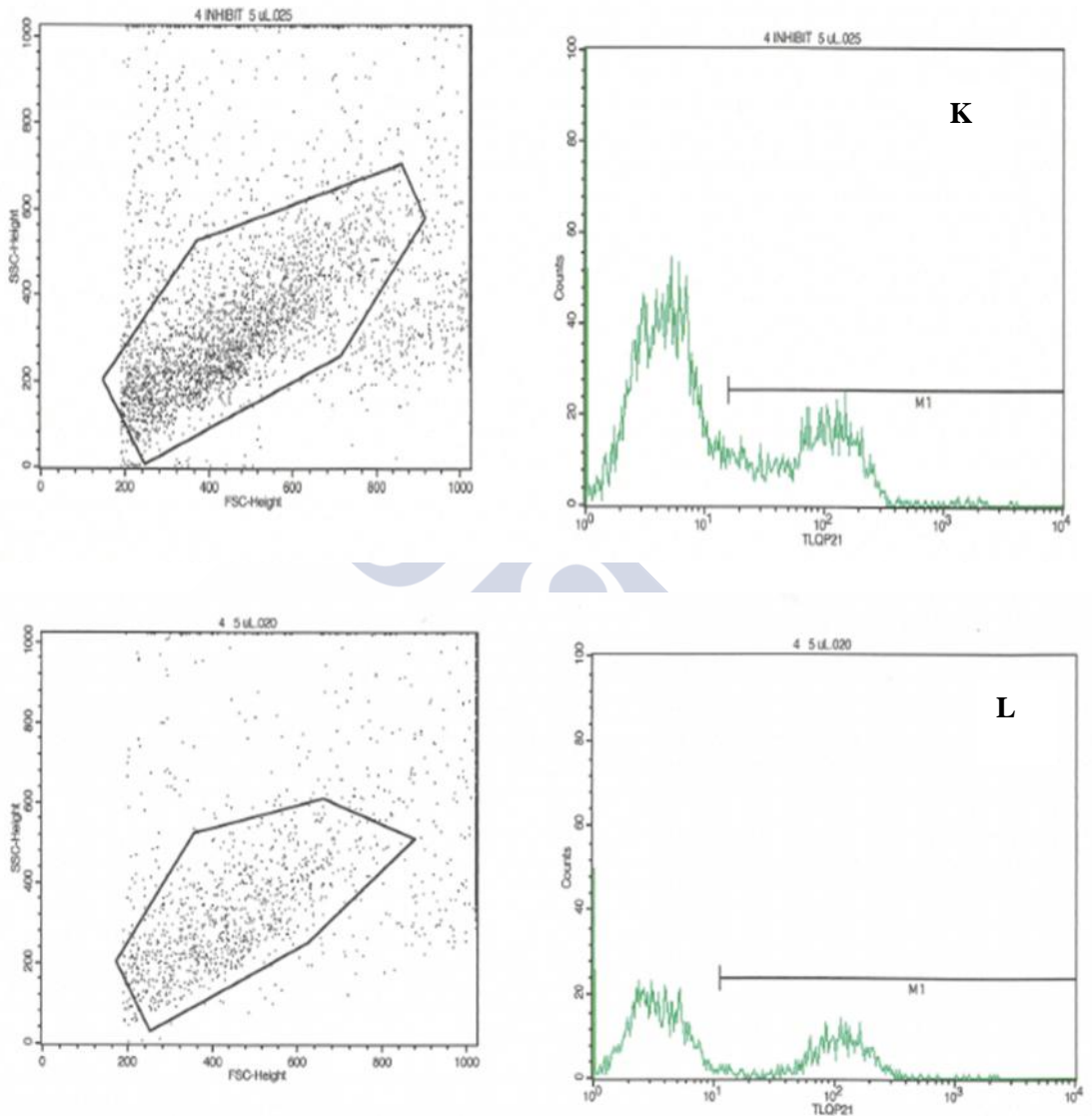


Figure 18(K-L): Expression of HSPA8 protein in SH-SY5Y cells reduced in flow cytometry assays (24 hours treatment). Incubation of SH-SY5Y cells with 28 μ l of 0.1 mM Biotin-TLQP-21 followed by staining with avidin, fluorescein conjugated (20 μ g/ml) showed surface binding of biotin-TLQP-21 as 30.78% (with inhibitor, K), and 32.13% (without inhibitor, L).

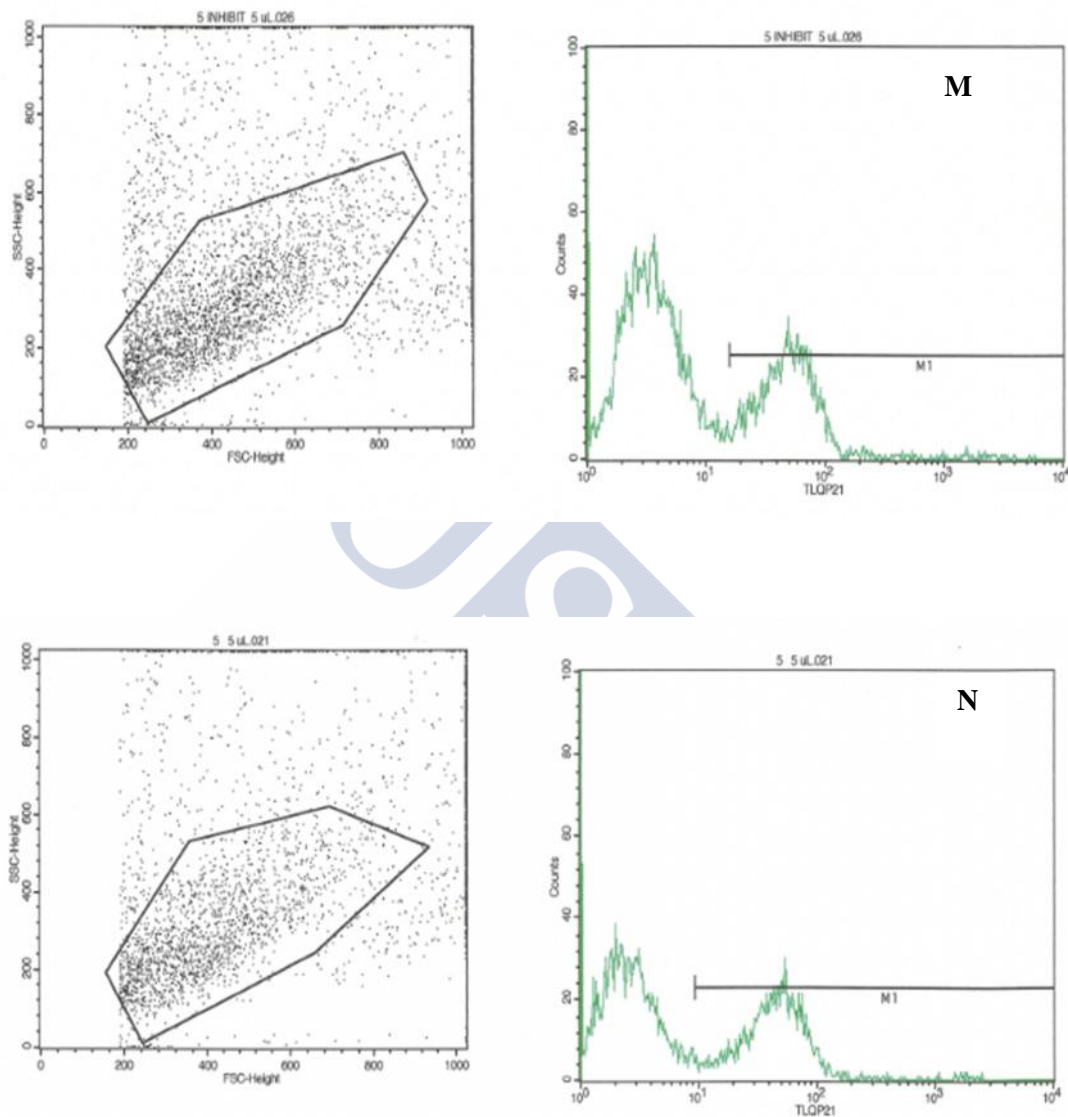


Figure 18(M-N): Expression of HSPA8 protein in SH-SY5Y cells reduced in flow cytometry assays (24 hours treatment). Incubation of SH-SY5Y cells with 10 μ l of 0.1 mM Biotin-TLQP-21 followed by staining with avidin, fluorescein conjugated (20 μ g/ml) showed surface binding of biotin-TLQP-21 as 32.64% (with inhibitor, M), and 40.75% (without inhibitor, N).

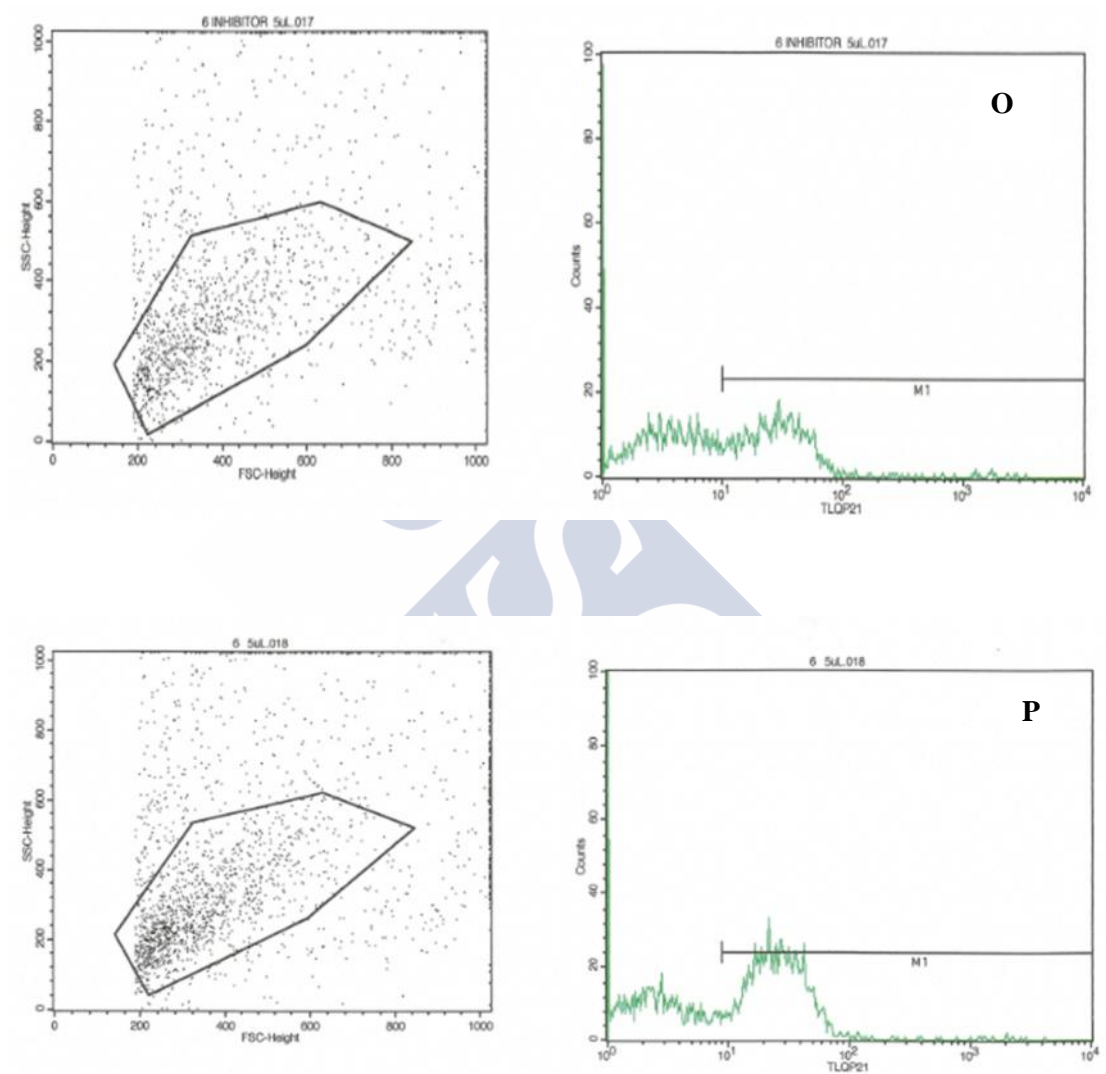


Figure 18(O-P): Expression of HSPA8 protein in SH-SY5Y cells reduced in flow cytometry assays (24 hours treatment). Incubation of SH-SY5Y cells with 5 μ l of 0.1 mM Biotin-TLQP-21 followed by staining with avidin, fluorescein conjugated (20 μ g/ml) showed surface binding of biotin-TLQP-21 as 50.36% (with inhibitor, O), and 61.16% (without inhibitor, P).

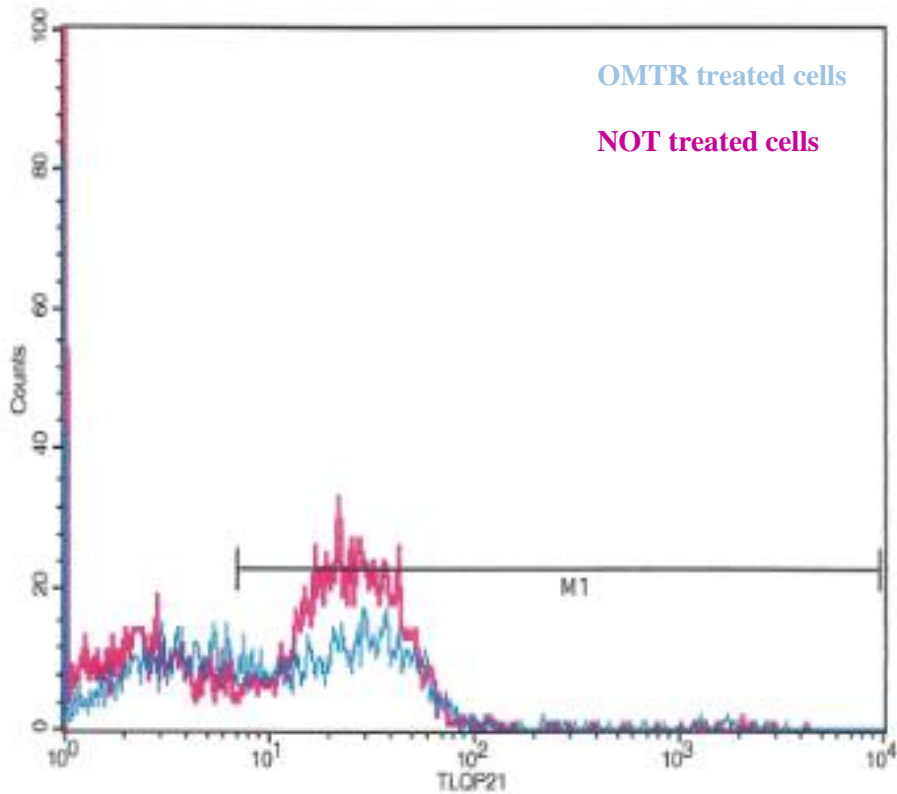


Figure 19: Representative histogram showing decreased binding of Biotin-TLQP-21 to the surface of intact, live SH-SY5Y cells treated with OMTR vs not treated cells in flow cytometry.

Of note, it has been shown by Wang and co-workers (2010) that OMTR treatment had no lethal effect on cells both in short term therapy (84 hours) and long term therapy (8 months). Moreover, the down regulatory effect of OMTR was detected only in HSPA8 but not in other heat shock protein (HSP) members like HSP90 and HSPA4 (Wang et al., 2010).



C3AR1 not trapped by TLQP-21 affinity chromatography:

In 2013, Hannedouche et al., confirmed and later in 2014, Cero et al., confirmed C3AR1 as a putative receptor of the murine TLQP-21 peptide. Hence, the same PVDF membrane used for probing with Anti-HSPA8 antibody, was stripped and probed with anti-C3AR1 antibody but it was nullified here that it was not the C3AR1 protein (Figure 20).

Fraction from T-21 column Fraction from C column
1 2 3 4 5 6

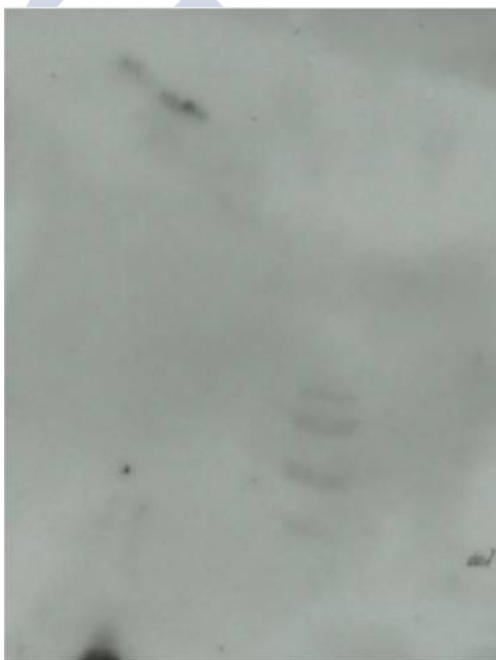


Figure 20: C3AR1, a ~53 kDa protein, does not bind biotin-TLQP-21 following Monomeric Avidin-agarose based affinity chromatography. The PVDF membrane, previously used for immunochemical validation of HSPA8 (Figure 11), was stripped, incubated with C3AR1 Ab but could not be detected, confirming that C3AR1 was not present in the eluate.

Proteomic study:

To date, little is known about the signaling mechanisms in which TLQP-21 and its receptor(s) take(s) part. For this reason a preliminary proteomic analysis was carried out using protein extracts of control and SH-SY5Y cells treated with the peptide, to know which proteins are modulated. It should be noted here that, besides confirming that TLQP-21 exerts biological effects in our model system, the ultimate objective is to investigate whether this modulation is due to the interaction between TLQP-21 and its receptor HSPA8 or not, which will be done in future studies.

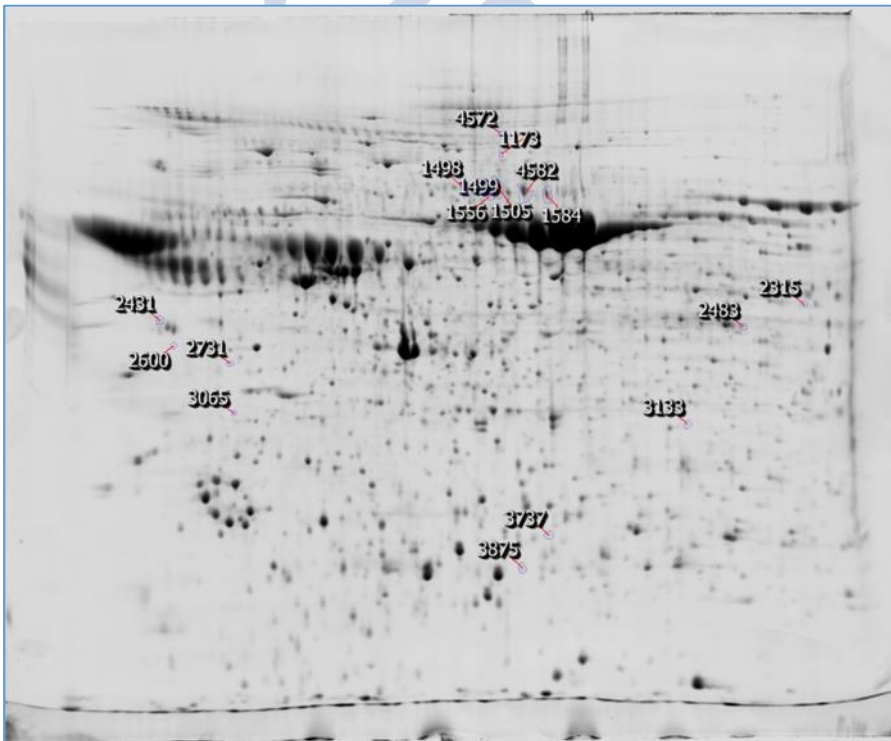


Figure 21: Representative gel obtained from the proteomic analysis. Identified spots are designated with number.

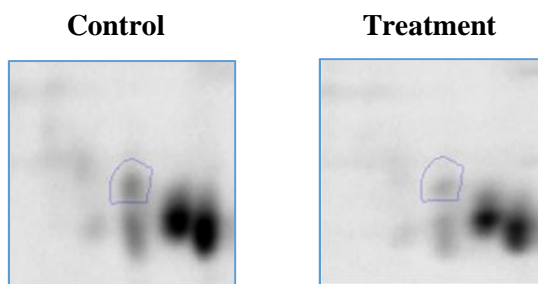


Figure 22: Representative spots from the proteomic study showing altered protein expression in SH-SY5Y cells. Samples from cells treated with TLQP-21 shows less intensity of spots in comparison to control.

Six gels of each condition were processed; one representative gel is shown in Figure 21. An example of one of the spots showing differential intensity in treated vs. not treated cells is shown in Figure 22. A list of all the proteins whose expression was found to be modified is presented in Table 8.

Table 8: List of proteins with altered expression levels in SH-SY5Y cells.

Protein	Score	MW(Da)	Sequence coverage	Function
Mediator of RNA polymerase II transcription subunit 24	71	111716	11%	Involved in the regulated transcription of nearly all RNA polymerase II-dependent genes
Adenylosuccinatesynthetase isozyme 2	64	50465	14%	Plays an important role in the de novo pathway and in the salvage pathway of purine nucleotide biosynthesis. Catalyzes the first

				committed step in the biosynthesis of AMP from IMP.
Spindle and kinetochore-associated protein 2	65	14236	49%	Essential for proper chromosome segregation. Required for timely anaphase onset during mitosis,
1-phosphatidylinositol 3-phosphate 5-kinase (type III PIP kinase)	58	239609	7%	Participates in phosphatidylinositol signaling system and regulation of actin cytoskeleton.
Heat shock protein beta-1	80	22826	37%	Chaperone activity, thermotolerance, inhibition of apoptosis, regulation of cell development, and cell differentiation, signal transduction.
Endothelial differentiation-related factor 1	63	16359	46%	Transcriptional coactivator stimulating NR5A1 and ligand-dependent NR1H3/LXRA and PPARG transcriptional activities. Enhances the DNA-binding activity of ATF1, ATF2, CREB1 and NR5A1. Regulates nitric oxid synthase

A total of 6 proteins were found to be in altered expression, listed in the Table 8. Out of them, one is 1-phosphatidylinositol 3-phosphate 5-kinase with MW ~240 kDa and another one is adenylosuccinate synthetase isozyme 2 with MW ~51 kDa.

Preliminary phosphoproteomic study:

A preliminary phosphoproteomic study was carried out to further validate that TLQP-21 exerts biological effects in the model system (SH-SY5Y cells) used and as a starting point for future, more comprehensive studies. Cell homogenates from TLQP-21 treated or control cells were subjected to 1D SDS-PAGE followed by staining with the phosphorous-specific dye Pro-Q Diamond. As seen in Figure 23, differences in band intensity were seen. Thus, the bands' intensity at <56 and >212 kDa were less in the samples treated with the peptide in comparison to control ones suggesting that the peptide on SH-SY5Y cells might provoke dephosphorylation of specific phosphoproteins. In consistent with the proteomic study, the intensity of the band was less in sample with the peptide treatment.

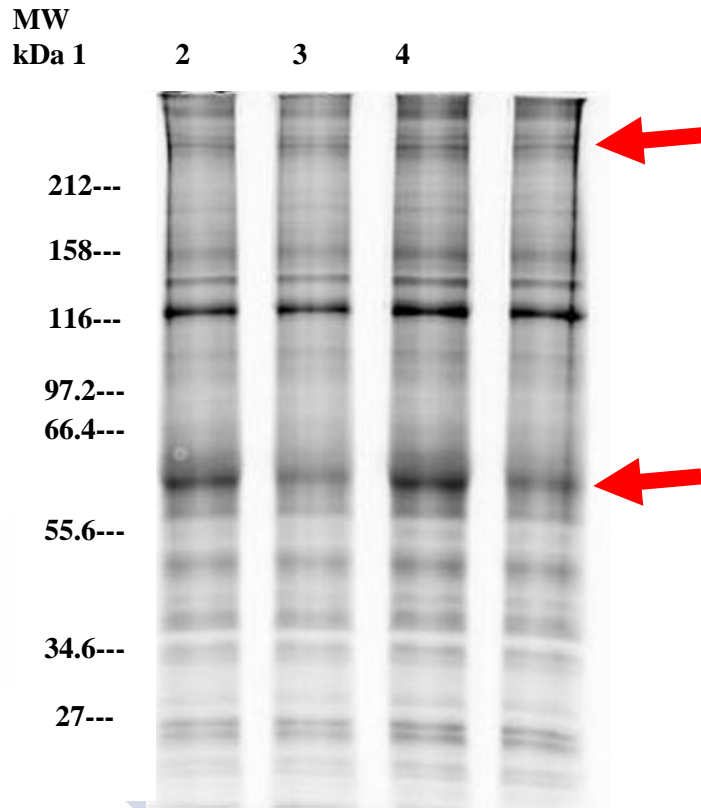


Figure 23: Phosphoprotein detection in SDS-polyacrylamide gels using Pro-Q Diamond dye. Incubation of SH-SY5Y cells with TLQP-21 at a concentration of $1\mu\text{g/ml}$ (Hunsberger et al., 2007) followed by staining with Pro-Q Diamond dye showed difference in phosphoprotein expression at <56 and >212 kDa proteins of control, SH-SY5Y cell homogenates not treated with the peptide (1 and 3) and cell homogenates, treated with the peptide (2 and 4).

Further studies are required to validate that the interaction of the peptide TLQP-21 with its receptor, HSPA8 is involved in the altered protein expressions as found in the proteomic study.



Discussion



Within the last two decades, if not more, increasing data illustrating the role of neuropeptides in modulating behavior has encouraged researchers to look for neuropeptide receptors (Griebel and Holsboer, 2012). Some researchers have even claimed the inception and development of a separate discipline termed as 'receptorology' (Ariens, 1984). To ease the task for searching out for the receptors and to exploit all the potential outcomes, a number of techniques and strategies have been adopted. In the present work, the VGF derived peptide TLQP-21 was modified with N-terminal biotin and C-terminal cysteine for effective cross linking, affinity chromatography purification, and easy detection, leading to successful search to 'fish' out HSPA8 as a receptor of the VGF derived peptide human TLQP-21.

Identification of HSPA8 as a receptor of human TLQP-21:

The VGF-derived peptide TLQP-21 was modified by attachment of biotin at the N terminal via the amide bond and with an extra cysteine residue at the C terminal to facilitate the search for receptor of TLQP-21, specially to serve multiple purposes like detection of any binding with receptor/binding partner and the peptide itself using streptavidin-HRP, also for purification from affinity columns.

Biotin-TLQP-21-C was mixed with an SH-SY5Y cell homogenate and cross-linked to putative TLQP-21-binding proteins using the water-soluble analog of EMCS, Sulfo-EMCS (N-(epsilon -maleimidocaproyloxy) sulfosuccinimide ester). Sulfo-EMCS is a heterobifunctional crosslinker containing two groups: N-hydroxysuccinimide (NHS) ester reacts at pH 7-9 with primary amines (-amine groups on lysine residues) by nucleophilic attack, releasing N -hydroxysulfosuccinimide as a byproduct (Hermanson, 1996) and forms amide bonds, on the other hand, maleimide reacts with sulfhydryl groups at pH 6.5-7.5 forming stable thioester bonds (Heitz et al., 1968). In aqueous

solutions, the maleimide group is comparatively more stable than the N-hydroxysuccinimide (NHS) ester group but will be hydrolyzed slowly, and at pH > 7.5, reaction specificity for sulfhydryl groups diminishes. Considering all these factors, conjugation experiments with Sulfo-EMCS are carried on at pH 7.2-7.5.

Peptides were incubated with SH-SY5Y cell homogenate for crosslinking. The cross-linking experiment identified a 75 kDa band, not in the control (reaction mixture without peptide) (Figure 8).

Once that the presence in SH-SY5Y cell homogenates of a TLQP-21-binding protein had been confirmed, an affinity chromatography-based approach was set up to identify it. Biotin-TLQP-21-C peptides were attached to the affinity column through their biotin tags, and SH-SY5Y cell homogenates were loaded to the column. The eluates from affinity chromatography were analysed by SYPRO[®] Ruby staining, following SDS-PAGE. A specific 75 kDa protein band was present in the eluates from the TLQP-21-containing column, not in the corresponding control fractions (Figure 9).

The band was excised and analysed by nanoHPLC-electrospray MS.MASCOT analysis of the spectra confirmed 3 proteins (Table 7): HSPA8 (MW 71 kDa), HSPA9/mortalin (MW 74 kDa), and HSPA5 (72 kDa). Out of these three, HSPA5 was excluded due to its lowest sequence coverages, scores and more importantly, for number of unique peptides. The number of unique peptides for HSPA5 was only 3 and cut-off parameter was set at 3 ((Nesvizhskii et al., 2007; Ayub, 2012). It seems that the band excised and analyzed here contains all these three proteins as the molecular weight (MW) of the proteins are close to each other but following stringent filtering parameters, HSPA8 and HSPA9/mortalin were considered as the target proteins, excluding HSPA5. It has been observed that HSPA8 is a multiligand binding, multifunctional protein that has affinity for a variety of ligands. Its localization to cell surface to perform directly as a receptor

was already well established (for details, see the section: HSPA8). Taken together all these into account, in this study, HSPA8 was given more preference and was confirmed by immunostaining. Later on, couple of experiments validated the presence of HSPA8 in cell surface and binding the peptide TLQP-21 (see below).

On the other hand, the localization of HSPA9 remains mostly restricted to one compartment of the cell, namely the mitochondria (Stricher et al., 2013); hence they are also known as 'mtHSP70'. But taken together all the data regarding the localization of HSPA9, it can be concluded that HSPA9/mortalins are mostly found in mitochondrial localizations, though surface expressed mortalins are evident (Deocaris et al., 2008; Wadhwa et al., 2002; Deocaris et al., 2006; Bhattacharyya et al., 1995). However, at this moment its role as a second TLQP-21 receptor cannot be ruled out. Further studies are required to assess whether TLQP-21 binds HSPA9/mortalin on the cell surface (like those applied to HSPA8) or not.

The samples, in which the 75 kDa bands were detected by Sypro[®] ruby staining (Figure 9), subjected to Western blot analysis with an anti-HSC70 (HSPA8) antibody. The antibody reacted positively with the protein at 71 kDa band (Figure 11).

Hannedouche et al. (2013) have identified C3AR1 as a putative receptor of murine TLQP-21. Hence, we probed the same membranes with an anti-C3AR1 antibody but no signal was detected (Figure 20).

Binding of biotinylated TLQP-21 to HSPA8 on the SH-SY5Y membrane:

Since for practical reasons, whole cell homogenates were used to identify HSPA8 as a human TLQP-21 receptor, there was the possibility that its interaction with TLQP-21 might be artifactual, i.e., that TLQP-21 bound to intracellular HSPA8 made available after homogenization. Therefore, it was necessary to prove that TLQP-21 actually binds HSPA8 on the cell membrane.

For this, biotinylated TLQP-21 was added to intact, live SH-SY5Y cells and cross-linked to putative membrane receptors with sulfo-EMCS. Subsequently, the cells were homogenized and the homogenate subjected to affinity chromatography using the monomeric avidin column. Eluted fractions were resolved by SDS-PAGE, blotted, and membranes probed with anti-HSPA8 antibody. A positive 71 kDa band corresponding to HSPA8 was detected in elutant fractions of the avidin column, not in the control samples (homogenate of cells not treated with biotinylated TLQP-21). The small mass increment added by biotinyl-TLQP-Cys (2820.33 Da) to HSPA8 is not sufficient to be detected in our SDS-PAGE system (Figure 12).

**Binding of biotin-TLQP-21 to the surface of intact, live SH-SY5Y cells:
Demonstration by FACS analysis:**

Viable, live SH-SY5Y cells were incubated biotin-TLQP-21. Subsequently, cells were treated with fluorescein-conjugated avidin and subjected to FACS analysis. Phenotypic expression of surface binding of biotinyl-TLQP-21 by the cells increased in the dose-dependent manner of biotin-TLQP-21, not on the increasing amount of fluorescein-conjugated avidin. Even in both the concentrations (10 μ g/ml and 20 μ g/ml) (Figures 13 and 14) of Immunopure Avidin, Fluorescein Conjugated, SH-SY5Y cells were stained in more/less same manner/amount. However, out of the whole cell population maximum

10.37% cells were proved to display positive staining expression of surface binding of biotinyl-TLQP-21 by the cells in consistent with Daudi cells where constitutive cell surface expression of the 60 kDa heat shock protein (Hsp 60) was limited to about 10% (Cicconi et al., 2004).

Using affinity chromatography and mass spectrometry-based protein identification, HSPA8 was identified as a receptor of the human VGF-derived peptide TLQP-21. In agreement with Pino et al., 2013; Shin, et al., 2003; Vega, et al., 2008; Altin and Pagler, 1995 who confirmed the abundance of several HSPs including HSPA8 on cell surface, cross-linking and FACS studies here confirmed that TLQP-21 binds to HSPA8 on the surface of SH-SY5Y cells. Furthermore, molecular modeling studies show that TLQP-21 can be docked into the peptide binding pocket of HSPA8.

OMTR down regulates the expression of HSPA8:

FACS studies, as described before, confirmed that TLQP-21 binds to HSPA8 on the surface of SH-SY5Y cells. But when OMTR, an inhibitor of the expression of HSPA8 (Wang et al., 2010), was used; binding of TLQP-21 to the surface of cells decreased (Figures 17, 18 and 19), strongly suggesting that TLQP-21 binding was through HSPA8.

Molecular dynamics study:

A docking and simulation study, prompted by the identification of HSPA8 as a receptor of TLQP-21, was carried out by Sandipan Chakraborty, Department of Microbiology, University of Calcutta, India. This collaborative study concluded that the ligand human TLQP-21 directly fits into the receptor HSPA8, as detailed in the Annex II.

Molecular dynamics simulation study explored the structural dynamics of TLQP-21 bound to the HSPA8 receptor binding site. Protein-peptide docking was designed to investigate the recognition mechanism of the ligand peptide TLQP-21 by receptor, HSPA8. TLQP-21 appropriately fits within the substrate binding site of the HSPA8 showing strong interaction with the β -sheet region of the HSPA8. The bound TLQP-21 keeps its helical conformation in bound condition with HSPA8. Thus, molecular docking study confirms an appropriate spatial fit of the peptide inside the cavity of HSPA8 (Annex II, Figure 26).

During the simulation of the complex HSPA8 and TLQP-21 any dissociation of the complex was not noticed suggesting that the peptide TLQP-21 formed strong, steady complex with HSPA8. As the simulation progresses goes on, the formation of more number of hydrogen bonds functions as one of the principal driving forces that allows stronger interaction of the peptide, TLQP-21, within HSPA8 substrate binding site. With the simulation process continuation, the peptide comes closer and settled around at an optimum distance guided by strong surface complementarity and increasing hydrogen bonding possibilities (Annex II, Figure 30).

It is obvious from the electrostatic surface potential of HSPA8, the peptide binding region of the protein is highly charged and contains negatively charged residues,

facilitating binding interaction between TLQP-21 and HSPA8. From the middle of the peptide positively charged Arg residues R₁₀-R₁₁, in addition, R₂₁, from the C-terminal region of the peptide TLQP-21, predominantly interacts strongly with the negatively charged region of the HSPA8 substrate binding site (Annex II, Figure 30). In relation to this, it is noteworthy that peptide binding affinity of the HSPA8 domain was found to increase significantly for basic sequences with Arg-Arg (RR) (Takenaka et al., 1995).

HSPA8:

HSPA8 (Heat shock cognate protein A8, 71 kDa), a constitutively expressed protein, is a fascinating member of the HSP70 (Heat shock protein) family. It is also known as stress-inducible protein.

Distribution:

While HSPA8 is mostly localized in the cytoplasm and nucleus, where it carries out a number of functions that are discussed below, it can also be found in a membrane-bound manner on cell surfaces, particularly in cancer cells, undifferentiated human embryonic stem cells, virus transformed B cells (Liao and Tang, 2014; Mambula et al., 2006; Kettner et al., 2007; Powers et al., 2008). It is present in lipid rafts isolated from rat forebrain and cerebellum (Chen et al, 2005). In this respect, HSPA8 is not the only member of the HSP family to be found on cell surfaces: HSP60 has been found present on the surface of the human leukemic CD4-positive T-cell line CEM-SS (Soltys and Gupta, 1997), where it localizes in response to infection (Belles et al., 1999); in turn, HSP70 interacts with phosphatidylserine on the surface of PC12 cells, resulting in a

decrease of viability (Arispe et al., 2004). HSPA8 can also be found extracellularly (Barreto et al., 2003; Evdokimovskaya et al., 2010; Nirdé P et al., 2010; Clayton et al., 2005). Shin et al., 2003 obtained a profile of the cell surface proteome of SH-SY5Y neuroblastoma, A549 lung adenocarcinoma, LoVo colon adenocarcinoma, Sup-B15 acute lymphoblastic leukemia and ovarian tumor cells, found HSPs including HSPA8 at cell surface and postulated that these proteins reach the cell surface either by active transportation from their site of synthesis to maintain structural integrity among receptor complexes, or by accompanied misfolded proteins or peptide fragments out of the cytosol via a non-classic pathway.

Functions:

While HSPA8 is involved in housekeeping chaperoning functions (He M et al., 2010; Pfaffenbach et al., 2010; Daugaard et al., 2007; Powers et al., 2008), that is not its only role: additionally, it carries out biological functions relevant to immunity, antigenicity, hematopoiesis, and autophagy (Stricher et al., 2013). HSPA8 is also involved in exocytosis, endocytosis and vesicular trafficking and participates in multiple cellular signalling pathways (Meimaridou et al., 2009) (for further description, see below).

HSPA8 signaling:

HSPA8 not only functions to play important roles in intracellular response but also as extracellular signal molecules participating in a number of signaling pathways. There are couple of secretion mechanisms of HSPA8 (Liao and Tang, 2014): firstly, cell lysis, HSPA8 is secreted by necrotic tumor cells into the blood stream via this mechanism.

Secondly, it follows secretory vesicles pathway to be secreted in exosomes, for example, B cells secrete HSPA8 following this pathway (Clayton et al., 2005). Thirdly, secretory lysosomal endosomes pathway, tumor cells and macrophages release HSPA8 via this pathway (Chen et al., 2005). Of note, HSPA8 release has more multiple cellular functions than other HSPs as the constitutive HSPA8 is much more abundantly secreted than other HSPs in most of the cells, interacting with multiple molecules/partners.



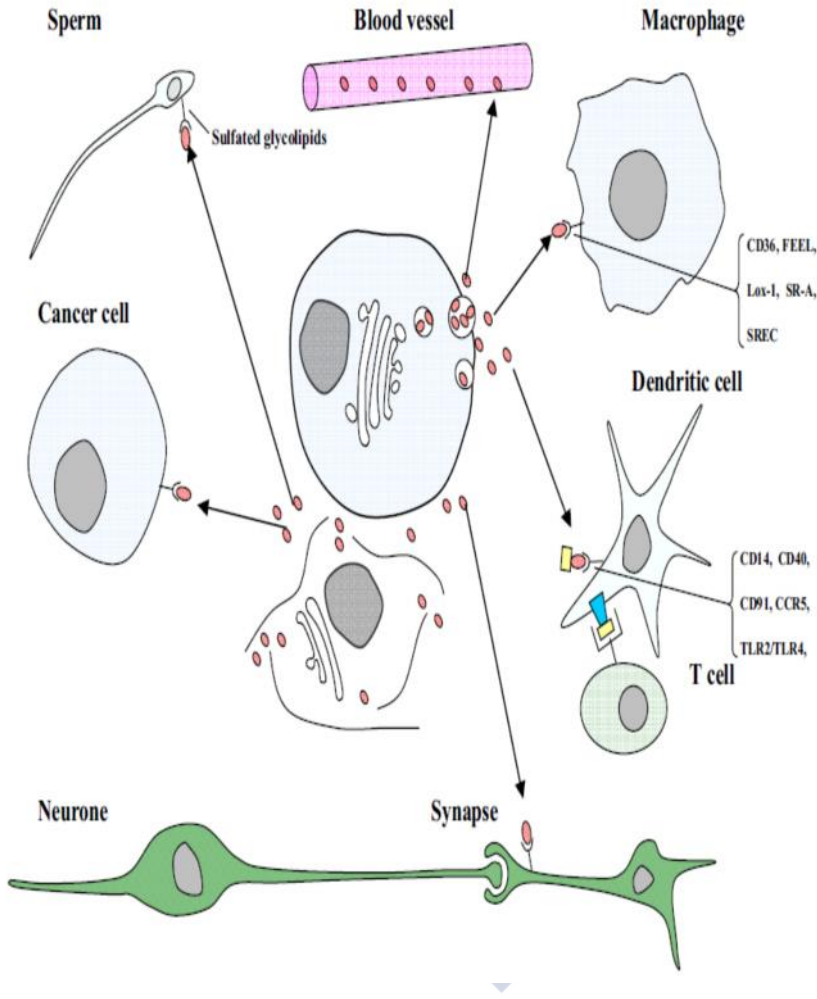


Figure 32: Interactions of HSPA8 (red ellipses) with a wide range of target molecules. After being released, extracellular HSPA8 interact with neuronal cells, macrophages, cancer cells, sperm, antigenic peptides (yellow squares) and by dendritic cells (act as antigen presenting cells) or enter the blood circulation. Antigenic peptides undergo cross-presentation caused by major histocompatibility class I molecules (blue trapezium) and activate CD8+ T lymphocytes (From Liao and Tang, 2014).

After being released into the extracellular microenvironment, HSPA8 interacts with surface signaling molecules including CD14, CD40, CD91, TLR2/TLR4, CCR5, CD36, FEEL, Lox-1, SR-A, and SREC (Calderwood et al., 2007), initiating extracellular signal transduction cascades (Figure 27). HSPA8 also interacts with TLR2/TLR4, induce cytokine expression, TNF- α , IL-1 β , and IL-6, and finally activates p38MAPK, NF- κ B pathways (Zou et al., 2008). HSPA8 can trigger inflammatory response, combinedly with macrophage and dendritic cells (DCs). Extracellular HSPA8 was found to regulate the proliferation of human cancer cells, as demonstrated by Derocq and Nirdé. HSPA8 was found to bind with sulfated glycolipids on the apical region of the sperm head, inducing the cell signalings between the oviductal cells and spermatozoa (Figure 32) (Elliott et al., 2009; Gadella et al., 1995). Consequently, this binding of HSPA8 affects the activity of both cell types: the oviductal cells and spermatozoa (Fazeli et al., 2003).

Although HSPA8 has been found to be an important signaling molecule interacting with a wide range of molecules, the molecular mechanisms involved remained largely elusive.

Protein folding:

One important cellular function of HSPA8 is its involvement in protein folding. For refolding mechanisms, HSPA8 in most of the cases, functions simultaneously with a variety of co-chaperones, upon ATP hydrolysis in order to bind nascent polypeptides inducing its refolding (Beckmann et al., 1990; Frydman et al., 1996), that take place in a protected environment formed by chaperones and cochaperones, and is directly coupled to translation (Thulasiraman et al., 1999). It is noteworthy that HSPA8 binds

unfolded neo-synthesized proteins, interacting with different protein aggregates to reduce their formation (Watanabe et al., 2001; Wang et al., 2009).

Protein import:

There are reports confirming the involvement of HSPA8 to import protein into organelles or cellular compartments like nucleus, mitochondria and ER: Upon ATP hydrolysis, HSPA8 was found to shuttle between nucleus and cytoplasm (Mandell et al., 1990; Kodiha et al., 2005) to import cytoplasmic proteins into the nucleus (Imamoto et al., 1992; Okuno et al., 1993). Furthermore, it facilitates the import of proteins for other organelles like mitochondria, ER (Chirico et al., 1988; Deshaies et al., 1988) and microtubules in an ATP dependent manner (Tsai et al., 2000; Terada et al., 2010).

Immunity:

HSPA8 has been found as highly immunogenic and central in the immunity system. Interacting with MHC molecules (Auger et al., 1996), HSPA8 was found to be involved in binding and protecting peptide for MHC-II molecules (Panjwani et al., 1999). HSPA8 was found to function as antigen: in rheumatoid arthritis (Hayem et al., 1999), SLE (Hayem et al., 1999; Minota et al., 1988), lupus (Stricher et al., 2013) and mixed-connective disease (Hayem et al., 1999; Minota et al., 1988), increased concentrations of IgG and IgM antibodies to HSPA8 were observed.

Hematopoiesis:

In combination with other co-chaperones like HSP40, BAG4, STUB1 and ST13/HIP, HSPA8 acts on BCL2L11/BIM mRNA stability in order to regulate total cell number (Matsui et al., 2007). Of note, BCL2L11-deficient mice show hyperplasia and increased WBCs (Bouillet et al., 1999).

Autophagy:

The involvement of HSPA8 in microautophagy was reported: in this process, HSPA8 is involved to engulf cytosolic material by the lysosome via invaginations of the membrane of the lysosome (Li et al., 2012), followed by internalization and degradation via endosomal microautophagy (Sahu et al., 2011). In macroautophagy, cytosolic material with a large portion are engulfed inside autophagosome, the double membrane vesicle, followed by degradation by lysosomes. To remove damaged organelles and intracellular proteins aggregates, this pathway plays a significant role (Wong et al., 2011).

Thus, a variety of cellular functions: Protein folding, import, immunity, hematopoiesis and autophagy; have been attributed to HSPA8.

HSPA8 as receptor/binding partner:

There are multiple evidences showing the ability of HSPA8 to interact with variety of ligands/binding partners of cellular, bacterial, and viral origin, illustrating their functional consequences downward, though in most cases they are still to be more clarified. Already HSPA8 has been known as a multifunctional and multiligand binding protein with multi-location.

It also localizes to the cell surface for cell recognition by immune cells, even more directly performing as a receptor (Tsuboi et al., 1994; Fishelson et al., 2001; Page et al., 2011; Kishi et al., 2001; Sagara et al., 1998; Guerrero et al., 2012). For example, the first ever demonstration of HSPA8's involvement in cell protection from complement-mediated damage showed that sublytic complement activation provoked the translocation of HSPA8 from the cytosol to the exoplasmic side of the plasma membrane of human erythroleukemia cells, K562. Treatment with HSPA8 inhibitor,

deoxyspergualin (DSG) sensitized K562 cells to complement lysis, on the other hand, treatment with HSPA 8 inducers like ethanol, butanol or hemin, protected the cells from complement-mediated lysis. Moreover, on the surface of intact, viable complement-stressed cells, HSPA8 was identified by antibodies. All these data validated the role of HSPA8 in cell defense against complement as well as its translocation to the plasma membrane of the cells (Fishelson et al., 2001).

The HSPA8 proteins were also found to interact with rat CD3+, CD4-, CD8-, T-cell receptor (TCR) alphabeta-, natural killer receptor-P1- T cells (Kishi et al., 2001). Moreover, the HSPA8 was found to perform directly as a receptor: P140, a phosphopeptide issued from the spliceosomal U1-70K small nuclear ribonucleoprotein protein, showed defensive property in MRL/lpr lupus-prone mice. The interaction between the ligand, P140 peptide and its receptor, HSPA8, induced the endogenous (auto)antigen processing affecting MRL/lpr antigen-presenting B cells, that led to the observed decrease of autoreactive T-cell priming and signaling via a mechanism involving a lysosomal degradation pathway (Page et al., 2011).

With respect to the functions of membrane-associated HSPA8, HSPA8 localized on the cell surface was shown to act as a cellular receptor for HTLV-1 induced syncytium formation (Sagara et al., 1998). Also, a peptide analogue phosphorylated on Ser140 termed peptide P140 was seen to bind 'a unique cell surface receptor', HSPA8 (Page et al., 2009) through the HSPA8 N-terminal domain (Stricher et al., 2013), and P140 has successfully completed phase II clinical trials as a potential treatment of systemic lupus erythematosus (Muller et al., 2008; Zimmer et al., 2013); phase III clinical trials are ongoing (Stricher et al., 2013).

HSPA8 possesses a peptide binding domain (Wang, 1993), a feature it shares with other members of the HSP70 family although each one exhibits exclusive and diversified peptide binding features (Fourie et al., 1994). Peptide binding affinity of the HSPA8 domain was seen to increase dramatically for heptamers compared with hexamers containing basic sequences with at least KK, KR, or RR from a phage display peptide library (Takenaka et al., 1995). Interestingly, the peptide sequence of TLQP-21 contains RR sequence at the region R₉- R₁₀- R₁₁.

Further, a circular dichroism study has shown the conformational change of HSPA8 due to binding of a decapeptide (Park et al., 1993). HSPA8 has also been shown to bind proteins, such as the prion protein (Wilkins et al., 2010) or the listeria adhesion protein, for which it acts as a receptor in caco-2 cells (Wampler et al., 2004). HSPA8 has been proved to interact with phosphatidylserine on the surface of PC12 cells (Arispe et al., 2004). Binding site has also been unveiled on HSPA8 for 15-deoxyspergualin, DSG (Nadler et al., 1998).

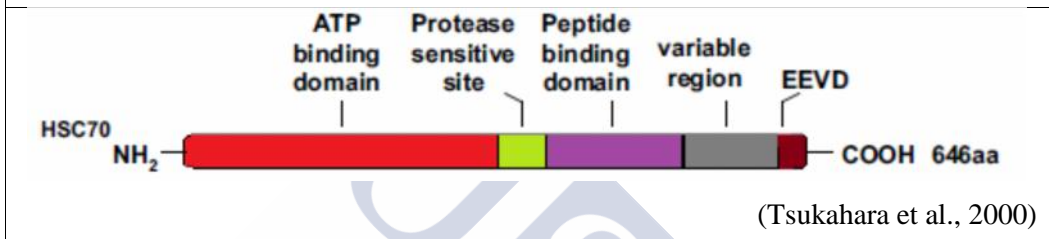
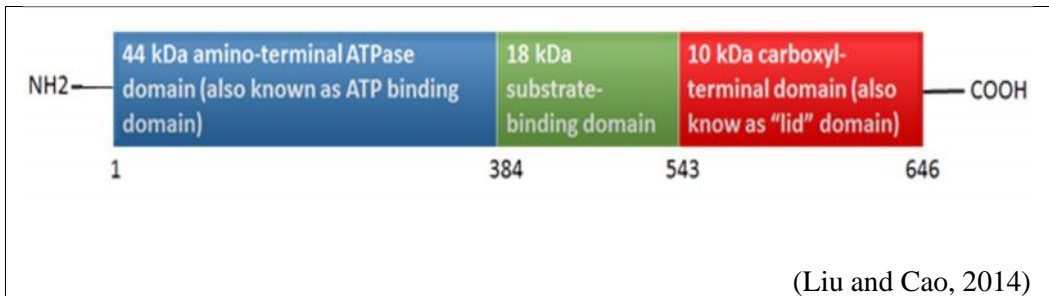
It is also suggested that chaperones like HSPA8 function through ‘transient exposure’ of their ‘interactive surface’ (regions of intramolecular or intermolecular contact) (Gatenby and Ellis, 1990) important in maintaining their interactions with other proteins (Park et al., 1993).

HSPs inducers:

Both the extrinsic factors (hypothermy , toxins, radiation, wound, infection, hypoxia, autophagy and aging) and the intrinsic factors (ER and genetic stress) can induce HSPA8 expression (Liao and Tang, 2014; Preuss et al., 2008; Kettner et al., 2007; Pfaffenbach and Lee , 2010). (For details, see the Table: 9)

Table 9: HSPA8, at a glance.

Name	HSPA8 (Heat shock cognate 71 kDa protein A8)
Other names	HSC70, HSC54, HSC71, HSP71, HSP73, HSPA10, LAP1, NIP71(Liu and Cao, 2014).
Location	11q24.1
Gene	Nine exons and eight introns : the promoter region of the HSPA8 gene includes a TATA box, two CCAAT boxes, two SP1 elements and two sets of heat shock response elements (HSE) where the heat shock transcriptional factors bind (Chen et al., 2002).
Structure	The basic structure of human HSC70 includes three parts: a 44 kDa ATPase domain, an 18 kDa peptide (substrate) binding domain and a 10 kDa carboxyl-terminal domain, also known as "lid" domain.



Expression factors	Increase HSPA8 expression	Decrease HSPA8 expression
	Stress, Heat, Exercise, Organochlorine, Sodium arsenite, Azetidine, Heavy metals (Nickel, Copper, Lead, Cadmium), Antimony containing Drugs, Geranylgeranylacetone, Ethanol, Estrogen, Progesterone, IL-1 beta, Kruppel like factor 4, Phorbol 12-myristate 13-	Sodium-4 phenylbutarate, Butarate, Glycerol, Arginase, Quercetin, 3,3',4,4',5-Pentachlorinated biphenyl (PCB 26), Mototane (in mitochondria), Deoxyspergualin (DSG), D-Galactose amine, cAMP, Lipopolysaccharide (LPS), INF gamma, TNF alpha, Oxymatrine, HSP 70 over expression (Liu et al., 2012)

	<p>acetate, Insulin (Liu et al., 2012), toxins, radiation, wound, infection, hypoxia, autophagy, aging, ER and genetic stress (Liao and Tang, 2014; Preusset al., 2008; Kettner et al., 2007; Pfaffenbach and Lee, 2010).</p>	
<p>Localization</p>	<p>Both extracellular and intracellular location have been proved (Barreto et al, 2003; Evdokimovskaya et al, 2010; Nirdé et al, 2010; Clayton et al., 2005) : major cytosolic molecular chaperone (Place and Hofmann, 2005), also located in various cellular locations such as nuclear and close to cellular membrane (Arispe and Maio, 2000). Interact with the lipid bilayer in the cellular membrane directly (Otto et al., 2001), cell surface (Shin, et al., 2003; Virginia et al., 2008; Altin and Pagler, 1995). Allied with cell surface for cell recognition by immune cells, even more directly carry out function as a receptor (Tsuboi et al., 1994; Fishelson et al., 2001; Page et al., 2011; Kishi et al., 2001; Sagara et al., 1998; Guerrero et al., 2012).</p>	

Functions	As a molecular chaperone, it regulates protein folding, protein maturation, maintains protein normal structure and functions, and protects cells from physical and chemical damage, interacts with nascent polypeptides in the process of new protein synthesis (Beckmann et al., 1990; Beckmann et al., 1992), regulates the translocation of proteins into different cellular organelles such as endoplasmic reticulum and mitochondria (Chirico et al., 1988, Sheffield et al., 1990). Cellular signaling and functions such as steroid receptor maturation (Kimmins and MacRae, 2000), Akt signaling pathway (Shiota et al., 2010). Regulating apoptosis, embryonic development and aging (Beere, 2004; Sreedhar and Csermely, 2004; Kodiha et al., 2005), immunity, antigenicity, hematopoiesis, autophagy, etc. (Stricher et al, 2013), exocytosis, endocytosis, vesicular trafficking, etc. and its association in the regulation of multiple cellular signalling pathways (Meimaridou et al., 2009).
Implications in diseases/physiology	Diabetes (Tiss et al., 2014), Cancers: colon cancer (Kubota et al., 2010), lung cancer (Rusin et al., 2004), Cardiovascular diseases (Dupont et al., 2008), (Chen et al., 2006). Neurological diseases : Parkinson's disease (Mak et al., 2010), Huntington's disease (Bauer et al., 2010), Liver diseases (Wang et al., 2010), obesity (Tiss et al., 2014), Fertility (Moein-Vaziri et al., 2014;

	<p>Zapranova et al., 2013; Kaur et al, 2013; Elliott et al., 2009). Ulcer (Tsukimi et al., 2001), Gastronomy (Bondia-Pons et al, 2011; Daniell et al., 2012). Hypertension (Lian et al., 2014; Oguri et al., 2009; Kato et al., 2008; Timofeeva et al., 2006), Stress (Singh et al., 2014; Magdeldin et al., 2015; Niu et al., 2014).</p>
<p>Noteworthy</p>	<p>Sagara Y et al., 1998 confirmed that HSPA8 expressing on the cell surface performed as a cellular receptor for HTLV-1(Human T-cell Lymphotropic Virus Type 1) induced syncytium formation.</p> <p>Page et al, 2009 validated HSPA8 as ‘a unique cell surface receptor’ as P140 peptide (a peptide analogue phosphorylated on Ser¹⁴⁰) bound with it through N-terminal domain of HSPA8 and P140 has successfully completed phase IIa and IIb clinical trials for SLE (systemic lupus erythematosus) by ImmuPharma France (Muller et al., 2008; Zimmer et al., 2013). Phase III clinical trial was on-going. (Stricher et al., 2013).</p>

The HSP family of proteins:

HSPs, the protein family to which HSPA8 belongs, are ubiquitously distributed and highly expressed in tissues (Hantschelet al., 2000). There are evidences of plasma membrane localization of cytoplasmic HSPs ranging from 70 to 90 KDa, though some of them term it as 'unusual plasma membrane localization of cytoplasmic HSPs' (Altmeyer et al., 1996; Ferrarini et al., 1992; Multhoff et al., 1995; Piselli et al., 1995; Tamura, et al., 1993). In fact, HSPs are contained intracellularly but they are translocated into the plasma membrane and released into the extracellular environment especially after various pathological conditions (Campisi, 2003; Singh-Jasuja, 2001; Srivastava, 2002, Vega et al., 2008). It is now well established that the HSPs act in various intracellular compartments (Buchner, 1996; Frydman and Hohfeld, 1997; Hartl, 1996; Hightower, et al., 1994; Melnick, and Argon, 1995), although there are evidences suggesting the function of certain HSPs after being expressed on the cell surface (Kaur, et al., 1993, Takashima, et al., 1996; Tamura, et al., 1993; Tsuboi, et al., 1994). HSPs interact with the proteins in unfolded, misfolded or aggregated states but do not react with the folded counterparts. However, they can interact with a limited set of native proteins (Mayer, 2013; Mayer and Bukau, 2005, Meimaridou, 2009). A list of wide variety of chemical scaffolds like polyamines, fatty acids, sulfoglycolipids, adenosines and peptides have been identified which show remarkable affinity for HSPs (Evans et al., 2010).

In stress conditions, HSPs are up-regulated and play an important role in cellular repair and protective mechanisms. For example, they bind as well as refold the denatured proteins due to be in stress, whereas in unstressed normal conditions, they perform their routine works like proper folding, assembly, and intercellular trafficking of newly synthesized proteins (Becker and Craig, 1994; Hartl, 1996, Lindquist and Craig, 1988).

Physiological relevance of the TLQP-21 and HSPA8 interaction:

Although it may be unanticipated at first sight that HSPA8 be a receptor for TLQP-21, this is consistent with several earlier and very recent findings. First, expression of HSPA8 has been found to increase in association with obesity and diabetes (Tiss et al., 2014). Increased expression of HSPs is required in persons with obesity to minimize inflammatory and metabolic stresses imposed by obesity. HSPs are believed to play crucial role in renovating cellular and metabolic homeostasis (McArdle et al., 2002; Morton et al., 2006) by decreasing inflammation, uprising skeletal muscle oxidation (Morino et al., 2008; Gupte et al., 2009; Liu et al., 2012; Henstridge et al., 2014). In consistent with the finding of less expression of HSPs in T2DM (Kurucz et al., 2002; Bruce et al., 2003); HSPs have been considered with importance for the treatment of insulin resistance and obesity related T2DM (Chung et al., 2008; Literati-Nagy et al., 2009). In fact, the role of HSPs was under-recognized previously in the maintenance of homeostasis in the physiology, with reference to the obesity-driven inflammation that promotes insulin resistance (Hooper and Hooper, 2009). All these lend support to the argument in favour of a TLQP21-HSPA8 connection in modulating obesity. In this respect, it should be remembered that TLQP-21 is the first identified VGF-derived peptide involved in energy homeostasis (Bartolomucci et al., 2007) and considered as putative target to treat obesity related disorders (Cero et al., 2014) as its role in diabetes (Zhang et al., 2013; Stephens et al., 2012), hypertension (Fargali et al., 2014) and lipolysis (Possenti et al., 2012) has already been confirmed.

TLQP-21 exerts important effects on energy metabolism, its administration decreased food intake and increased energy expenditure in Siberian hamsters (Jethwa et al., 2007). It also decreased body weight and WAT in mice fed high fat diet for 14 days, blocking

hormonal changes associated with this diet and provoking the autonomic activation of the adrenal medulla and adipose tissue. Furthermore, intracerebroventricular administration of TLQP-21 reduced early phase diet induced obesity (Bartolomucci et al., 2006). It is therefore noteworthy that expression of HSPA8 has been shown to be modulated by diet. Thus, significant downregulation was seen in liver from rats fed high-fat sucrose diet versus starch-rich control diet (Bondia-Pons et al., 2011), and in response to increased bean consumption (Daniell et al., 2012).

Another argument favoring the physiological relevance of this newly discovered TLQP-21/HSPA8, ligand-receptor relationship comes from the study of reproduction. HSPA8 contributes to survival of sperm in the oviduct (Elliott et al., 2009). And enhances the ability of spermatozoa to bind oviductal epithelial cells, boosting up in-vitro fertilization performance (Moein-Vaziri et al., 2014). Furthermore, HSPA8 has crucial protective functions in the process of spermatogenesis and epididymal maturation of male germ cells under stress conditions (Zaprjanova et al., 2013). SRY (sex determining region on the Y chromosome) plays a key role in mammalian sex determination within the nucleus. HSPA8 plays a key role in calcium-binding protein, calmodulin (CaM) dependent nuclear import of SRY (Kaur et al., 2013). On the other hand, after administration of TLQP-21 on adolescent males with chronic food deprivation, the gonadotrophin response of hypothalamic-pituitary-gonadal (HPG) axis was found to be reduced and in fed males it caused puberty delay (Pinilla et al., 2011), consistent with the infertility found in male VGF knockout mice (Hahm et al., 1999; 2002).

HSPA8 was reported to be involved in the healing of acetic acid-induced gastric ulcers in rats. The protein was expressed highly in the normal mucosa and ulcerated tissue, though the level of protein expression was not changed during the ulceration and ulcer

healing process (Tsukimi et al., 2001). Remarkably, the central inhibitory effect of TLQP-21 on gastric acid secretion was proved, confirming that it is mediated by endogenous somatostatin and prostaglandins and requires the integrity of sensory nerve fibres (Sibilia et al., 2012).

Altered gene expression of HSPA8 was also found to be involved in hypertension in patients with blood-stasis syndrome (Lian et al., 2014), in Japanese individuals with chronic kidney disease (Oguri et al., 2009), patients with thoracic aortic aneurysm (Kato et al., 2008), patients with arterial hypertension (Timofeeva et al., 2006). The findings that acute and chronic administration of the VGF-derived peptide TLQP-21 to rodents improved hypertension (Fargali et al., 2014) indicates that the action of TLQP-21 may be mediated by the receptor HSPA8.

The findings highlighting the physiological relevance of the HSPA8 and TLQP-21 connection give more credence to the interaction of HSPA8 and TLQP-21 or at least the probable involvement of HSPA8 in TLQP-21 induced biological actions. In fact, due to all these physiological relevances of HSPA8 and TLQP-21, it is highly likely that the HSPA8-TLQP-21 interaction prompts various cellular responses, though the consequences of HSPA8-TLQP-21 are still elusive and need more clarification in signaling pathways.

Recent identification of murine TLQP-21 receptors:

gC1qR (Chen et al, 2013) and C3AR1 (Cero et al., 2014; Hannedouche et al, 2013) have been reported as receptors of murine TLQP-21. gC1qR was identified as the receptor of the peptide TLQP-21 using chemical crosslinking and monomeric avidin column purification following by MS analysis : the conjugated peptide (confirmed by MALDI-TOF) was crosslinked to the protein preparations showing ~30 kDa band (Ayub, 2012). Then the peptide attachment to monomeric avidin column, followed by the application of membrane protein and the elutants showed the ~30 kDa band, confirming it as gC1qR after MS analysis (Chen et al., 2013).

Hannedouche and his co-workers used the TLQP-21 responsive CHO-K1 cells to search for its receptor. Following unbiased genome wide sequencing of the transcriptome from CHO-K1 cells, possible GPCRs responsible for bringing about the TLQP-21 induced biological activities in the cells were listed. The TLQP-21 response in the cells were found reduced by the gene knockdown with the siRNAs targeting C3AR1. Moreover, the C3AR1 antagonist, SB290157 was shown to inhibit the TLQP-21 response in CHO-K1 cells. All these validate that the binding of TLQP-21 to its receptor C3AR1 has biological effects in CHO-K1 cell line, though this finding was not demonstrable to the human receptor (Hannedouche et al., 2013).

Even more recently, Cero et al., 2014 confirmed the binding of murine TLQP-21 to C3AR1 in CHO and 3T3L1 cells by photoactivated crosslinking method. In addition, structural analysis of TLQP-21 alone and in the presence of 3T3L1 cells, wild type splenocyte, C3AR1 knockout splenocyte and C3AR1 antagonists confirmed that the peptide goes from a disordered to ordered transition upon targeting cells expressing the C3AR1 and adopts a helical conformation, in consistent with the findings of a molecular dynamics study (Chakraborty et al., 2015). Based on the contraction of

stomach fundus strips (Severini et al., 2009) : one of the most reliable bioassays for TLQP-21; hot spots responsible for the function of the peptide were found lying at the C-terminal sequence (HFHH-10) whereas TLQP-11 (TLQPPASSRRR), the one without the C-terminal sequence was found inactive. Additional study by β -arrestin recruitment assay using HTLA cells transfected with human C3AR1 receptor revealed that the rodent version of the peptide possesses higher potency than human version of the peptide towards human C3AR1. It is hypothesized that the human version of the peptide differs by 4 amino acids compared to rodent version (as cited by Bartolomucci et al., 2011 but apparently human version of TLQP-21: TLQPPSALRRRHYHHALPPSR shows extensive homology but also substantial differences with mouse TLQP-21: TLQPPASSRRRHFHHALPPAR by 5 amino acids), resulting in the lower potency of the human TLQP-21 towards both of the human and rodent C3AR1 receptor (Cero et al., 2014).

Receptor(s) for human vs rodent TLQP-21:

Both human and rodent version of the peptide contains basic sequence RR to which the binding affinity of the HSPA8 was found to increase considerably (Takenaka et al., 1995). Structural dynamics of TLQP-21 bound to the HSPA8 receptor binding site explored by molecular dynamics simulation also reported that R₁₀-R₁₁ of the peptide TLQP-21 interacts strongly with the HSPA8 substrate binding site (For details, see the annex II).

However, to date most of the works focusing the characterization of TLQP-21 effects were based on rodent models, rather on human beings (Zhang et al., 2013). In fact, very few studies have been carried out with TLQP-21 using human cells. It is important to note here that for the first time Stephens et al., 2012 showed the controlled TLQP-21 secretion from human islets and effect of TLQP-21 on human pancreatic islet cells was

established by the same group (Stephens et al., 2012). Later on, in 2013, Zhang et al ascertained that in human umbilical vascular endothelial cells (HUVECs) TLQP-21 was capable of stopping apoptosis when the cells were treated with high glucose concentration; additionally they validated the signaling pathway in HUVECs: TLQP-21 uplifts the synthesis of NADPH and GSH (glutathione) in response to the boost up expression of G6PD (glucose-6-phosphate dehydrogenase), finally restoring the ROS (reactive oxygen species). All these data suggest that the peptide has effects in human cells but there might be different processing mechanism than rodents leading to a different receptor recognition in humans (Hannedouche et al., 2013). Recently, Cero et al., 2014 showed that human TLQP-21 with a S20A substitution binds to human C3AR1; however though the binding was found to be weaker in comparison to that of rodent TLQP-21. Moreover, human TLQP-21 was found to exert only a limited biological activity, five times less than the corresponding rodent TLQP-21 (Hannedouche et al., 2013), upon interaction with the rodent C3AR1 receptor (Cero et al, 2014).

All these data support the existence of different receptors for human vs rodent TLQP-21 that will potentiate 100 % biological activity in humans.

Downstream effects of human TLQP-21 binding to its receptor:

Till now, what is known about the downstream effects of binding of murine TLQP-21 to its receptors: TLQP-21 was found to increase the calcium levels in macrophages in a gC1qR dependent manner in rats (Chen et al., 2013). The biological activity of TLQP-21 signaling was also reported as mediated by G protein coupled receptor (GPCR) in CHO-K1 cell line. In CHO-K1 cells it was found that there is increase in intracellular calcium in response to TLQP-21, though to get strong signal ATP priming was required (Hannedouche et al., 2013). However, these outcomes were not possible to translate in human suggesting that human TLQP-21 might not work very well in those systems. Since it is unknown that whether similar effects, as cited by Chen et al., 2013 and Hannedouche et al., 2013, would be exerted by human TLQP-21 in the experimental system of this study, a proteomic as well as phosphoproteomic study was carried out. Of note, it is also important to validate that TLQP-21 is indeed having a biological effect in the model used in this study. Further, this is a starting point and pioneer work for future studies regarding the binding of the human version of the peptide to its receptor HSPA8.

Till now, HSPA8 was shown to interact with variety of ligands/binding partners with its functional consequences downward. But in most cases they are still to be more clarified. HSPA8 was reported to interact with TLR2/TLR4, induce cytokine expression, TNF- α , IL-1 β , and IL-6, initiating p38MAPK, NF- κ B pathways (Zou et al., 2008). It was also found to interact with surface signaling molecules including CD14, CD40, CD91, TLR2/TLR4, CCR5, CD36, FEEL, Lox-1, SR-A, and SREC (Calderwood et al., 2007), commencing signal transductions (Liao and Tang, 2014). HSPA8 found to provoke the endogenous (auto)antigen processing affecting antigen-presenting B cells, reducing

autoreactive T-cell priming; via a signalling mechanism involving a lysosomal degradation pathway (Page et al., 2011).

Here both the proteomic and the phosphoproteomic study showed altered protein expressions. Further investigations required to validate the result, also to confirm whether HSPA8 is involved in this altered protein expression or not. As a whole, further studies are required to clarify the overall downstream signaling pathways involved in the interaction of TLQP-21 and HSPA8.

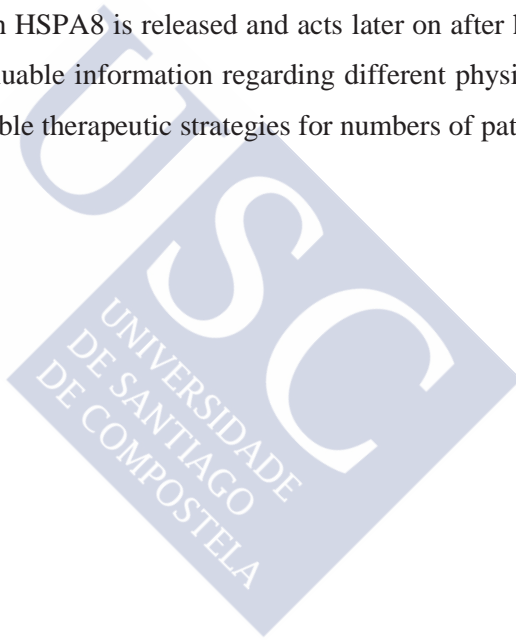
Concluding remarks:

So far it is known, HSPA8 is the first putative receptor of TLQP-21 in human cells. Considering all these aspects, identification of HSPA8 as a receptor of human TLQP-21 would open new approaches for diagnostics and therapeutics for a wide range of human diseases related with VGF, in particular those in which TLQP-21 has been shown to have an effect. Further advance exploration into the HSPA8-TLQP-21 interaction emphasizing, specially the downstream consequences is an essential need now.

In this study, HSPA9/mortalin, another member of the HSP-70 family, was found to bind TLQP-21. Further validation is required to make sure that TLQP-21 binds HSPA9/mortalin on the cell surface like HSPA8.

Future prospective:

The ligand TLQP-21 and its putative receptor HSPA8 is in its infancy and extensive work remains before to make it clear how the interaction between the receptor and the ligand, HSPA8 – TLQP-21 can be best exploited. Future works should aim to have a better understanding of the downstream consequences of the cell treatment with TLQP-21 which would uncover the proteins (both qualitative and quantitative) being regulated in TLQP-21 treated cells, also intracellular molecular mechanisms of TLQP-21 actions. The mechanisms by which HSPA8 is released and acts later on after having bound with TLQP-21 will provide valuable information regarding different physiological processes as well as will provide viable therapeutic strategies for numbers of pathologic conditions treatment.





Conclusions



-HSPA8 was identified as the receptor of human TLQP-21 using SH-SY5Y cells.

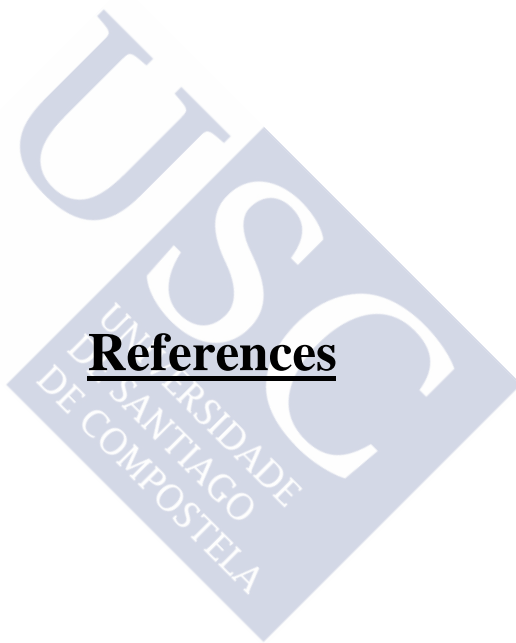
-Cross-linking of biotinylated TLQP-21 to putative membrane receptors of SH-SY5Y cells with subsequent cell homogenization, affinity chromatography using a monomeric avidin column and Western blot could detect a ~71 kDa band corresponding to HSPA8.

-Surface binding of biotinylated TLQP-21 by the SH-SY5Y cells was increased in the dose-dependent manner of biotin-TLQP-21, demonstrated by FACS analysis.

- TLQP-21 can be docked into the peptide binding pocket of HSPA8: illustrated by molecular modeling studies.

-TLQP-21 induced altered protein expressions in SH-SY5Y cells: confirmed by proteomic and phosphoproteomic study.





References



-
- Abbadie, C., Lindia, J. A., Cumiskey, A. M., Peterson, L. B., Mudgett, J. S., Bayne, E. K., DeMartino, J. A., MacIntyre, D. E., Forrest, M. J. (2003) Impaired neuropathic pain responses in mice lacking the chemokine receptor CCR2. *Proc. Natl. Acad. Sci. U.S.A.* **100**: 7947–795
- Aguilar, E., Pineda, R., Gayta´ n, F., Sa´nchez-Garrido, M. A., Romero, M., Romero-Ruiz, A., Ruiz-Pino, F., Tena-Sempere, M., and Pinilla, L. (2013) Characterization of the reproductive effects of the Vgf-derived peptide TLQP-21 in female rats: in vivo and in vitro studies. *Neuroendocrinology* **98**: 38–50
- Alder, J., Thakker-Varia, S., Bangasser, D. A., Kuroiwa, M., Plummer, M. R., Shors, T. J., Black, I. B. (2003) Brain-derived neurotrophic factor-induced gene expression reveals novel actions of VGF in hippocampal synaptic plasticity. *J Neurosci.* **26** 23(34): 10800-8
- Altmeyer, A., Maki, R. G., Feldweg, A. M., Heike, M., Protopopov, V. P., Masur, S. K., Srivastava, P. K. (1996) Tumor-specific cell surface expression of the KDEL containing, endoplasmic reticular heat shock protein gp96. *Int J Cancer.* **69**: 340–349
- Ames, R. S., Lee, D., Foley, J. J., Jurewicz, A. J., Tornetta, M. A., Bautsch, W., Settmacher, B., Klos, A., Erhard, K. F., Cousins, R. D., Sulpizio, A. C., Hieble, J. P., McCafferty, G., Ward, K. W., Adams, J. L., Bondinell, W. E., Underwood, D. C., Osborn, R. R., Badger, A. M., Sarau, H. M. (2001) Identification of a selective nonpeptide antagonist of the anaphylatoxin C3a receptor that demonstrates antiinflammatory activity in animal models. *J Immunol.* **15**: 166 (10): 6341-8
- Amir, S., Schiavetto, A. (1990) Injection of prostaglandin E2 into the anterior hypothalamic preoptic area activates brown adipose tissue thermogenesis in the rat. *Brain Res* **528**: 138–142
- Ariëns, E. J. (1984) Receptors: perspectives in pathology and clinical medicine. *J Recept Res.* **4** (1-6): 1-17

References

Arispe, N., Doh, M., Simakova, O., Kurganov, B., De Maio, A. (2004) Hsc70 and Hsp70 interact with phosphatidylserine on the surface of PC12 cells resulting in a decrease of viability. *FASEB J.* **18**: 14, 1636-1645

Arispe, N., De Maio, A. (2000) ATP and ADP modulate a cation channel formed by Hsc70 in acidic phospholipid membranes. *J Biol Chem.* **6** 275 (40): 30839-43

Auger, I., Escola, J. M., Gorvel, J. P., Roudier, J. (1996) HLA-DR4 and HLA-DR10 motifs that carry susceptibility to rheumatoid arthritis bind 70-kD heat shock proteins. *Nat Med* **2**: 306-10; PMID:8612229; <http://dx.doi.org/10.1038/nm0396-306>

Ayub, M. (2012) *Investigating the mechanisms of action of VGF-derived peptides in the nervous system.* Ph D thesis. Imperial College, London. Print.

Bachman, E. S., Dhillon, H., Zhang, C. Y., Cinti, S., Bianco, A. C., Kobilka, B. K., Lowell, B. B. (2002) beta-AR signaling required for diet-induced thermogenesis and obesity resistance. *Science* **297**: 843-845

Barreto, A., Gonzalez, J. M., Kabingu, E., Asea, A., Fiorentino, S. (2003) Stress-induced release of HSC70 from human tumors. *Cell Immunol.* **222** (2) : 97-104

Bartolomucci, A., Bresciani, E., Bulgarelli, I., Rigamonti, A. E., Pascucci, T., Levi, A., Possenti, R., Torsello, A., Locatelli, V., Muller, E. E., Moles, A. (2009) Chronic intracerebroventricular injection of TLQP-21 prevents high fat diet induced weight gain in fast weight-gaining mice. *Genes Nutr.* **4** (1): 49-57. doi: 10.1007/s12263-009-0110-0. Epub 2009 Feb 27

Bartolomucci, A., Moles, A., Levi, A., Possenti, R., (2008) Pathophysiological role of TLQP-21: gastrointestinal and metabolic functions. *Eat Weight Disord.* **13**(3): e49-54. PMID: 19011364

Bartolomucci, A., Corte, G. L., Possenti, R., Locatelli, V., Rigamonti, A. E., Torsello, A., Bresciani, E., Bulgarelli, I., Rizzi, R., Pavone, F., D'Amato, F. R., Severini, C., Mignogna, G., Giorgi, A., Schinina, M. E., Elia, G., Brancia, C., Ferri, G. L., Conti, R., Ciani, B., Pascucci, T., Dell'Omo, G., Muller, E. E.,

- Levi, A., Moles, A. (2006) TLQP-21, a VGF-derived peptide, increases energy expenditure and prevents the early phase of diet-induced obesity, *Proc. Natl. Acad. Sci. U. S. A.* **103** : 14584–14589
- Bartolomucci, A., Pasinetti, G. M., Salton, S.R.J. (2010) Granins as disease-biomarkers: translational potential for psychiatric and neurological disorders. *Neuroscience* **170**: 289–297
- Bartolomucci, A., Possenti, R., Levi, A., Pavone, F., Moles, A. (2007) The role of the vgf gene and VGF-derived peptides in nutrition and metabolism. *Genes Nutr.* **2** (2): 169-80
- Bartolomucci, A., Possenti, R., Mahata, S. K., Fischer-Colbrie, R., Loh, Y. P., Salton, S. R. (2011) The extended granin family: structure, function, and biomedical implications. *Endocr Rev.* **32** (6): 755-97
- Bauer, P. O., Goswami, A., Wong, H. K., Okuno, M., Kurosawa, M., Yamada, M., Miyazaki, H., Matsumoto, G., Kino, Y., Nagai, Y., Nukina, N. (2010) Harnessing chaperone-mediated autophagy for the selective degradation of mutant huntingtin protein. *Nat Biotechnol.* **28** (3): 256-63
- Becker, F., Craig, E. (1994) Heat shock proteins as molecular chaperones. *Eur J Biochem.* **219**: 11–23
- Beckmann, R. P., Mizzen, L. E., Welch, W. J. (1990) Interaction of Hsp 70 with newly synthesized proteins: implications for protein folding and assembly. *Science.* **248** (4957): 850-4. PMID: 2188360; <http://dx.doi.org/10.1126/science.2188360>
- Beckmann, R. P., Lovett, M., Welch, W. J. (1992) Examining the function and regulation of hsp 70 in cells subjected to metabolic stress. *J Cell Biol.* **117** (6): 1137-50
- Beere, H. M. (2004) The stress of dying: the role of heat shock proteins in the regulation of apoptosis. *J Cell Sci.* **1**: 117(Pt 13): 2641-51

References

- Belles, C., Kuhl, A., Nosheny, R., Carding, S. R. (1999) Plasma membrane expression of heat shock protein 60 *in vivo* in response to infection. *Infection and Immunity*, **67** (8): 4191–4200
- Bhattacharyya, T., Karnezis, A. N., Murphy, S. P., Hoang, T., Freeman, B. C., Phillips, B., Morimoto, R. I. (1995) Cloning and subcellular localization of human mitochondrial hsp70. *J. Biol. Chem.* **270**: 1705–1710
- Biedler, J. L., Helson, L., Spengler, B. A. (1973) Morphology and growth, tumorigenicity, and cytogenetics of human neuroblastoma cells in continuous culture. *Cancer Res.* **33** (11): 2643–52
- Biedler, J. L., Roffler-Tarlov, S., Schachner, M., Freedman, L. S. (1978) Multiple neurotransmitter synthesis by human neuroblastoma cell lines and clones. *Cancer Res.* **38** : 3751–7
- Bondia-Pons, I., Boqué, N., Paternain, L., Santamaría, E., Fernández, J., Campión, J., Milagro, F., Corrales, F., Martínez, J. A. (2011) Liver proteome changes induced by a short-term high-fat sucrose diet in wistar rats. *J Nutrigenet Nutrigenomics.* **4** (6): 344-53
- Borges, C. R.; Watson, J. T. (2003) Recognition of cysteine-containing peptides through prompt fragmentation of the 4-dimethylaminophenylazophenyl-4' - maleimide derivative during analysis by MALDI-MS. *Protein Science* **12**: 1567–1572
- Bouillet, P., Metcalf, D., Huang, D. C., Tarlinton, D. M., Kay, T. W., Köntgen, F., Adams, J. M., Strasser, A. (1999) Proapoptotic Bcl-2 relative Bim required for certain apoptotic responses, leukocyte homeostasis, and to preclude autoimmunity. *Science* **286**: 1735-8; PMID:10576740; <http://dx.doi.org/10.1126/science.286.5445.1735>
- Bozdagi, O., Rich, E., Tronel, S., Sadahiro, M., Patterson, K., Shapiro, M. L., Alberini, C. M., Huntley, G. W., Salton, S. R. (2008) The neurotrophin-inducible gene Vgf regulates hippocampal function and behavior through a brain-derived neurotrophic factor-dependent mechanism. *J Neurosci.* **28** (39): 9857-69

- Brown, D. M., Donaldson, K., Borm, P. J., Schins, R. P., Dehnhardt, M., Gilmour, P., Jimenez, L. A., Stone, V. (2004) Calcium and ROS-mediated activation of transcription factors and TNF- cytokine gene expression in macrophages exposed to ultrafine particles. *Am. J. Physiol. Lung Cell. Mol. Physiol.* **286**: L344–353
- Bruce, C. R., Carey, A. L., Hawley, J. A., Febbraio, M. A. (2003) Intramuscular heat shock protein 72 and heme oxygenase-1 mRNA are reduced in patients with type 2 diabetes: evidence that insulin resistance is associated with a disturbed antioxidant defense mechanism. *Diabetes.* **52**: 2338-2345
- Buchner, J. (1996) Supervising the fold: functional principles of molecular chaperones. *FASEB.* **10**: 10-19
- Busse, S., Bernstein, H. G., Busse, M., Bielau, H., Brisch, R., Mawrin, C., Müller, S., Sarnyai, Z., et al. (2012) Reduced density of hypothalamic VGF-immunoreactive neurons in schizophrenia: a potential link to impaired growth factor signaling and energy homeostasis. *Eur Arch Psychiatry Clin Neurosci.* **262** (5): 365-74. doi: 10.1007/s00406-011-0282-7. Epub 2011 Dec 14
- Cai, X., Wang, G. J., Qu, Y., Fan, C. H., Zhang, R. Q., Xu, W. S. (1997) Clinical efficacy of oxymatrine in the treatment of chronic hepatitis B. *Acad. J. Sec. Mil. Med. Univ.* **18**:47–49
- Calderwood, S. K., Mambula, S. S., Gray, P. J. Jr., Theriault, JR. (2007) Extracellular heat shock proteins in cell signaling. *FEBS Lett* **581**: 3689-94
- Campisi, J., Leem, T. H., Fleshner, M. (2003) Stress-induced extracellular Hsp72 is a functionally significant danger signal to the immune system. *Cell Stress Chaperones.* **8**: 272-286
- Cannon, B., Nedegaard, J. (2004) Brown adipose tissue: function and physiological significance. *Physiol Rev* **84**: 277–359

References

Canu, N., Possenti, R., Ricco, A.S., Rocchi, M., Levi, A. (1997a) Cloning, structural organization analysis, and chromosomal assignment of the human gene for the neurosecretory protein VGF. *Genomics* **45**: 443-446

Canu, N., Possenti, R., Rinaldi, A. M., Trani, E., Levi, A. (1997b) Molecular cloning and characterization of the human VGF promoter region. *J Neurochem* **68**: 1390-1399

Cassina, V., Torsello, A., Tempestini, A., Salerno, D., Brogioli, D., Tamiazzo, L., Bresciani, E., Martinez, J., Fehrentz, J. A., Verdié, P., Omeljaniuk, R. J., Possenti, R., Rizzi, L., Locatelli, V., Mantegazza, F. (2013) Biophysical characterization of a binding site for TLQP-21, a naturally occurring peptide which induces resistance to obesity. *Biochim Biophys Acta.* **1828** (2): 455-60. doi: 10.1016/j.bbamem.2012.10.023. Epub 2012 Oct 30.

Cattaneo, A., Sesta, A., Calabrese, F., Nielsen, G., Riva, M. A., Gennarelli, M. (2010) The expression of VGF is reduced in leukocytes of depressed patients and it is restored by effective antidepressant treatment. *Neuropsychopharmacology* **35**: 1423-1428

Cederberg, A., Grønning, L. M., Ahren, B., Tasken, K., Carlsson, P., Enerback, S. (2001) FOXC2 is a winged helix gene that counteracts obesity, hypertriglyceridemia, and diet-induced insulin resistance. *Cell* **106**: 563-573

Cero, C., Vostrikov, V. V., Verardi, R., Severini, C., Gopinath, T., Braun, P. D., Sassano, M. F., Gurney, A., Roth, B. L., Vulchanova, L., Possenti, R., Veglia, G., Bartolomucci, A. (2014) The TLQP-21 peptide activates the G-protein-coupled receptor C3aR1 via a folding-upon-binding mechanism. *Structure* **22**: 1744-1753

Chakraborty, S., Akhter, S., Requena, J. R., Basu, S. (2015) Probing the conformational dynamics of the bioactive peptide TLQP 21 in solution: A molecular dynamics study. *Chemical biology and drug design*. 'Accepted Article', doi: 10.1111/cbdd.12541

- Cheishvili, D., Maayan, C., Smith, Y., Ast, G., Razin, A. (2007) IKAP/hELP1 deficiency in the cerebrum of familial dysautonomia patients results in down regulation of genes involved in oligodendrocyte differentiation and in myelination. *Hum. Mol. Genet.* **16**: 2097–2104
- Chen, H. S., Jia, J., Su, H. F., Lin, H. D., Chen, J. W., Lin, S. J., Yang, J. Y., Lai, H. C., Mestril, R., Wang, P. H. (2006) Downregulation of the constitutively expressed Hsc70 in diabetic myocardium is mediated by insulin deficiency. *J Endocrinol.* **190** (2): 433-40
- Chen, M. S., Goswami, P. C., Laszlo, A. (2002) Differential accumulation of U14 snoRNA and hsc70 mRNA in Chinese hamster cells after exposure to various stress conditions. *Cell Stress Chaperones.* **7** (1): 65-72
- Chen, S., Bawa, D., Besshoh, S., Gurd, J. W., Brown, I. R. (2005) Association of heat shock proteins and neuronal membrane components with lipid rafts from the rat brain. *Journal of Neuroscience Research* **81**: 522–529
- Chen, Y. C., Pristerá, A., Ayub, M., Swanwick, R. S., Karu, K., Hamada, Y., Rice, A. S., Okuse, K. (2013) Identification of a receptor for neuropeptide VGF and its role in neuropathic pain. *J BiolChem.* **288** (48): 34638-46
- Chen, Z., Stokes, D. L., Rice, W. J., Jones, L. R. (2003) Spatial and Dynamic Interactions between Phospholamban and the Canine Cardiac Ca² Pump Revealed with Use of Heterobifunctional Cross-linking Agents. *J. Biol. Chem.* **278**: 48348-48356
- Chirico, W. J., Waters, M. G., Blobel, G. (1988) 70K heat shock related proteins stimulate protein translocation into microsomes. *Nature* **28** 332 (6167): 805-10; PMID:3282179; <http://dx.doi.org/10.1038/332805a0>
- Cho, K. O., Skarnes, W. C., Minsk, B., Palmieri, S., Jackson-Grusby, L., Wagner, J. A. (1989) Nerve growth factor regulates gene expression by several distinct mechanisms. *Mol. Cell. Biol.* **9**: 135–143

References

- Chubb, J. E., Bradshaw, N. J., Soares, D. C., Porteous, D. J., Millar, J. K. (2008) The DISC locus in psychiatric illness. *Mol Psychiatry*. **13** (1): 36-64
- Chung, J., Nguyen, A. K., Henstridge, D. C., Holmes, A. G., Chan, M. H., Mesa, J. L., et al. (2008) HSP72 protects against obesity-induced insulin resistance. *Proceedings of the National Academy of Sciences of the United States of America* **105**: 1739-1744
- Cicconi, R., Delpino, A., Piselli, P., Castelli, M., Vismara, D. (2004) Expression of 60 kDa heat shock protein (Hsp60) on plasma membrane of Daudi cells. *Molecular and Cellular Biochemistry* **259**: 1-7
- Clayton, A., Turkes, A., Navabi, H., Mason, M. D., Tabi, Z. (2005) Induction of heat shock proteins in B-cell exosomes. *J Cell Sci* **118**: 3631-8
- Coull, J. A., Beggs, S., Boudreau, D., Boivin, D., Tsuda, M., Inoue, K., Gravel, C., Salter, M. W., De Koninck, Y. (2005) BDNF from microglia causes the shift in neuronal anion gradient underlying neuropathic pain. *Nature* **438**: 1017-1021
- Daniell, E. L., Ryan, E. P., Brick, M. A., Thompson, H. J. (2012) Dietary dry bean effects on hepatic expression of stress and toxicity-related genes in rats. *Br J Nutr*. **108** Suppl 1: S37-45
- Daugaard, M., Rohde, M., Jäättelä, M., (2007) The heat shock protein 70family: Highly homologous proteins with overlapping and distinct functions. *FEBS Lett* **581**: 3702-10
- Dedio, J., Jahnen-Dechent, W., Bachmann, M., Muller-Esterl, W. (1998) The multiligand-binding protein gC1qR, putative C1q receptor, is a mitochondrial protein. *J Immunol* **160**: 3534-3542
- Deftos, L. J., Murray, S. S., Burton, D. W., Parmer, R. J., O'Connor, D. T., Deleage, A. M., Mellon, P. L. (1986) A cloned chromogranin A (CgA) cDNA detects a 2.3kb mRNA in diverse neuroendocrine tissues. *Biochemical and Biophysical Research Communications* **137**: 418-423

- Deocaris, C. C., Kaul, S. C., Wadhwa, R. (2008) From proliferative to neurological role of an hsp70 stress chaperone, mortalin. *Biogerontology* **9**(6): 391-403
- Deocaris, C. C., Kaul, S. C., Wadhwa, R. (2006) On the brotherhood of the mitochondrial chaperones mortalin and heat shock protein 60. *Cell Stress Chaperones*. **11**(2): 116–128
- Deshaies, R. J., Koch, B. D., Werner-Washburne, M., Craig, E. A., Schekman, R. (1988) A subfamily of stress proteins facilitates translocation of secretory and mitochondrial precursor polypeptides. *Nature* **332**: 800-5; PMID:3282178; <http://dx.doi.org/10.1038/332800a0>
- Dugas, J. C., Tai, Y. C., Speed, T. P., Ngai, J., Barres, B. A. (2006) Functional genomic analysis of oligodendrocyte differentiation. *J Neurosci.* **25**; 26(43): 10967-83
- Dupont, A., Chwastyniak, M., Beseme, O., Guihot, A. L., Drobecq, H., Amouyel, P., Pinet, F. (2008) Application of saturation dye 2D-DIGE proteomics to characterize proteins modulated by oxidized low density lipoprotein treatment of human macrophages. *J Proteome Res.* **7**(8): 3572-82. doi: 10.1021/pr700683s. Epub 2008 Jun 13.
- Elliott, R. M. A., Lloyd, R. E., Fazeli, A., Sostaric, E., Georgiou, A. S. Satake1, N., Watson, P. F., Holt, W. V. (2009) Effects of HSPA8, an evolutionarily conserved oviductal protein, on boar and bull spermatozoa. *Reproduction* **137**: 191–203
- Evans, C. G., Chang, L., Gatwick, J. E. (2010) Heat shock protein 70 (Hsp70) as an emerging drug target. *J Med Chem.* **24**: 53 (12): 4585–4602
- Evans, R. M., Barish, G. D., Wang, Y-X. (2004) PPARs and the complex journey to obesity. *Nat Med* **10**: 1–7

References

- Evdokimovskaya, Y., Skarga, Y., Vrublevskaya, V., Morenkov, O. (2010) Secretion of the heat shock proteins HSP70 and HSC70 by baby hamster kidney (BHK-21) cells. *Cell BiolInt* **34**: 985-90
- Fairbanks, C. A., Peterson, C. D., Speltz, R. H., Riedl, M. S., Kitto, K. F., Dykstra, J. A., Braun, P. D., Sadahiro, M., Salton, S. R., Vulchanova, L. (2014) The VGF-derived peptide TLQP-21 contributes to inflammatory and nerve injury-induced hypersensitivity. *Pain* **155**: 1229–1237
- Fargali, S., Garcia, A. L., Sadahiro, M., Jiang, C., Janssen, W. G., Lin, W. J., Cogliani, V., Elste, A., Mortillo, S., Cero, C., et al. (2014) The granin VGF promotes genesis of secretory vesicles, and regulates circulating catecholamine levels and blood pressure. *FASEB J.* **28**: 2120–2133
- Fazeli, A., Elliott, R. M., Duncan, A. E., et al. (2003) In vitro maintenance of boar sperm viability by a soluble fraction obtained from oviductal apical plasma membrane preparations. *Reproduction* **125**: 509-17
- Ferrarini, M., Heltai, S., Zocchi, M. R., Rugarli, C. (1992) Unusual expression and localization of heat-shock proteins in human tumor cells. *Int J Cancer.* **51**: 613–619
- Fischer-Colbrrie, R., Hagn, C., Schober, M. (1987) Chromogranins A, B, and C: widespread constituents of secretory vesicles. *Annals of the New York Academy of Sciences* **493**: 120-134
- Fishelson, Z., Hochman, I., Greene, L. E., Eisenberg, E. (2001) Contribution of heat shock proteins to cell protection from complement-mediated lysis. *Int Immunol* **13**: 983-91
- Fourie, A. M., Sambrook, J. F., Gething, M. J. (1994) Common and divergent peptide binding specificities of hsp70 molecular chaperones. *J Biol Chem.* **269**(48): 30470-8
- Francis K., Lewis B. M., Akatsu H., Monk P. N., Cain S. A., Scanlon M. F., Morgan B. P., Ham J., Gasque P. (2003) Complement C3a receptors in the

- pituitary gland: a novel pathway by which an innate immune molecule releases hormones involved in the control of inflammation. *FASEB J.* **17**: 2266–2268
- Frydman, J., Hohfeld, J. (1997) Chaperones get in touch: the Hip-Hop connection. *Trends Biochem. Sci.* **22** : 87
- Frydman, J., Hartl, F. U. (1996) Principles of chaperone-assisted protein folding: differences between in vitro and in vivo mechanisms. *Science* **272**: 1497-502; PMID:8633246; <http://dx.doi.org/10.1126/science.272.5267.1497>
- Gaboriaud, C., Juanhuix, J., Gruez, A., Lacroix, M., Darnault, C., Pignol, D., Verger, D., Fontecilla-Camps, J. C., Arlaud, G. J. (2003) The crystal structure of the globular head of complement protein C1q provides a basis for its versatile recognition properties. *J Biol Chem.* **278**(47): 46974-82
- Gadella, B. M., Lopes-Cardozo, M., van Golde, L. M., *et al.*(1995) Glycolipid migration from the apical to the equatorial subdomains of the sperm head plasma membrane precedes the acrosome reaction. Evidence for a primary capacitation event in boar spermatozoa. *J Cell Sci* **108**: 935-46
- Gatenby, A. A., Ellis, R. J. (1990) Chaperone function: The assembly of ribulose biphosphate carboxylase-oxygenase. *Annu. Rev. Cell Biol.* **6**: 125-149
- Ghebrehwet, B., Lim, B. L., Kumar, R., Feng, X., Peerschke, E. I. (2001) gC1q-R/p33, a member of a new class of multifunctional and multicompartmental cellular proteins, is involved in inflammation and infection. *Immunol Rev* **180**: 65-77
- Ghebrehwet, B., Lu, P. D., Zhang, W., Lim, B. L., Eggleton, P., Leigh, L. E., Reid, K. B., Peerschke, E. I. (1996) Identification of functional domains on gC1Q-R, a cell surface protein that binds to the globular "heads" of C1Q, using monoclonal antibodies and synthetic peptides. *Hybridoma* **15**: 333-342
- Gilhooley, M. J. (2010) Adult neurogenesis and depression: An introduction. *Psychiatr Danub.* **1**: S85-7.

References

Griebel, G., Holsboer, F. (2012) Neuropeptide receptor ligands as drugs for psychiatric diseases: the end of the beginning? *Nature Reviews Drug Discovery* **462**: 478

Guerrero, C. A., Moreno, L. P. (2012) Rotavirus receptor proteins Hsc70 and integrin $\alpha 3$ are located in the lipid microdomains of animal intestinal cells. *Acta Virol* **56**: 63-70

Gupte, A. A., Bomhoff, G. L., Swerdlow, R. H., Geiger, P. C. (2009) Heat treatment improves glucose tolerance and prevents skeletal muscle insulin resistance in rats fed a high-fat diet. *Diabetes* **58**: 567-578

Hahm, S., Fekete, C., Mizuno, T. M., Windsor, J., Yan, H., Boozer, C. N., Lee, C., Elmquist, J. K., Lechan, R. M., Mobbs, C. V., et al. (2002) VGF is required for obesity induced by diet, gold thioglucose treatment, and agouti and is differentially regulated in pro-opiomelanocortin- and neuropeptide Y-containing arcuate neurons in response to fasting. *J Neurosci* **22**: 6929-6938

Hahm, S., Mizuno, T. M., Wu, T. J., Wisor, J. P., Priest, C. A., Kozak, C. A., Boozer, C. N., Peng, B., McEvoy, R. C., Good, P., et al. (1999) Targeted deletion of the Vgf gene indicates that the encoded secretory peptide precursor plays a novel role in the regulation of energy balance. *Neuron* **23**: 537-548

Hannedouche, S., Beck, V., Leighton-Davies, J., Beibel, M., Roma, G., Oakeley, E. J., Lannoy, V., Bernard, J., Hamon, J., Barbieri, S., Preuss, I., Lasbennes, M. C., Sailer, A. W., Suply, T., Seuwen, K., Parker, C. N., Bassilana, F. (2013) The identification of the C3a Receptor (C3AR1) as the target of the VGF derived peptide TLQP-21 in rodent cells. *J Biol Chem.* **20**; 288(38): 27434-43. doi: 10.1074/jbc.M113.497214. Epub 2013 Aug 12.

Hantschel, M., Pfister, K., Jordan, A., Scholz, R., Andreesen, R., Schmitz, G., Schmetzer, H., Hiddemann, W., Multhoff, G. (2000) Hsp70 plasma membrane expression on primary tumor biopsy material and bone marrow of leukemic patients. *Cell Stress Chaperones* **5**(5): 438-42

- Harsha, H. C., Kandasamy, K., Ranganathan, P., Rani, S., Ramabadran, S., Gollapudi, S., Balakrishnan, L., Dwivedi, S. B., Telikicherla, D., Selvan, L. D., Goel, R., Mathivanan, S., Marimuthu, A., Kashyap, M., Vizza, R. F., Mayer, R. J., Decaprio, J. A., Srivastava, S., Hanash, S. M., Hruban, R. H., Pandey, A. (2009) A compendium of potential biomarkers of pancreatic cancer. *PLoS Med.* **6**(4): 1000046
- Hartl, F. U. (1996) Molecular chaperones in cellular protein folding. *Nature* **381**: 571–580
- Hayem, G., De Bandt, M., Palazzo, E., Roux, S., Combe, B., Eliaou, J. F., Sany, J., Kahn, M. F., Meyer, O. (1999) Anti-heat shock protein 70 kDa and 90 kDa antibodies in serum of patients with rheumatoid arthritis. *Ann Rheum Dis* **58**: 291-6; PMID:10225814; <http://dx.doi.org/10.1136/ard.58.5.291>
- He, M., Guo, H., Yang, X., et al. (2010) Genetic variations in HSPA8 gene associated with coronary heart disease risk in a Chinese population. *PLoS One* **5**: 9684
- Heapy, C. G., Jamieson, A., Russell, N. J. W. (1987) Afferent C-fibre and A-delta activity in models of inflammation. *British journal of pharmacology* **90**: 164
- Heitz, J. R., Anderson, C. D., Anderson, B. M. (1968) Inactivation of yeast alcohol dehydrogenase by N -alkylmaleimides. *Arch. Bio- chem. Biophys.* **127**: 627
- Heleniak, E. P., Aston, B. (1989) Prostaglandins, brown fat and weight loss. *Med Hypotheses* **28**: 13–33
- Henstridge, D. C., Bruce, C. R., Drew, B. G., Tory, K., Kolonics, A., Estevez, E., et al., (2014) Activating HSP72 in rodent skeletal muscle increases mitochondrial number and oxidative capacity and decreases insulin resistance. *Diabetes* **63**: 1881-1894
- Hermanson, G. T. (1996) Bioconjugate Techniques. Academic Press: San Diego, CA; 37. ISBN 0-12-342336-8

References

Hightower, L. E., Sadis, S. E., and Takenaka, I. M. (1994) Interactions of vertebrate hsc70 and hsp70 with unfolded proteins and peptides. In "The Biology of Heat Shock Proteins and Molecular Chaperones." (R.I. Morimoto, A. Tissieres and C. Georgopoulos, Eds.), Cold Spring Harbor Press, Cold Spring.

Hooper, P. L., Hooper, P. L. (2009) Inflammation, heat shock proteins, and type 2 diabetes. *Cell Stress and Chaperones*. **14**: 113–115

Hooshmand and Hooshang (1993) Chronic pain: reflex sympathetic dystrophy prevention and management. *Boca Raton, FL: CRC Press LLC*. 44. ISBN 0-8493-8667-5

Huang, J. T., Leweke, F. M., Oxley, D., Wang, L., Harris, N., Koethe, D., Gerth, C. W., Nolden, B. M., Gross, S., Schreiber, D., Reed, B., Bahn, S. (2006) Disease biomarkers in cerebrospinal fluid of patients with first-onset psychosis. *PLoS Med*. **3** (11): e428.

Hunsberger, J. G., Newton, S. S., Bennett, A. H., Duman, C. H., Russell, D. S., Salton, S. R., Duman, R. S. (2007) Antidepressant actions of the exercise-regulated gene VGF. *Nat Med* **13**: 1476-1482

Imamoto, N., Matsuoka, Y., Kurihara, T., Kohno, K., Miyagi, M., Sakiyama, F., Okada, Y., Tsunasawa, S., Yoneda, Y. (1992) Antibodies against 70-kD heat shock cognate protein inhibit mediated nuclear import of karyophilic proteins. *J Cell Biol* **119**: 1047-61; PMID:1332978; <http://dx.doi.org/10.1083/jcb.119.5.1047>

Jethwa, P. H., Ebling, F. J. (2008) Role of VGF-derived peptides in the control of food intake, bodyweight and reproduction. *Neuroendocrinology* **88**: 80-87. DOI:10.1159/000127319

Jethwa, P. H., Warner, A., Nilaweera, K. N., Brameld, J. M., Keyte, J. W., Carter, W. G., Bolton, N., Bruggraber, M., Morgan, P. J., Barrett, P., et al. (2007) VGF-derived peptide, TLQP-21, regulates food intake and body weight in Siberian hamsters. *Endocrinology* **148**: 4044-4055

- Jimenez, M., Leger, B., Canola, K., Lehr, L., Arboit, P., Seydoux, J., Russell, A. P., Giacobino, J. P., Muzzin, P., Preitner, F. (2002) α 1/ α 2/ α 3-adrenoreceptor knockout mice are obese and cold sensitive but have normal lipolytic responses to fasting. *FEBS Lett* **530**: 37–40
- Kaput, J., Astley, S., Renkema, M., Ordovas, J., van Ommen, B. (2006) Harnessing Nutrigenomics: Development of web-based communication, databases, resources, and tools. *Genes Nutr.* **1** (1): 5–11. doi: 10.1007/BF02829931.
- Kato, K., Oguri, M., Kato, N., Hibino, T., Yajima, K., Yoshida, T., Metoki, N., Yoshida, H., Satoh, K., Watanabe, S., Yokoi, K., Murohara, T., Yamada, Y. (2008) Assessment of genetic risk factors for thoracic aortic aneurysm in hypertensive patients. *Am J Hypertens.* **21**(9): 1023-7
- Kaur, G., Lieu, K. G., Jans, D. A. (2013) 70-kDa Heat Shock Cognate Protein hsc70 Mediates Calmodulin-dependent Nuclear Import of the Sex-determining Factor SRY. *J Biol Chem.* **288**(6): 4148–4157
- Kaur, I., Voss, S. D., Gupta, R. S., Schell, K., Fisch, P., Sondel, P. M. (1993) Human Peripheral yd T cells recognize hsp60 molecules on Daudi Burkitt's lymphoma cells. *J. Immunol* **150**: 2046-2055
- Kettner, S., Kalthoff, F., Graf, P., Priller, E., Kricek, F., Lindley, I., Schweighoffer, T. (2007) EWI-2/CD316 is an inducible receptor of HSPA8 on Human Dendritic Cells. *Mol Cell Biol* **27**: 7718-26
- Kim, K. B., Kim, B. W., Choo, H. J., Kwon, Y. C., Ahn, B. Y., Choi, J. S., Lee, J. S., Ko, Y. G. (2009) Proteome analysis of adipocyte lipid rafts reveals that gC1qR plays essential roles in adipogenesis and insulin signal transduction. *Proteomics* **9**: 2373–2382
- Kimmins, S., MacRae, T. H. (2000) Maturation of steroid receptors: an example of functional cooperation among molecular chaperones and their associated proteins. *Cell Stress Chaperones.* **5** (2): 76-86

References

Kishi, A., Ichinohe, T., Hirai, I., Kamiguchi, K., Tamura, Y., Kinebuchi, M., Torigoe, T., Ichimiya, S., Kondo, N., Ishitani, K., et al. (2001) The cell surface-expressed HSC70-like molecule preferentially reacts with the rat T-cell receptor Vdelta6 family. *Immunogenetics* **53**: 401-9

Klos, A., Wende, E., Wareham, K. J., Monk, P. N. (2013) International Union of Pharmacology. LXXXVII. Complement peptide C5a, C4a, and C3a receptors. *Pharmacol. Rev.* **65** (1): 500-43

Kodiha, M., Chu, A., Lazrak, O., Stochaj, U. (2005) Stress inhibits nucleocytoplasmic shuttling of heat shock protein hsc70. *Am J Physiol Cell Physiol.* **289** (4): C1034-41 PMID:15930140; <http://dx.doi.org/10.1152/ajpcell.00590.2004>

Konsman, J. P., Parnet, P., Dantzer, R. (2002) Cytokines-induced sickness behavior: mechanisms and implications. *Trends Neuro-sci* **25**: 154-159

Korhonen, R., Kankaanranta, H., Lahti, A., Lähde, M., Knowles, R. G., Moilanen, E. (2001) Bi-directional effects of the elevation of intracellular calcium on the expression of inducible nitric-oxide synthase in J774 macrophages exposed to low and to high concentrations of endotoxin. *Biochem. J.* **354**: 351-358

Kubota, H., Yamamoto, S., Itoh, E., Abe, Y., Nakamura, A., Izumi, Y., Okada, H., Iida, M., Nanjo, H., Itoh, H., Yamamoto, Y. (2010) Increased expression of co-chaperone HOP with HSP90 and HSC70 and complex formation in human colonic carcinoma. *Cell Stress Chaperones.* **15** (6): 1003-11

Kurucz, I., Morva, A., Vaag, A., Eriksson, K. F., Huang, X., Groop, L., et al. (2002) Decreased expression of heat shock protein 72 in skeletal muscle of patients with type 2 diabetes correlates with insulin resistance. *Diabetes.* **51**: 1102-1109

Larsen, T. M., Toubro, S., van Baak, M. A., Gottesdiener, K. M., Larson, P., Saris, W. H. M., Astrup, A. (2002) Effect of a 28-d treatment with L-796568, a novel β_3 -adrenergic receptor agonist, on energy expenditure and body composition in obese men. *Am J Clin Nutr* **76**: 780-788

- Levi, A., Eldridge, J. D., Paterson, B. M. (1985) Molecular cloning of a gene sequence regulated by nerve growth factor. *Science* **229**(4711): 393-395
- Levi, A., Ferri, G-L., Watson, E., Possenti, R., Salton, S. R. J. (2004) Processing, distribution, and function of VGF, a neuronal and endocrine peptide precursor. *Cell Mol Neurobiol.* **24** (4): 517-33
- Li, W. W., Li, J., Bao, J. K. (2012) Microautophagy: lesser-known self-eating. *Cell Mol Life Sci* **69**: 1125- 36; PMID:22080117; <http://dx.doi.org/10.1007/s00018-011-0865-5>
- Lian, Y. H., Fang, M. X., Chen, L. G. (2014) Constructing protein-protein interaction network of hypertension with blood stasis syndrome via digital gene expression sequencing and database mining. *J Integr Med.* **12**(6): 476-82
- Liao, Y., Tang, L., (2014) The Critical Roles of HSC70 in Physiological and Pathological Processes. *Current Pharmaceutical Design* **20**: 101-107
- Lin, P., Wang, C., Xu, B., Gao, S., Guo, J., Zhao, X., Huang, H., Zhang, J., Chen, X., Wang, Q., Zhou, W. (2014) The VGF-derived peptide TLQP62 produces antidepressant-like effects in mice via the BDNF/TrkB/CREB signaling pathway. *Pharmacol Biochem Behav.* **120**: 140-8
- Lin, H., Sassano, M. F., Roth, B. L., Shoichet, B. K. (2013) A pharmacological organization of G protein-coupled receptors. *Nat Methods.* **10**(2): 140-6. doi: 10.1038/nmeth.2324
- Lindquist, S., Craig, E. A. (1988) The heat-shock proteins. *Annu Rev Genet* **22**: 631-677
- Ling, J. Y., Zhang, G. Y., Cui, Z. J., Zhang, C. K. (2007) Supercritical fluid extraction of quinolizidine alkaloids from *Sophora flavescens* Ait and purification by high-speed counter-current chromatography. *J. Chromatogr. A* **1145**:123-127
- Literati-Nagy, B., Kulcsar, E., Literati-Nagy, Z., Buday, B., Peterfai, E., Horvath, T., et al. (2009) Improvement of insulin sensitivity by a novel drug, BGP-15, in

References

- insulin-resistant patients: a proof of concept randomized doubleblind clinical trial. *Hormone and Metabolic Research*. **41**: 374-380
- Liu, C. T., Brooks, G. A. (2012) Mild heat stress induces mitochondrial biogenesis in C2C12 myotubes. *Journal of Applied Physiology* **112**: 354-361
- Liu, J. W., Andrews, P. C., Mershon, J. L., Yan, C., Allen, D. L., Ben-Jonathan, N. (1994) Peptide V: a VGF-derived neuropeptide purified from bovine posterior pituitary. *Endocrinology* **135**: 2742-2748
- Liu, T., Cao, S. (2014) HSPA8 (heat shock 70kDa protein 8). *Atlas Genet Cytogenet Oncol Haematol*. **18**(3): 169-173
- Liu, T., Daniels, C. K., Cao, S. (2012) Comprehensive review on the HSC70 functions, interactions with related molecules and involvement in clinical diseases and therapeutic potential. *Pharmacol Ther*. **136** (3): 354-74
- Liu, T., van Rooijen, N., Tracey, D. J. (2000) Depletion of macrophages reduces axonal degeneration and hyperalgesia following nerve injury. *Pain* **86**: 25-32
- Lowell, B. B., Flier, J. S. (1997) Brown adipose tissue, β -adrenergic receptors, and obesity. *Annu Rev Med* **48**: 307-316
- Lowell, B. B., Spiegelman, B. M. (2000) Toward a molecular understanding of adaptive thermogenesis. *Nature* **404**: 652-660
- Magdeldin, S., Blaser, R. E., Yamamoto, T., Yates, J. R. (2015) Behavioral and Proteomic Analysis of Stress Response in Zebrafish (*Danio rerio*). *J Proteome Res*. **14**(2): 943-52. doi: 10.1021/pr500998e. Epub 2014 Nov 26.
- Mahata, S. K., Mahata, M., Fischer-Colbrie, R., Winkler, H. (1993) In situ hybridization: mRNA levels of secretogranin II, VGF and peptidylglycine alpha-amidating monooxygenase in brain of saltloaded rats. *Histochemistry* **99**: 287-293

- Mak, S. K., McCormack, A. L., Manning-Bog, A. B., Cuervo, A. M., Di Monte, D. A. (2010) Lysosomal degradation of alpha-synuclein in vivo. *J Biol Chem.* **30**: 285(18): 13621-9
- Mamane, Y., Chung Chan, C., Lavallee, G., Morin, N., Xu, L. J., Huang, J., Gordon, R., Thomas, W., Lamb, J., Schadt, E. E., Kennedy, B. P., Mancini, J. A. (2009) The C3a anaphylatoxin receptor is a key mediator of insulin resistance and functions by modulating adipose tissue macrophage infiltration and activation. *Diabetes* **58**: 2006–2017
- Mambula, S. S., Calderwood, S. K. (2006) Heat Shock Protein 70 is secreted from tumor cells by a nonclassical pathway involving lysosomal endosomes. *J Immunol* **177**: 7849-57
- Mandell, R. B., Feldherr, C. M. (1990) Identification of two HSP70-related *Xenopus* oocyte proteins that are capable of recycling across the nuclear envelope. *J Cell Biol* **111**: 1775-83; PMID:2229173; <http://dx.doi.org/10.1083/jcb.111.5.1775>
- Maratou, K., Wallace, V. C., Hasnie, F. S., Okuse, K., Hosseini, R., Jina, N., Blackbeard, J., Pheby, T., Orengo, C., Dickenson, A. H., McMahon, S. B., Rice, A. S. (2009) Comparison of dorsal root ganglion gene expression in rat models of traumatic and HIV-associated neuropathic pain. *Eur. J. Pain* **13**: 387–398
- Matsui, H., Asou, H., Inaba, T. (2007) Cytokines direct the regulation of Bim mRNA stability by heat-shock cognate protein 70. *Mol Cell* **25**: 99-112; PMID:17218274; <http://dx.doi.org/10.1016/j.molcel.2006.12.007>
- Mayer, M. P. (2013) Hsp70 chaperone dynamics and molecular mechanism. *Trends Biochem Sci.* **38**(10): 507-14
- Mayer, M. P., Bukau, B. (2005) Hsp70 chaperones: cellular functions and molecular mechanism. *Cell. Mol. Life Sci.* **62**: 670–684

References

McArdle, A., Jackson, M. (2002) Stress proteins and exercise-induced muscle damage. In exercise and stress response. The role of stress proteins. Edited by Locke FM, Noble EG, Boca R. London: CRC; 137–150

McNamara, C. R., Mandel-Brehm, J., Bautista, D. M., Siemens, J., Deranian, K. L., Zhao, M., Hayward, N. J., Chong, J. A., Julius, D., Moran, M. M., et al. (2007) TRPA1 mediates formalin-induced pain. *Proceedings of the National Academy of Sciences of the United States of America* **104**: 13525-13530

Meimaridou, E., Gooljar, S. B., Chapple, J. B. (2009) From hatching to dispatching: the multiple cellular roles of the Hsp70 molecular chaperone machinery. *J MolEndocrinol.* **42**: 1-9

Melnick, J., Argon, Y. (1995) Molecular chaperones and the biosynthesis of antigen receptors. *Immunol.Today.* **16**: 243-250

Merskey and Bogduk (Eds.) (1994) Classification of chronic pain. Seattle: *IASP Task Force on Taxonomy*. IASP Press, Seattle. Part III: Pain Terms, A Current List with Definitions and Notes on Usage. **2**: 209-214

Mert, T., Gunay, I., Ocal, I., Guzel, A. I., Inal, T. C., Sencar, L., Polat, S. (2009) Macrophage depletion delays progression of neuropathic pain in diabetic animals. *Naunyn Schmiedebergs Arch. Pharmacol.* **379**: 445–452

Minota, S., Cameron, B., Welch, W. J., Winfield, J. B. (1988) Autoantibodies to the constitutive 73-kD member of the hsp70 family of heat shock proteins in systemic lupus erythematosus. *J Exp Med* **168**:1475-80; PMID:3171482; <http://dx.doi.org/10.1084/jem.168.4.1475>

Moein-Vaziri, N., Phillips, I., Smith, S., Almi ana, C., Maside, C., Gil, M. A., Roca, J., Martinez, E. A., Holt, W. V., Pockley, A. G., Fazeli, A. (2014) Heat-shock protein A8 restores sperm membrane integrity by increasing plasma membrane fluidity. *Reproduction* **147**(5): 719-32

- Morino, S., Kondo, T., Sasaki, K., Adachi, H., Suico, M.A., Sekimoto, E., et al. (2008) Mild electrical stimulation with heat shock ameliorates insulin resistance via enhanced insulin signaling. *PLoS ONE* **3**: 4068
- Morton, J. P., MacLaren, D. P., Cable, N. T., Bongers, T., Griffiths, R. D., Campbell, I. T., Evans, L., Kayani, A., McArdle, A., Drust, B. (2006) Time course and differential responses of the major heat shock protein families in human skeletal muscle following acute nondamaging treadmill exercise. *J Appl Physiol*. **101**: 176–182
- Moss, A., Ingram, R., Koch, S., Theodorou, A., Low, L., Baccei, M., Hathway, G. J., Costigan, M., Salton, S. R., Fitzgerald, M. (2008) Origins, actions and dynamic expression patterns of the neuropeptide VGF in rat peripheral and central sensory neurones following peripheral nerve injury. *Mol Pain* **4**: 62. doi: 10.1186/1744-8069-4-62.
- Mueller, M., Wacker, K., Ringelstein, E. B., Hickey, W. F., Imai, Y., Kiefer, R. (2001) Rapid response of identified resident endoneurial macrophages to nerve injury. *Am. J. Pathol.* **159**: 2187–2197
- Muller, S., Monneaux, F., Schall, N., Rashkov, R. K., Oparanov, B. A., Wiesel, P., Geiger, J. M., Zimmer, R. (2008) Spliceosomal peptide P140 for immunotherapy of systemic lupus erythematosus: results of an early phase II clinical trial. *Arthritis Rheum* **58**: 3873 - 83
- Nadler, S. G., Dischino, D. D., Malacko, A. R., Cleaveland, J. S., Fujihara, S. M., Marquardt, H. (1998) Identification of a binding site on Hsc70 for the immunosuppressant 15-deoxyspergualin. *Biochem Biophys Res Commun.* **9**: 253(1): 176-80
- Nesvizhskii, A. I. (2007) Protein identification by tandem mass spectrometry and sequence database searching. *Methods in molecular biology* **367**: 87-119

Netea, M. G., Joosten, L. A., Lewis, E., Jensen, D. R., Voshol, P. J., Kullberg, B. J., Tack, C. J., van Krieken, H., Kim, S. H., Stalenhoef, A. F., van de Loo, F. A., Verschueren, I., Pulawa, L., Akira, S., Eckel, R. H., Dinarello, C. A., van den Berg, W., van der Meer, J. W. (2006) Deficiency of interleukin-18 in mice leads to hyperphagia, obesity and insulin resistance. *Nat Med* **12**: 650–656

Nirdé, P., Derocq, D., Maynadier, M., Chambon, M., Basile, I., Gary-Bobo, M., Garcia, M. (2010) Heat shock cognate 70 protein secretion as a new growth arrest signal for cancer cells. *Oncogene* **29**: 117- 27

Niu R, Zhang Y, Liu S, Liu F, Sun Z, Wang J. (2014) Proteome alterations in cortex of mice exposed to fluoride and lead. *Biol Trace Elem Res*. [Epub ahead of print]

Obici, S., Feng, Z., Arduini, A., Conti, R., Rossetti, L. (2003) Inhibition of hypothalamic carnitine palmitoyltransferase-1 decreases food intake and glucose production. *Nat Med* **9**: 56–61

Oguri, M., Kato, K., Yokoi, K., Watanabe, S., Metoki, N., Yoshida, H., Satoh, K., Aoyagi, Y., Nishigaki, Y., Yoshida, H., Nozawa, Y., Yamada, Y. (2009) Association of polymorphisms of THBS2 and HSPA8 with hypertension in Japanese individuals with chronic kidney disease. *Mol Med Rep.* **2**(2): 205-11

Okuno, Y., Imamoto, N., Yoneda, Y. (1993) 70-kDa heat-shock cognate protein colocalizes with karyophilic proteins into the nucleus during their transport in vitro. *Exp Cell Res* **206**: 134-42; PMID:8482354; <http://dx.doi.org/10.1006/excr.1993.1129>

Opstal-van Winden A. W., Vermeulen R. C., Peeters P. H., Beijnen J. H., van Gils C. H. (2012) Early diagnostic protein biomarkers for breast cancer: how far have we come? *Breast Cancer Res. Treat.* **134**: 1–12

Otto, H., Dreger, M., Bengtsson, L., Hucho, F. (2001) Identification of tyrosine-phosphorylated proteins associated with the nuclear envelope. *Eur J Biochem.* **268**(2): 420-8

-
- Page, N., Gros, F., Schall, N., Décossas, M., Bagnard, D., Briand, J. P., Muller, S. (2011) HSC70 blockade by the therapeutic peptide P140 affects autophagic processes and endogenous MHCII presentation in murine lupus. *Ann Rheum Dis* **70**: 837-43
- Page, N., Schall, N., Strub, J-M., Quinternet, M., Chaloin, O., Décossas, M., Cung, M. T., Dorsselaer, A. V., Briand, J-P., Muller, S (2009) The spliceosomal phosphopeptide P140 controls the lupus disease by interacting with the HSC70 protein and via a mechanism mediated by T cells. *PLoS ONE* **4**(4): 5273
- Panjwani, N., Akbari, O., Garcia, S., Brazil, M., Stockinger, B. (1999) The HSC73 molecular chaperone: involvement in MHC class II antigen presentation. *J Immunol* **163**: 1936-42; PMID:10438929
- Park, K., Flynn, G. C., Rothman, J. E., Fasman, G. D. (1993) Conformational change of chaperone Hsc70 upon binding to a decapeptide: A circular dichroism study. *Protein science* **2**: 325-330
- Peerschke, E. I., Ghebrehwet, B. (2007) The contribution of gC1qR/p33 in infection and inflammation. *Immunobiology* **212**: 333-342
- Peerschke, E. I., Yin, W., Grigg, S. E., Ghebrehwet, B. (2006) Blood platelets activate the classical pathway of human complement. *J Thromb Haemost* **4**: 2035-2042
- Petersen-Mahrt, S. K., Estmer, C., Ohrmalm, C., Matthews, D. A., Russell, W. C., Akusjarvi, G. (1999) The splicing factor-associated protein, p32, regulates RNA splicing by inhibiting ASF/SF2 RNA binding and phosphorylation. *The EMBO journal* **18**: 1014-1024
- Peterson, K. L., Zhang, W., Lu, P. D., Keilbaugh, S. A., Peerschke, E. I., Ghebrehwet, B. (1997) The C1q-binding cell membrane proteins cC1q-R and gC1q-R are released from activated cells: subcellular distribution and immunochemical characterization. *Clin Immunol Immunopathol* **84**: 17-26

Pfaffenbach, K. T., Lee, A. S. (2010) The critical role of GRP78 in physiologic and pathologic stress. *Curr Opin Cell Biol* **23**: 150-6

Pinilla, L., Pineda, R., Gaytan, F., Romero, M., Garcia-Galiano, D., Sanchez-Garrido, M.A., Ruiz-Pino, F., Tena-Sempere, M., and Aguilar, E. (2011) Characterization of the reproductive effects of the anorexigenic VGF-derived peptide TLQP-21: in vivo and in vitro studies in male rats. *American journal of physiology Endocrinology and metabolism* **300**: 837-847

Pino, M. F., Zhang, G., Rosser, C. J., Goodison, S., Urquidi, V. (2013) Heat shock cognate protein HSPA8 (Hsc70) regulates migration and xenograft growth of breast tumor cell lines. [Abstract]. In: Proceedings of the 104th Annual Meeting of the American Association for Cancer Research; 2013 Apr 6-10; Washington, DC. Philadelphia (PA): AACR; *Cancer Res* **73**(8 Suppl): Abstract nr 3798

Piselli, P., Vendetti, S., Poccia, F., Cicconi, R., Mattei, M., Bolognesi, A., Stripe, F., Colizzi, V., (1995) In vitro and in vivo efficacy of heat shock protein specific immunotoxins on human tumor cells. *J Biol Regul Homeost Agents*. **9**: 55–62

Place, S. P., Hofmann, G. E. (2005) Comparison of Hsc70 orthologs from polar and temperate notothenioid fishes: differences in prevention of aggregation and refolding of denatured proteins. *Am J Physiol Regul Integr Comp Physiol*. **288** (5): R1195-202

Porro, C. A., Cavazzuti, M. (1993) Spatial and temporal aspects of spinal cord and brainstem activation in the formalin pain model. *Prog Neurobiol* **41**: 565-607

Possenti, R., Eldridge, J. D., Paterson, B. M., Grasso, A., Levi, A. (1989) A protein induced by NGF in PC12 cells is stored in secretory vesicles and released through the regulated pathway. *EMBO J*. **8**(8): 2217-2223

Possenti, R., Muccioli, G., Petrocchi, P., Cero, C., Cabassi, A., Vulchanova, L., Riedl, M. S., Manieri, M., Frontini, A., Giordano, A., Cinti, S., Govoni, P., Graiani, G., Quaini, F., Ghè, C., Bresciani, E., Bulgarelli, I., Torsello, A., Locatelli, V., Sanghez, V., Larsen, B. D., Petersen, J. S., Palanza, P., Parmigiani, S., Moles, A., Levi, A., Bartolomucci, A. (2012) Characterization of a novel

- peripheral pro-lipolytic mechanism in mice: role of VGF-derived peptide TLQP-21. *Biochem J* **441** (1): 511-22
- Possenti, R., Rinaldi, A. M., Ferri, G. L., Borboni, P., Trani, E., and Levi, A. (1999) Expression, processing, and secretion of the neuroendocrine VGF peptides by INS-1 cells. *Endocrinology* **140**: 3727–3735
- Powers, M. V., Clarke, P. A., Workman, P. (2008) Dual targeting of HSC70 and HSP72 inhibits HSP90 function and induces tumor-specific apoptosis. *Cancer Cell* **14**: 250-62
- Preuss, J., Dettmeyer, R., Poster, S., Lignitz, E., Madea, B. (2008) The expression of heat shock protein 70 in kidneys in cases of death due to hypothermia. *ForensicSci Int* **176**: 248-52
- Ramos, A., Rodríguez-Seoane, C., Rosa, I., Trossbach, S. V., Ortega-Alonso, A., Tomppo, L., Ekelund, J., Veijola, J., Järvelin, M. R., Alonso, J., Veiga, S., Sawa, A., Hennah, W., García, A., Korth, C., Requena, J. R. (2014) Neuropeptide precursor VGF is genetically associated with social anhedonia and underrepresented in the brain of major mental illness: its downregulation by DISC1. *Hum Mol Genet.* **23** (22): 5859-65. doi: 10.1093/hmg/ddu303
- Razzoli, M., Bo, E., Pascucci, T., Pavone, F., D'Amato, F.R., Cero, C., Sanghez, V., Dadomo, H., Palanza, P., Parmigiani, S., et al. (2012) Implication of the VGF-derived peptide TLQP-21 in mouse acute and chronic stress responses. *Behav. Brain Res.* **229**: 333–339
- Riedl, M. S., Braun, P. D., Kitto, K. F., Roiko, S. A., Anderson, L. B., Honda, C. N., Fairbanks, C. A., Vulchanova, L. (2009) Proteomic analysis uncovers novel actions of the neurosecretory protein VGF in nociceptive processing. *J Neurosci* **29**: 13377–13388
- Riu, E., Ferre, T., Hidalgo, A., Mas, A., Franckhauser, S., Otaegui, P., Bosch, F. (2003) Overexpression of c-myc in the liver prevents obesity and insulin resistance. *FASEB J* **17**: 1715–1717

References

- Rizzi, R., Bartolomucci, A., Moles, A., D'Amato, F., Sacerdote, P., Levi, A., La Corte, G., Ciotti, M. T., Possenti, R., Pavone, F. (2008) The VGF-derived peptide TLQP-21: a new modulatory peptide for inflammatory pain. *Neurosci Lett* **441**: 129–133
- Rusin, M., Zientek, H., Krzesniak, M., Malusecka, E., Zborek, A., Krzyzowska-Gruca, S., Butkiewicz, D., Vaitiekunaite, R., Lisowska, K., Grzybowska, E., Krawczyk, Z. (2004) Intronic polymorphism (1541-1542delGT) of the constitutive heat shock protein 70 gene has functional significance and shows evidence of association with lung cancer risk. *Mol Carcinog.* **39** (3): 155-63
- Sagara, Y., Ishida, C., Inoue, Y., Shiraki, H., Maeda, Y. (1998) 71-kilodalton heat shock cognate protein acts as a cellular receptor for syncytium formation induced by human T-cell lymphotropic virus type 1. *J Virol* **72**: 535-41
- Sahu, R., Kaushik, S., Clement, C. C., Cannizzo, E. S., Scharf, B., Follenzi, A., Potalicchio, I., Nieves, E., Cuervo, A. M., Santambrogio, L. (2011) Microautophagy of cytosolic proteins by late endosomes. *Dev Cell* **20**: 131-9; PMID:21238931; <http://dx.doi.org/10.1016/j.devcel.2010.12.003>
- Salton, S. R., Fischberg, D. J., Dong, K. W. (1991) Structure of the gene encoding VGF, a nervous system-specific mRNA that is rapidly and selectively induced by nerve growth factor in PC12 cells. *Mol. Cell. Biol.* **11**: 2335–2349
- Schwartz, M. W., Woods, S. C., Porte, D. Jr., Seeley, R. J., Baskin, D. G. (2000) Central nervous system control of food intake. *Nature* **404**: 661–671
- Seidah, N. G., Chretien, M. (1999) Proprotein and prohormone convertases: A family of subtilases generating diverse bioactive polypeptides. *Brain Res.* **848**: 45–62
- Severini, C., Ciotti, M. T., Biondini, L., Quaresima, S., Rinaldi, A. M., Levi, A., Frank, C., Possenti, R. (2008) TLQP-21, a neuroendocrine VGF-derived peptide, prevents cerebellar granule cells death induced by serum and potassium deprivation. *J Neurochem* **104**: 534-544

- Severini, C., La Corte, G., Improta, G., Broccardo, M., Agostini, S., Petrella, C., Sibilìa, V., Pagani, F., Guidobono, F., Bulgarelli, I., et al. (2009) In vitro and in vivo pharmacological role of TLQP-21, a VGF-derived peptide, in the regulation of rat gastric motor functions. *British journal of pharmacology* **157**: 984-993
- Sha, L., MacIntyre, L., Machell, J. A., Kelly, M. P., Porteous, D. J., Brandon, N. J., Muir, W. J., Blackwood, D. H., Watson, D. G., Clapcote, S. J., Pickard, B. S. (2012) Transcriptional regulation of neurodevelopmental and metabolic pathways by NPAS3. *Mol Psychiatry*. **17** (3): 267-79. doi: 10.1038/mp.2011.73. Epub 2011 Jun 28.
- Sheffield, W. P., Shore, G. C., Randall, S. K. (1990) Mitochondrial precursor protein. Effects of 70-kilodalton heat shock protein on polypeptide folding, aggregation, and import competence. *J Biol Chem*. **5** 265 (19): 1 1069-76
- Shevchenko, A., Tomas, H., Havlis, J., Olsen, J. V., Mann, M. (2006) In-gel digestion for mass spectrometric characterization of proteins and proteomes. *Nature protocols* **1**: 2856
- Shimazawa, M., Tanaka, H., Ito, Y., Morimoto, N., Tsuruma, K., Kadokura, M., Tamura, S., Inoue, T., Yamada, M., Takahashi, H., et al. (2010) An inducer of VGF protects cells against ER stress-induced cell death and prolongs survival in the mutant SOD1 animal models of familial ALS. *PLoS ONE* **5** (12): e15307. doi: 10.1371/journal.pone.0015307.
- Shin, B. K., Wang, H., Marie, A., Naour, F. L., Brichory, F., Jang, J. H., Zhao, R., Puravs, E., Tra, J., Michael, C. W., Misek, D. E., Hanash, S. M. (2003) Global profiling of the cell surface proteome of cancer cells uncovers an abundance of proteins with chaperone function. *J. Biol. Chem*. **278**: 7607-7616. Epub 2002 Dec 18.
- Shiota, M., Kusakabe, H., Izumi, Y., Hikita, Y., Nakao, T., Funae, Y., Miura, K., Iwao, H. (2010) Heat shock cognate protein 70 is essential for Akt signaling in endothelial function. *Arterioscler Thromb Vasc Biol*. **30** (3) : 491-7

References

- Sibilia, V., Pagani, F., Bulgarelli, I., Mrak, E., Broccardo, M., Improta, G., Severini, C., Possenti, R., Guidobono, F. (2010a) TLQP-21, a VGF-derived peptide, prevents ethanol-induced gastric lesions: insights into its mode of action. *Neuroendocrinology*. **92** (3): 189-97. doi: 10.1159/000319791
- Sibilia, V., Pagani, F., Bulgarelli, I., Tulipano, G., Possenti, R., Guidobono, F. (2010b) Characterization of the mechanisms involved in the gastric antisecretory effect of TLQP-21, a vgf-derived peptide, in rats. *Amino Acids* **10**.1007/s00726-010-0818-6
- Sibilia, V., Pagani, F., Bulgarelli, I., Tulipano, G., Possenti, R., Guidobono, F., (2012) Characterization of the mechanisms involved in the gastric antisecretory effect of TLQP-21, a vgf-derived peptide, in rats. *Amino Acids*. **42** (4): 1261-8. doi: 10.1007/s00726-010-0818-6. Epub 2010 Dec 4.
- Singh, A. K., Upadhyay, R. C., Malakar, D., Kumar, S., Singh, S. V. (2014) Effect of thermal stress on HSP70 expression in dermal fibroblast of zebu (Tharparkar) and crossbred (Karan-Fries) cattle. *J Therm Biol*. **43**: 46-53
- Singh-Jasuja, H., Hilf, N., Arnold-Schild, D., Schild, H. (2001) The role of heat shock proteins and their receptors in the activation of the immune system. *Biol. Chem*. **382**: 629-636
- Snyder, S. E., Salton, S. R. (1998) Expression of VGF mRNA in the adult rat central nervous system. *J Comp Neurol* **394**: 91-105
- Snyder, S. E., Li, J., Salton, S. R. (1997) Comparison of VGF and trk mRNA distributions in the developing and adult rat nervous systems. *Brain Res Mol Brain Res*. **49** (1-2): 307-11
- Snyder, S. E., Peng, B., Pintar, J. E., Salton, S. R. (2003) Expression of VGF mRNA in developing neuroendocrine and endocrine tissues. *J Endocrinol*. **179** (2): 227-35
- Soltys, B. J., Gupta, R. S. (1997) Cell surface localization of the 60 kda heat shock chaperonin protein (Hsp60) in mammalian cells. *Cell Biology International* **21**(5): 315-320

- Sreedhar, A. S., Csermely, P. (2004) Heat shock proteins in the regulation of apoptosis: new strategies in tumor therapy: a comprehensive review. *Pharmacol Ther.* **101** (3): 227-57
- Srivastava, P. (2002) Roles of heat-shock proteins in innate and adaptive immunity. *Nat. Rev. Immunol.* **2**: 185-194
- Steiner, D. F. (1998) The proprotein convertases. *Curr. Opin. Chem. Biol.* **2**: 31–39
- Stephens, S. B., Schisler, J. C., Hohmeier, H. E., An, J., Sun, A. Y., Pitt, G. S., Newgard, C. B. (2012) A VGF-derived peptide attenuates development of type 2 diabetes via enhancement of islet β -cell survival and function. *Cell Metab.* **16** (1): 33-43. doi: 10.1016/j.cmet.2012.05.011.
- Strachan, E., Mallia, A. K., Cox, J. M., Antharavally, B., Desai, S., Sykaluk, L., O'Sullivan, V., Bell, P. A. (2004) Solid-phase biotinylation of antibodies. *J. Mol. Recognit.* **17**(3): 268–276 DOI:10.1002/jmr.669
- Stricher, F., Macri, C., Ruff, M., Muller, S. (2013) HSPA8/HSC70 chaperone protein Structure, function, and chemical targeting. *Autophagy* **9**: (12), 1937–1954
- Succu, S., Cocco, C., Mascia, M. S., Melis, T., Melis, M. R., Possenti, R., Levi, A., Ferri, G. L., Argiolas, A. (2004) Pro-VGF-derived peptides induce penile erection in male rats: possible involvement of oxytocin. *Eur J Neurosci* **20**: 3035-3040
- Succu, S., Mascia, M. S., Melis, T., Sanna, F., Melis, M. R., Possenti, R., Argiolas, A. (2005) Pro-VGF-derived peptides induce penile erection in male rats: Involvement of paraventricular nitric oxide. *Neuropharmacology* **49**: 1017-1025
- Takashima, S., Sato, N., Kishi, A., Tamura, Y., Hirai, I., Torigoe, T., Yagihashi, A., Takahashi, S., Sagae, S., Kudo, R., Kikuchi, K. (1996) Involvement of peptide antigens in the cytotoxicity between 70-kDa heat shock cognate protein-like molecule and CD3+, CD4⁻, CD8⁺, TCR α / β - killer T cells. *J. Immunol.* **157**: 3391-3395

References

Takenaka, I. M., Leung, S. M., McAndrew, S. J., Brown, J. P., Hightower, L. E. (1995) Hsc70-binding peptides selected from a phage display peptide library that resemble organellar targeting sequences. *J Biol Chem.* **270** (34): 19839-44

Tamura, Y., Tsuboi, N., Sato, N., Kikuchi, K. (1993) 70 kDa heat shock cognate protein is a transformation-associated antigen and a possible target for the host's anti-tumor immunity. *J Immunol.* **151**: 5516-5524

Terada, S., Kinjo, M., Aihara, M., Takei, Y., Hirokawa, N. (2010) Kinesin-1/Hsc70-dependent mechanism of slow axonal transport and its relation to fast axonal transport. *EMBO J* **29**: 843-54; PMID:20111006; <http://dx.doi.org/10.1038/emboj.2009.389>

Thakker-Varia, S., Behnke, J., Doobin, D., Dalal, V., Thakkar, K., Khadim, F., Wilson, E., Palmieri, A., Antila, H., Rantamaki, T., Alder, J. (2014) VGF (TLQP-62)-induced neurogenesis targets early phase neural progenitor cells in the adult hippocampus and requires glutamate and BDNF signaling. *Stem Cell Res.* **12** (3): 762-77. doi: 10.1016/j.scr.2014.03.005.

Thakker-Varia, S., Jean, Y. Y., Parikh, P., Sizer, C. F., Jernstedt Ayer, J., Parikh, A., Hyde, T. M., Buyske, S., Alder, J. (2010) The neuropeptide VGF is reduced in human bipolar postmortem brain and contributes to some of the behavioral and molecular effects of lithium. *J Neurosci.* **30**: 9368-80

Thakker-Varia, S., Krol, J. J., Nettleton, J., Bilimoria, P. M., Bangasser, D. A., Shors, T. J., Black, I. B., Alder, J. (2007) The neuropeptide VGF produces antidepressant-like behavioral effects and enhances proliferation in the hippocampus. *J Neurosci.* **27**: 12156-67

Thulasiraman, V., Yang, C. F., Frydman, J. (1999) In vivo newly translated polypeptides are sequestered in a protected folding environment. *EMBO J* **18**: 85-95; PMID:9878053; <http://dx.doi.org/10.1093/emboj/18.1.85>

Timofeeva, A. V., Goryunova, L. E., Khaspekov, G. L., Kovalevskii, D. A., Scamrov, A. V., Bulkina, O. S., Karpov, Y. A., Talitskii, K. A., Buza, V. V., Britareva, V. V., Beabealashvilli, R. S. (2006) Altered gene expression pattern in

peripheral blood leukocytes from patients with arterial hypertension. *Ann N Y Acad Sci.* **1091**: 319-35

Tiss A., Khadir, A., Abubaker, J., Abu-Farha, M., Al-Khairi, I., Cherian, P., John, J., Kavalakatt, S., Warsame, S., Al-Ghimlas, F., Elkum, N., Behbehani, K., Dermime, S., Dehbi, M. (2014) Immunohistochemical profiling of the heat shock response in obese non-diabetic subjects revealed impaired expression of heat shock proteins in the adipose tissue. *Lipids in Health and Disease* **13**: 106

Tjolsen, A., Berge, O. G., Hunskaar, S., Rosland, J. H., and Hole, K. (1992) The formalin test: an evaluation of the method. *Pain* **51**: 5-17

Toshinai, K., Nakazato, M. (2009) Neuroendocrine regulatory peptide-1 and -2: Novel bioactive peptides processed from VGF. *Cell. Mol. Life Sci.* **66** (11-12): 1939 – 1945

Toshinai, K., Yamaguchi, H., Kageyama, H., Matsuo, T., Koshinaka, K., Sasaki, K., Shioda, S., Minamino, N., Nakazato, M. (2010) Neuroendocrine regulatory peptide-2 regulates feeding behavior via the orexin system in the hypothalamus. *Am J Physiol Endocrinol Metab* **299**: E394–E401. doi: 10.1152/ajpendo.00768.2009. Epub 2010 Jun 15.

Trani, E., Ciotti, T., Rinaldi, A. M., Canu, N., Ferri, G. L., Levi, A., Possenti, R. (1995) Tissue-specific processing of the neuroendocrine protein VGF. *J. Neurochem.* **65**: 2441–2449

Trani, E., Giorgi, A., Canu, N., Amadoro, G., Rinaldi, A. M., Halban, P. A., Ferri, G. L., Possenti, R., Schinina, M. E., Levi, A. (2002) Isolation and characterization of VGF peptides in rat brain. Role of PC1/3 and PC2 in the maturation of VGF precursor. *J Neurochem.* **81**(3): 565-74

Tsai, M. Y., Morfini, G., Szebenyi, G., Brady, S. T. (2000) Release of kinesin from vesicles by hsc70 and regulation of fast axonal transport. *Mol Biol Cell* **11**: 2161-73; PMID:10848636; <http://dx.doi.org/10.1091/mbc.11.6.2161>

References

Tsuboi, N., Ishikawa, M., Tamura, Y., Takayama, S., Tobioka, H., Matsuura, A., Hirayoshi, K., Nagata, K., Sato, N., Kikuchi, K. (1994) Monoclonal antibody specifically reacting against 73-kilodalton heat shock cognate protein: possible expression on mammalian cell surface. *Hybridoma* **13**: 373-81

Tsukahara, F., Yoshioka, T., Muraki, T. (2000) Molecular and functional characterization of HSC54, a novel variant of human heat-shock cognate protein 70. *Mol Pharmacol* **58**: 1257-63

Tsukimi, Y., Nakai, H., Itoh, S., Amagase, K., Okabe, S. (2001) Involvement of heat shock proteins in the healing of acetic acid-induced gastric ulcers in rats. *J Physiol Pharmacol.* **52**(3): 391-406

Van den Pol, A.N., Bina, K., Decavel, C., Ghosh, P. (1994). VGF expression in the brain. *J Comp Neurol* **347**: 455-469

Van den Pol, A. N., Decavel, C., Levi, A., Paterson, B. (1989) Hypothalamic expression of a novel gene product, VGF: Immunocytochemical analysis. *J Neurosci.* **9** (12): 4122-37

Vega, V. L., Rodríguez-Silva, M., Frey, T., Gehrman, M., Diaz, J. C., Steinem, C., Multhoff, G., Arispe, N., De Maio, A. (2008) Hsp70 translocates into the plasma membrane after stress and is released into the extracellular environment in a membrane-associated form that activates macrophages. *The Journal of Immunology* **180**: 6, 4299-4307. doi: 10.4049/jimmunol.180.6.4299

Wadhwa, R., Taira, K., Kaul, S. C. (2002) An Hsp70 family chaperone, mortalin/mthsp70/PBP74/Grp75: what, when, and where? *Cell Stress Chaperones.* **7**(3): 309-16

Wakonigg, G., Zernig, G., Berger, I., Fischer-Colbrie, R., Laslop, A., Saria, A. (2002) Lack of a distinctive behavioural effect of chromogranin-derived peptides in rodents. *Regul Pept.* **15**; 103 (2-3): 85-91

- Wampler, J. L., Kim, K-P., Jaradat, Z., Bhunia, A. K. (2004) Heat shock protein 60 acts as a receptor for the listeria adhesion protein in Caco-2 cells. *Infect Immun.* **72**(2): 931–936
- Wang, J., Farr, G. W., Zeiss, C. J., Rodriguez-Gil, D. J., Wilson, J. H., Furtak, K., Rutkowski, D. T., Kaufman, R. J., Ruse, C. I., Yates, J. R. 3rd, et al. Progressive aggregation despite chaperone associations of a mutant SOD1-YFP in transgenic mice that develop ALS. *Proc Natl Acad Sci U S A* **106**: 1392-7; PMID:19171884; <http://dx.doi.org/10.1073/pnas.0813045106>
- Wang, T. F., Chmg, J-H., Wang, C. (1993) Identification of the peptide binding domain of hsc70, 18-kilodalton fragment located immediately after atpase domain is sufficient for high affinity binding. *J Biol Chem* **268**: 35, 26049-26051
- Wang, Y., Lee, C-H., Tiep, S., Yu, R. T., Ham, J., Kang, H., Evans, R. M. (2003) Peroxisome-proliferator-activated receptor δ activates fat metabolism to prevent obesity. *Cell* **113**: 159–170
- Wang, Y. P., Liu, F., He, H. W., Han, Y. X., Peng, Z. G., Li, B. W., You, X. F., Song, D. Q., Li, Z. R., Yu, L. Y., Cen, S., Hong, B., Sun, C. H., Zhao, L. X., Kreiswirth, B., Perlin, D., Shao, R. G., Jiang, J. D. (2010) Heat stress cognate 70 host protein as a potential drug target against drug resistance in hepatitis B virus. *Antimicrob Agents Chemother.* **54**(5):2070-7. doi: 10.1128/AAC.01764-09.epub 2010 Feb 22
- Watanabe, M., Dykes-Hoberg, M., Culotta, V. C., Price, D. L., Wong, P. C., Rothstein, J. D. (2001) Histological evidence of protein aggregation in mutant SOD1 transgenic mice and in amyotrophic lateral sclerosis neural tissues. *Neurobiol Dis* **8**: 933-41; PMID:11741389; <http://dx.doi.org/10.1006/nbdi.2001.0443>
- Wilkins, S., Choglay, A. A., Chapple, J. P., van der Spuy, J., Rhie, A., Birkett, C. R., Cheetham, M. E. (2010) The binding of the molecular chaperone Hsc70 to the prion protein PrP is modulated by pH and copper. *Int J Biochem Cell Biol.* **42** (7): 1226-32

References

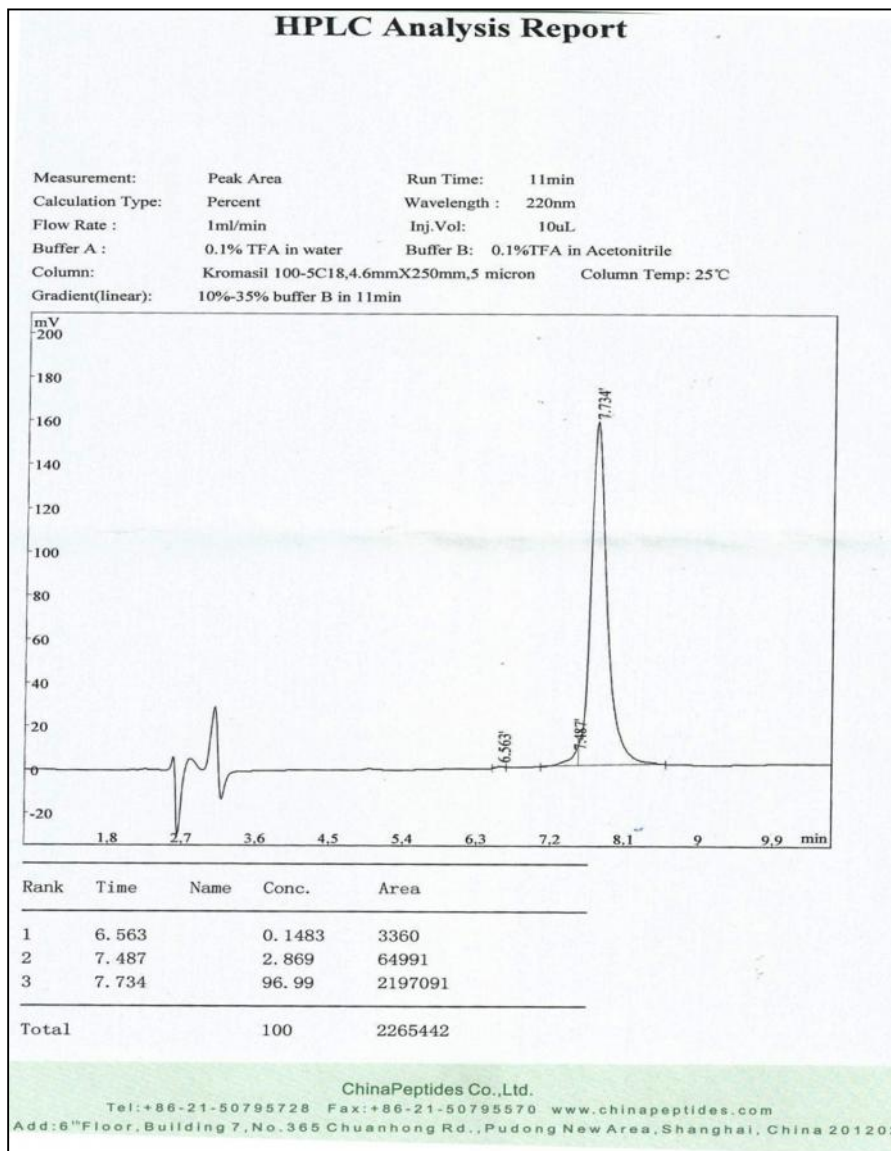
- Wong, A. S., Cheung, Z. H., Ip, N. Y. (2011) Molecular machinery of macroautophagy and its deregulation in diseases. *Biochim Biophys Acta* **1812**: 1490-7; PMID:21787863; <http://dx.doi.org/10.1016/j.bbadis.2011.07.005>
- Xu, Z., Hirasawa, A., Shinoura, H., Tsujimoto, G. (1999) Interaction of the alpha(1B)-adrenergic receptor with gC1q-R, a multifunctional protein. *The Journal of biological chemistry* **274**: 21149- 21154
- Yamaguchi, H., Sasaki, K., Satomi, Y., Shimbara, T., Kageyama, H., Mondal, M. S., Toshinai, K., Date, Y., Gonzalez, L. J., Shioda, S., Takao, T., Nakazato, M., Minamino, N. (2007) Peptidomic identification and biological validation of neuroendocrine regulatory peptide-1 and -2. *J Biol Chem* **282**: 26354-26360
- Zaprianova, S., Rashev, P., Zasheva, D., Martinova, Y., Mollova, M. (2013) Electrophoretic and immunocytochemical analysis of Hsp72 and Hsp73 expression in heat-stressed mouse testis and epididymis. *Eur J Obstet Gynecol Reprod Biol.* **168**(1): 54-9
- Zhang, J. V., Ren, P. G., Avsian-Kretchmer, O., Luo, C. W., Rauch, R., Klein, C., Hsueh, A. J. (2005) Obestatin, a peptide encoded by the ghrelin gene, opposes ghrelin's effects on food intake. *Science* **310**: 996–999
- Zhang, W., Ni, C., Sheng, J., Hua, Y., Ma, J., et al. (2013) TLQP-21 protects human umbilical vein endothelial cells against high-glucose-induced apoptosis by increasing G6PD expression. *PLoS ONE* **8**(11): 79760
- Zimmer, R., Scherbarth, H. R., Rillo, O. L., Gomez-Reino, J. J., Muller, S. (2013) Lupuzor/P140 peptide in patients with systemic lupus erythematosus: a randomised, double-blind, placebo-controlled phase IIb clinical trial. *Ann Rheum Dis* **72**: 1830 – 5
- Zou, N., Ao, L., Cleveland, J. C. Jr., et al. (2008) Critical role of extracellular heat shock cognate protein 70 in the myocardial inflammatory response and cardiac dysfunction after global ischemia-reperfusion. *Am J Physiol Heart Circ Physiol* **294**: 2805-13

Annex I:

HPLC and MS analysis report of TLQP-21



A.



B.

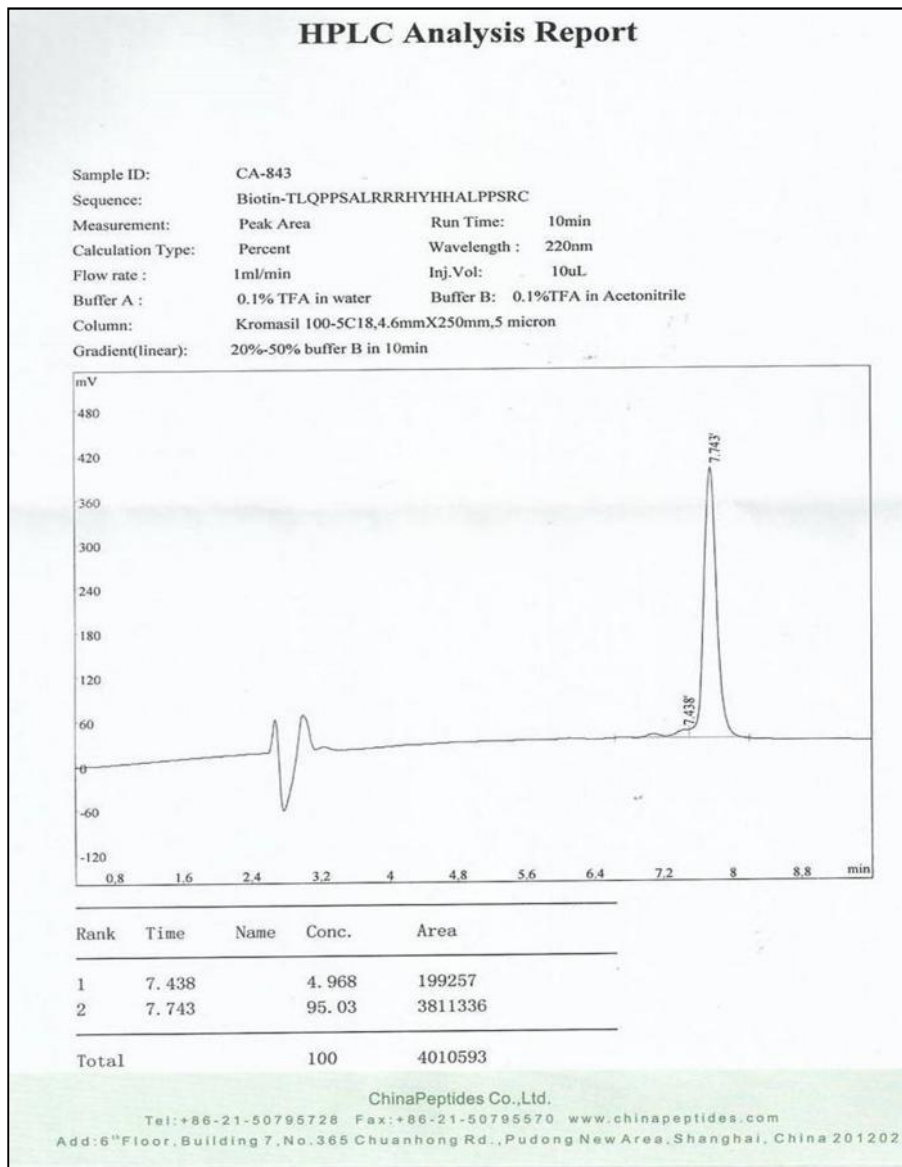
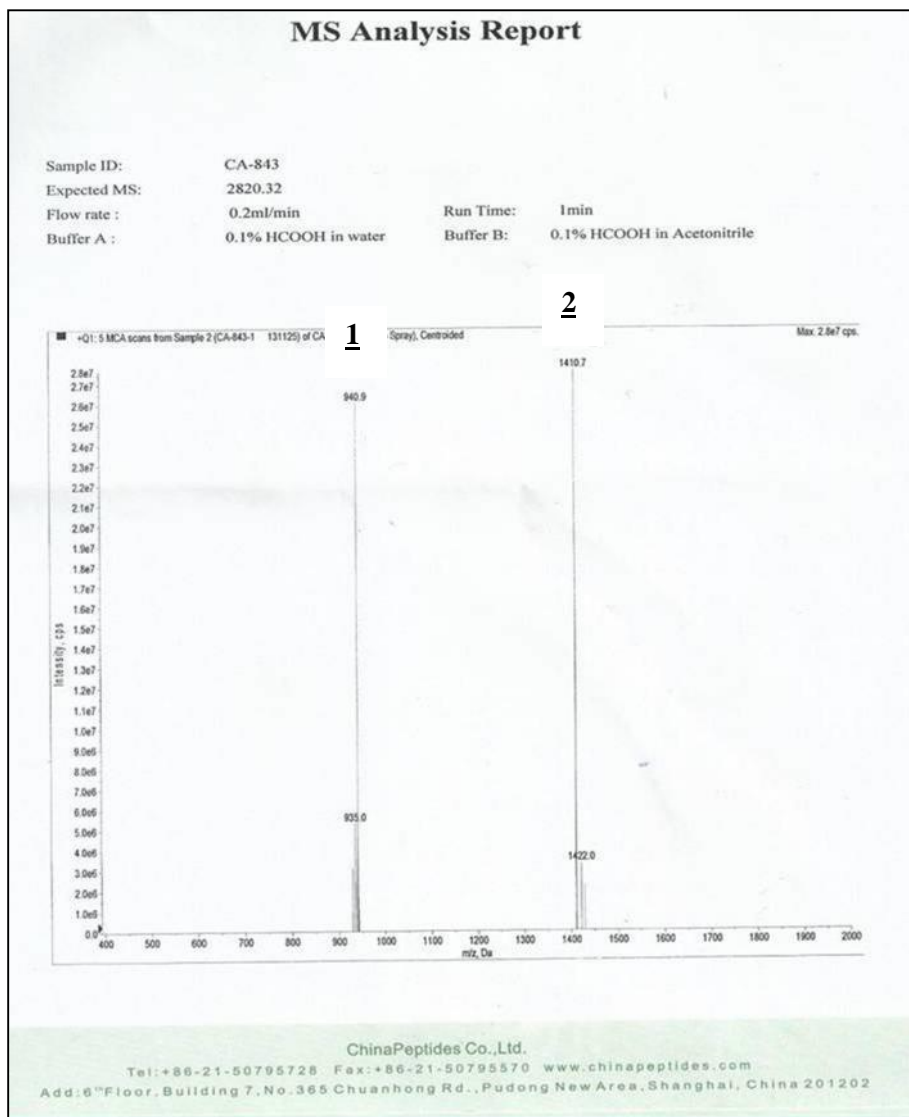


Figure 24: HPLC analysis report of TLQP-21 (A) and biotin-TLQP-21-Cys (B).

A.



B.

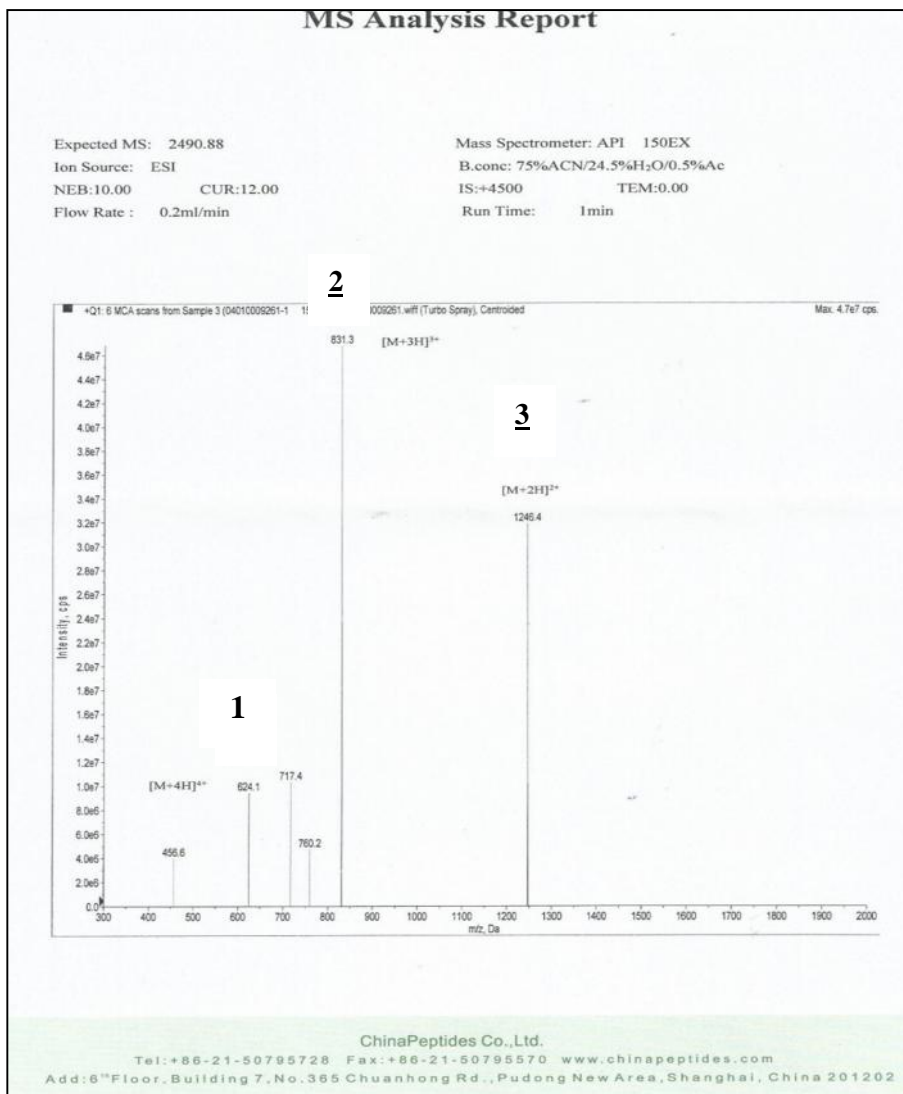


Figure 25: MS analysis report confirming biotin-TLQP-21-Cys. A. (1) The peak at m/z 940.9 corresponds to the biotin-TLQP-21-C, in its triple protonated form $[(\text{biotin-TLQP-C} + \text{H}^+)/3]$. **(2)** The peak at m/z 1410.7 represents to the doubly protonated biotin-TLQP-21-C, $[(\text{biotin-TLQP-21-C} + \text{H}^+)/2]$. **B. (1)** The peak at m/z 624.1 corresponds to TLQP-21, in its quadrupole protonated form $[(\text{TLQP} + \text{H}^+)/4]$. **(2)** The peak at m/z 831.3 represents to the triple protonated TLQP-21, $[(\text{TLQP-21} + \text{H}^+)/3]$. **(3)** Peak at m/z 1246.4 represents to the doubly protonated TLQP-21, $[(\text{TLQP-21} + \text{H}^+)/2]$.

Annex II:

**Structural dynamics of TLQP-21 bound to the HSPA8 receptor binding site:
explored by molecular dynamics simulation**



Structural dynamics of TLQP-21 bound to the HSPA8 receptor binding site: Explored by molecular dynamics simulation

This part of the work was performed by Sandipan Chakraborty, Department of Microbiology, University of Calcutta, India. The study was directly prompted by our findings that HSPA8 is a receptor of the human VGF-derived bioactive peptide TLQP-21 as described in this report. Data reported here will be submitted for publication together with data reported in the results section of this thesis, and are presented here with permission of Sandipan Chakraborty. In the Figures of this part, HSPA8 has been cited as HSC70.

Introduction

Structural details of the interactions needed for TLQP-21 recognition have been explored by molecular modeling studies. TLQP-21 is a highly flexible peptide. Recent NMR study suggest that TLQP-21 is probably unstructured in solution devoid of any defined secondary structure and in the presence of 3T3L1 cells expressing its putative receptor induces a conformational change with more α -helical propensity (1). Recently, we used an extensive 550 ns molecular dynamics to explore the folding energy landscape of the peptide to identify the probable native structure of the peptide in solution and found that the most populated structure of the peptide adopts a highly compact globular form stabilized by several hydrogen bonding interactions and π -cationic interactions (2). Thus the peptide is an interesting biological system exhibiting exquisite structural flexibility which is highly sensitive of its environment. Here, we also explored the structural dynamics of TLQP-21 bound to the HSPA8 receptor binding site has been explored by molecular dynamics simulation and compare the peptide dynamics when it is in water.

Material and Methods

Free peptide simulation:

TLQP-21 is known to be highly flexible peptide and there is no structural information available about the native structure of the peptide. We performed secondary structure analysis of human TLQP-21 (TLQPPSALRRRRHYHHALPPSR) from its amino acid sequence using Jpred3 web-interface (3, 4). The program predicts a strong helical propensity in the region 6-13. So, the peptide initially has been modeled as helical and both the C and N terminal amino and carboxylic group were prepared in neutral form. The initial model was then subjected to molecular dynamics simulation using GROMACS 4.5 (5, 6) simulation package using OPLS force field (7). The peptide was subjected to a short 100 steps energy minimization using the steepest descent algorithm *in vacuo* which is followed by 3000 steps of *in vacuo* conjugate gradient minimization. Then the minimized peptide was solvated with TIP3P explicit water model in a cubic box with periodic boundary condition. The box dimension was chosen such that all the protein atoms were at a distance equal to or greater than 10 Å from the box edges. The simulated system was then made neutral by adding appropriate number of Cl⁻ ions and the protonation state considered for each residue was consistent with neutral pH. The solvated system was then subjected to 500 steps of energy minimization using steepest descent algorithm in water. Simulation was carried out in the isothermalisobaric (NPT) ensemble at 300 K, using an external bath with a coupling constant of 0.1 ps. The pressure was kept constant (1 bar) by using pressure coupling with the time-constant set to 1 ps. The LINCS algorithm was used to constrain the bond lengths involving hydrogen atoms, allowing the use of 2.0 fs time step. Electrostatic interactions were calculated using particle mesh Ewald summation method. Van der Waals interactions were truncated at 14 Å. The trajectories were stored at every 5 ps.

Modeling the HSPA8:

The HSPA8 shows high degree of conformational flexibility. It is an ATP binding chaperone and has intrinsic ATPase activity which hydrolyzes ATP into ADP. HSPA8 hydrolyzing ATP initiates the conformational change of HSPA8 and further causes substrate binding by HSPA8. But in all the available PDB of the HSPA8 is in closed conformation where lid moves over the substrate binding domain to close the cavity opening. This conformation does not allow the binding of the peptide TLQP-21. Thus we modeled the HSPA8 in open conformation where the lid is further away from the substrate binding domain using SWISS-MODEL web-server (8) and the quality of the generated model was judged using ANOLEA and QMEAN analysis. We used the structural homolog of HSPA8, E.coli DnaK in open conformation, which has a sequence identity of 52.82 % to model the protein using homology modeling. The modeled HSPA8 was then subjected to a short 500 steps energy minimization using the steepest descent algorithm *in vacuo* which is followed by 500 steps of energy minimization using steepest descent algorithm in water using TIP3P explicit water model in a cubic box with periodic boundary condition. The minimized structure was then subjected to further 1500 steps of energy minimization using conjugate gradient algorithm in explicit water.

Protein-peptide Docking:

To dock TLQP-21 within HSPA8 substrate binding site, we have used protein-peptide docking procedure. Firstly, we have used ClusPro 2.0 web-interface (9, 10) to dock the TLQP-21 with HSPA8. ClusPro uses a fast Fourier transform (FFT) based rigid body docking algorithm to explore all possible binding poses of the peptide within the active site by a systematic rotation and translation of the peptide. Then 1000 lowest energy solution judged by a balanced scoring function are clustered and solutions from

the 10 best clusters are reported. The best solution was selected which has the most favorable energy and also belongs to the most populated cluster.

Molecular dynamics simulation of the HSPA8-TLQP-21 complex:

Conformational dynamics of both free TLQP-21 and HSPA8-TLQP-21 complex were studied using extensive molecular dynamics simulation with the aid of GROMACS 4.5 packages 95, 6) with OPLS force field (7).

Both free and HSPA8 bound TLQP-21 complex were subjected to a preliminary short energy minimization *in vacuo* using the steepest descent algorithm. Then each system was solvated with TIP3P explicit water model in a cubic box with periodic boundary condition. The box dimension was chosen such that all the protein atoms were at a distance equal to or greater than 10 Å from the box edges. The simulated system was then made charge neutral by adding appropriate number of counter ions. The solvated system was then subjected to 1000 steps of energy minimization using steepest descent algorithm which is followed by 5000 steps of minimization using conjugate gradient algorithm. After that, a 100 ps position restrained dynamics was carried out where the protein/complex was restrained by adding restraining forces while the water molecules were allowed to move freely. It allows proper equilibration of solvent around the solute. It was then followed by 100 ps of NVT simulation at 300 K and 100 ps of NPT simulation to achieve proper equilibration of the system to be simulated. Final production simulations were performed in the isothermal isobaric (NPT) ensemble at 300 K, using an external bath with a coupling constant of 0.1 ps. The pressure was kept constant (1 bar) by using pressure coupling with the time-constant set to 1 ps. The LINCS algorithm was used to constrain the bond lengths involving hydrogen atoms, allowing the use of 2.0 fs time step. Electrostatic interactions were calculated using particle mesh Ewald summation method. Van der Waals interactions were truncated at

14 Å. The trajectories were stored at every 5 ps. Analyses were carried out with the trajectory analysis tools implemented in GROMACS.

Result and Discussion

Recognition of TLQP-21 by HSPA8:

To explore the recognition mechanism of TLQP-21 by HSPA8, we have employed protein-peptide docking implemented in ClusPro 2.0 web-interface. It is to be noted that we have modeled the HSPA8 in open conformation where lid is further away from the substrate binding domain. In this lowest energy docking complex, TLQP-21, binds properly within the substrate binding domain of HSPA8. Structures of the TLQP-21-HSPA8 complex obtained from ClusPro shown in Figure 21.

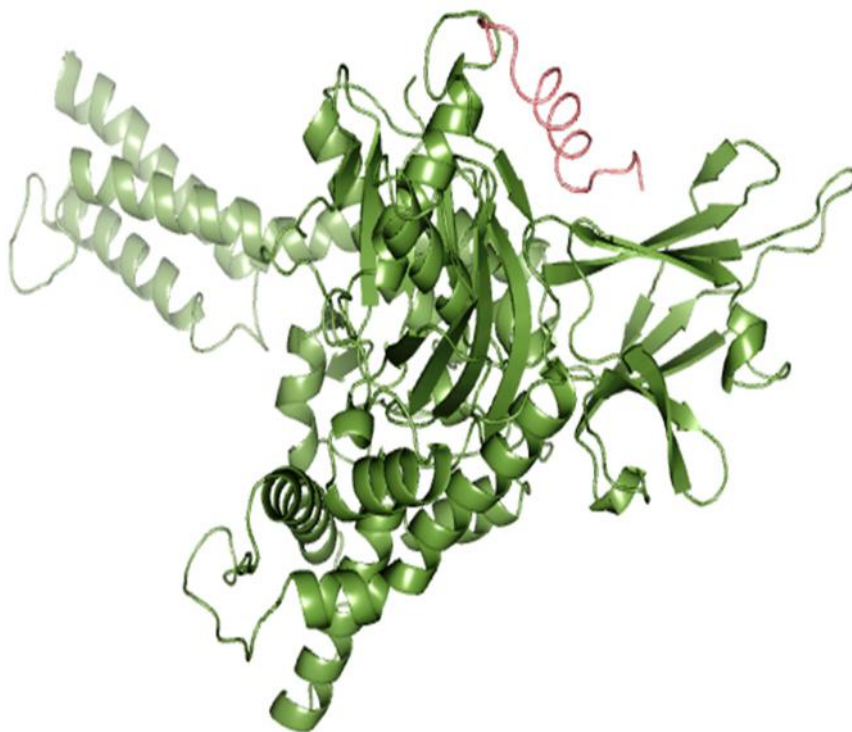


Figure 26: Structures of the TLQP-21- HSPA8 obtained from molecular docking study in cartoon representation. HSPA8 is colored in green whereas the bound TLQP-21 is colored in pink.

As evident from the figure, TLQP-21 appropriately orients within the substrate binding site of the HSPA8. The peptide interacts strongly with the twisted β -sheeted plate sheet region of the HSPA8 substrate binding site. The complex displays high steric compatibility in size and shape between the TLQP-21 and HSPA8, resulting a tighter spatial fit of the peptide inside the cavity. The bound TLQP-21 still maintains its helical conformation.

Molecular dynamics simulation:

To further investigate the conformational dynamics of TLQP-21 in its free and receptor bound state, we have used molecular dynamics (MD) simulation using GROMACS packages (5, 6) for both free and HSPA8 bound TLQP-21 obtained from docking studies.

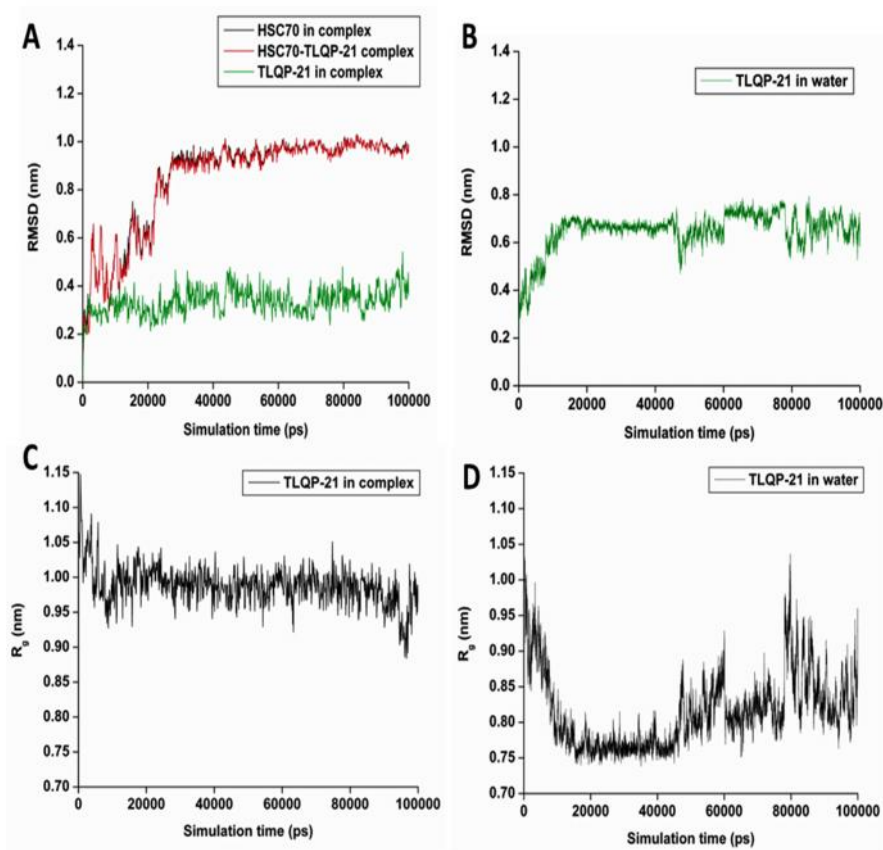


Figure 27: Variations of RMSD (A, B) and R_g (C, D) with simulation time for TLQP-21 in complex with HSPA8 and free TLQP-21 in solution obtained from molecular dynamics simulation.

Figure 22 depicts the variations of two global structural parameters root mean square deviation (RMSD) and radius of gyration (R_g) for both free and HSPA8 bound TLQP-21. The RMSD (root means square deviations) of the backbone C atoms of the simulated protein over time can be used to analyze the structural stability of the system. Figure 22A shows that the complex undergoes significant conformational changes during the first 25 ns of the simulation, after that the system monotonically reaches to an equilibrium state, evident from the stable RMSD profile of the complex. We then analyzed the variations of the RMSD of each of the component of the complex, i.e., HSPA8 and TLQP-21, during the simulation. As evident from the Figure 22A, changes in the observed in the complex during the initial period of the simulation is mainly contributed by the receptor HSPA8. It is to be noted that the HSPA8 is a highly flexible protein that undergoes significant conformation changes upon substrate binding and dependent on ATP hydrolysis. We have modeled the HSPA8 in open conformation where the lid is further away from the substrate binding domain. Thus it is expected that upon peptide binding there should be significant conformational changes. Throughout the simulation, we do not find any dissociation of the complex, indicating that the peptide TLQP-21 form strong, stable complex with HSPA8. It is to be noted that we modeled TLQP-21 in helical form and interestingly we found that this helical form is highly stable upon complex formation. Figure 22A shows that the peptide within the complex undergoes very small changes in its RMSD profile during very initial equilibration period of the simulation after that it is highly stable throughout the simulation and settled down ~ 0.3 nm with respect to the initial helical conformation of the peptide while it is bound to the HSPA8 substrate binding site. But the TLQP-21 in solution is highly flexible as evident from the RMSD profile of the peptide, shown in Figure 22B. The initial helical conformation of the peptide, TLQP-21, changes significantly up to 0.7 nm during ~ 20 ns of the simulation with respect to the initial helical conformation of the peptide in water. During the simulation period, particularly during 50 to 100 ns of the

simulation the RMSD profiles varies significantly indicating that the peptide is highly flexible in solution and accessing different conformation states during simulation.

On the other hand, radius of gyration (R_g) provides insight into the overall dimension and shape of the protein. The plot of R_g of TLQP-21 in bound and free states with simulation time is shown in Figure 22C and 22D. The initial helical conformation of the peptide TLQP-21 when bound to HSPA8 is highly stable during the 100 ns simulation of the complex, evident from a highly stable R_g profile of the peptide in bound condition throughout the simulation. While during the simulation of the peptide in free state, the initial helical conformation of the peptide changes rapidly and adopts a more compact form, evident from a sharp decrease of R_g from 1.10 nm to 0.75 nm. This conformation fluctuates between numerous states throughout the simulation time evident from the changes of the R_g profile and the sharp spikes indicate metastable states with partial unfolded structures. Overall the RMSD and R_g profile reveals the peptide, TLQP-21, in water adopt a highly flexible conformation and fluctuates between many conformations during simulation, while receptor binding provides stabilization of its initial helical conformation.

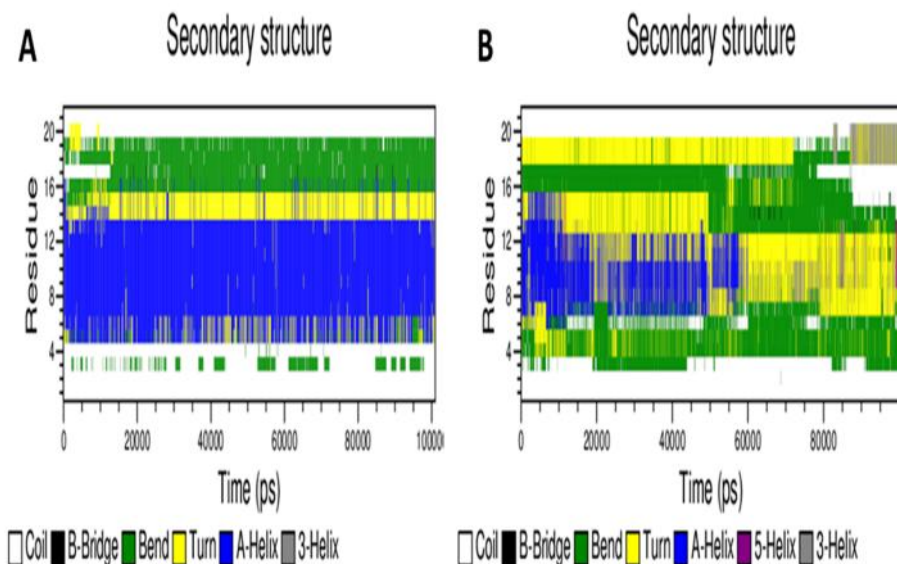


Figure 28: A: Secondary structural propensity variation analysis of each residue of the peptide with simulation time when complex with HSPA8. B: Secondary structural propensity variation analysis of each residue of the free peptide with simulation time in solution.

Secondary structural propensity analysis of each residue of the peptide in bound and free state throughout simulation time is shown in Figure 23. TLQP-21 when bound to the HSPA8, the peptide possess strong helical propensity and it's helical is highly stable throughout the simulation. Particularly, the region 4-14 exists as α -helix when bound to the receptor binding site. Interestingly, in solution the peptide is highly flexible and mostly unstructured in solution which corroborates well with the existing assumptions. Most of the residues of the peptide possess high turn/bend propensity. Residues of the

region S₆-R₁₀/R₁₁ shows some helical propensity during the initial period but it rapidly dissolves during the later period of the simulation.

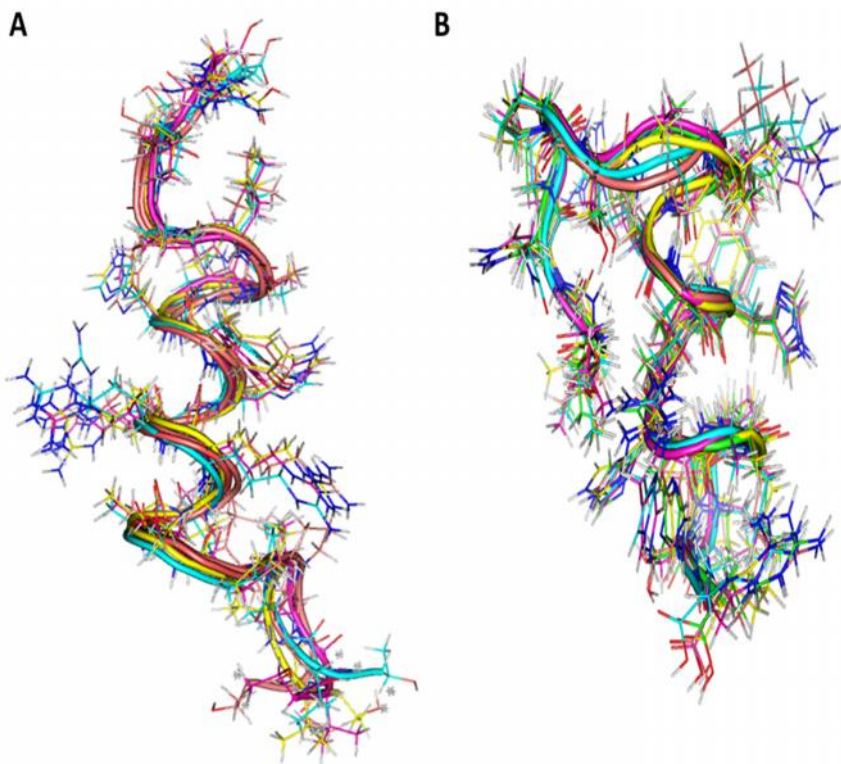


Figure 29: Superimposed structure of the five most populated conformations of the peptide TLQP-21 obtained from cluster analysis. A: Peptide conformations obtained from the cluster analysis from the TLQP-21- HSPA8 complex simulation. B: Free peptide simulation in solution.

To identify most frequently visited conformations during MD simulation, cluster analysis has been performed over the 100 ns trajectory using a stringent RMSD cutoff of 0.1 nm using gromos algorithm. Analysis on the whole trajectory of the complex simulation results in 907 clusters of TLQP-21 peptide conformations while in solution

the peptide conformations observed during the simulation resulted 2816 conformations. This observation again indicates that the peptide is highly stable upon binding with the receptor, HSPA8 while in solution it is highly flexible accessing many conformations. Average conformation of the peptide, TLQP-21, of the five most populated clusters from TLQP-21- HSPA8 complex simulation and simulation of the peptide in solution is also shown in Figure 24. When peptide is bound to HSPA8 substrate binding site (Figure 24A), all the five conformations of the peptide have very similar side-chain orientations and exist as long α -helix. In solution, all the five structures of the peptide adopt a highly compact globular form in contrast to their initial long helical form. This observation is in accordance with the R_g distribution. Most of the conformations in the MD simulation are centered ~ 0.75 nm of R_g , represent highly globular forms. All the five conformations of the peptide are highly flexible with widely distributed side-chain orientations. Although a helical propensity is observed for a very short region of the peptide, but most of the residues are in coil/turn conformation.

We then analyzed the essential interactions responsible for TLQP-21 recognition by HSPA8. Analysis of the average center of mass distance variations between TLQP-21 and HSPA8 reveals that the initial docked complex varies greatly with the simulation and as the simulation progresses TLQP-21 comes closer and binds strongly to the HSPA8 binding site (Figure 25A).

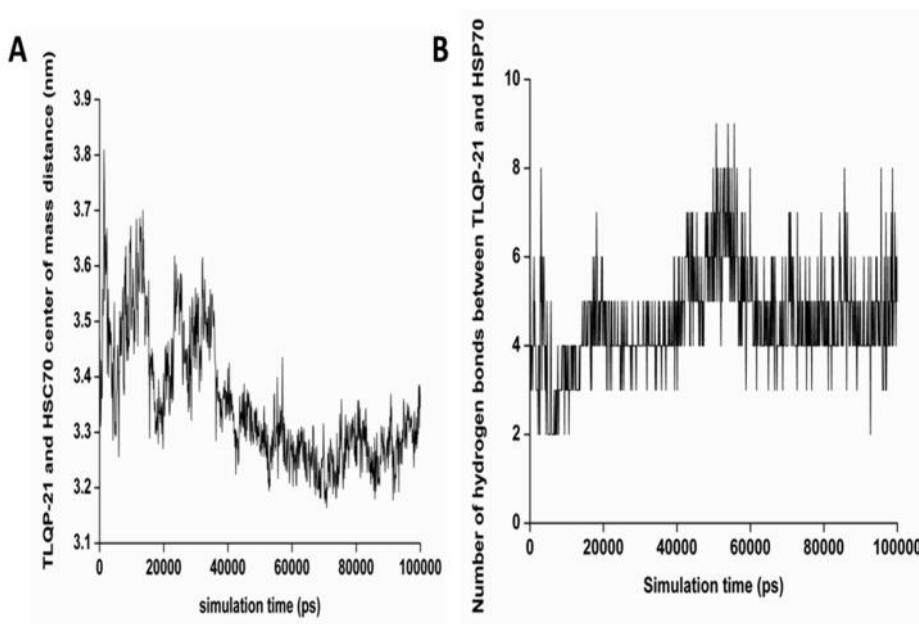
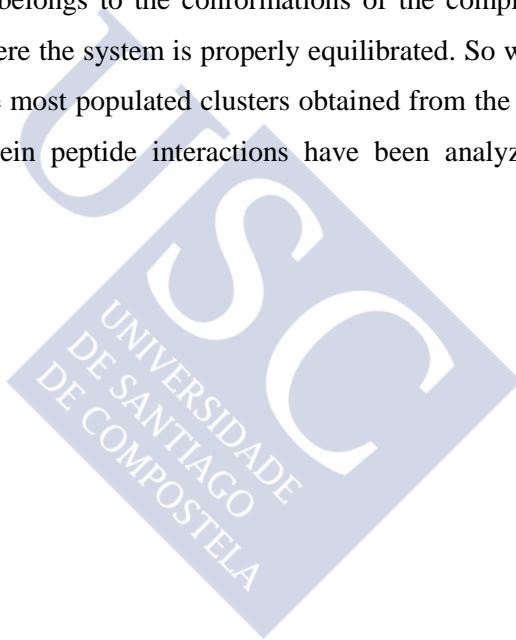


Figure 30: Variations of center of mass distance (A) and hydrogen bonding (B) between TLQP-21 and HSPA8 with simulation time.

One of the principal driving force that allows stronger interaction of the peptide, TLQP-21, within HSPA8 substrate binding site as the simulation progresses is the formation of more number of hydrogen bonds. Figure 25B demonstrates the variation of number of hydrogen bonds between TLQP-21 and HSPA8. As evident from the figure, with simulation time, the number of hydrogen bonds increases compared to the number of hydrogen bonds observed in the docked complex. Also evident from the RMSD profile of the complex (Figure 25A), during the initial 30 ns of the simulation, the docked complex undergoes conformational readjustment. During this time the peptides comes closer to the HSPA8 binding site and during this period number of hydrogen bonds with the receptor varies greatly. With the simulation, the peptide comes closer and settled around at an optimum distance guided by strong surface complementarity and increasing

hydrogen bonding possibilities. During latter half of the simulation, the number of hydrogen bonds between TLQP-21 and HSPA8 settled ~ 5-6.

Variations of RMSD fluctuations of the complex, center of mass distance between TLQP-21 and HSPA8 as well as the protein-peptide hydrogen bonding reveal that the complex reaches a stable equilibrated state in the later 50 ns of the simulation. We then performed the cluster analysis of the TLQP-21- HSPA8 complex reveals that the most populated conformations belongs to the conformations of the complex from the latter half of the simulation, where the system is properly equilibrated. So we have chosen the average structure from the most populated clusters obtained from the TLQP-21- HSPA8 complex simulation. Protein peptide interactions have been analyzed and shown in Figure 26.



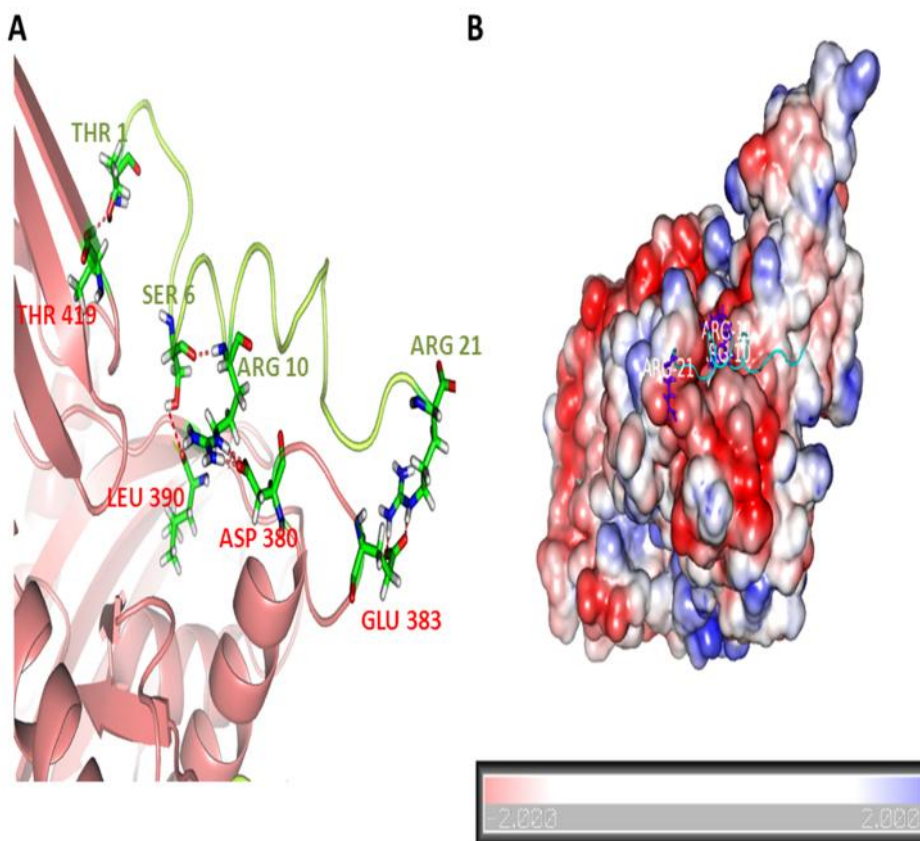
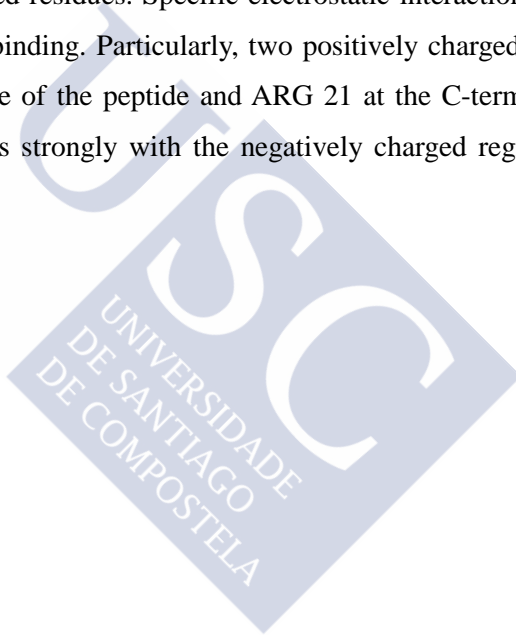


Figure 31: Details of the interactions involved in TLQP-21 recognition by HSPA8.

A: Details of the hydrogen bonding interactions between TLQP-21 and HSPA8. HSPA8 and TLQP-21 are colored as salmon and lime-green color, respectively. B: Electrostatic surface potential of HSPA8 when TLQP-21 is bound to the protein. Regions of positively and negatively charged surface area are colored in blue and red color.

We have also analyzed the hydrogen bonding interactions between TLQP-21 and HSPA8 using PIC web-server (11). Details of hydrogen bonding interactions between TLQP-21 and HSPA8 are shown in Figure 26A. THR 1 at the N-terminal of the TLQP-21 is involved in hydrogen bonding interaction with THR 419 of HSPA8. At the middle of the

peptide, SER 6 and ARG 10 are involved in hydrogen bonding interactions with LEU 390 and ASP 380, respectively at the HSPA8 receptor binding site. These interactions might play crucial role in mainlining the helical structure of the peptide within receptor binding site. At the C-terminal region, ARG 21 of TLQP-21 is involved in a hydrogen bonding interaction with GLU 383 of HSPA8. Figure 26B shows electrostatic interactions between HSPA8 and TLQP-21. As evident from the electrostatic surface potential of HSPA8, the peptide binding region of the protein is highly charged and contains negatively charged residues. Specific electrostatic interactions between TLQP-21 and HSPA8 facilitate binding. Particularly, two positively charged residues ARG 10 and ARG 11 at the middle of the peptide and ARG 21 at the C-terminal region of the peptide TLQP-21 interacts strongly with the negatively charged region of the HSPA8 substrate binding site.



References

1. Cero, C., Vostrikov, V. V., Verardi, R., Severini, C., Gopinath, T., Braun, P. D., Sassano, M. F., Gurney, A., Roth, B. L., Vulchanova, L., Razzoli, M., Lodola, A., Possenti, R., Veglia, G., Bartolomucci, A. (2014) The TLQP-21 Peptide Activates the G-Protein-Coupled Receptor C3aR1 via a Folding-upon-Binding Mechanism. *Structure*; **22** : 1744–1753
2. Chakraborty, S., Akhter, S., Requena, J. R., Basu, S. (2015) Probing the conformational dynamics of the bioactive peptide TLQP 21 in solution: A molecular dynamics study. *Chem Biol Drug Des*:doi: 10.1111/cbdd.12541.
3. Cole, C, Barber, J. D., Barton, G. J. (2008) The Jpred 3 secondary structure prediction server. *Nucleic Acids Res*; **36** : W197-W201
4. Cuff, J. A., Clamp, M. E., Siddiqui A. S., Finlay, M., Barton G. J. (1998) Jpred: A Consensus Secondary Structure Prediction Server. *Bioinformatics*; **14** : 892-893
5. Spoel, D. V. D., Lindahl, E., Hess, B., Groenhof, G., Mark, A. E., Berendsen, H. J. (2005) GROMACS: fast, flexible, and free. *J Comput Chem*; **26** : 1701–1718
6. Lindahl, E., Hess, B., Spoel, D. V. D. (2001) GROMACS 3.0: a package for molecular simulation and trajectory analysis. *J Mol Model*; **7** : 306–317
7. Jorgensen, W. L., Rives, T. (1988) Development and testing of the OPLS all-atom force field on conformational energetic and properties of organic liquids. *J Am Chem Soc*; **110** : 1657–1666
8. Arnold, .K, Bordoli, L., Kopp, J., Schwede, T. (2006) The SWISS-MODEL Workspace: A web-based environment for protein structure homology modelling. *Bioinformatics*; **22** : 195-201

9. Comeau, S. R., Gatchell, D. W., Vajda, S., Camacho, C. J. (2004) ClusPro: an automated docking and discrimination method for the prediction of protein complexes. *Bioinformatics*; **20** : 45-50
10. Kozakov, D., Brenke, R., Comeau, S. R., Vajda, S. (2006) PIPER: An FFT-based protein docking program with pairwise potentials. *Proteins: Struct Func Bioinfo*; **65** : 392-406
11. Tina, K.G., Bhadra, R., Srinivasan, N. (2007) PIC: Protein interactions calculator. *Nucleic Acid Res*; **35**: W473–W47.



Annex III:

Probing the conformational dynamics of the bioactive peptide TLQP-21 in solution: A molecular dynamics study

This part of the study was performed as a collaborative work with Sandipan Chakraborty and Soumalee Basu, Department of Microbiology, University of Calcutta, India. The study was directly prompted by our findings that HSPA8 is a receptor of the human VGF-derived bioactive peptide TLQP-21 as described in this report. Data reported here has already been published in the Journal of Chemical Biology and Drug design (CBDD).



Received Date : 29-Nov-2014

Revised Date : 04-Feb-2015

Accepted Date : 05-Feb-2015

Article type : Research Letter

**Probing the conformational dynamics of the bioactive peptide TLQP 21 in solution: A
molecular dynamics study**

Sandipan Chakraborty^{1*}, Shamim Akhter^{2,3}, Jesús R Requena², Soumalee Basu¹

¹Department of Microbiology, University of Calcutta, 35 Ballygunge Circular Road, Kolkata - 700 019, India.

²CIMUS Biomedical Research Institute and Department of Medicine, University of Santiago de Compostela-IDIS, Avenida de Barcelona s/n 15782, Santiago de Compostela, Spain.

³Biotechnology and Genetic Engineering Discipline, Khulna University, Bangladesh.

*Corresponding author: Sandipan Chakraborty: sandipanchakraborty.13@gmail.com;

This article has been accepted for publication and undergone full peer review but has not been through the copyediting, typesetting, pagination and proofreading process which may lead to differences between this version and the Version of Record. Please cite this article as an 'Accepted Article', doi: 10.1111/cbdd.12541

This article is protected by copyright. All rights reserved.

Abstract

VGF derived peptide, TLQP-21, is a physiologically active neuropeptide exhibiting important roles in energy expenditure and balance, gastric contractility, reproduction, pain modulation, and stress. Although the physiological functions of the peptide constitute a research area of considerable interest, structural information is clearly lacking. Here, using extensive 550 ns molecular dynamics simulation in explicit water model, we have explored the folding energy landscape of the peptide. Principal component analysis and cluster analysis have been used to identify highly populated conformational states of the peptide in solution. The most populated structure of the peptide adopts a highly compact globular form stabilized by several hydrogen bonding interactions and π -cationic interactions. Strong surface complementarity of hydrophobic residues allows tighter spatial fit of the residues within the core region of the peptide. Our simulation also predicts that the peptide is highly flexible in solution and that the region A₇-R₉ and three C-terminal residues, P₁₉-R₂₁, possess strong helical propensity.

Keywords: TLQP-21; Neuropeptide; Folding energy landscape; Molecular dynamics simulation; Globular conformation.

Introduction

Regulation of energy homeostasis is a complex physiological function due to the cross-talk between several biological pathways. Identification of novel genes which regulate energy homeostasis and metabolism keeps on adding even more complexity (1-3). Among several such genes, *vgf* has recently received particular attention due to the fact that VGF^{-/-} mice have been found to be lean with a hypermetabolic phenotype (4). The human VGF gene is located on

This article is protected by copyright. All rights reserved.

chromosome 7 and is specifically expressed within neuroendocrine cells. Expression of VGF (nonacronymic), an acidic, proline and glycine rich protein (5), is up-regulated by nerve growth factor (NGF), and is modulated by DISC1 (6). Besides its role in regulation of energy metabolism, VGF shows antidepressant-like actions in rodents (7, 8). It is up-regulated in rodent hippocampi during electroconvulsive treatment (9), voluntary exercise (7), or treatment with brain-derived neurotrophic factor (BDNF) (10) or serotonin (8), while it is down regulated in rodent brain subjected to animal depression paradigms (8). Its expression is also reduced in post-mortem brain of patients with chronic mental disease (11, 6). VGF is a precursor protein that encodes different physiologically active neuropeptides. Among several bioactive peptides derived from VGF, TLQP-21 emerges as a multi-functional peptide exhibiting important role in energy expenditure and balance, gastric contractility, reproduction, pain modulation, stress, etc. (12). Initially, the peptide was immunopurified from rat brain (13) and found to be expressed in hypothalamus, hippocampus, pituitary gland, cerebral cortex, olfactory system and in brain stem which play many important roles in energy homeostasis, reproduction, stress and pain modulation (4).

Although the physiological role of TLQP21 is of considerable interest, very little information is available regarding the probable receptor through which the peptide elicits its effect. Recently, C3AR1 (14) and gC1qR (15) have been identified as receptors of TLQP-21. Also TLQP-21 has been demonstrated to bind to adipocyte membranes (16). Although these findings indicate the existence of cell surface receptors of TLQP-21, no structural information has been reported for TLQP-21 in its free state. In a recent publication, Cero et al (2014) using solution NMR study, demonstrated that the peptide TLQP-21 adopted α -helical structure (17) in the presence of 3T3L1 cells expressing the putative receptor of the peptide, but they were unable to obtain the

This article is protected by copyright. All rights reserved.

structure of unbound TLQP-21 due to high degree of flexibility. Thus the peptide is an interesting biological system exhibiting exquisite structural flexibility which is highly sensitive to its environment. But absence of any structural information regarding the native state of the peptide in solution is the main limitation to study the dynamic transition of the peptide and limits further structural insight of the peptide bound to the receptor. Here, we have used an extensive 550 ns molecular dynamics simulation to explore the folding energy landscape of the peptide to identify the probable native structure of the peptide in solution.

Material and Methods:

TLQP-21 is known to be a highly flexible peptide with no structural information about the native structure of the peptide. We therefore performed secondary structure analysis of human TLQP-21 (TLQPPSALRRRHYYHHALPPSR) from its amino acid sequence using Jpred3 web-interface (18, 19). Since the program predicts a strong helical propensity in the region 6-13, so, the peptide has been modeled as helical preparing both the C and N terminal amino and carboxylic groups in neutral form. The initial model was then subjected to molecular dynamics simulation using the GROMACS 4.5 (20, 21) simulation package using OPLS force field (22). The peptide was subjected to a short 100 steps energy minimization using the steepest descent algorithm *in vacuo* which is followed by 3000 steps of *in vacuo* conjugate gradient minimization. Then the minimized peptide was solvated with TIP3P explicit water model in a cubic box with periodic boundary condition. The box dimension was chosen such that all the protein atoms were at a distance equal to or greater than 10 Å from the box edges. The simulated system was then made neutral by adding appropriate number of Cl⁻ ions and the protonation state considered for each residue was consistent with neutral pH. The solvated system was then subjected to 500 steps of

This article is protected by copyright. All rights reserved.

energy minimization using steepest descent algorithm in water. Simulation was carried out in the isothermalisobaric (NPT) ensemble at 300 K, using an external bath with a coupling constant of 0.1 ps. The pressure was kept constant (1 bar) by using pressure coupling with the time-constant set to 1 ps. The LINCS (23) algorithm was used to constrain the bond lengths involving hydrogen atoms, allowing the use of 2.0 fs time step. Electrostatic interactions were calculated using particle mesh Ewald summation method. Van der Waals interactions were truncated at 14 Å. The trajectories were stored at every 5 ps.

Analyses were carried out with the trajectory analysis tools implemented in GROMACS and the secondary structure assignments were carried out with DSSP (24) module. The RMSD matrix was then computed on the trajectory by least square fitting on main-chain atoms and then processed using the GROMOS algorithm to extract clusters of similar conformations. Principal component analysis (PCA) was then performed on the trajectory. Mass weighted covariance matrix of the atomic positional fluctuations was calculated on C α atom and essential subspace was then described by the variance retained by the reduced representation defined by calculated eigenvectors.

Result and discussions:

VGF-derived peptide TLQP-21 is a multifunctional peptide that is considered to be a highly flexible unstructured protein. We have explored structural preferences of the human peptide in solution using atomistic simulation. Analysis of residue wise secondary structure preference from the sequence using Jpred3 web-interface (18, 19), reveals a strong helical propensity in the region 6-13. So, we initially modeled the peptide as helical and studied the conformational

This article is protected by copyright. All rights reserved.

preferences of the peptide utilizing a long 550 ns all-atom molecular dynamics simulations using OPLS force field.

Figure 1A reveals variations of the two structural parameters, root mean square deviation (RMSD) and radius of gyration (R_g), of the peptide along with simulation time. Variations of each structural parameter with simulation time and 2-D scatter plot between RMSD and R_g is shown in Figure S1 (Supplementary material). RMSD of the backbone C α atoms of the simulated peptide over time can be used to analyze the structural flexibility of the system while the radius of gyration (R_g) provides insight into the overall dimension and shape of the peptide. The initial helical conformation of the peptide changes rapidly and adopts a more compact form, evident from a sharp decrease of R_g from 1.10 nm to 0.75 nm. This conformation fluctuates between numerous states throughout the simulation time as evident from the changes of the RMSD and R_g profile with the sharp spikes indicating metastable states with partial unfolded structures. Broadly, the RMSD and R_g profile reveals a highly flexible nature of the peptide that fluctuates between many conformations during the simulation. The initial long helical conformation is not stable rather the peptide refolds in a more compact form. Variations of RMSD with R_g indicate that most of the conformations visited during the simulation are confined within the RMSD range of 0.6-0.8 nm with respect to the initial conformation with corresponding R_g varying between 0.75-0.95 nm. Solvent accessible surface area (SASA) calculations reveal that the conformations with low R_g values are tightly packed into the globular form with low SASA (Figure 1B). Relative contributions from both hydrophobic and hydrophilic residues reveal that hydrophobic residues are packed inside the protein core with the progress of the simulation evident from the reduction of SASA from 13-14 \AA^2 to 9-10 \AA^2 . But the SASA of the hydrophilic residues change from $\sim 10.3 \text{\AA}^2$ to $\sim 9.75 \text{\AA}^2$ during the simulation (Data not

This article is protected by copyright. All rights reserved.

shown). Secondary structural propensity analysis of each residue of the peptide throughout the simulation time is shown in Figure 2. In general, the peptide is highly flexible and mostly unstructured in solution which corroborates well with the existing assumptions (17). Most of the residues of the peptide possess high turn/bend propensity. Interestingly, we observed two distinct regions of helical propensity in the peptide during the simulation. Residues of the region S₆-R₁₀/R₁₁ maintain its helical propensity until 300 ns after that the region appear as 3_{10} -helix and the secondary structure remains stable for the remaining simulation time (Figure 2A). Interesting observation is the gain of helical structure in the region P₁₈-R₂₁ with two consecutive prolines. Initially this region remains highly unstructured but later it gains helical propensity and appear as 3_{10} -helix at ~ 300 ns and remains stable throughout the simulation. Variations of the number of residues with different types of secondary structure propensity with simulation time are shown in Figure 2B.

Figure 2B reveals with simulation time, the number of residues with 3_{10} -helical structure increases and in later half of the simulation α -helical propensity decreases. Interestingly, between the timescale 100-300 ns, there is strong propensity of four residues to adopt π -helix. Particularly, residues R₉-Y₁₃ have some π -helical propensities. With simulation time, the number of residues in coil conformation increases. At the very beginning there are four residues in coil conformation. Within 100 ns the propensity increases to 8 residues and maintains the coil conformation during the remaining 450 ns.

To identify most frequently visited conformations during MD simulation, cluster analysis has been performed over the 550 ns trajectory using a stringent RMSD cutoff of 0.1 nm using GROMOS algorithm. Analysis on the whole trajectory of TLQP-21 simulation results in 1999 clusters. Distribution of number of conformations of the peptide in 50 most populated clusters is

This article is protected by copyright. All rights reserved.

shown in Figure 3A. As evident from the figure, first five clusters are highly populated. Average structure from each of the five clusters is also shown in Figure 3A. All the five structures adopt a highly compact globular form in contrast to their initial long helical form. This observation is in accordance with the R_g distribution. Most of the conformations in the MD simulation are centered ~ 0.75 nm of R_g , representing highly globular forms. All the five conformations of the peptide are highly flexible with most of the residues existing in coil/turn conformation. Secondary structural propensity of each residue in all the five conformations has been analyzed using the STRIDE algorithm, as shown in Figure 3B.

In summary, most of the residues have strong turn propensity. Residues A₇-R₉ in the average structures of all the five clusters, except cluster II, have strong helical propensity adopting the structure of 3_{10} -helix. This region in the conformations from cluster II exists as helical turn. C-terminal residues on the other hand exist as helical turn/random coil in most of the clusters except cluster III and V, where they exist as 3_{10} -helix.

Analysis of per residue fluctuations (Figure 3C) reveals that residues with defined secondary structural element are less flexible compared to the region that is devoid of any secondary structural element. Particularly, the N-terminal 3_{10} -helix spanning residues A₇-R₁₀ is highly stable throughout the simulation.

MD simulation visits numerous conformations during the simulation time scale. To identify most probable solution structure of the peptide we have used principal component analysis (PCA). PCA is an efficient data reduction technique where the dimensionality of the essential subspace of the peptide is defined by the reduced subspace represented by eigenvectors or principal components (PCs). There are 189 PCs needed to define the variations observed in the MD

This article is protected by copyright. All rights reserved.

simulation. First few components are more informative as evident with high eigenvalues while the latter components carry very little information about the peptide dynamics (Figure 4A). Particularly, PC1 being the most informative component requires special mention. Cosine contents of first 10 principal components are low enough to ensure that the simulations represent the intrinsic dynamical behavior of the peptide rather than representing random diffusion dynamics. Free energy surface of the peptide has been represented in terms of the first two PCs (PC1 and PC2) and is shown in Figure 4B. Surface has been constructed on the basis of most frequently visited conformational clusters in the bi-dimensional scatter plot of first two PCs. Structures with very similar conformations tend to cluster together in 2-D essential sub-space constructed by first two PCs.

The free energy surface representation, shown in Figure 4B, reveals three main peaks. It is to be noted that these peaks are distributed within very narrow region in PC2 (-2 to 6) but widely distributed along PC1 (-10 to 10). This is in accordance with the eigenvalue distribution plot where the eigenvalue of PC1 is ~ 2.5 times higher than the eigenvalue of PC2. Peak centered on ~8 of PC1 scale represents most prominent peak in the energy surface and represents conformations of cluster I, III and V. This is in accordance with the cluster analysis (Figure 3B) where the average conformation of the peptide belonging to these three clusters share highly similar secondary structural profile. On the other hand, peak centered on ~-0.5 and ~ -10 of PC1 scale represent conformations belonging to cluster II and IV, respectively. Secondary structure analysis of cluster average structure from these two clusters (Figure 3B) reveals that the secondary structural propensity of conformations from these two clusters is distinctively different than other clusters.

This article is protected by copyright. All rights reserved.

Cluster analysis identified cluster I as the most populated conformational cluster observed during the MD simulation. Also the most prominent peak in energy surface computed by first two PCs, represents conformations from this cluster. Average structure of cluster I has been further analyzed to provide essential interactions that stabilize the structure in atomistic details, shown in Figure 5.

The peptide adopts a highly compact globular structure stabilized by several hydrogen bonding interactions and strong surface complementarity of hydrophobic residues allows tighter spatial fit of the residues within the core region of the peptide. Details of the hydrogen bonding interactions are shown in Figure 5A. THR 1 is involved in a hydrogen bonding interaction with HIS 12. ARG 10 is involved in several hydrogen bonding contacts with GLN 3, SER 6 and ALA 7. LEU 8 interacts with TYR 13. HIS 14 is involved in two hydrogen bonds with LEU 17 and SER 20. LEU 17 is also involved in a hydrogen bonding interaction with SER 20 as is HIS 14 with ALA 16. Interestingly, side chains of all the polar residues are extending outwards and those polar atoms buried inside the core are involved in hydrogen bonding interactions. All hydrophobic residues are clustered together to form two distinct patches of hydrophobic cluster (Figure 5B). PRO 4 and PRO 5 along with ALA 7 and LEU 8 form a cluster. The second cluster is formed by PRO 18 and PRO 19 in tighter packing with LEU 17. It is to be noted that LEU 2 of the N-terminal region folds back to form strong van der Waals interactions with the second cluster. There is also a π -cationic interaction between ARG 9 and TYR 13 with a distance of 4.87 Å (Figure 5C).

This article is protected by copyright. All rights reserved.

Conclusions and future directions:

Present study provides possible solution structure of the biogenic peptide TLQP-21 through an efficient sampling of the folding energy landscape using extensive 550 ns molecular dynamics simulation in explicit water model. In accordance to current hypothesis, our simulation also predicts that the peptide is highly flexible in solution. Most of the residues of the peptide possess high turn/bend propensity which is supported by the solution NMR study, where a chemical shift index of a typical random coil conformation has been observed (17). Interestingly, our simulation shows that the peptide is not absolutely random coil but contains stretches of defined structure. Residues A₇-R₉ have high helical propensity and during the simulation this region fluctuates between π -helix and 3_{10} -helix. Also, three end residues fluctuate between 3_{10} -helix and turn. Recently, solution state NMR study by Cero *et al.*, demonstrates that the TLQP-21 peptide adopts a well-defined α -helical conformation upon receptor binding. Thus the peptide undergoes a folding upon-binding transition within the receptor binding site (17). We also suggest that the traces of helical structures present in its native state in solution are crucial to adopt the α -helical structure of the peptide upon binding to the receptor interface. Random coil to helix is a common mechanism for activating GPCRs of the secretin family (25-26). Cero *et al.*, suggested that the driving forces of TLQP-21 peptide folding-upon binding mechanism are distinctively different than most of the other peptides. While formation of amphipathic helix where hydrophobic residues are embedded within the binding surfaces, has been considered to be the primary driving force for the conformational transition of most of the peptides upon binding with their cognate receptor, but in TLQP-21 hydrophobic and hydrophilic residues are randomly distributed throughout the peptide sequence, suggesting a different mechanism of folding upon binding [17]. Presence of helical residues in the middle of the peptide in solution observed in our simulation

This article is protected by copyright. All rights reserved.

might be a crucial structural motif that might play an important role in receptor binding and may be the nucleating structure that initiates the refolding of the peptide in helical form within the receptor binding site.

The most populated structure of the peptide obtained from MD simulation adopts a highly compact globular structure stabilized by several hydrogen bonding interactions and π -cationic interactions. Strong surface complementarity of hydrophobic residues allows tighter spatial fit of the residues within the core region of the peptide whereas polar atoms within the peptide core are involved in hydrogen bonding thus allowing efficient folding of the peptide. This study for the first time provides structural insight into the conformational dynamics of the physiologically important peptide TLQP-21 in solution and further extending the idea to understand its interaction with its receptor in critical details.

Acknowledgments

Authors gratefully acknowledge BIOGENE high performance computing facility at the Bioinformatics Resources and Applications Facility (BRAAF) and the Centre for High Performance Computing for Modern Biology, Ballygunge Science College, University of Calcutta, India, for providing us the computational facility. JRR was funded by ERANET-NEURON grant DISCover (ISCIH PI09/2688); SA is supported by an EXPERTS II-Erasmus Mundus fellowship

Conflict of Interest

Authors do not have any competing interest.

This article is protected by copyright. All rights reserved.

References

1. Cederberg A., Grønning L.M., Ahren B., Tasken K., Carlsson P., Enerback S. (2001) FOXC2 is a winged helix gene that counteracts obesity, hypertriglyceridemia, and diet-induced insulin resistance. *Cell*;106:563–573.
2. Riu E., Ferre T., Hidalgo A., Mas A., Franckhauser S., Otaegui P., Bosch F. (2003) Overexpression of c-myc in the liver prevents obesity and insulin resistance. *FASEB J*;17:1715–1717.
3. Zhang J.V., Ren P.G., Avsian-Kretchmer O., Luo C.W., Rauch R., Klein C., Hsueh A.J. (2005) Obestatin, a peptide encoded by the ghrelin gene, opposes ghrelin's effects on food intake. *Science*;310:996–999.
4. Bartolomucci A., Possenti R., Levi A., Pavone F., Moles A. (2007) The role of the vgf gene and VGF-derived peptides in nutrition and metabolism. *Genes Nutr*;2:169–180.
5. Chakraborty T.R., Tkalych O., Nanno D., Garcia A.L., Devi L.A., Salton S.R. (2006) Quantification of VGF-and pro-SAAS-derived peptides in endocrine tissues and the brain, and their regulation by diet and cold stress. *Brain Res*;1089:21-32.
6. Ramos A., Rodríguez-Seoane C., Rosa I., Trossbach S.V., Ortega-Alonso A., Tomppo L., Ekelund J., Veijola J., Järvelin M.R., Alonso J., Veiga S., Sawa A., Hennah W., García Á., Korth C., Requena J.R. (2014) Neuropeptide precursor VGF is genetically associated with social anhedonia and underrepresented in the brain of major mental illness: its downregulation by DISC1. *Hum Mol Genet*;23:5859-5865.

This article is protected by copyright. All rights reserved.

7. Hunsberger J.G., Newton S.S., Bennett A.H., Duman C.H., Russell D.S., Salton S.R., Duman R.S. (2007). Antidepressant actions of the exercise-regulated gene VGF. *Nature Med*;13:1476-1482.
8. Thakker-Varia S., Krol J.J., Nettleton J., Bilimoria P.M., Bangasser D.A., Shors T.J., Black I.B., Alder J. (2007) The neuropeptide VGF produces antidepressant-like behavioral effects and enhances proliferation in the hippocampus. *J Neuroscience*;27:12156-12167.
9. Newton S.S., Collier E.F., Hunsberger J., Adams D., Terwilliger R., Selvanayagam E., Duman R.S. (2003) Gene profile of electroconvulsive seizures: induction of neurotrophic and angiogenic factors. *J Neuroscience*;23:10841-10851.
10. Alder J., Thakker-Varia S., Bangasser D.A., Kuroiwa M., Plummer M.R., Shors T.J., Black I.B. (2003) Brain-derived neurotrophic factor-induced gene expression reveals novel actions of VGF in hippocampal synaptic plasticity. *J Neuroscience*;23:10800-10808.
11. Thakker-Varia S, Jean Y.Y., Parikh P, Sizer C.F., Ayer J.J., Parikh, A., Hyde T.M., Buyske S., Alder J. (2010) The neuropeptide VGF is reduced in human bipolar postmortem brain and contributes to some of the behavioral and molecular effects of lithium. *J Neuroscience*;30:9368-9380.
12. Ferri G.L., Noli B., Brancia C., D'Amato F., Cocco C. (2011) VGF: An inducible gene product, precursor of a diverse array of neuro-endocrine peptides and tissue-specific disease biomarkers. *J Chem Neuroanat*;42:249-261.

This article is protected by copyright. All rights reserved.

13. Bartolomucci A., Corte G.L., Possenti R., Locatelli V., Rigamonti A.E., Torsello A., Bresciani E., Bulgarelli I., Rizzi R., Pavone F., D'Amato F.R., Severini C., Mignogna G., Giorgi A., Schininà M.E., Elia G., Brancia C., Ferri G.-L., Conti R., Ciani B., Pascucci T., Dell'Omo G., Muller E.E., Levi A., Moles A. (2006) TLQP-21, a VGF-derived peptide, increases energy expenditure and prevents the early phase of diet-induced obesity. *Proc Natl Acad Sci*;103:14584-14589.
14. Hannedouche S., Beck V., Leighton-Davies J., Beibel M., Roma G., Oakeley E.J., Lannoy V., Bernard J., Hamon J., Barbieri S., Preuss I., Lasbennes M.C., Sailer A.W., Suply T., Seuwen K., Parker C.N., Bassilana F. (2013) Identification of the C3a Receptor (C3AR1) as the Target of the VGF-derived Peptide TLQP-21 in Rodent Cells. *J Biol Chem*;288:27434-27443.
15. Chen Y.-C., Pristerá A., Ayub M., Swanwick R.S., Karu K., Hamada Y., Rice A.S.C., Okuse K. (2013) Identification of a receptor for neuropeptide VGF and its role in neuropathic pain. *J Biol Chem*;288:34638-34646.
16. Possenti R., Muccioli G., Petrocchi P., Cero C., Cabassi A., Vulchanova L., Riedl M.S., Manieri M., Frontini A., Giordano A., Cinti S., Govoni P., Graiani G., Quaini F., Ghè C., Bresciani E., Bulgarelli I., Torsello A., Locatelli V., Sanghez V., Larsen B.D., Petersen J.S., Palanza P., Parmigiani S., Moles A., Levi A., Bartolomucci A. (2012) Characterization of a novel peripheral pro-lipolytic mechanism in mice: role of VGF-derived peptide TLQP-21. *Biochem J*;441:511-522.
17. Cero C., Vostrikov V.V., Verardi R., Severini C., Gopinath T., Braun P.D., Sassano M.F., Gurney A., Roth B.L., Vulchanova L., Razzoli M., Lodola A., Possenti R., Veglia G.,

- Bartolomucci A. (2014) The TLQP-21 Peptide Activates the G-Protein-Coupled Receptor C3aR1 via a Folding-upon-Binding Mechanism. *Structure*;22:1744–1753.
18. Cole C, Barber J.D., Barton G.J. (2008) The Jpred 3 secondary structure prediction server. *Nucleic Acids Res*;36:W197-W201.
19. Cuff J.A., Clamp M.E., Siddiqui A.S., Finlay M. Barton G.J. (1998) Jpred: A Consensus Secondary Structure Prediction Server. *Bioinformatics*;14:892-893.
20. Spoel D.V.D., Lindahl E., Hess B., Groenhof G., Mark A.E., Berendsen H.J. (2005) GROMACS: fast, flexible, and free. *J Comput Chem*;26:1701–1718.
21. Lindahl E., Hess B., Spoel D.V.D. (2001) GROMACS 3.0: a package for molecular simulation and trajectory analysis. *J Mol Model*;7:306–317.
22. Jorgensen W.L., Rives T. (1988) Development and testing of the OPLS all-atom force field on conformational energetic and properties of organic liquids. *J Am Chem Soc*;110:1657–1666.
23. Hess B., Bekker H., Berendsen H.J.C., Fraaije J. (1997) LINCS: a linear constraint solver for molecular simulations. *J Comput Chem*;18:1463–1472.
24. Kabsch W., Sander C. (1983) Dictionary of protein secondary structure: pattern recognition of hydrogen-bonded and geometrical features. *Biopolymers*;22:2577–2637.
25. Shoichet B.K., Kobilka B.K. (2012) Structure-based drug screening for G-protein-coupled receptors. *Trends Pharmacol Sci*;33:268–272.
26. Hollenstein K., de Graaf C., Bortolato A., Wang M.W., Marshall F.H., Stevens R.C. (2014) Insights into the structure of class B GPCRs. *Trends Pharmacol Sci*;35:12–22.

This article is protected by copyright. All rights reserved.

Figure legends:

Figure 1: A: 2-D plot of variations among RMSD, R_g and simulation time. B: Variations of solvent accessible surface area (SASA) with R_g .

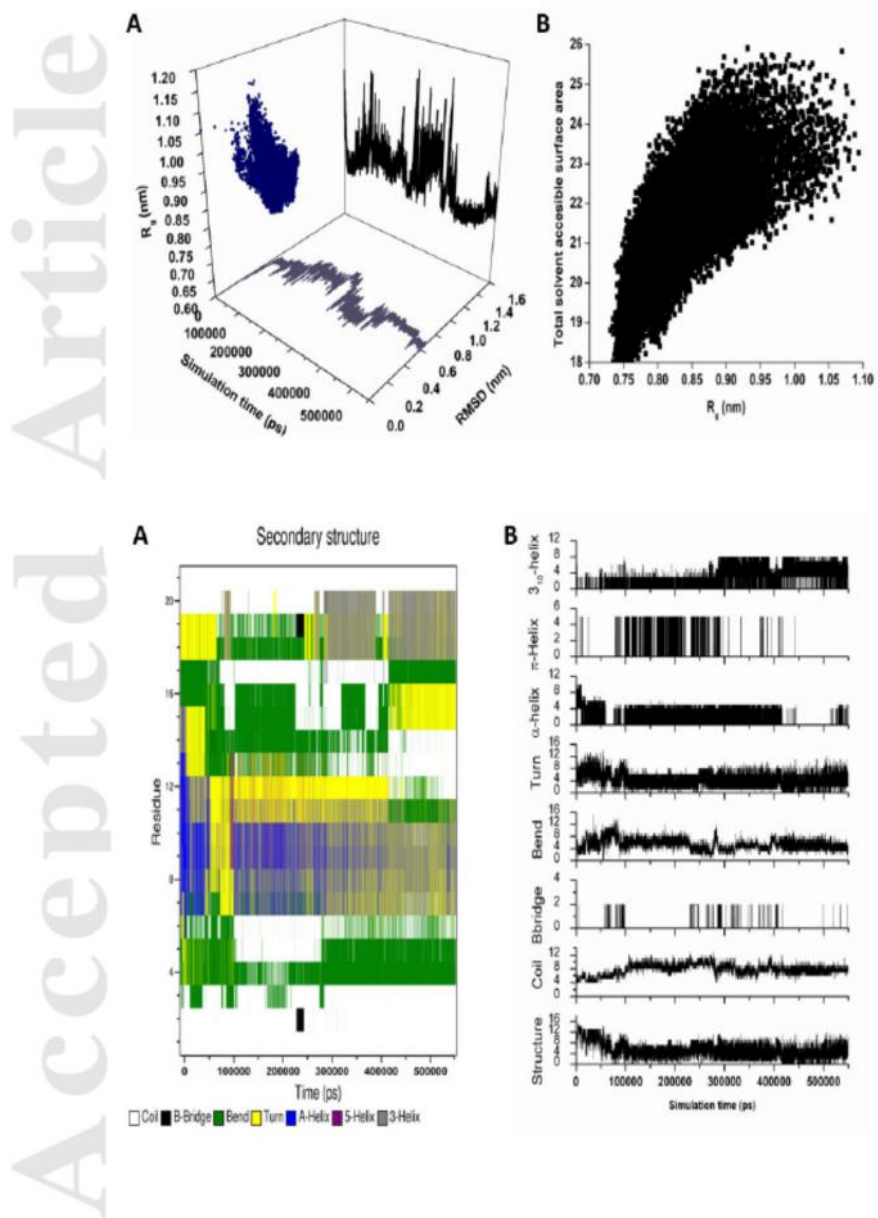
Figure 2: A: Secondary structural propensity variation analysis of each residue of the peptide during simulation time. B: Variations of number of residues in each type of secondary structural region with simulation time.

Figure 3: A: Distribution of number of conformations of the peptide in 50 most populated clusters obtained from cluster analysis on MD trajectory along with the cartoon representations of the average structure from each of the five most populated clusters. B: Secondary structural propensity of the five conformations using STRIDE algorithm. C: RMSF analysis of MD trajectory.

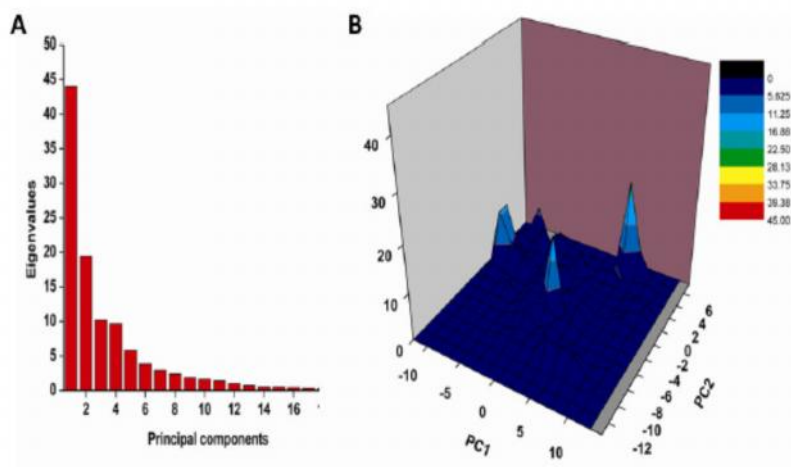
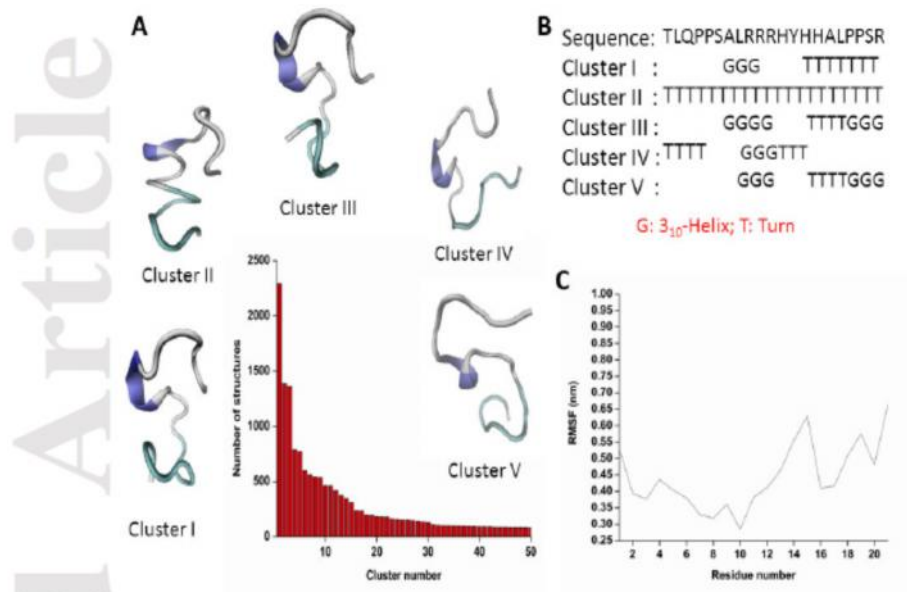
Figure 4: A: Eigenvalue analysis of the calculated principal components obtained from PCA analysis. B: Free energy surface representation of the peptide obtained from MD simulation in terms of PC1 and PC2.

Figure 5: Cartoon representation of the average conformation of the most populated structure of TLQP-21 obtained from MD simulation. A: Hydrogen bonding residues are labeled and represented as sticks. B: Hydrophobic residues are represented in green CPK mode. C: π -cationic interaction between ARG 9 and TYR 13.

This article is protected by copyright. All rights reserved.

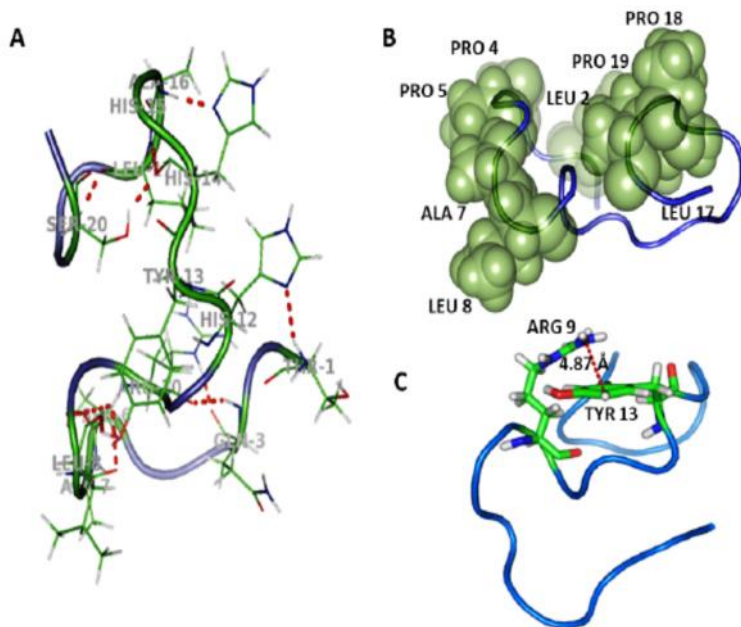


This article is protected by copyright. All rights reserved.



This article is protected by copyright. All rights reserved.

Accepted Article



This article is protected by copyright. All rights reserved.

Annex IV:

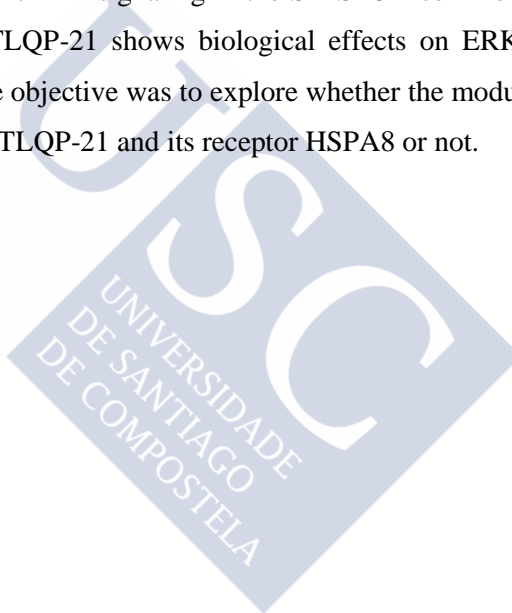
A study on the effect of TLQP-21 on ERK/AKT signaling in SH-SY5Y cells



A study on the effect of TLQP-21 on ERK/AKT signaling in SH-SY5Y cells

Introduction

Taken together all the data into consideration, as presented in the Figure 1 and 2; ERK/AKT signaling pathway was chosen to perform a study to have a read out whether the peptide potentiates ERK/AKT signaling in the SH-SY5Y cell model or not. Of note, besides confirming that TLQP-21 shows biological effects on ERK and AKT in our model system, the ultimate objective was to explore whether the modulation effect is due to the interaction between TLQP-21 and its receptor HSPA8 or not.



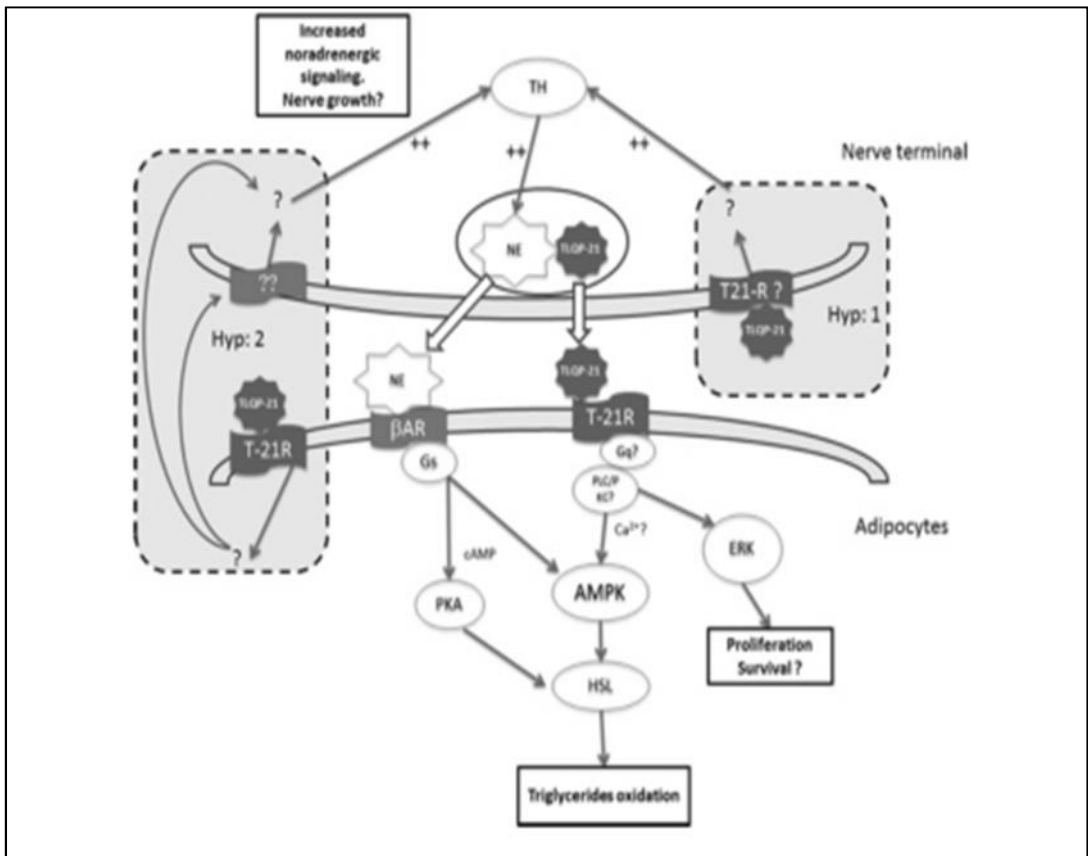


Figure 1: Proposed mechanism of action of TLQP-21: Intracellular signaling downstream in adipocyte membrane after activation of a putative TLQP-21 receptor activation (Possenti, et al. 2012).

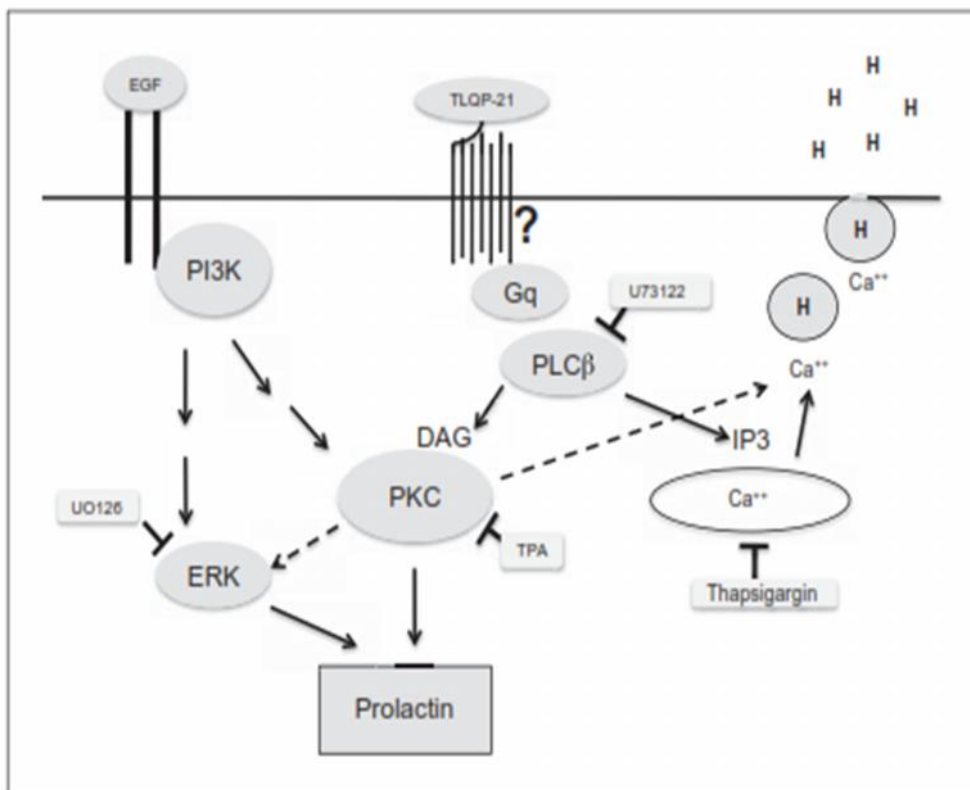


Figure 2: Schematic demonstration of TLQP-21 intracellular signaling (Passeri et al., 2013).

Materials and methods

Petri dishes with confluent SH-SY5Y cells were incubated for 6 hours with the peptide TLQP-21 at a concentration of 1µg/ml. SH-SY5Y cells in Petri dishes were washed twice with cold PBS, followed by solubilization in lysis buffer, composed of 20 mM HEPES, 2mM EGTA, 1mM DTT, 1mM sodium orthovanadate, 1% Triton X-100, 10%

Glycerol, 2 μ M leupeptin, 400 μ M PMSF, 50 μ M β -glycerophosphate, 100 μ g/ml trasylol. The cells were scrapped on ice for 10 minutes and were incubated on ice for 30 minutes with periodic vortexing at each 5 minutes interval, followed by centrifugation for 20 minutes at 14000g at 4 °C. The supernatant was saved for further use. Protein concentration was quantified using the BCA protein assay kit (Pierce Chemical). As control, cells without peptide incubation were grown, then homogenized under the same conditions as treated cells.

Cell homogenate samples (20 μ l) were boiled in 2X Laemmli buffer (Bio-Rad) for 10minutes at 100 °C, spun, and loaded to SDS-PAGE gel. After electrophoresis (200V, 01h), proteins were transferred onto Polyvinylidene fluoride (PVDF) membrane (Millipore, Bedford, MA) in the condition of 0.8 mA/cm² for 90 minutes using semi-dry method (Trans-blot SD semi-dry transfer cell, Biorad). The PVDF membrane was then blocked by 5% BSA (Bovine Serum Albumin) in TBS-T solution (Tris-buffered saline with 0.1% tween 20) for 01 hour at room temperature, followed by three washes by TBS-T each for 10 minutes and then, the membranes were probed by primary antibodies in TBS-T, as specified in the Table 1.

Table 1: Specifications of the antibodies used.

Antibody	Commercial source	Dilution	Other specifications
pERK(Thr202/Tyr204)	Cell signaling	1:2000	Overnight incubation
ERK	Cell signaling	1:1000	Overnight incubation
p ^{AKT} (Ser473)	Cell signaling	1:1000	Overnight incubation
AKT	Cell signaling	1:1000	Overnight incubation
GAPDH	Sigma-Aldrich	1: 5000	Overnight incubation

Then the PVDF membrane was washed 3 times with TBS-T for 10 minutes each wash, followed by incubation with the secondary Anti-rabbit antibody (Dako) at 1 : 2000 dilution in TBS-T. The control was performed using a GAPDH antibody, as specified in the Table 1. The membrane was washed 3 times with TBS-T for 10 minutes each wash. Subsequently, the membrane was incubated with chemiluminescence solution Luminata Forte Western HRP substrate (Merck Millipore) for 5 minutes covering the membrane containing container to protect it from light and was developed using Hypercassette and Amersham hyperfilm (GE Healthcare).

Results and discussion

With protein extracts obtained from TLQP-21 treated cells and not treated (control) cells, the following Western blot analyses were performed. The result obtained in this case showed no difference in expression of the proteins in SHSY-5Y cells. Results shown are from a single experiment and are representative of three separate experiments.

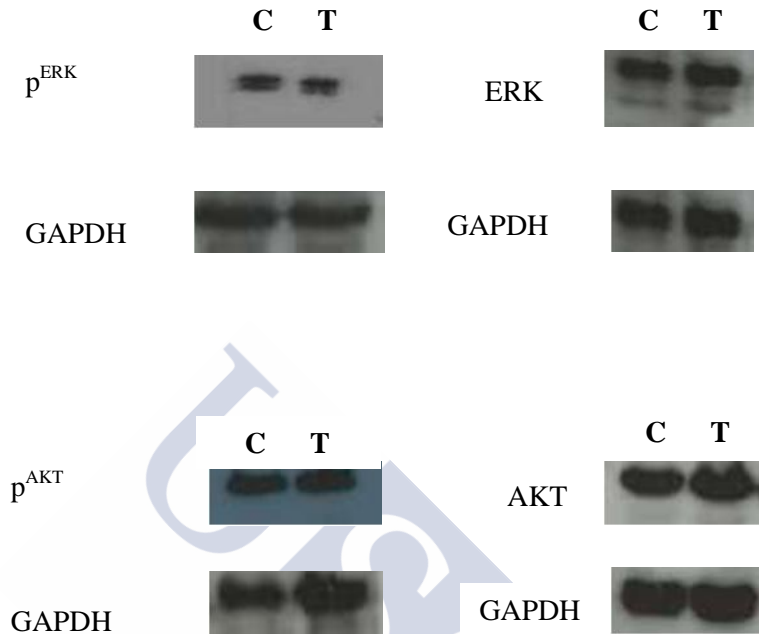


Figure 2: Representative Western blot showing that treatment of TLQP-21 did not alter in the expression of pERK, ERK, p^{AKT}(Ser473) and AKT. (C- Not treated with peptide, Control; T- Treated with TLQP-21). GAPDH was checked as load control.

Of note, in TLQP-21 treated rat pituitary tumor cell lines (GH3), no difference was found in p^{ERK} and p^{AMPK} though there was difference in expression of p^{AKT} and p-p³⁸ (Passeri et al., 2013). In another study, TLQP-21 was found to significantly activate ERK ½. Akt phosphorylation was found to be increased after 15 min of treatment with TLQP-21, while phosphorylation of Akt increased further after that time using insulin-like growth factor-1 (IGF-1). After 24 and 48 h of incubation, IGF-1 treatment increased Akt phosphorylation while TLQP-21 did not modify the amount of phosphorylated Akt,

although total Akt and α -tubulin were found to be increased in both cases (Severini et al., 2008).

Conclusion

In SH-SY5Y cells, TLQP-21 did not bring any alternation in the expression of ERK and AKT proteins.

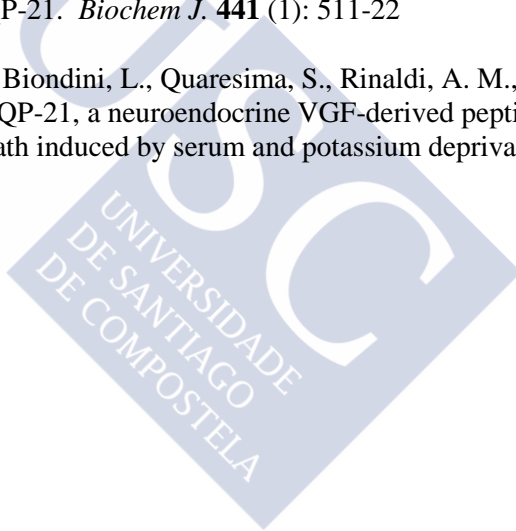


References

Passeri, P. P., Biondini, L., Mongiardi, M. P., Mordini, N., Quaresima, S., Frank, C., Baratta, M., Bartolomucci, A., Levi, A., Severini, C., Possenti, R. (2013) Neuropeptide TLQP-21, a VGF Internal Fragment, Modulates Hormonal Gene Expression and Secretion in GH3 Cell Line. *Neuroendocrinology* . **97**:212–224. DOI: 10.1159/000339855

Possenti, R., Muccioli, G., Petrocchi, P., Cero, C., Cabassi, A., Vulchanova, L., Riedl, M. S., Manieri, M., Frontini, A., Giordano, A., Cinti, S., Govoni, P., Graiani, G., Quaini, F., Ghè, C., Bresciani, E., Bulgarelli, I., Torsello, A., Locatelli, V., Sanghez, V., Larsen, B.D., Petersen, J. S., Palanza, P., Parmigiani, S., Moles, A., Levi, A., Bartolomucci, A. (2012) Characterization of a novel peripheral pro-lipolytic mechanism in mice: role of VGF-derived peptide TLQP-21. *Biochem J.* **441** (1): 511-22

Severini, C., Ciotti, M. T., Biondini, L., Quaresima, S., Rinaldi, A. M., Levi, A., Frank, C., Possenti, R. (2008) TLQP-21, a neuroendocrine VGF-derived peptide, prevents cerebellar granule cells death induced by serum and potassium deprivation. *J Neurochem* **104**: 534-544



Annex V:

A comparative study on the phosphoproteins and total proteins in TLQP-21 treated vs. control SH-SY5Y cells



A comparative study on the phosphoproteins and total proteins in TLQP-21 treated vs. control SH-SY5Y cells

Introduction

In addition to the phosphoproteomic study of SH-SY5Y cells treated with TLQP-21 described before in the thesis, a preliminary analysis of total protein expression was also carried on using the same cell extracts. Comparison of simple 1D SDS-PAGE gels stained with SYPRO[®] Ruby protein gel stain was carried out. The purpose of this study was to assess whether changes in protein expression could be seen even at such low separation resolution.

Materials and methods

The materials and methods used for Pro-Q[®] Diamond phosphoprotein gel staining as well as mass spectrometry in this part of the work were exactly as same as it has been described in the Materials and Methods section of the thesis.

For SYPRO[®] Ruby protein gel staining : Samples (25 µl) from cell homogenates of the cells treated with the peptide and not treated were boiled in 2X Laemmli buffer (Bio-Rad) for 10 minutes at 100 °C, spun, and loaded to SDS-PAGE gel. After electrophoresis (200V, 01h), the gel was washed in dH₂O for 10 minutes. Then the gel was incubated with fixing solution (10% methanol, 7% acetic acid) for 1 hour at room temperature in an orbital shaker step at 50 rpm, followed by overnight incubation with SYPRO[®] Ruby Protein Gel Stain at room temperature with shaking. The gel was then placed into a

staining container covering with a lid to protect it from the light, in addition, the container was wrapped in aluminum foil to further shield the stain from light during the staining process, as per instruction of the supplier. After overnight staining, the gel was transferred to a clean staining dish, washed with the fixing solution in the same condition of staining followed by 5 minutes washing in dH₂O. Finally, the gel was taken from the container to take the image in a Molecular Imager® Gel Doc™ system (Bio Rad, Hercules) using the highest sensitivity of the CCD camera at a resolution of 1392 x 1040 pixels with 12 bit gray scale levels per pixel.

Results and discussion

As supplementary confirmation that TLQP-21 exerts biological effects in the model system, SH-SY5Y cells; homogenates from TLQP-21 treated or not treated (control) cells were subjected to 1D SDS-PAGE followed by staining with the dye Pro-Q Diamond, followed by SYPRO® Ruby dye. As seen in the Figure 1 : At positions 3, 4 and 5; band intensity becomes higher in SYPRO® Ruby dye staining indicate the nonphosphorylated proteins. Several bands with altered intensity in the SYPRO® Ruby experiment were of the same positions in the gels as those in the Pro Q® Diamond, suggesting that both techniques were detecting, to some extent, similar changes. This also suggested that the proteins with altered phosphorylation status were probably abundant proteins, hence their changes were "picked up" by SYPRO® Ruby staining. Differences in band intensity were seen at positions 1 to 5 of the gels. The bands' intensity at 1 (A, Pro Q® Diamond) and 3 (both in A, Pro Q® Diamond and B, SYPRO® Ruby dye) were less in the samples treated with the peptide in comparison to not treated (control) ones suggesting that the peptide on SH-SY5Y cells might provoke dephosphorylation of specific phosphoproteins.

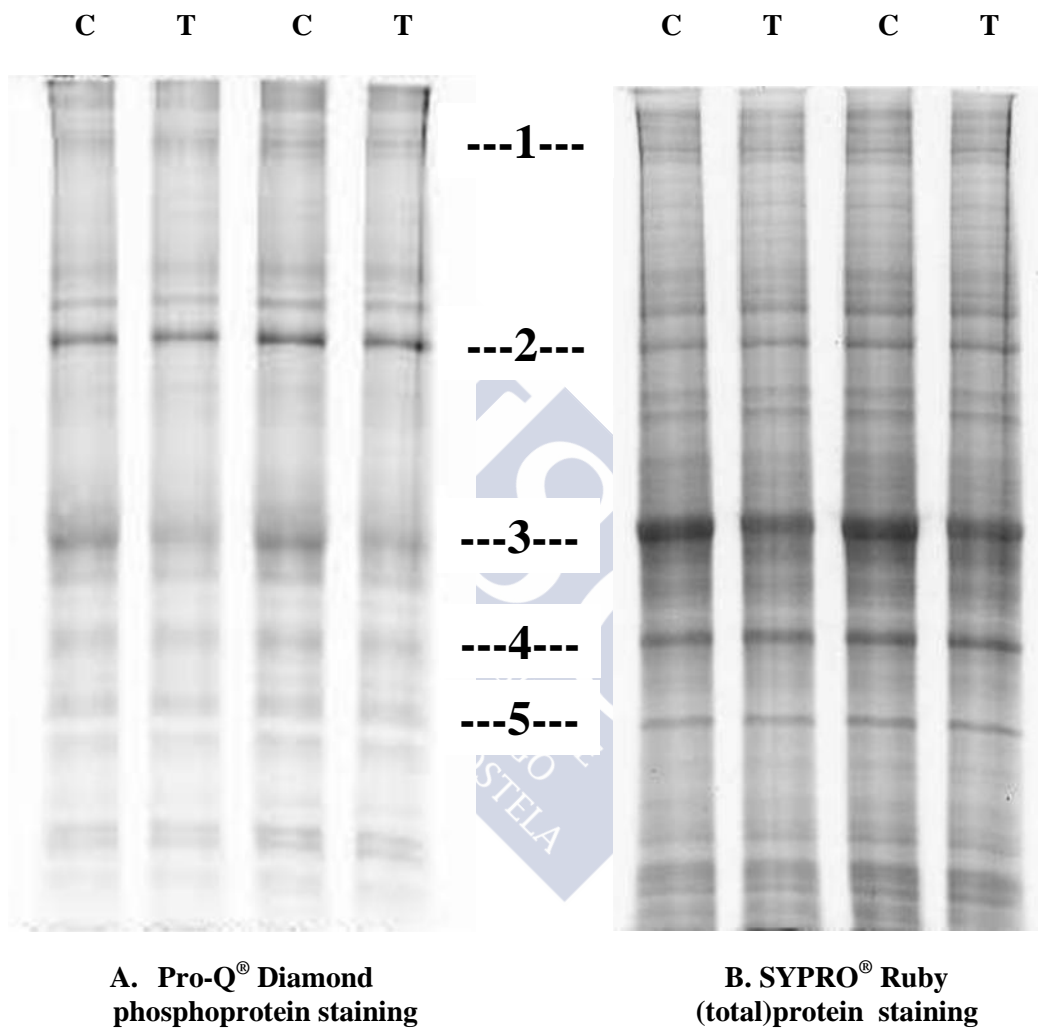


Figure 1: Comparative selectivity of A. Pro-Q[®] Diamond phosphoprotein staining and B. SYPRO[®] Ruby (total) protein staining. Gel, at first, was stained with Pro-Q Diamond dye. Same gel poststained with SYPRO Ruby protein gel stain to visualize all proteins of the cell homogenates treated (T) and not treated (C) with the peptide showing differences in protein expression at position 1, 2, 3, 4 and 5.

The bands at position 1 and 3 from A, Pro Q® Diamond stained gel was cut and analysed by mass spectrometry, as described in the Materials and Methods section; results are detailed in the Table 1.

Table 1: List of proteins with altered expression levels in Pro Q® Diamond stained gel. Proteins of the cell homogenates treated (T) and not treated (C) with the peptide.

A 1

Control (C)

Treated (T)

Protein 1: Microtubule-associated protein 1B OS=Homo sapiens GN=MAP1B, Score: 360.0, MW [kDa]: 270.5	Protein 1: Microtubule-associated protein 1B OS=Homo sapiens GN=MAP1B Score: 245.8
Protein 2: Cytoplasmic dynein 1 heavy chain 1 OS=Homo sapiens GN=DYNC1H1, Score: 157.9, MW [kDa]: 532.1	Protein 2: DNA-dependent protein kinase catalytic subunit - Homo sapiens (Human) Score: 111.7
Protein 3: Alpha-2-macroglobulin OS=Homo sapiens GN=A2M, Score: 157.2, MW [kDa]: 163.2	Protein 3: Filamin-A OS=Homo sapiens GN=FLNA ,Score: 80.5
Protein 4: Filamin-A OS=Homo sapiens GN=FLNA, Score: 136.4, MW [kDa]: 280.6	Protein 4: Cytoplasmic dynein 1 heavy chain 1 OS=Homo sapiens GN=DYNC1H1 ,Score: 41.6
Protein 5: DNA-dependent protein kinase catalytic subunit - Homo sapiens (Human) Score: 37.5, MW [kDa]: 468.8	Protein 5: Alpha-2-macroglobulin OS=Homo sapiens GN=A2M ,Score: 40.0
	Protein 6: Neuroblast differentiation-associated protein AHNAK OS=Homo sapiens, GN=AHNAK, Score: 38.5, MW [kDa]: 628.7
	Protein 7: Solute carrier family 25 member 42 OS=Homo sapiens GN=SLC25A42 Score: 34.2, MW [kDa]: 35.4

A3**Control (C)****Treated (T)**

Protein 1: Protein disulfide-isomerase A3 OS=Homo sapiens GN=PDIA3, Score: 266.6, MW [kDa]: 56.7	Protein 1: Tubulin beta chain OS=Homo sapiens GN=TUBB , Score: 297.2
Protein 2: Tubulin beta chain OS=Homo sapiens GN=TUBB, Score: 232.4, MW [kDa]: 49.6	Protein 2: Protein disulfide-isomerase A3 OS=Homo sapiens GN=PDIA3 , Score: 286.1
Protein 3: Serum albumin precursor - Homo sapiens (Human), Score: 211.7, MW [kDa]: 69.3	Protein 3: Serum albumin precursor - Homo sapiens (Human), Score: 244.2
Protein 4: Tubulin beta-4A chain OS=Homo sapiens GN=TUBB4A, Score: 177.6, MW [kDa]: 49.6	Protein 4: Tubulin beta-4B chain OS=Homo sapiens GN=TUBB4B , Score: 203.0
Protein 5: Tubulin alpha-1A chain OS=Homo sapiens GN=TUBA1A, Score: 123.7, MW [kDa]: 50.1	Protein 5: Adenylyl cyclase-associated protein 1 OS=Homo sapiens GN=CAPI , Score: 109.9
Protein 6: Adenylyl cyclase-associated protein 1 OS=Homo sapiens GN=CAPI, Score: 106.0 MW [kDa]: 51.9	Protein 6: Tubulin alpha-1A chain OS=Homo sapiens GN=TUBA1A , Score: 107.5
Protein 7: Tryptophan--tRNA ligase, cytoplasmic OS=Homo sapiens GN=WARS Score: 104.6, MW [kDa]: 53.1	Protein 7: Alpha-2-HS-glycoprotein OS=Homo sapiens GN=AHSG , Score: 103.9
Protein 8: Alpha-2-HS-glycoprotein OS=Homo sapiens GN=AHSG , Score: 47.6, MW [kDa]: 39.3	Protein 8: Tryptophan--tRNA ligase, cytoplasmic OS=Homo sapiens GN=WARS , Score: 103.0
	Protein 9: Pyruvate kinase isozymes M1/M2 OS=Homo sapiens GN=PKM ,Score: 85.6, MW [kDa]: 57.9
	Protein 10: Dihydrolipoyl dehydrogenase, mitochondrial OS=Homo sapiens GN=DLD Score: 37.9, MW [kDa]: 54.1

Out of the proteins listed in the Table 1, several proteins like Microtubule-associated protein 1B (MW 271 kDa), Tubulin beta chain (MW 57 kDa), Tubulin beta-4B chain (MW 50 kDa), Alpha-2-macroglobulin (MW 163 kDa) were of interests. Further studies are required to validate the results obtained from mass spectrometry.

Conclusion

Changes in protein expression were detected even with a low resolution (1D) separation technique, suggesting that more complete, 2D separation-based proteomic studies should be carried out.



Annex VI:

**A study on the effect of TLQP-21 on the expression of Egr-2 and Grb-2
in SH-SY5Y cells.**



A study on the effect of TLQP-21 on the expression of Egr-2 and Grb-2 in SH-SY5Y cells.

Introduction

Egr-2 and Grb-2 genes were found as VGF (AQEE-30: 1µg/ml) induced genes in PC12 cells (Figure 1, Hunsberger et al., 2007). So, it was of interest to study the effect of TLQP-21 treatment on Egr-2 and Grb-2 protein expression in SH-SY5Y cells in order to know the read out that either or both of the two proteins were modulated. In this connection it should be noted here that, besides confirming that TLQP-21 exerts biological effects on Egr-2 and Grb-2 in our model system, the ultimate objective was to investigate whether this modulation is due to the interaction between TLQP-21 and its receptor HSPA8 or not.



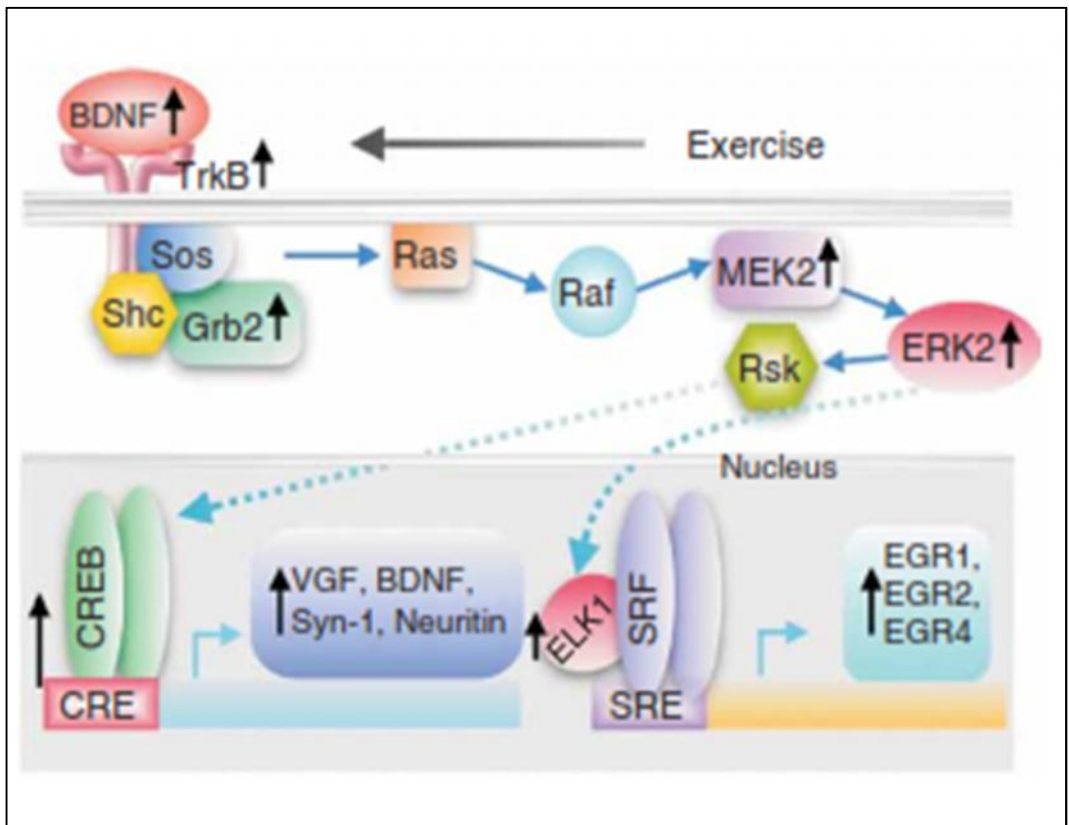


Figure 1: Schematic diagram of neurotrophic factor signaling pathway, showing target gene products, including Egr-2 and Grb-2 (Hunsberger et al., 2007).

Materials and methods

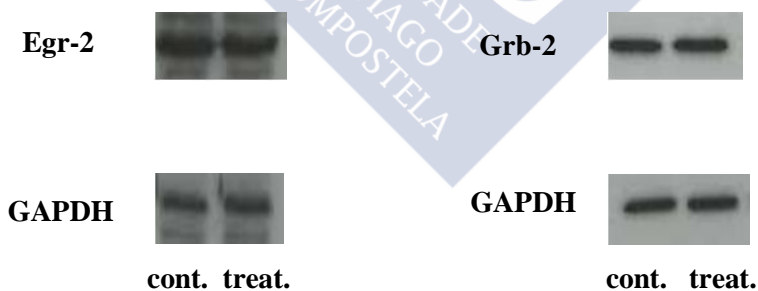
The materials and methods used in this part of the work were exactly same as it has been described in the materials and method section of annex IV, using the antibodies as specified in the Table 1.

Table: Specifications of the antibodies used.

Antibody	Commercial source	Dilution	Other specifications
Grb-2	Cell Signaling	1:1000	Overnight incubation
Egr-2	Santa Cruz Biotechnology	1: 500	Overnight incubation

Results and discussion

The level of expression of the proteins: Egr-2 and Grb-2 was measured by means of Western blot using protein extracts obtained from SH-SY5Y cells treated with the peptide TLQP-21 and not treated (control). Expression of the proteins remained unchanged, as shown in the Figure 2.

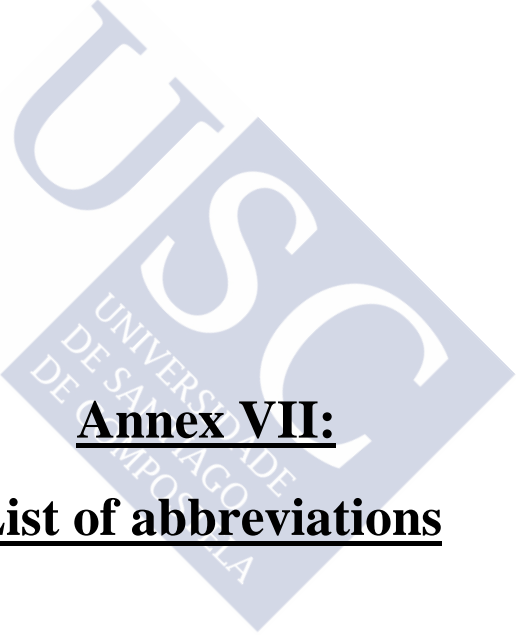
**Figure 2: Western blot analysis of Egr-2 and Grb-2 expression in SH-SY5Y cells.**

Conclusions

No change in the expression of the Egr-2 and Grb-2 proteins was found here. But another VGF derived bioactive peptide AQEE-30 was found to alter in the expression of the proteins in PC12 cells. It might be that AQEE-30 in PC12 cells altered the signaling of Egr-2 and Grb-2 protein expressions whereas in SH-SY5Y cells, TLQP-21 could not bring about such changing effect.

Reference

Hunsberger, J. G., Newton, S. S., Bennett, A. H., Duman, C. H., Russell, D. S., Salton, S. R., Duman, R. S. (2007) Antidepressant actions of the exercise-regulated gene VGF. *Nat Med* **13**: 1476-1482

The logo of the University of Santiago de Compostela (USC) is a diamond-shaped emblem. It features the letters 'USC' in a large, stylized font. Below the letters, the text 'UNIVERSIDADE DE SANTIAGO DE COMPOSTELA' is written in a smaller font, following the shape of the diamond.

Annex VII:
List of abbreviations



AA:	Amino acids
AD:	Alzheimer's disease
AFM:	Atomic force microscopy
ALS:	Amyotrophic lateral sclerosis
AR:	-adrenergic
BAT:	Brown adipose tissue
BDNF:	Brain derived neurotrophic factor
BSA:	Bovine serum albumin
C3a:	Complement component-3a
C3AR1:	Complement component-3a receptor 1
C4a:	Complement component-4a
cAMP:	Cyclic adenosine monophosphate
cDNA:	Complementary deoxyribonucleic acid
CgA:	Chromogranin A
CGCs:	Cerebellar granule cells
CHO:	Chinese hamster ovary
CNS:	Central nervous system
COX-2:	Cyclooxygenase-2
CSF:	Cerebrospinal fluid
Da:	Daltons
DISC1:	Disrupted in Schizophrenia 1
DRG:	Dorsal root ganglion
DSG:	15-deoxyspergualin
EBSS:	Earle's balanced salt solution
ER:	Endoplasmic reticulum
ERK:	Extracellular-signal-regulated kinase
FACS:	Fluorescence-activated cell sorting

FBS:	Foetal bovine serum
FFA:	Free fatty acids
FSH:	Follicle stimulating hormone
FSH:	Follicle-stimulating hormone
FTD:	Fronto-temporal dementia
G6PD:	Glucose-6-phosphate dehydrogenase
gC1q-R:	Receptor (R) for globular head (g) region of C1q
GIP:	Glucose-dependent insulintropic polypeptide
Gln:	Glutamine
GLP-1:	Glucagon-like peptide-1
GnRH:	Gonadotrophin releasing hormone
GPCR:	G-protein coupled receptor
GSIS:	Glucose-stimulated insulin secretion
hCG:	Human chorionic gonadotrophin
HFD:	High-fat diet
HPG:	Hypothalamic-pituitary-gonadal
HPLC:	High performance liquid chromatography
HRP:	Horseradish peroxidase
HSP70:	Heat shock protein 70 (family)
HSPA5:	Heat shock protein A5
HSPA8:	Heat shock cognate protein A8
HSPA9:	Heat shock protein A9
HSPs:	Heat shock proteins
HUVECs:	Human umbilical vascular endothelial cells
i.c.v.:	Intracerebroventricular
IL-8:	Interleukin-8
Ip:	Intraperitoneal

Iv:	Intravenous
kDa:	Kilo Dalton
LC-MS:	Liquid chromatography mass spectrometry
LH:	Leutinizing hormone
mA:	Milliampere
MALDI-TOF:	Matrix Assisted Laser Desorption Ionization Time-of-Flight
MAPK:	Mitogen-activated protein kinase
MDD:	Major depressive disorder
MM:	Molecular mass
MS:	Mass spectrometry
NEAA:	Non-Essential Amino Acids
NERPs:	Neuroendocrine regulatory peptides
NGF:	Nerve growth factor
NHS:	N-hydroxysuccinimide
NPCs:	Neural progenitor cells
P/S:	Penicillin-Streptomycin
PAGE:	Polyacrylamide gel electrophoresis
PBS:	Phosphate buffered saline
PCs:	Prohormone convertases
PG:	Prostaglandin
PGE2:	Prostaglandin E2
PKA:	Protein kinase A
PNS:	Peripheral nervous system
PSNL:	Partial sciatic nerve ligation
PTX:	Pertussis toxin
PVDF:	Polyvinylidene fluoride
ROS:	Reactive oxygen species

Annex VII: List of abbreviations

SCZ:	Schizophrenia
SDS:	Sodium dodecyl sulphate
SgII:	Secretogranin II
ShRNA:	Small hairpin RNA/ short hairpin RNA
siRNA:	Small interfering ribonucleic acid
SN:	Secretoneurin
T2DM:	Type 2 diabetes mellitus
TBS:	Tris-buffered saline
TG:	Triglycerides
TNF- :	Tumor necrosis factor alpha
TrkB:	Tropomyosin receptor kinase B
UCP1:	Uncoupling protein 1
VEGF:	Vascular endothelial growth factor
VGF:	Non acronymic, a neurotrophin
VIP:	Vasoactive intestinal peptide
WAT:	White adipose tissue



